This is to certify that the

thesis entitled

THE SYNTHESIS AND CHARACTERIZATION
OF MODELS FOR HEME-CONTAINING PROTEINS

presented by

Richard Hall Young

has been accepted towards fulfillment
of the requirements for

Ph.D. degree in Chemistry

Chi K. Chang
Major professor

Date May 18, 1984

THE SYNTHESIS AND CHARACTERIZATION OF MODELS FOR HEME-CONTAINING PROTEINS

By

Richard Hall Young

A DISSERTATION

Submitted to
Michigan State University
in partial fulfillment of the requirements
of the degree of

DOCTOR OF PHILOSOPHY

Department of Chemistry

1986

ABSTRACT

THE SYNTHESIS AND CHARACTERIZATION OF MODELS FOR HEME-CONTAINING PROTEINS

By

Richard Young

The synthesis of a series of blocked and imidazole appended diphenylporphyrins is described. The hybrid porphyrin is synthesized by the condensation of o-nitrobenzaldehyde with 4,4'-diethyl-3,3'-dimethyl-2,2'-dipyrrylmethane in methanol followed by oxidation and reduction. The effectiveness of the blocking groups is supported by the formation of stable ferric hydroxides in the doubly protected system; trans 5,15-bis(o-(p-t-butylbenzamido)phenyl)-2,8,12,18-tetraethyl-3,7,13,17-tetramethylporphyrin. This complex was characterized by UV-visible, ^{1}H NMR, IR, and cyclic voltammetry. The ability of the m-benzamido linkage to enforce imidazole coordination is shown by ^{1}H NMR studies on the ferric bis imidazole complexes of free, and covalently linked systems.

The diphenyl porphyrins are also used in the construction of binuclear systems, including a mixed cofacial diporphyrin. The effectiveness of chelating ligands is supported by electron spin resonace studies.

Synthetic analogues of hydroporphyrins are constructed from gemini-alkylated ketones resulting from the oxidation of octaethyl porphyrin. The synthesis of simple chlorins, bacteriochlorins, isobacteriochlorins, and imidazole linked systems are described. These stabilized hydroporphyrins are fully characterized by UV-visible, ^{1}H NMR, and cyclic voltammetry.

To Dad, Mom

George, Leonard, Martin,

Robert, Kathy,

and Jim.

ACKNOWLEDGMENTS

The author would first of all like to thank his parents and family for their never ending support and understanding. The author is also indebted to Dr. C.K. Chang for his support and guidance. Gratitude is also extended to Dr. R.W. Fish for his foresight and compassion. I am also grateful to Michigan State University, the National Science Foundation, and the National Institute of Health for the opportunity and freedom to complete this research.

A special thanks is also extended to all those who made my stay worthwhile: Brian, for teaching me how to laugh at myself; Ivy, for intiating and enduring a friendship; Susan and Nancy, for helping me tread that fine line; and (MAM)X2, for caring enough to fight back. In addition; Steve, Larry, Steve, Paul, Steve, Tim, and the rest of the Megahurtz, Aromatics, Zero's, and Alkanes for making winning and losing so much fun.

TABLE OF CONTENTS

LIST OF TABLES

LIST OF FIGURES

LIST OF

APPENDIX FIGURES

A1

A1

A1

A1

A1

A1

A1

A2

A2

A2

A2

A2

A2

A2

A2

CHAPTER 1

THE SYNTHESIS AND CHARACTERIZATION OF BLOCKED AND LIGAND APPENDED HEMES DERIVED FROM ATROPISOMERIC DIPHENYL PORPHYRINS

Introduction

The construction of synthetic metalloporphyrin complexes which mimic heme-containing proteins has been one of the most powerful methods in studying reaction mechanisms and structure-function relationships of hemoproteins. Most model systems are based on two families of porphyrins; the β-substituted porphyrins (e.g. protoporphyrin) and the meso-substituted tetraphenyl (TPP) derivatives. These two types of porphyrins have been manipulated extensively and in the last decade a large number of interesting model systems with colorful names have been created. [1-4] The β-substituted compounds resemble more closely the naturally occurring hemes, however, the excessive floppiness of the side chains used in functionalization is often undesirable. The tetraphenyl systems, particularly those functionalized with o-anilido groups (e.g. "picket fence" heme), are structurally more rigid. Nevertheless, they suffer from the fact that synthetically it is very difficult to derivatize one particular phenyl group (out of four in TPP) on the prophyrin ring in order to attache special appendages. Recently, Gunter and Mander [5] reported the synthesis of a hybrid meso-diphenylporphyrin. This system appears to be attractive for model building purposes in that the atropisomers of the o-amino substituted derivative can be separated and manipulated individually to yield a wide variety of useful heme model compounds. While these authors described the synthesis of heme-copper complex based on one of the atropisomers [5,6] no other work has been reported

exploiting this useful system. We describe here an improved synthesis of this hybrid porphyrin as well as a large number of protected and chelated heme model compounds that can be derived from this porphyrin.

The diphenyl porphyrins 1 and 2, substituted with ethyl and methyl groups are easier to synthesize and are substantially more soluble in organic solvents than the octamethyl analogue. The ring methyl groups in this system hinder the rotation of the neighboring phenyl rings allowing isolation of the atropisomers. This steric constraint and the conformational rigidity of amides can be employed to enforce selective ligation and/or blockage of the porphyrin coordination site. Our synthetic targets summarized in Table 1, demonstrate that a large number of novel porphyrins capable of tetrapenta-, and hexa-coordination can be generated conveniently using this approach. These synthetic hemes have been applied in modeling studies of O_2 and CO binding in hemoglobins and myoglobins.

Synthesis

The parent compound, 5, 15-bis(o-aminophynyl)-2,8,12,18-tetraethyl 3,7,13,17-tetramethylporphine, or $(NH_2)_2$-DPE 1 (amino-diphenyl etioporphyrin II) was synthesized by condensation of equivalent amounts of 5, 5'- unsubstituted dipyrrylmethane 3, and o-nitrobenzaldehyde in methanol with a catalytic amount of p-toluenesulfonic acid, Scheme 1. The resulting porphyrinogen 4, was oxidized with o-chloranil and reduced to the corresponding atropisomeric diamino porphyrins. The prerequisite decarboxylation of the dipyrrylmethane was found to proceed readily in one step from its diester precursor.

Table 1. Blocked and Ligand Appended Diphenyl Porphyrins.

Table 1. Blocked and Ligand Appended Diphenyl Porphyrins.

Precursors			NMR, Figure #
(amino)$_2$DPE	trans	1	
	cis	2	1a
(amino),(p-tBu-benzamide)DPE	trans	5	1b
(amino),(m-BrCH$_2$benzamide)DPE	cis	6	A3
(amino),(m-ImCH$_2$benzamide)DPE	trans	7	A4
	cis	8	A4
Symmetric			
(p-tBu-benzamide)$_2$DPE	trans	9	1c
	cis	10	1d
(m-ImCH$_2$benzamide)$_2$DPE	trans	11	A5
	cis	12	A5
(acetamide)$_2$DPE	trans	13	A6
	cis	14	
(Im(CH$_2$)$_2$CONH)$_2$DPE	trans	15	A7
(Im(CH$_2$)$_3$CONH)$_2$DPE	trans	16	A7
(Im(CH$_2$)$_3$NHCONH)$_2$DPE	trans	17	A7
(Br(CH$_2$)$_3$CONH)$_2$DPE	trans	18	
	cis	19	A8
lactam((CH$_2$)$_3$CON)$_2$DPE	trans	20	A8
(m-NMe$_3^+$CH$_2$benzamide)$_2$DPE	trans	21	A9
Phenols and Esters			
(hydroxy)$_2$DPE	trans	22	A11
	cis	23	A12
(p-tBu-benzoate)$_2$DPE	trans	24	A13
(m-ImCH$_2$benzoate)$_2$DPE	trans	25	A14

Trans (p-tBu-benzamide)DPE		NMR, Figure #
(m-BrCH$_2$benzamide)	26	A15
(m-ImCH$_2$benzamide)	27	1E,A16
(m-AcSCH$_2$benzamide)	28	A15
(Im(CH$_2$)$_2$CONH)	29	A17
(Im(CH$_2$)$_3$CONH)	30	A17
(Im(CH$_2$)$_3$NHCONH)	31	A18
Trans (m-ImCH$_2$benzamide)DPE		
3, 5(CO$_2$Et)$_2$benzamide	32	A19
3, 5(CO$_2$Bu)$_2$benzamide	33	A19
3, 5(CONH-nBu)$_2$benzamide	34	A20
3, 5(CONEt$_2$)$_2$benzamide	35	A21
3, 5(CON-iPr$_2$)$_2$benzamide	36	A21
3, 5(COS-nBu)$_2$benzamide	37	A22
3, 5(CH$_2$OH)$_2$benzamide	38	A23
3, 5(CH$_2$OMe)$_2$benzamide	39	A24
3 (NMe$_2$CH$_2$)benzamide	40	A25
3 (NMe$_3^+$CH$_2$)benzamide	41	A26
3 (NEt$_3^+$CH$_2$)benzamide	42	A27
(acetamide) trans	43	A28a
cis	44	A28b
Malonyl		
NH$_2$	45	A29
NH-tBu	46	A30
NMe$_2$	47	A31

Scheme 1.

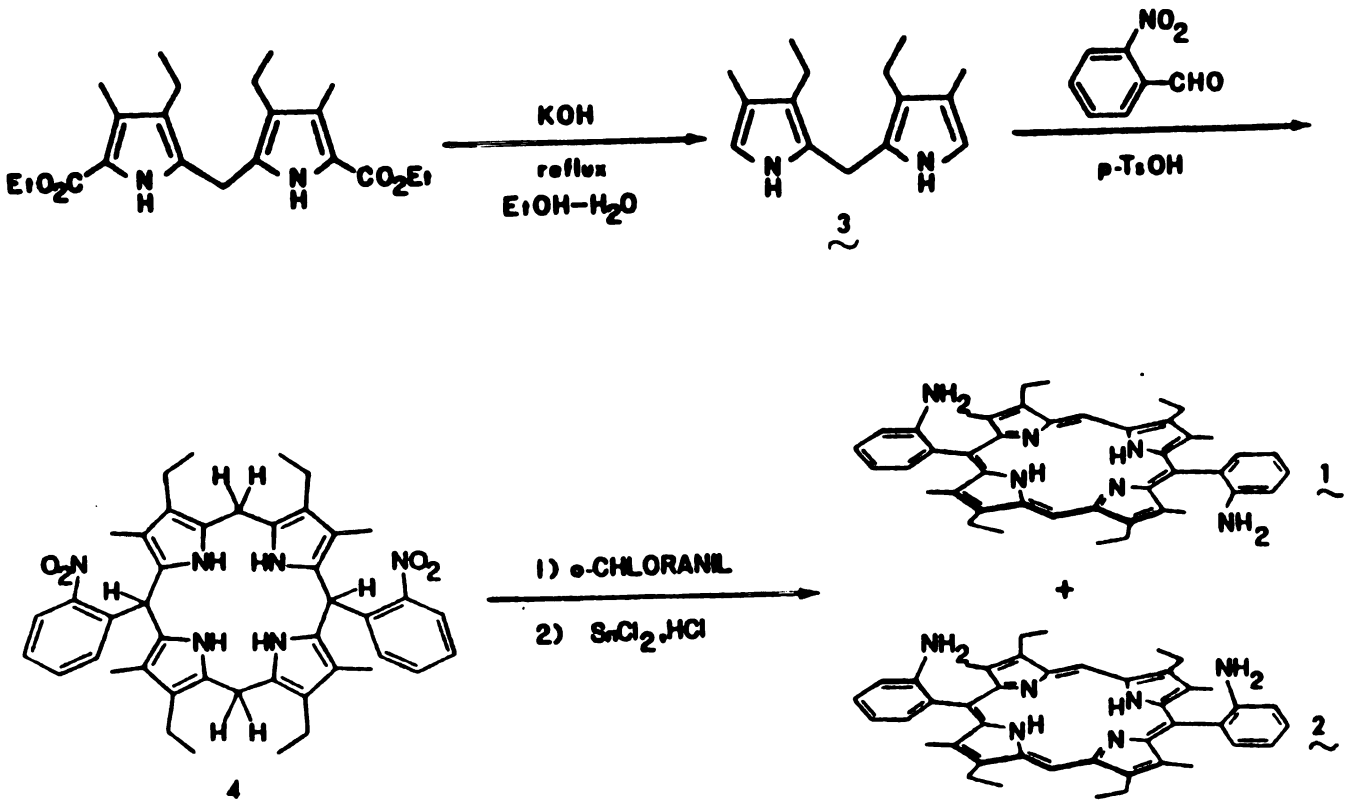
KOH
reflux
EtOH–H2O
3
NO2
CHO
p-TsOH
4
1) o-CHLORANIL
2) SnCl2.HCl
1
+
2

In contrast, the tetramethyldipyrrylmethane used by Gunter and Mander[5] was notoriously difficult to prepare and required a bomb reactor to effect decarboxylation. In the present scheme, the yields were better than 70% in each step. The diamino prophyrins have good solubility in organic solvents and separation of atropisomers can be carried out directly in large scale on silica gel columns. The isolated individual atropisomers were found to be conformationally rigid, only under prolonged heating at >100°C could they be thermally equilibrated to 1:1 mixtures of cis:trans isomers. The activation energy needed for thermal interconversion of the two isomers was found to be 26.2 Kcal/mol for the parent diaminoporphyrin and 28.8 Kcal/mol for the acetamido derivative. The rotational barrier and conformation of the amides should allow attachment an direction of specific groups over the prophyrin core. These groups can serve a wide variety of functions and be readily modifiable without causing severe changes in the overall complex.

To prepare anilido derivatives, the most efficient method was found to be direct coupling between acid chlorides and the aminoporphyrins. The yields were routinely >60% when the acid chlorides could be isolated. In cases where the acid chloride could not be isolated, we have employed with success ethyl chloroformate and trifluoroacetic anhydride in mixed anhydride couplings. The symmetrically substituted anilides were initially constructed to develop the required synthetic methods and aid in the characterization of more complex systems.

A simple soluble protected porphyrin can be constructed by

treating the trans diamine 1, with an excess of p-t-butylbenzoyl chloride. The resulting trans (p-t-butylbenzamido)$_2$ DPE 9 isolated in > 90% yield, possesses phenyl rings held above and below the porphyrin ring. The protons of these phenyl groups were shifted upfield, 6.42 ppm ($CDCl_3$), and appeared as a singlet in the ^1H NMR in a variety of solvents. The more crowded cis isomer, formed by the same sequence, showed the expected AB quartet for the phenyl protons in $CDCl_3$, but a singlet in DMSO-d_6. These results imply that the free rotation necessary to equilibrate the protons was restricted by solvation or aggregation in the cis, but not in the trans atropisomer.

A series of penta-coordinate ferrous hemes were constructed employing a stepwise coupling strategy (Scheme 2).

These differently appended systems needed in kinetic studies would reveal the possible importance of the imidazole preequilibrium, Equation 1, in O_2 and CO binding, Equation 2.

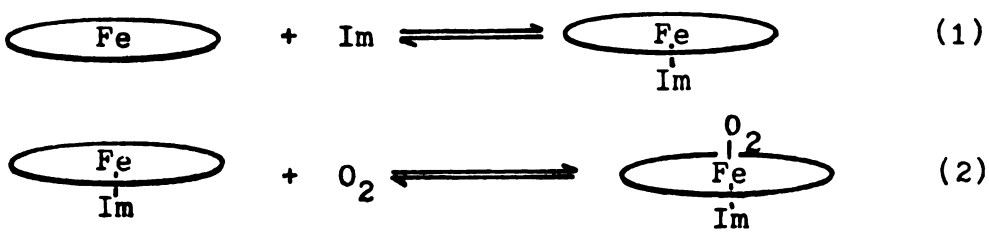

Scheme 2.

Scheme 2.

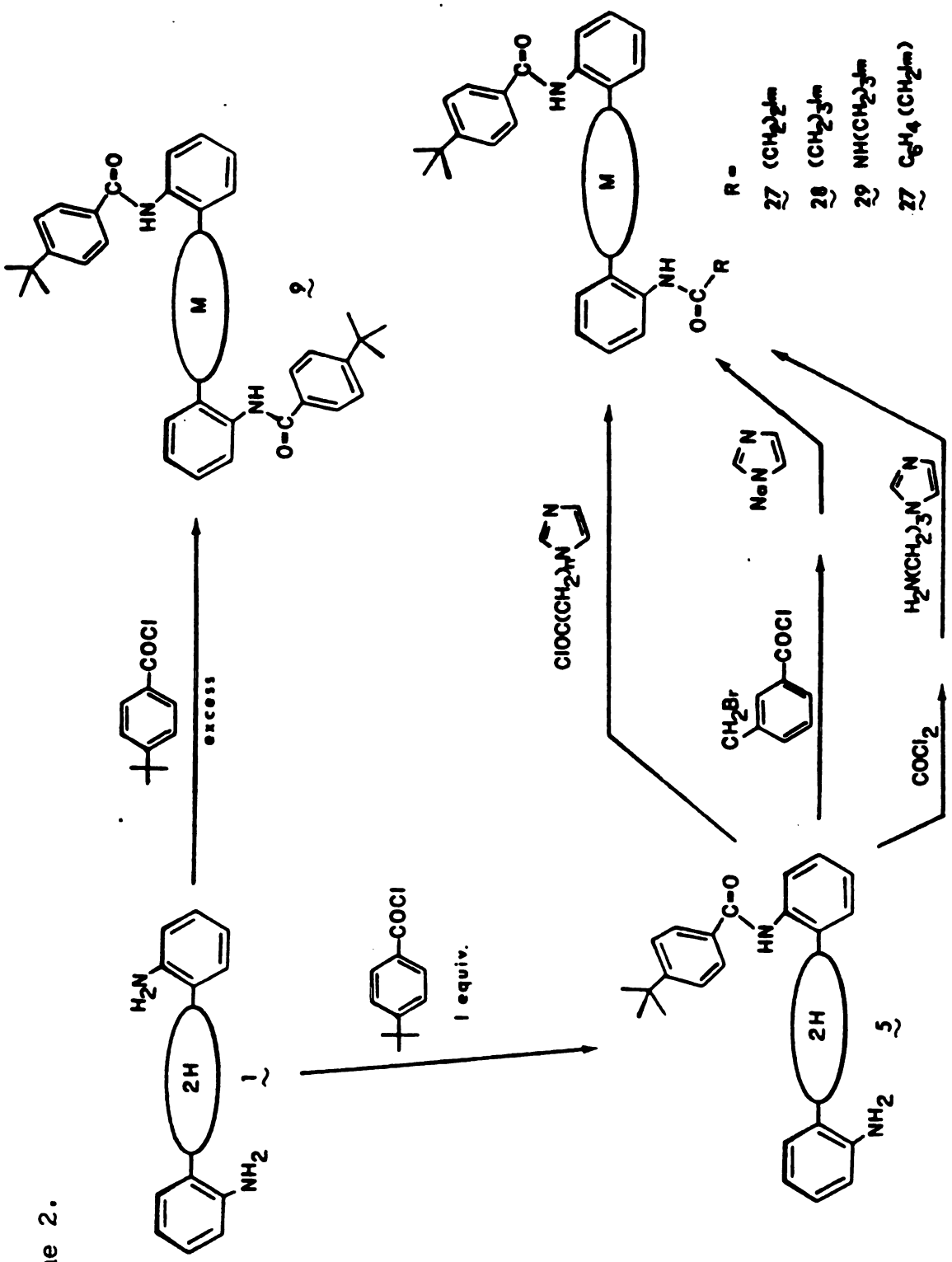
2H
M
excess
1 equiv.
COCl
COCl2
ClOC(CH2)2N
NaN
CH2Br
H2N(CH2)3N
R =
27 (CH2)2m
28 (CH2)3m
29 NH(CH2)3m
27 C6H4 (CH2m)

Reaction of porphyrin 1 with one equivalent of p-t-butylbenzoyl chloride followed by separation on silica gel yielded an almost statistical distribution of mono, di, and unsubstituted amino porphyrins. The mono-substituted porphyrin 5, can be easily appended with appropriate imidazole ligands. Initial attempts to generate the alkyl liinked imidazoles throught the bromo alkanoic anilides failed due to rapid lactam formation on treatment with base. Imidazole alkanoic acids were successfully synthesized and coupled by procedures analogous to those used in the synthesis of "tailed picket fence" porphyrins.[7]

There is evidence indicating that appended imidazoles via alkyl linkages are somewhat undisciplined and tend to form mixtures of bis-, mono-, and un-ligated ferrous hemes under many circumstances.[7] To overcome this randomness, a more orientation specific imidazole linkage was designed. The benzamide linkage is more rigid and should also serve as an effective blocking group, preventing μ-oxo dimer formation in ferric hemins. This linkage was constructed by coupling m-bromomethylbenzoyl chloride with the anilino porphyrin 5, followed by substitution with sodium imidazolate in acetonitrile. This two step sequence overcame the low solubility problem of m-(α-(N-imidazolyl)toluic acid. The benzyl halides formed were prone to hydrolysis during work-up in the presence of organic bases. This could be prevented by simply reacting the benzyl halides in situ.

Preliminary results on the CO and O_2 association rates indicate the affect of changing appendages is small and is of the same order for both CO and O_2.

Modifications of the blocking group near the ligand coordination site (trans to the imidazole) were made in order to model the polarity and steric effects inside the myoglobin heme pocket. The mono-benzyl-imidazole porphyrin 7 was easily prepared by treatment of the diamino DPE with one equivalent of α-bromotoluic acid chloride, followed by addition of sodium imidazolate in acetonitrile, and subsequent separation of the product mixture. The mono-imidazole porphyrin 7 can be carried through a variety of reaction sequences to produce blocked or functionally derivatized porphyrins of varing polarity and steric bulk (Scheme 3). Although the iron complexes of most of these compounds did not form isolable oxygen adducts at room temperature, kinetic studies have shown that local polar groups assume a principal role in determining CO and O_2 binding, Table 2 and 3. Detailed discussion and analysis of these results have been published elsewhere.[8]

The separation of functionalized porphyrins from by-products was tedious. In general, large excesses of reagents were required to prevent cross-coupling and polymerization. Two methods were generally employed for crude purification before final separation on preparative TLC plates or columns, both utilizing the difference in basicity

Scheme 3.

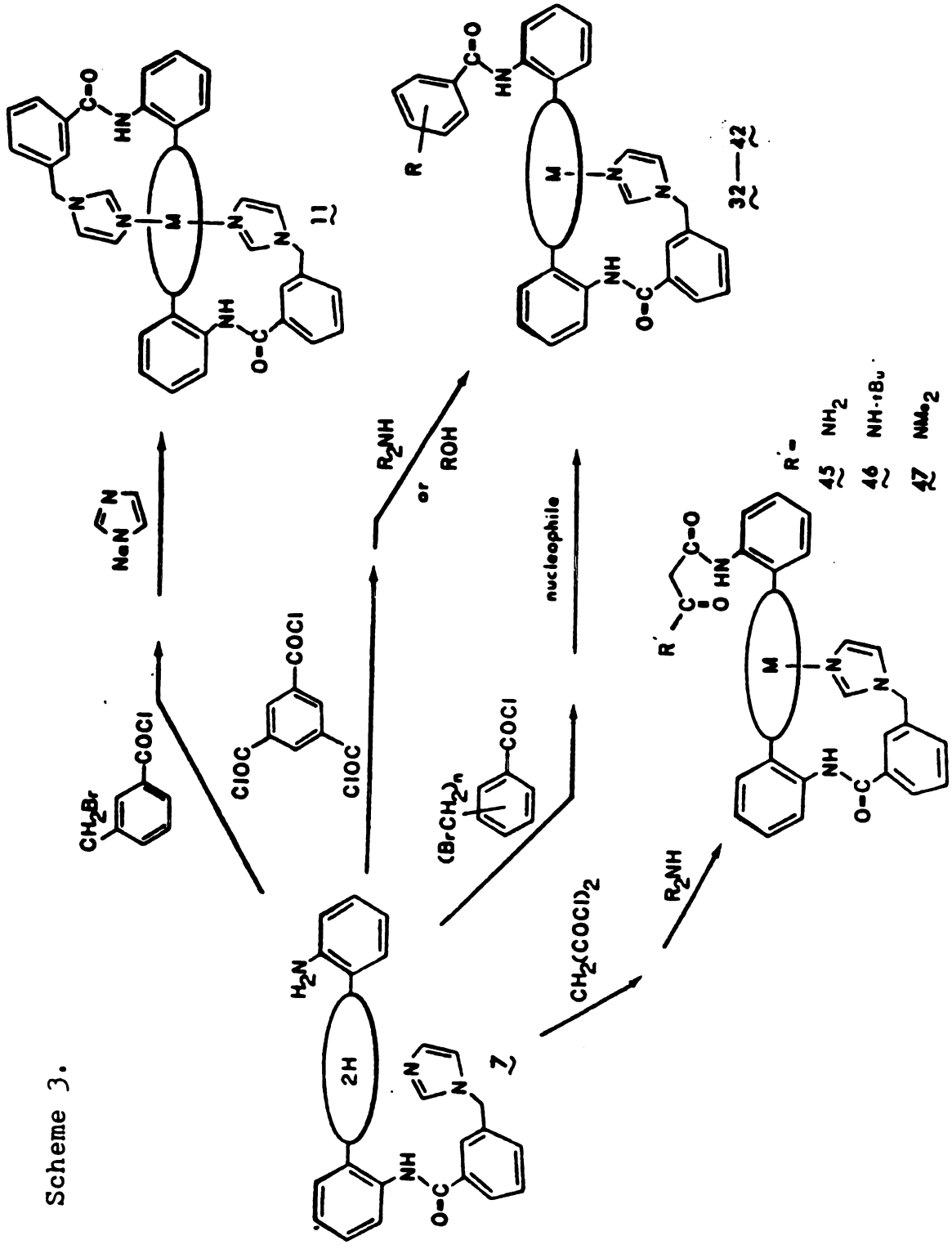
11
32—42
R₂NH
or ROH
nucleophile
R =
45 NH₂
46 NH-tBu
47 NMe₂
2H
7
CH₂(COCl)₂
R₂NH

Table 2 CO and O_2 Binding Constants of Diphenyl Hemes with Remote Polar Groups (20-22°C).[a]

Compound	k' (M^{-1} s^{-1})	k (s^{-1})	$P_{½}^{O_2}$ (torr)	1' (M^{-1} s^{-1})	1 (s^{-1})	$P_{½}^{CO}$ (torr)	M[e]
cis acetamide (44)	3×10^7[b]	38,000	126	2.3×10^6	0.12	0.0054	23,000
trans acetamide (43)	2.6×10^7	4,100	16	1.6×10^6	0.072	0.0045	3,550
ether strap[c,d]	3.0×10^8	40,000	18.6	6.8×10^7			
amide strap[c,d]	3.6×10^8	5,000	2	3.5×10^7			

[a] In toluene.

[b] Due to the low O_2 affinity high oxygen concentrations were necessary leading to pseudo-first order rate constants approaching the limits of detection.

[c] Axial base was a covalently attached pyridine.

[d] Reference 3e

[e] $P_{½}^{O_2}/P_{½}^{CO}$.

Table 3 *CO and O_2 Binding Constants of Diphenyl Hemes with Groups of Varying Polarity Situated Near the Ligand Binding Site*

Table 3 CO and O_2 Binding Constants of Diphenyl Hemes with Groups of Varying Polarity Situated Near the Ligand Binding Site (20-22°C).[a]

Compound		μ_g	k' (M^{-1} s^{-1})	k (s^{-1})	$P_{½}^{O_2}$ (torr)	l' (M^{-1} s^{-1})	l (s^{-1})	$P_{½}^{CO}$ (torr)	M[b]
4-t-Butyl	(27)	0.52	4.7×10^7	15,500	33	2.5×10^6	0.14	0.0057	5,800
3,5-CH_2OMe	(39)	1.3	2.6×10^7	9,900	38	1.1×10^6	0.028	0.0075	15,000
3,5-CH_2OH	(38)	1.7	2.3×10^7	2,900	13	1.2×10^6	0.090	0.0075	1,700
3,5-CO_2nBu	(33)	1.9	2.2×10^7	11,000	48	1.5×10^6	0.13	0.0086	5,600
3,5-CONHnBu	(34)	3.6	1.3×10^7	300	2.3	1.3×10^6	0.042	0.0032	720
3,5-$CONEt_2$	(35)	3.8-3.9	1.4×10^7	4,750	34	0.59×10^6	0.048	0.0081	4,200
3,5-$CONiPr_2$	(36)	3.8-3.9	1.3×10^7	9,300	72	0.47×10^6	0.053	0.011	6,500

[a] Toluene.

[b] $P_{½}^{O_2}/P_{½}^{CO}$.

between the desired porphyrin and by-products. The first method involved extraction of the porphyrins into 80% phosphoric acid, several washings with methylene chloride, and subsequent neutralization and extraction. The second method, generally giving a higher recovery, involved chromatographic separation of the protonated species. Reaction mixtures were protonated with acetic acid and then washed through a column of silica gel. The by-products were eluted with methylene chloride-acetic acid, followed by the desired porphyrin which was freed with triethylamine.

Thermal Atropisomerization

The isolation of atropisomers in tetraphenyl porphyrins [1a, 2c, 7] and now diphenyl porphyrins is evidence for the restricted rotation of phenyl rings. To allow ring rotation, the porphyrin skeleton must undergo severe deformations to minimize steric constraints between o-substituents and pyrrole protons or ring methyl groups. The energy barrier for this rotation by thermal and photochemical processes in TPP systems has been the subject of an investigation.

The activation energies for thermal rotation in the o-diamino and o-diacetamido DPE have been obtained. The kinetic studies were carried out by monitoring the rate of isomerization using thin layer chromatography and UV-vis spectroscopy at several different temperatures. Table 4 lists the temperatures, rates, and ΔG^{+} calculated for the acetamido, amino, and related TPP systems.

Table 4. Rate Constants and Activation Parameters for the Thermal Atropisomerism of Diphenyl Porphyrins and Related Tetraphenyl Porphyrins.

Diphenyl Porphyrin	T°C	k, s^{-1}	$\Delta G^{\ddagger}$
$(acetamide)_2$, cis	115	9.7×10^{-4}	28.2
	120	1.9×10^{-3}	28.0
	132	5.5×10^{-3}	28.1
	141	1.5×10^{-2}	27.9
$(amino)_2$, cis	87	7.9×10^{-4}	26.2
	98	2.6×10^{-3}	26.2
	109	7.8×10^{-3}	26.2
	112	1.1×10^{-2}	26.1
	123	2.5×10^{-2}	26.2
Tetraphenyl Porphyrin			
$(o\text{-hexadecylamide})_4$*	81	1.7×10^{-4}	27.0
	108	4.5×10^{-4}	28.3
	136	2.2×10^{-3}	29.2
$(o\text{-pivalylamide})_4$*	108	2.5×10^{-5}	30.5
	138	5.6×10^{-4}	30.4

* reference 9.

The slower rates for the diamino versus diacetamido DPE are expected due to the increased size of the substituent which interacts with the ring methyls during isomerization. The value of 28 Kcal/mol of the diacetamido is comparable to those of acyl substituted tetra(o-aminophenyl) porphyrins.[9] Intuitively, the addition of flanking methyl groups should bring more hindrance than the β-pyrrole protons in preventing rotation. However, the absence of an increase in ΔH^{+} for the DPE system suggests that this is not true. This may be due to the more flexible nature of the diphenyl porphyrin. To minimize interaction between phenyl rings and beta-substituents during rotation, the ring skeleton must twist around the methine carbons. In the diphenyl system, since two phenyl rings are replaced by two protons at the meso positions, ring distortions may occur easier. Therefore the added steric constraints introduced by the beta-methyl groups may be compensated by the greater flexibility of diphenyl porphyrin.

^{1}H NMR of Free Base Porphyrins

The ^{1}H NMR spectra of all free base porphyrins, recorded on a 250 MHz instrument, have proven essential in the identification of mono- and di-substituted porphyrins used in construction of these unique heme models. As shown in Figure 1, the ring methyl groups flanking the phenyl rings in the DPE derivatives appear uniformly shifted ca. 1 ppm upfield versus etioporphyrin II due to the diamagnetic ring current of phenyl rings. The peripheral ethyl groups and methine protons are not affected by the phenyl rings but would be expected to

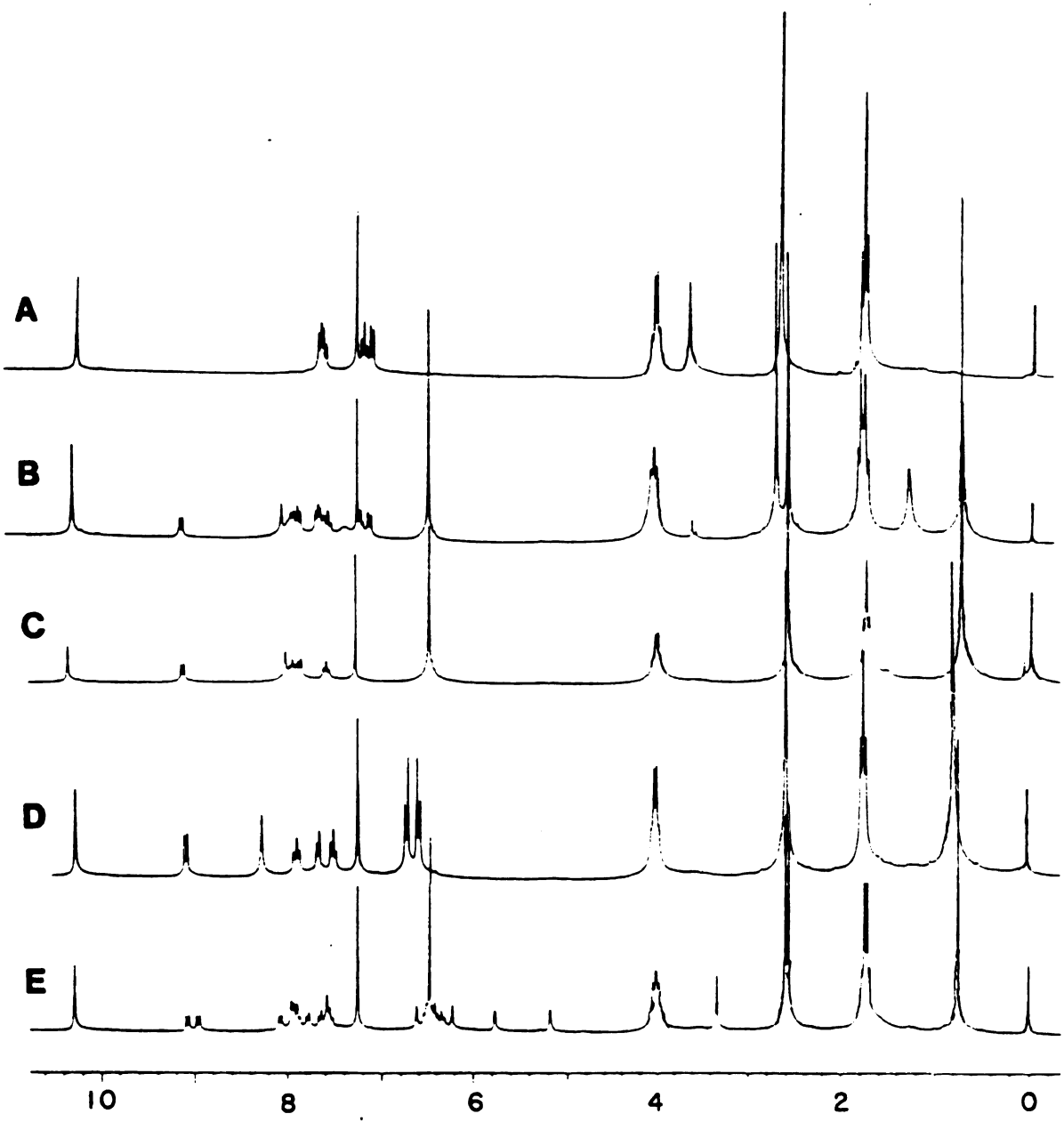

Figure 1. Comparative 250 MHz ^{1}H NMR spectra of derivatized diphenyl porphyrins: (A) (amino)$_2$DPE, trans (1); (B) (amino),(p-tBu-benzamide)DPE, trans (5); (C) (p-tBu-benzamide)$_2$DPE, trans (9); (D) (p-tBu-benzamide)$_2$DPE, cis (10); (E) (m-Im-CH_2-benzamide)$_2$DPE, trans (27).

reflect any reduction in porphyrin ring current if large distortions in the skeleton are present. Since no deviation was observed, we believe that the DPE derivatives are essentially as flat as other ordinary porphyrins. The planarity of the system, however, cannot be used to judge the flexibility of the macrocycle as the system would assume a planar configuration to maximize delocalization. The ring methyl groups served as a diagnostic tool in probing the symmetry of products. Figure 1A, C, D illustrate unsubstituted and symmetrically substituted systems, showing a singlet for the ring methyls. Figure 1B, E are typical of assymmetrical substitutions, hence a pair of singlets for the four methyl groups. The ethyl groups also reflect symmetry but the patterns are more complex. In the aromatic region, amide formation causes large downfield shifts of the protons ortho to the amine, due to deshielding by the carbonyl group. The NH proton of the amide appears at δ6.9ppm for the aliphatic acids and δ8ppm for benzoic acids, again due to the deshielding by the phenyl ring held above.

The aromatic protons of the bis-p-t-butylbenzamide DPE 9 and 10, Figure 1C, D appear as a singlet in the trans isomer but the expected AA'BB' pattern in the cis isomer. As DMSO-d_6 was added portion wise to a $CDCl_3$ solution of the cis isomer, Figure 2, the quartet collapsed into a singlet. The cis isomer is more congested than the trans isomer and aggregation or solvation serves to prevent free rotation and equilibration of the aromatic protons of the blocking group.

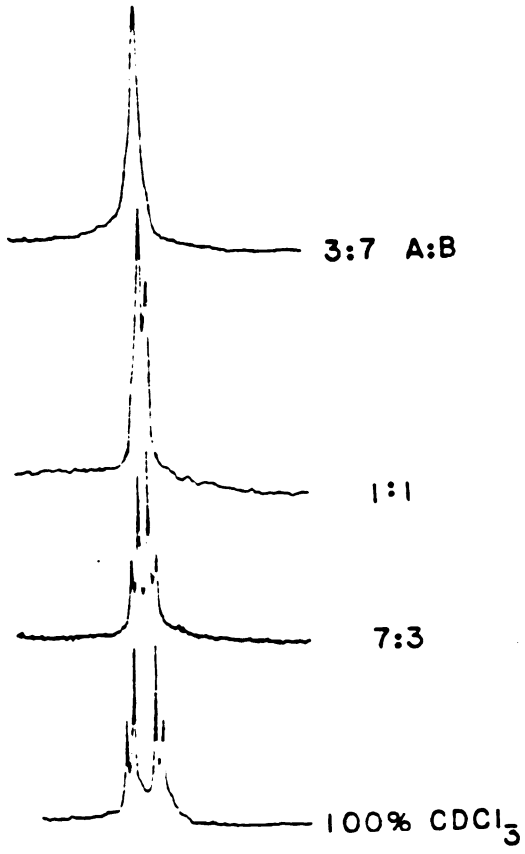

Figure 2. Effect of solvent on the resonances for the aromatic protons of the blocking group in (p-tBu-benzamide)$_2$DPE, cis (10). A = $CDCl_3$, B = DMSO-d_6.

Attachment of imidazoeyl ligands was easily determined by the appearance of the imidazole protons which usually appeared as three singlets, Figure 1E. The resonances were shifted upfield relative to the free ligand, due to coordination to the inner pyrrolic NH protons.

Electronic Spectra

Diphenyl porphyrins exhibit a phyllo-type spectra, bands IV > II> III> I, characteristic of mono and di-meso substituted porphyrins. The spectra of the free base porphyrins, Table 5, are nearly independent of substituent effect due to the insulating effect of the phenyl rings.

Large effects due to coordination are observed in the spectra of zinc and iron DPE, Table 6. Coordination of appended imidazole by zinc results in an overall red shift, c.a. 10 nm, in the electronic spectrum. Pronounced effects are also observed in the ferric hemes which can assume several spin states depending upon the coordination sphere. Systems containing one appended imidazole exhibited a ferric heme chloride spectra unique to those without coordinating ligands. The high local concentration of imidazole in appended systems favors the formation of the monoimidazole hemin chloride complex which would be impossible to observe in non-appended systems. The high local imidazole concentration was also evidenced in the spectra of bis appended systems, which at room temperature showed the bis coordinated species. Similar results could not be obtained with non-appended systems unless the temperature was reduced or a large excess of extraneous ligand was added, Fig. 3. The addition of acids to the appended systems generated spectra identical to the non-appended systems due to protonation of ligands and disruption of coordination.

NMR, Iron DPE

The 250 ^{1}H NMR of key paramagnetic iron diphenylporphyrins have

Table 5. Electronic Spectra Data of Selected Free Base Diphenyl Porphyrins.

	I	II	III	IV	Soret
(amino)$_2$ DPE, cis (2)					
2H	625(1.9)[a]	576(6.6)	541(5.6)	507(16.1)	409(186)
Zn		574(11.2)	539(18.0)	500(2.7)	412(350)
H^+	624(6.7)	574(12.2)	534(5.0)		420(220)
(p-tBu-benzamide)$_2$ DPE, trans (9)					
2H	625(3.8)	575(8.7)	542(6.9)	508(15.0)	409(180)
Zn		576(13.9)	540(19.4)	502(3.5)	413(347)
(p-tBu-benzamide)(m-ImCH$_2$ benzamide)DPE, trans (27)					
2H	625(3.0)	575(7.7)	542(7.7)	508(14.8)	410(182)
Zn		582(7.4)	552(20.1)		424(328)
H^+	624(8.3)	576(14.2)	535(3.5)		438(223)
(m-ImCH$_2$ benzamide)$_2$ DPE, trans (11)					
2H	628(2.7)	575(7.5)	542(7.1)	508(15.5)	410(187)
Zn		586(6.8)	552(20.6)	509(3.0)	425(358)
H^+	622(8.0)	575(13.5)	537(3.2)		439(210)
(NO$_2$)$_2$ DPE, cis and trans					
2H	629(2.8)	578(6.7)	545(6.1)	509(17.5)	408(175)
H^+	617(6.4)	572(13.7)	535(2.7)		429(290)
(OH)$_2$ DPE, trans (22)					
2H	625(2.9)	573(6.8)	541(6.9)	506(15.3)	405(190)

[a] Wavelength in nm; extinction coefficient X 10^{-4} in parentheses.

Table 6. Electronic Spectra Data of Selected Iron(III) Diphenyl Porphyrin Complexes.

(p-tBu-benzamide)$_2$ DPE, trans[a] (9)						
FeCl	646(4.4)	583(2.9)	539(6.9)	509(9.0)	413(62.8)	388(90.3)
FeOH		578(8.2)		475(13.4)	404(86.1)	362(43.8)
FeIm$_2$			534(9.1)		412(114)	
(p-tBu-benzamide)$_2$ DPE, cis[a] (10)						
FeCl	643(4.3)	586(2.6)	537(7.6)	511(9.6)	414(70.5)	388(100)
FeOH		585(8.0)		476(15.6)	405(107)	360(50.2)
Fe_2O		594(5.4)	565(10.7)	440(36.2)	397(84.9)	354(48.5)
(Im(CH$_2$)$_3$NHCONH)$_2$, trans[b] (17)						
FeIm$_2$			535(0.83)		408(1.0)	
(acetamide)$_2$DPE, trans[b] (13)						
FeCl	645(0.04)	586(0.03)	540(0.08)	510(0.10)	386(1.0)	
FeOH		575(0.97		473(0.16)	402(1.0)	362(0.56)
(m-ImCH$_2$ benzamide)$_2$ DPE[b] (11)						
FeIm$_2$		562(0.04)	527(0.07)		412(1.0)	
Fe(HCl)	643(0.04)	581(0.03)	541(0.07)	510(0.09)	439(0.36)	389(1.0)
(p-tBu-benzamide),(m-ImCH$_2$ benzamide)DPE[b] (27)						
FeCl	629(0.03)	574(0.04)		508(0.08)	408(1.0)	
FeIm$_2$			539(0.09)		407(1.0)	
FeOH		579(0.07)		493(0.11)	406(1.0)	

[a] Wavelength in nm; extinction coefficients X 10^{-4} in parentheses.

[b] Extinction coefficients relative to soret in parentheses.

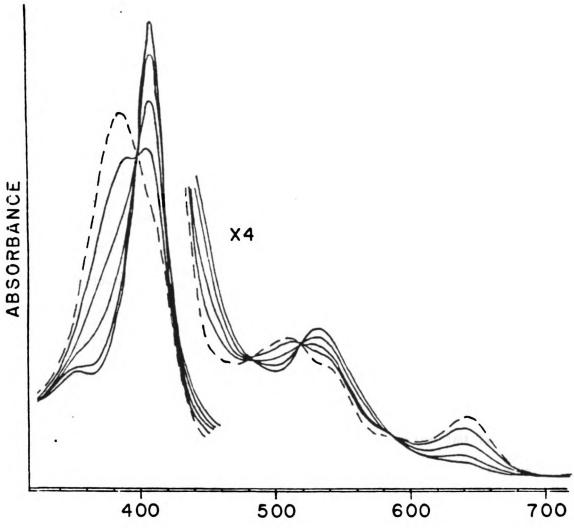

Figure 3. Electronic spectra of Fe(III)PCl complex of (p-tBu-benzamide)$_2$DPE, trans (9) (----); and the effect of adding excess imidazole (____).

been recorded, Table 7. The proton NMR of these complexes routinely span several hundred ppm due to large scale isotropic shifts resulting from contact and dipolar spin interactions. Spectral assignments are difficult due to the lack of observable spin-spin splittings, distortions of peak intensities due to the wide spectral widths required, as well as the complexity of the systems. Partial assignments were based on correlation with well characterized FeOEP and FeTPP systems [10, 11, 12] and variable temperature measurements which distinguish paramagnetically shifted signals, e.g., as the temperature is lowered upfield shifted peaks will shift further upfield and downfield shifted peaks will shift further downfield. The integrity of the iron compounds was verified by converting them to the low spin Fe(II)ImCO complexes. These diamagnetic systems appeared to be less symmetric than the parent free base porphyrins.

Analysis of ambient and variable temperature spectra proved invaluable in determining the effectiveness of blocking and ligating groups. The characteristic isotropic shifts and splitting patterns revealed the spin states (coordination sphere) and oxidation state of the central metal in these complex systems.

Sterically Protected Heme and Hemin Hydroxide

It is well known that in the presence of OH^-, ferric hemes dimerize in solution to yield the $Fe(III)_2O$ μ-oxo species[13], which makes the isolation of hemin hydroxide nearly impossible for most iron porphyrins. The μ-oxo dimer is also formed when ferrous hemes undergo autoxidation. This is the major drawback in the use of simple

Table 7. Observed NMR Shifts of Protons in Selected Iron(II)/(III) Diphenyl Porphyrin Complexes.

Iron Diphenyl Porphyrins

porphyrin	ring CH_3	CH_2	ArH, NH	CH_3	meso	tBu
(p-tBu-benzamide)$_2$DPE, trans (9)						
Fe(III)Cl	-54	-39, -37	-15 - -9	-6.5	65	1, 2
Fe(III)OH	-38	-31, -27	-13 - -5	-4.5	45	0.5, 0.8
Fe(III)Im$_2$	-15.5	-9 - -6		0.8		-2.6
Fe(II)ImCO	2.41, 2.42	3.8	9.1-6.3	1.6	10	0.7, 0.9
(p-tBu-benzamide)$_2$DPE, cis (10)						
Fe(III)Cl	-54	-39	-16 - -8	-6.6	65	1.5
Fe(III)$_2$O	-1.0	-4.2	-8 - 5	-0.7	-9	-0.5
(acetamide)$_2$DPE, trans (13)						CH_3CO
Fe(III)Cl	-54	-40, -37, -36	-16 - -8	-6.5	61	0.4, 2.1
Fe(III)Im$_2$	-16.4	-3.9	-9 - -5	0.6		
(acetamide)$_2$DPE, cis (14)						
Fe(III)Cl	-55	-39, -38	-16 - -8	-6.8	59	3.7
Fe(III)OH	-40	-32, -30	-13 - -7	-5.2		-0.8
(m-ImCH$_2$ benzamide)$_2$DPE, trans (11)						
Fe(III)Im$_2$	-26	-5.2	-9 - -5	-0.4		
Fe(II)Im$_2$	2.4	3.9	9 - 6.5	1.7	9.7	
Fe(II)ImCO	2.4, 2.3	3.8	9 - 6.2	1.7	9.8	
(Im(CH$_2$)$_3$NHCONH)$_2$DPE, trans (17)						
Fe(III)Im$_2$	-14.1	-12 - -3		0.3,0.4		
Fe(II)ImCO	2.39, 2.42	3.8	7.2 - 8.6	1.7	9.8	
(p-tBu-benzamide), (m-ImCH$_2$benzamide)DPE, trans (27)						tBu
Fe(III)Cl	-54	-43, -41, -39, -37	-14 - -6	-6.5	63	1, 2
Fe(III)Im$_2$	-15.3, -15.1	-14 - -5		0.8	65	-2.0
Fe(II)ImCO	2.3, 2.4	3.8	6.3 - 9.1	1.6	10.1	0.7
(p-tBu-benzamide), (Im(CH$_2$)$_3$NHCONH)DPE trans (31)						
Fe(III)Cl	-58.5, -59.0	-54, -53, -40, -38	-13 - -6	-6.5	60	1.5
Fe(II)ImCO	2.4	3.8	6.3 - 9.1	1.7	9.8	0.7
(p-tBu-benzamide), (Im(CH$_2$)$_2$CONH)DPE, trans (29)						
Fe(III)Cl	-58.0, -56.5	-43, -38	-9 - -6	-6.8	60	1.2
(p-tBu-benzoate)$_2$DPE, trans (24)						
Fe(III)Cl	-56.1, -55.6	-42, -37	-15 - -8	-6.8		0.19, 0.23
(m-ImCH$_2$ benzoate)$_2$DPE, trans (25)						
Fe(III)Im$_2$	-23.1	-6.4	-10 - -6	-0.23		

hemes as models for studying O_2 binding in the hemoglobin and myoglobin. In the protein, the heme prosthetic group is invariably immobilized within the polypeptide matrix, therefore, formation of hemin hydroxide (hematin) is commonplace. In fact, such hydroxide species may be crucial in the enzymatic functions of catalase, peroxidase, and cytochrome oxidase.

In order to prevent μ-oxo dimer formation in iron popphyrins, steric blockage must be incorporated to protect both faces of the heme group. A large number of encumbered heme models aiming at producing stable O_2 complexes have been synthesized, but these compounds are generally protected only on one face.[1,2,3] Only recently have studies been made on the preparation of doubly protected systems capable of forming stable hemin hydroxides.[14-18] A tetra(5-anthryl) porphinato ferric hydroxide was mentioned in a communication by Cense and LeQuan.[15] Balch and coworkers synthesized ferric hydroxides of tetra(2, 4, 6-trimethoxyphenyl)porphyrin and tetramesitylporphyrin via air oxidation of ferrous hemes or by the metathesis of hemin chlordie with aqueous sodium hydroxide.[14] Formation of hemin hydroxide was also observed with tetra (2, 4, 6-triphenylphenyl)porphyrin by Suslick.[17] Except for Balch's work, most of these compounds are difficult to prepare and have not been fully characterized. Our trans amino-DPE 1, if property derivatized should offer a simple alternative for the preparation of hemin hydroxides.

Both the cis- and trans- bis(p-t-buylbenzamide)-DPE, 9 and 10, were converted to the hemin chloride by standard procedures. Exchange

of the anion was carried out either by elution of the halide through basic alumina or washing a dichloromethane solution with aqueous NaOH. After completion of the exchange, as evidenced by changes in the visible spectra, Figure 4, the solutions were dried and evaporated to dryness. The cis isomer dimerized readily to the thermodynamically more stable μ-oxo dimer as shown by spectral changes, and can be easily crystallized from methanol-CH_2Cl_2. The trans hemin hydroxide did not dimerize upon isolation but crystallization in methanol often gave mixtures due to the formation of methoxide. Thus, a solid form of trans hemin hydroxide was simply obtained by lyophilization from benzene or precipitation from hexane.

Cyclic voltammograms of the cis and trans hemin chlorides, as expected, are identical. However, the isolated products following metathesis are unique. As shown in Figure 5, the voltammogram of the open-face cis isomer is indicative of a μ-oxo dimer exhibiting oxidation of both rings in a stepwise fashion. The voltammogram of the trans product indicates the $E_{1/2}$ for the Fe(III)/Fe(II) couple is about 500 mV more negative in the hydroxide than in the chloride. The greater difficulty in reduction can be accounted for by the higher electron density of the central metal, due to the electron donating ability of the hydroxide ligand.

Infrared spectroscopy provided unambiguous evidence of the presence of an OH group in the trans product, Figure 6. The hydroxide exhibits a sharp peak at 3615 cm^{-1}, which is absent in either the trans chloride or cis μ-oxo dimer. Previous investigators have used

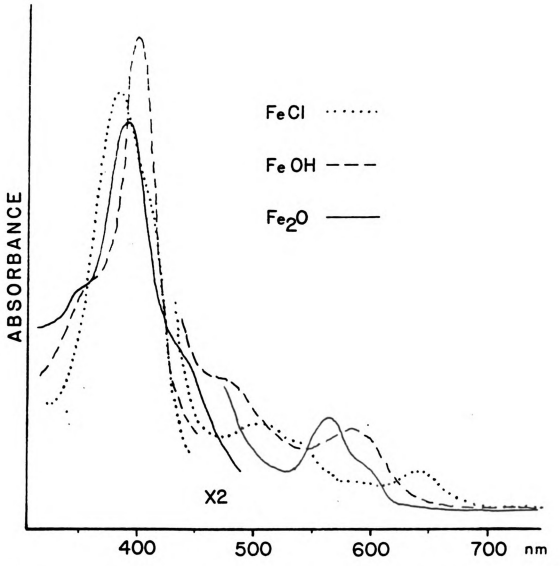

Figure 4. Electronic spectra of Fe(III) complexes of (p-tBu-benzamide)$_2$DPE, cis (10); Fe(III)PCl (····); Fe(III)POH (----); Fe(III)P_2O (——).

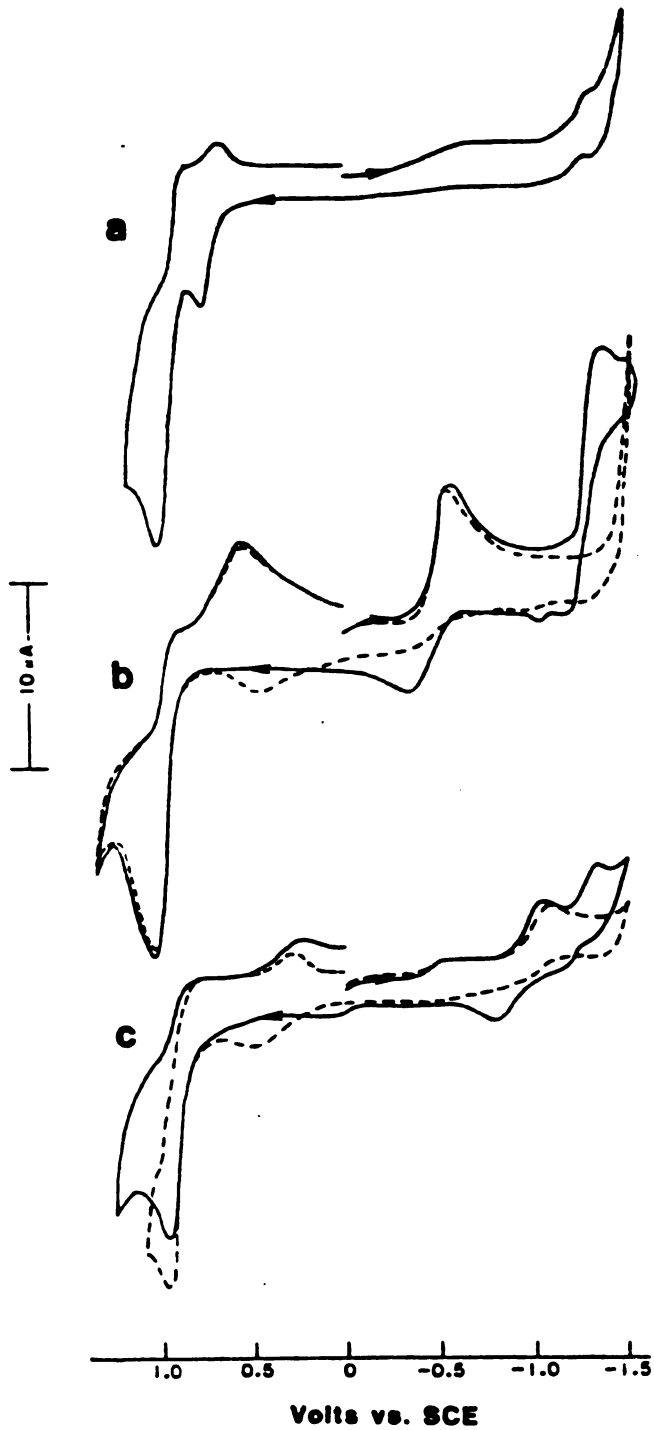

Figure 5. Cyclic voltammograms of Fe(III) complexes of (p-tBu-benzamide)$_2$DPE (a) cis, Fe(III)P$_2$O; (b) trans, Fe(III)$_2$PCl; (c) trans, Fe(III)POH in the presence of CO (····).

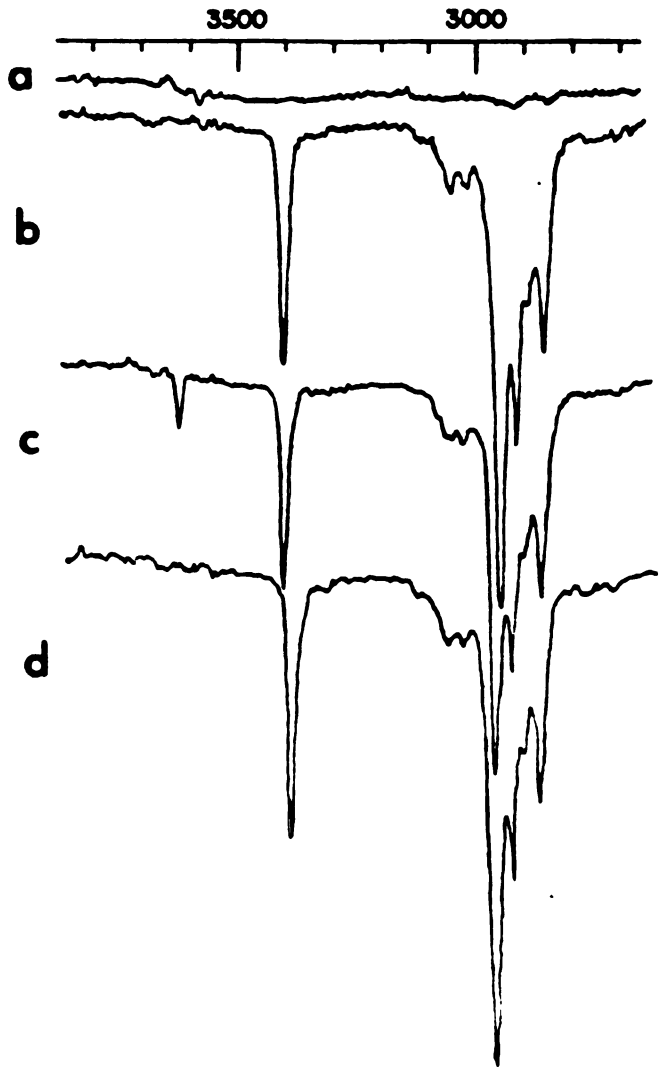

Figure 6. Infrared spectra of Fe(III) complexes of (p-tBu-benzamide)$_2$DPE in CCl_4, (a) solvent; (b) trans, Fe(III)$_2$PCl; (c) trans, Fe(III)POH; (d) cis, Fe(III)P_2O.

the presence of this peak for the formation of hemin hydroxides.[16, 18,19] Balch and co-workers, however, did not observe this peak in any of their systems, only a broad band centered at 3400 cm^{-1} which can be attributed to occluded water.[14]

The ^1H NMR of the cis μ-oxo dimer, Figure 7, is indicative of a strongly antiferromagnetically coupled species: there are no resonances beyond δ10 ppm. (For paramagnetic species, we conform to the convention that downfield shifts from TMS take the negative sign.) The trans hydroxide shows large isotropic shifts for the ring methyl groups and the CH_2 protons centered at δ-38 and -30 ppm, respectively. The features of this spectrum are similar to the high spin ferric hemin chloride: there are large isotropic shifts and splitting of CH_2 and t-butyl peaks. The isotropic shifts of the trans hydroxide also exhibit a near Curie behavior with linear dependence on reciprocal of temperature, Figure 8. The curvature of the Curie plot can be accounted for by the dipolar contribution[11,20] to the isotropic shift:

$$H/H_o = C_{con}/T + C_{dip}/T^2$$

where $C_{con} = A/h\ (35g/(12K/2))\ 12K/2$

$$C_{dip} = 28g^2B^2\ (3COS^2\theta-1)\ D/9k^2r^3$$

The calculated value of D is 10.0 cm^{-1}, very similar to that measured for the tetramesitylporphyrin Fe-OH.[14]

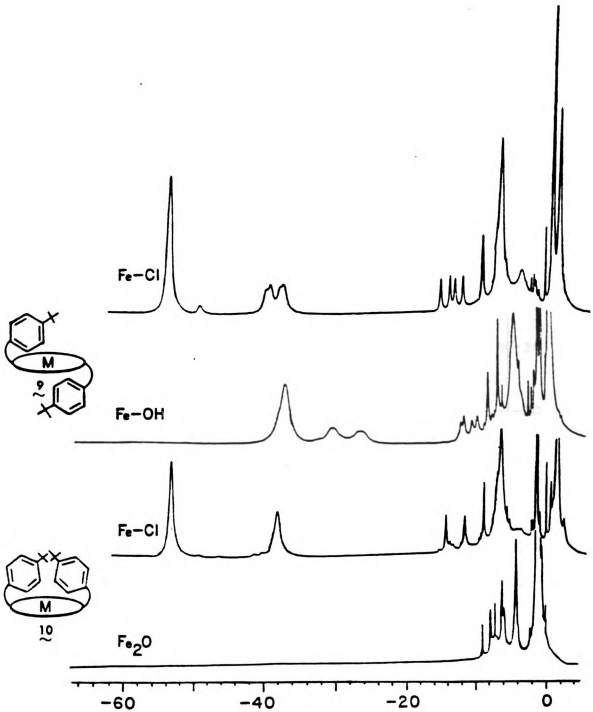

Figure 7. Comparative ^1H NMR spectra of paramagnetic Fe(III) complexes of DPE $\underset{\sim}{9}$ & $\underset{\sim}{10}$.

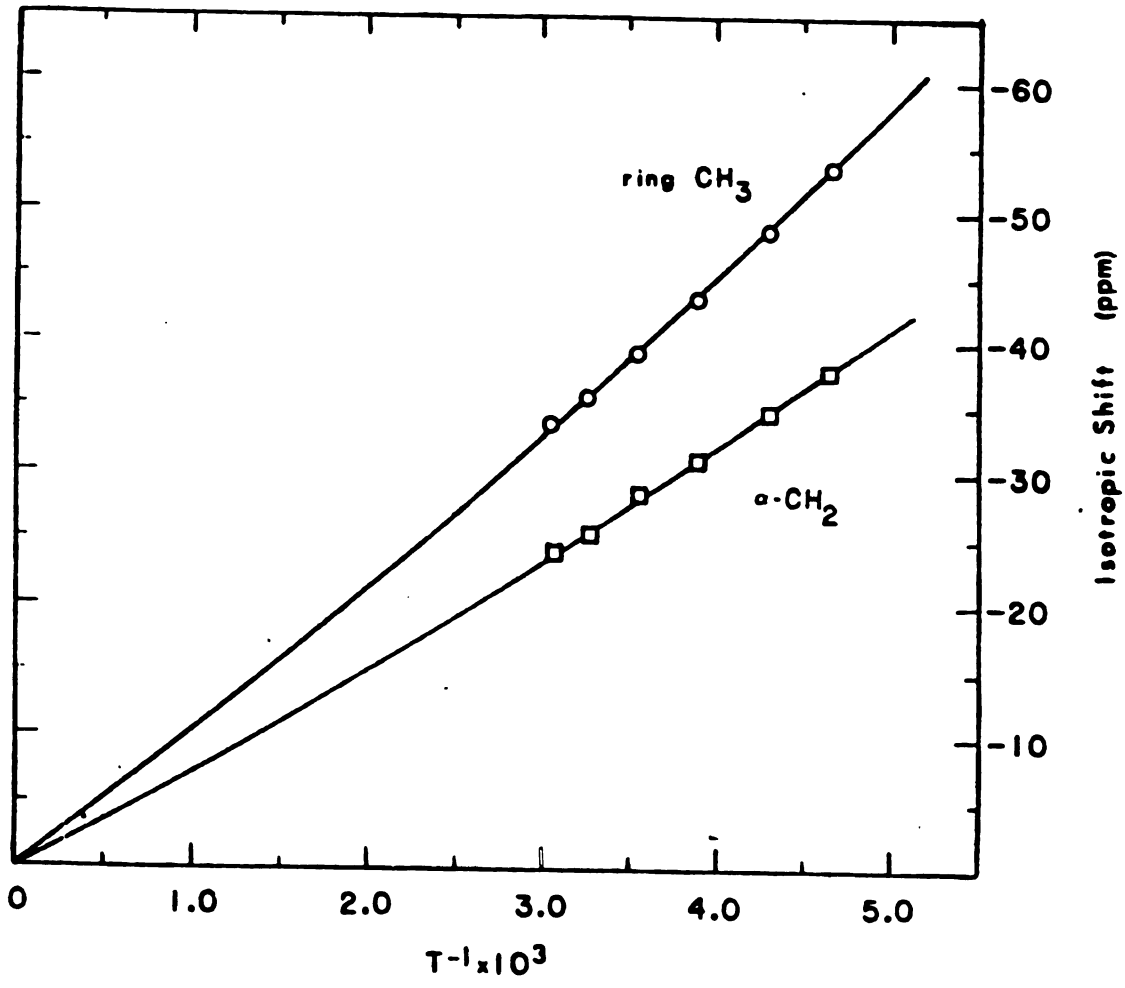

Figure 8. Curie plot for the Fe(III)POH complex of diphenyl porphyrin 9.

The observed change in the isotropic shifts between hemin chloride and hydroxide for our trans bis(p-t-butylbenzamide)DPE 9 is 15 ppm, which is quite large in comparison with the ca. 1 ppm difference observed for the tetramesitylporphyrin system.[14] In principle, the isotropic shifts are extremely sensitive to spin density variations caused by ligand or conformational changes. Large changes in isotropic shifts have been observed in ferric hydroxides of flexible porphodimethenes.[21] The sensitivity of the shifts of α-methylenes units in 5,15-dimethyl octaethylporphodimethene were attributed to the folding of the ring skeleton, resulting in reduced transfer of spin density from the metal to the ring. The flexibility of the diphenylporphyrin system has already been alluded by the ease of atropisomerization. It is possible that the large changes in isotropic shift may be related to the intrinsic flexibility of the DPE ring.

Gunter and Mander[6] have observed a solvent dependent equilibrium between hemin chloride and hydroxide in octamethyl diphenylporphyrins. We have observed a similar equilibrium with unhindered DPE, e.g., cis-bis(acetamide)-DPE 14, however, no equilibrium was observed for the doubly protected DPE systems. Further evidence for this equilibrium was observed in bis-imidazole formation. Cense and Le Quan and Felton used ligand exchange reactions as evidence for hydroxide formation.[15,18] The ferric hydroxide should undergo metathesis while the strongly coupled μ-oxo dimers should be resistant. Both the μ-oxo dimers and ferric hydroxides of DPE undergo

reactions with extraneous imidazole, Figure 9, but at different rates. The slower exchange rate observed for the μ-oxo dimer indicates conversion to the hydroxide may precede ligand exchange, Equation 3.

$$Fe(III)P_2O + H_2O \rightleftharpoons 2\ Fe(III)POH \overset{Im}{\rightleftharpoons} 2\ Fe(III)PIm_2 \quad (3)$$

Hemes Appended with Imidazole Ligands

The presence and importance of the proximal histidyl imidazole in hemoglobin and myoglobin oxygen binding has been well established by studies on the natural systems as well as models. The histidyl ligand is also present in other heme proteins such as cytochromes c, b_5, cytochrome oxidase, and peroxidases. Therefore, it is not surprising that imidazole-iron porphyrin have been and continue to be a crucial model in biomimetic studies of heme-containing systems. However, the use of free imidazoles and simple hemes to generate 5-coordinate complexes is not possible due to the competing reaction to form 6-coordinate hemochromes. In compounds that are sterically protected on one face of the porphyrin ring, i.e., capped, crowned hemes[21,22] and cofacial diporphyrins, a bulky imidazole can be used effectively to prevent bis-coordination. In other less shielded systems, including our trans-(p-t-butylbenzamide) DPE derivatives, this approach is unsatisfactory. An alternative to generating 5-coordinate heme without the use of external ligand is to covalently attach an imidazole to the heme group. This tactic originally reported by Warme and Hager[23] and later successfully employed by Chang and

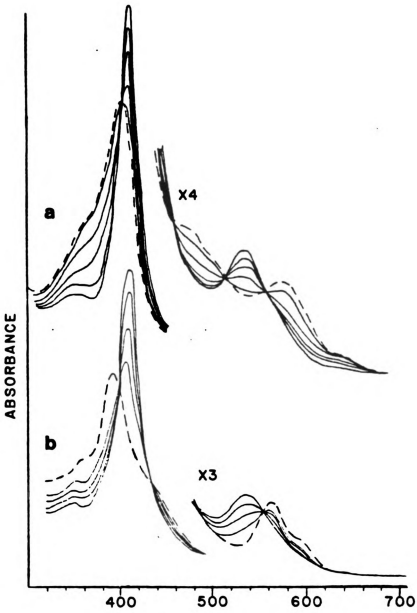

Figure 9. Electronic spectra of Fe(III) complexes of (p-tBu-benzamide)DPE, (a) trans, Fe(III)POH (----); and the effect of adding excess imidazole (——), (b) cis, Fe(III)P$_2$O(----); and the effect of adding excess N-Me imidazole (——).

Traylor[4] to allow equilibrium and kinetic studies of O_2 binding to a variety of myoglobin models.[7,24,25] The main advantage of strapped bases is the generation of a high local concentration of ligand near the metal center. In addition, perturbations affecting the imidazole coordination can be easily introduced by modifying the sidechain or spacer group connecting the base and the ring. This arrangement also more closely resembles the natural system where the interaction between heme iron and histidine is subject to protein conformational controls. Indeed, studies by Traylor and coworkers have shown that strain introduced by chain length or substitution has a dramatic effect on the electronic, spectroscopic, and chemical properties of heme models.[24]

Alkyl chain-linked imidazole can be easily added to the DPE system using two routes, Scheme 2. The trans mono-t-butylbenzamido-mono-amino-DPE $\underset{\sim}{5}$ was coupled with N-imidazolyl alkanoic acid chlorides of varying length. Alternatively, porphyrin $\underset{\sim}{5}$ was reacted with phosgene to generate the carbamoyl chloride which when combined with amino appendages produced the urea linked system in excellent yields. The structure of these imidazole-appended DPE's were characterized by NMR, IR, and elemental analysis. ^1H NMR spectra of the diamagnetic zinc complexes of these compounds provided additional support for the purported structure. Zinc porphyrins prepared by heating the porphyrin with a saturated methanolic solution of zinc acetate in methylene chloride, bind imidazole strongly. Thus, coordination of the intramolecularly linked base resulted in the upfield shift of

imidazole protons and protons of the alkyl strap which are held rigidly over the ring. Conversely, the addition of trifluoroacetic acid resulted in protonation of imidazole and disruption of coordination, thereby, causing downfield shift for the methylene protons as the side chain moved away from the porphyrin.

Our previous experience as well as the experiments described below suggest that an alkyl chain strapped imidazole is still able to form both inter- and intra-molecular complexes. In an effort to construct a more restricted system, porphyrin 27 (also 7 and 32-44) was designed (Scheme 2, 3). The m-benzyl linkage is less floppy and has fewer degrees of freedom of rotation than alkyl straps[7]. Synthetically, the imidazole m-toluic acid chloride was difficult to obtain because of the insolubility of the acid. A two-step method was therefore devised as described in the Synthesis section. The advantage of the benzyl linked imidazole is illustrated by the following ^1H NMR experiments using ferric hemes.

At room temperature, mixing a 2:1 stoichiometric ratio of 1-methylimidazole and the trans-diacetamido-DPE Fe(III)Cl gave a spectrum, Figure 10, typical of high-spin (s=5/2, d^5)species, which shows that 2 equivalents of external base are not sufficient to form appreciable amounts of 6-coordinate hemichrome. The equlibrium, of course, can be shifted to the bis-imidazole complex (s=1/2) by addition of excess base or lowering the temperature. As temperature was reduced, the spin equilibrium became obvious. Complete conversion to the 6-coordinate low spin complex was prevented by solubility

Figure 10. Temperature dependent ^{1}H NMR spectra of Fe(III)PCl complex of (acetamide)$_2$DPE, trans (13) containing 2 equivalents 1-methyl imidazole in $CDCl_3$.

limitations. The higher local concentration of imidazole in strapped imidazoles is seen in the spectrum of the bis urea linked imidazole heme, Figure 11. At room temperature, only the low-spin species was observed. However, the appearance of ring methyl groups as broad bands as well as the splitting of the alpha CH_2 protons when temperature was lowered suggests that mixtures of inter- and intro-molecularly bounds species exist in solution, Equation 4.

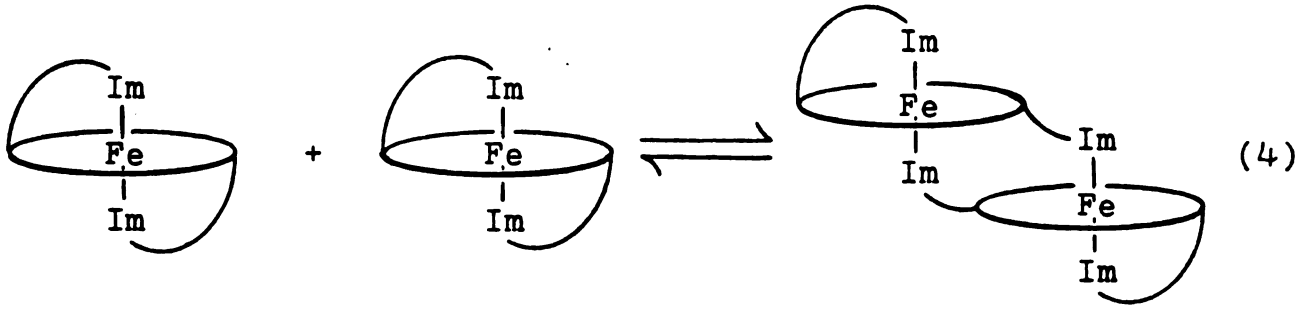

(4)

The bis-benzylimidazole heme exhibited a different type of behavior, Figure 12. A relatively sharp resonance at δ-26 ppm corresponding to the ring methyl protons was observed. Also as the temperature was reduced, the ring methyl and alpha CH_2 resonances remained as sharp singlets, reflecting a high degree of symmetry in the bis-imidazole complex. There was no indication of exchange.

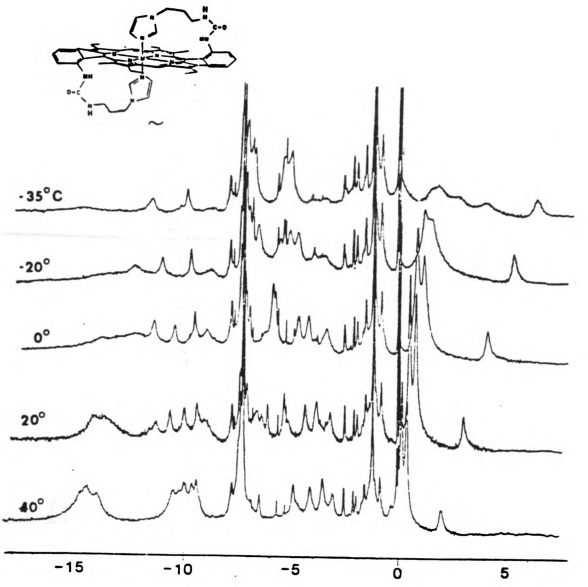

Figure 11. Temperature dependent ^1H NMR spectra of the Fe(III)PIm$_2$Cl complex of $(Im(CH_2)_3NCOHNH)_2$ DPE, trans-(17) in $CDCl_3$.

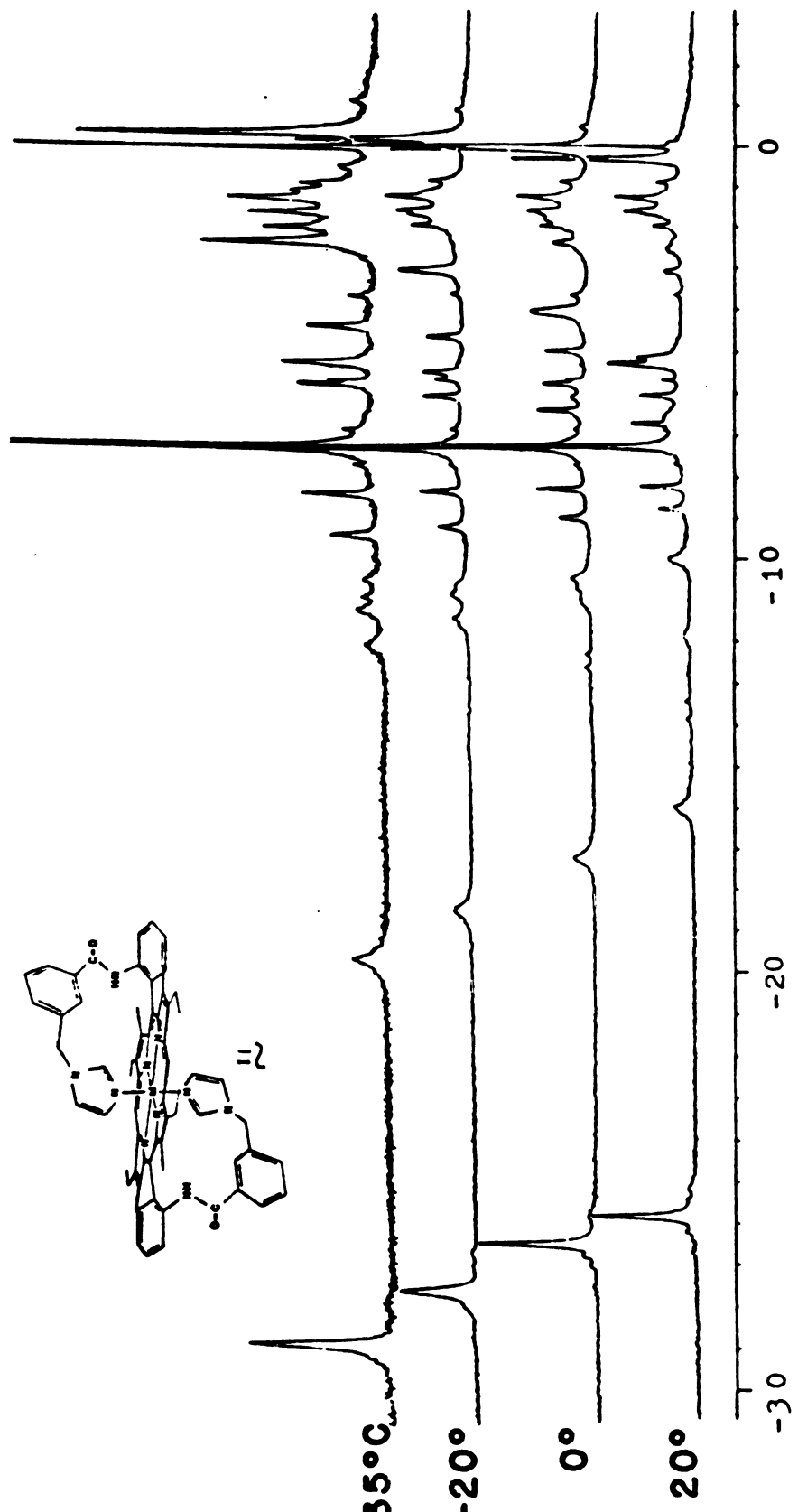

Figure 12. Temperature dependent ^1H NMR spectra of the Fe(III)PIm$_2$Cl complex of (m-ImCH$_2$benzamide)$_2$DPE, trans (11) in $CDCl_3$.

The large downfield shift of the ring methyl groups, observed at δ -26 ppm in the bis-benzylimidazole system is noteworthy. The ring methyl resonances of bis-imidazole complexes of model hemes, e.g., etioheme, occur around δ-16 ppm. As well, extrapolation of the shifts for non-covalently linked N-methylimidazole diphenyl heme system gives a signal around δ-17 ppm at room temperature; and for free N-benzylimidazole plus diacetamido-DPE hemin chloride, the peak is estimated at -16 ppm.

To determine the influence of the appended benzylimidazole , a mixed species consisting of trans-(p-t-butylbenzamido), (imidazolyl-toluamido)-DPE Fe(III)Cl, 27, and imidazole was prepared. The presence of the appended benzylimidazole to create a high local concentration facilitated coordination of the second (free) imidazole to form a bis adduct with only a small excess of ligand. The ring methyl protons appeared as a pair of singlets in this system indicating assymmetric coordination, Figure 13. Interestingly the shift was normal; δ-15.1 ppm and -15.3 ppm at room temperature. The ester analogue of the bis benzylimidazole appended system shows the ring methyl protons at δ-23 ppm.

These results concur with previous observations[24,26-28] that the spin density distribution at the peripheral substituents of ferric hemes are very sensitive to axial ligand orientation or ring distortion. The covalently bound bis-benzylimidazole either introduced distortion to the ring or more likely, assumed a coordination geometry at variance with the free ligand. In the mixed complex, the shift is

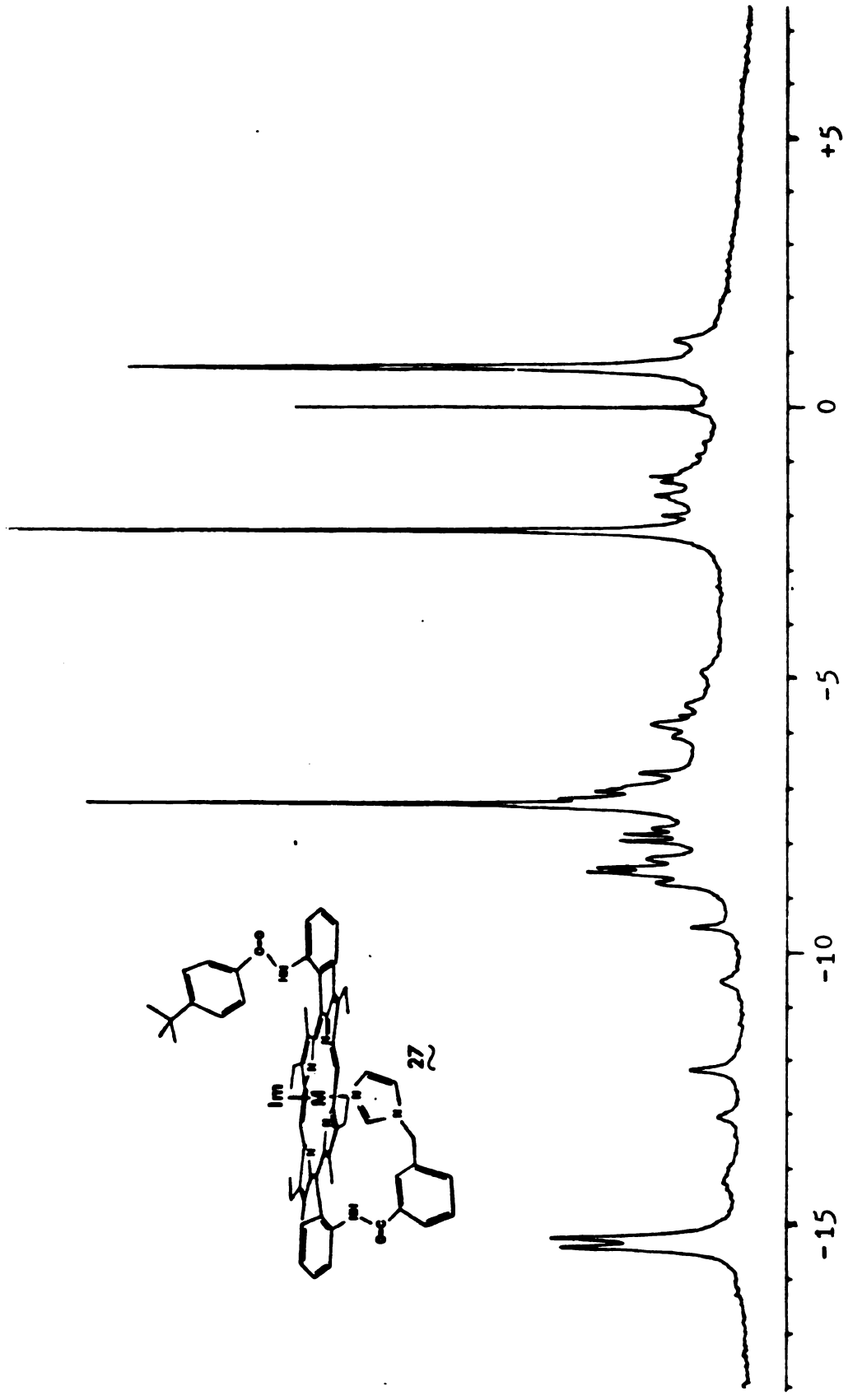

Figure 13. ^1H NMR spectrum of the Fe(III)PIm$_2$Cl complex of (p-tBu-benzamide), (m-ImCH$_2$benzamide)DPE, trans in $CDCl_3$ with 1.2 equivalents imidazole.

normal because whatever distortion brought about by the internal ligand is compensated for by the external ligand. In the ester analogue of the bis-benzylimidazole appended systems, the shifts are closer to the free systems because of the greater flexibility of the ester linkage, allowing a more favorable geometry or less distortion.

β-Ketoamide Appendages

In our effort to construct orientation specific groups appended to the hemes, we also explored the use of β-ketoamide groups as linkage units. β-Carbonyl groups may form hydrogen bonds to the amides, thereby, directing the attached functional groups over the porphyrin ring. The malonyl amide porphyrins (45-47) were synthesized by first treating the mono-imidazolyl toluamide DPE 7 with an excess of malonyl dichloride, followed by the appropriate amine.

The ability of the β-ketoamide linkage in directing groups over the porphyrin core was indicated by ^{1}H NMR spectra. The malonyl derivatives displayed an upfield shift for the terminal N-alkyl groups. For example, the t-butyl protons appear as a singlet at 1.3 ppm in t-butylacetamide, but at 0.6 ppm in the malonyl porphyrin.

Kinetic studies of CO binding to the malonamide hemes were performed to detect distal steric effects brought about by these more "peptide-like" blocking groups. However, little differences were found in the CO association rate as the amide varied from primary, secondary, to tertiary.[29] It has been shown previously that the CO association rates are sensitive to the steric crowdedness at the heme iron.[3,22,30] The lack of change in this rate would reflect on the

fact that the N-alkyl substituents need not be coplanar with the amide carbonyl and that they can assume conformations which have a minimum interaction with the incoming ligand. It thus may be difficult to control or predict the distal steric effect of malonamide appendages.

Phenolic and Ester linked Diphenyl Porphyrins

The ease in synthesis and versatility of the amino DPE led to the study of analogous systems. Phenolic and ester linked porphyrins, although less directed than the corresponding anilides, would serve as excellent models in studying orientational effects and distal polarity on CO and O_2 binding.

Initial attempts to generate these species with o-methoxybenzaldehyde led to excellent yields of the slightly soluble porphyrinogen and porphyrin. The low solubility of the products helps to drive the porphyrinogen formation to completion. Unfortunately, attempts to deprotect the phenols failed due to the low solubility of the methoxy porphyrins.

Salicylaldehyde was also found to react rapidly and the parent phenolic porphyrins were much more soluble. The reaction was carried out at 0°C to increase selectivity and zinc acetate was introduced to promote a template effect. The yields of the porphyrin isolated after oxidation were routinely > 40%. The high polarity of the cis atropisomer 21 versus the trans form 22 allowed an easy separation on silica gel. The individual isomers reacted under the same conditions as the analogous anilides to yield sterically encumbered and imidazole appended systems, 24 and 25.

Summary and Further Studies

The improved synthesis and utilization of hybrid diphenyl porphyrins was demonstrated. The increased rigidity due to ring alkyl groups allowed the construction of blocked and chelated iron porphyrins of fixed geometry. The effectiveness of the p-t-butyl-benzamide blocking group was demonstrated by the formation and characterization of ferric hydroxides. Chelated systems, incorporating a variety of appendages, provided a high local concentration of imidazole favoring formation of 5-coordinate intermediates useful for the heme-ligand binding studies.

Kinetic studies on systems having minor changes in the blocking group revealed the importance of local and distal polarity on oxygen association and dissociation rates. The importance of H-bonding in the stabilization of the heme-oxygen complex and steric factors in CO binding were also implied. [8a,8b]

Further studies would involve the clarification of polarity effects by utilizing blocking groups which cannot hinder coordination of ligands. The phenolic porphyrins can also be used in studying distal polarity effects and the possible role of the amide NH in stabilization of complexes. Reduced porphyrin derivatives can also be constructed by saturation of peripheral double bonds using standard techniques, e.g., diimide reduction yields the cis and trans diamino chlorins, 48. These systems can be derivatized in the same fashion as the porphyrins to reveal the influence of ring saturation. The presence of octa-alkyl substituents may also allow oxidation to the

versatile geminal ketones,[58] although steric congestion may be prohibitive.

Experimental

^1H NMR spectra were recorded on a Bruker WM-250 MHz instrument. Absorption spectra were measured using a Cary 219 spectrophotometer. IR spectra was obtained in KBr wafers on a Perkin Elmer 237B spectrometer. Elemental analysis were performed by Spang; C, H, N, analyses were within $\pm$0.42%. Methylene chloride was distilled from CaH_2 and THF was distilled from $LiAlH_4$ before use.

Thermal Atropisomerization

To ortho-xylene (50 ml) heated to constant temperatures in an oil bath was added the cis DPE (20 mg) in methylene chloride (5 ml). Aliquots were analyzed at intervals by TLC (silica gel, methylene chloride/hexane). The separated isomers were placed in a cuvette, diluted to a constant volume with 10% MeOH/CH_2Cl_2 and relative absorbance determined at 403 nm. The rates of isomerization were determined by least squares plots.

^1H NMR

Free base and iron porphyrin were measured in $CDCl_3$ (ca. 0.01 M) at 20°C. Fe(III)P(Im)$_2$ was prepared by addition of two equivalents of imidazole in $CDCl_3$. Fe(II)P(Im)CO was prepared by mixing a $CDCl_3$ solution of the iron porphyrin with aqueous sodium dithionite under CO atmosphere.

Fe Insertion

Porphyrin (20 mg) was dissolved in 1:1 THF:benzene (20 mL),

containing collidine (2 drops) and $FeBr_2$ (40 mg). The solution was heated under argon for ca. 30 min and the solvent was removed in vacuo. The residue was redissolved in CH_2Cl_2, extracted with 10% HCl, washed with water and eluted on alumina column. To obtain the ferric chloride form, the solution was washed with saturated NaCl in 0.1N HCl. The hydroxide was obtained by washing a CH_2Cl_2 solution with 10% NaOH. Alternatively the hemin chloride was eluted through a basic column of alumina until the absorption spectra indicated complete ligand exchange.

4,4'-Diethyl-3,3'-dimethyl-2,2'-dipyrrylmethane

5,5'-Bis(ethoxycarbonyl)-4,4'-Diethyl-3,3'-dimethyl-2,2'-dipyrryl methane (12) gm, 0.4 ml, which was obtained easily from ethyl 4-ethyl-3,5-dimethyl-pyrrole-2-carboxylate, was dissolved in hot ethanol (95%, 400 ml). To this solution after it was heated to a gentle reflux with stirring, a solution of NaOH (50 gm/100 ml water) was added carefully through the condenser. Refluxing was continued for 2 h, after which the condenser was removed and the volume was reduced to 1/3. The mixture was diluted with water (100 ml) and then brought to vigorous refluxing for 6 h without interruption. At the end of this period, a layer of brown oil was separated. The mixture was allowed to cool to room temperature, the solidified material was filtered off, washed with water until neutral, and dried (quantitative yield). The freshly prepared decarboxylated dipyrrylmethane has a light tan color and a characteristic chared bone smell; it slowly darkens in the air but can be stored indefinitely in a refrigerator.

^{1}H NMR ($CDCl_3$) δ1.12(t, 6H, Me), 2.03(s, 6H, Me), 2.47(q,4H, CH_2), 3.79(s, 2H, CH_2), 6.35(m, 2H, H), 7.26(br s, 2H, NH). m.p. 49-50°C. Mass Spectrum (70 eV), 230 (m+), calc. 230.

5,15-Bis(o-nitrophenyl)-2,8,12,18-tetraethyl-3,7,13,17-tetramethylporphyrin

4,4'-Diethyl-3,3'-dimethyl-2,2'-dipyrrylmethane (6 g, 26.1 mmol) and o-nitrobenzaldehyde (3.9 g, 26.1 mmol) was dissolved in methanol (300 ml). After the solution was deaerated by bubbling with argon for 10 min, p-toluene-sulfonic acid (1.4 g, 7.4 mmol) was added. The mixture was stirred for 15 min, then allowed to stand in the dark at room temperature. The crude yellow porphyrinogen began precipitating within 1 h. After 6 h at room temperature, the solution was cooled and kept at 4°C overnight. The solid was collected and washed with cold methanol.

The crude porphyrinogen 3 (2.5 g) was dissolved in tetrahydrofuran (200 ml) and treated with a solution of o-chloranil (2.5 g) in THF (20 ml). The solution was stirred at room temperature for 30 min. The porphyrin which precipitated out during this period was too finely divided to be filtered. Thus, the solvent was evaporated and the protonated residue was redissolved in methylene chloride. A solution of methanol-triethylamine (4:1) was added to reprecipitate the porphyrin. The product was collected by filtration and wash washed with cold methanol and THF (yield: 2.2g); ^{1}H NMR ($CDCl_3$-TFA) δ-1.84(br s, 4H, NH), 1.37(t, 12H, Me), 2.29(s, 12H, Me), 3.74(q, 8H, CH_2), 8.13(m, 4H, ArH), 8.48(m, 4H, ArH), 1.22(s, 2H, meso); UV-VIS

(dichloromethane) max (ϵmM) 629 nm (2.5), 578 (6.3), 545 (5.8), 509 (15.0), 408 (150).

Porphyrinogen, ^{1}H NMR ($CDCl_3$) δ1.15(m, 12H, Me), 2.27(s, 12H, Me), 2.41(q, 8H, CH_2), 4.21(s, 4H, meso CH_2), 4.71(br s, 4H, NH), 8.73(br s, 8H Ar).

5,15-Di(o-aminophenyl)-2,8,12,18-tetraethyl-3,7,13,17-tetramethylporphyrins (1), (2)

To a solution of the nitrophenylporphyrin 4 (4 g, 5.5 mnol) dissolved in 12 N HCl (180 ml) was added stannous chloride dihydrate (9.4 g, 41.3 mmol). The mixture was stirred at room temperature for 16 h. The solution was diluted with water (100 ml), neutralized with aqueous ammonia (75 ml) and extracted with methylene chloride (3 x 100 ml). The combined organic layers were washed with water, dried, and evaporated to dryness. The crude porphyrin was redissolved in a minimum amount of CH_2Cl_2, acidified with trifluoroacetic acid (1 ml) and irradiated under a sun lamp for 2 h to recover any over-reduced porphyrin. At the end of this treatment, the solution was diluted with CH_2Cl_2, washed with water and saturated $NaHCO_3$, and then evaporated to dryness. The crude product was purified on a silica column (6 x 30 cm) using 2% methanol- CH_2Cl_2. The trans isomer was eluted first, followed sluggishly by the cis isomer. Yields from a 2 g crude mixture: trans, 0.74 g (37%) and cis, 1.1 g (55%).

Cis-isomer (2) m.p. > 380°C; ^{1}H NMR ($CDCl_3$) δ-2.43(br s, 2H, pyrrole NH), 1.79(t, 12H, Et), 2.70(s, 12H, Me), 3.63 (s, 4H, NH_2), 4.04(q, 8H, Et), 7.1(d, 2H, Ar), 7.19(t, 2H, Ar), 7.60(t, 2H, Ar), 7.67(d, 2H, Ar), 10.25(s, 2H, meso).

Tr

NH

8H

1(

Tr

pc

ml

py

wi

se

Na

pu

m.

12H

2H

Tra

13,

chl

3 h

diss

solu

ml)

Trans-isomer (1) m.p. > 380°C; ^{1}H NMR ($CDCl_3$) δ-2.44(s, 2H, pyyrole NH), 1.79(t, 12H, Et), 2.70(s, 12H, Me), 3.67 (s, 4H, NH_2), 4.05(q, 8H, Et), 7.10(d, 2H Ar), 7.17(t, 2H, Ar), 7.57-7.65(m, 4H, Ar), 1023(s, 2H, meso).

Trans 5,15-di(o-acetamido)-2,8,12,18-tetraethyl-3,7,13,17-tetramethyl porphyrin (13)

Excess acetyl chloride (1 ml, 11 mmol) was added to a CH_2Cl_2 (100 ml) solution of trans diamino DPE (100 mg, 0.15 mmol), followed by pyridine (1 ml, 12 mmol). The mixture was stirred for 0.5 h, diluted with water and stirred for 1 h further. The organic layer was separated and washed successively with; 10% HCl, H_2O, sat. aqueous $NaHCO_3$, and then dried and evaporated to dryness. The product was purified on silica gel to yield the acetylated product, (105 mg, 95%); m.p. 365°C; ^{1}H NMR ($CDCl_3$) δ-2.42(s, 2H, NH), 1.30(s, 6H, Me), 1.77(t, 12H, Me), 2.54(s, 12H, Me), 4.05(q, 8H, CH_2), 6.92(s, 2H, NH), 7.51(t, 2H Ar), 7.83(m, 4H, Ar), 8.80(d, 2H, Ar), 1030(s, 2H, meso).

Trans-5,15-bis(o-(p-t-butylbenzamido)phenyl)-2,8,12,18-tetraethyl-3,7, 13,17-tetramethylporphyrin (9)

A mixture of p-t-butylbenzoic acid (2 g, 11.2 mmol) and thionyl chloride (2 ml) in chloroform (20 ml) was refluxed under nitrogen for 3 h. The solution was evaporated to dryness to yield a yellow oil.

A portion of the crude acid chloride (89 mg, 0.45 mmol) was dissolved in methylene chloride (10 ml) and added dropwise to a solution of bis-amino porphyrin 1 (300 mg, 0.45 mmol) in CH_2Cl_2 (100 ml) containing triethylamine (1 ml, 7.17 mmol). After completion of

the addition, the mixture was refluxed for 2 h under nitrogen before poured into water (100 ml). The organic layer was separated, washed successively 5% HCl (150 ml), with saturated $NaHCO_3$ solution (150 ml), and H_2O (150 ml). After drying over sodium sulfate, the mixture was evaporated to dryness and separated on a series of preparative silica gel TLC plates (Analtech 1500 micron) using CH_2Cl_2, and acidic alumina columns.

The first band, containing trans-bis(o-(p-t-butylbenzamido)phenyl) porphyrin 9 was collected and crystallized from CH_2Cl_2-MeOH to yield purple crystals (80 mg, 18%); IR: CO: 1670 cm^{-1}; ^1H NMR ($CDCl_3$) δ -2.33(br s, 2H, pyrrole NH), 0.73(s, 18H, t-butyl), 1.75(t, 12H, Et), 2.60 (s, 12H, CH_3), 4.05(q, 12H, Et), 6.42(s, 8H, Ar), 7.55(t, 2H, Ar), 7.82-7.96(m, 4H, Ar), 7.99(s, 2H, NH), 9.10(d, 2H, Ar), 11.32(s, 2H, meso); Anal. Calcd. for $C_{66}H_{72}N_4O_2$ C 80.78, H 7.40, N 8.75; Found C 80.63, H 7.31, N 8.42.

The second band, which is the major one, corresponds to trans-5-(o-aminophenyl)-15-(o-(p-t-butylbenzamido)phenyl) porphyrin 5, was also crystallized from CH_2Cl_2-MeOH (186 mg, 50%); ^1H NMR ($CDCl_3$) δ -2.40(br s, 2H, pyrrole NH), 0.70 (s, 9H, t-butyl), 1.72(t, 6H, Et), 1.76(t, 6H, Et), 2.57 (s, 6H, CH_3), 2.70(s, 6H, CH_3), 3.68(s, 2H, NH_2), 4.05(m, 8H, Et), 6.47(s, 4H, Ar), 7.10(d, 1H, Ar), 7.17(t, 2H, Ar), 7.5-7.95(m, 6H, Ar), 8.05(s, 1H, NH), 9.10(d, 2H, Ar), 10.26(s, 2H, meso); Anal. Calcd. for $C_{55}H_{60}N_6O$ C 80.45, H 7.36, N 10.24; Found C 80.22, H 7.27, N 10.16.

The third band was the recovered starting material,

t

T

t

p

wa

wh

ac

at

et

ch

an

ch

cl

CH_2

yel

aci

N_2

an

adde

prog

comp

sepa

ml),

trans-5,15-bis(o-aminophenyl) porphyrin 1, (92 mg, 31%).

Trans-5-(o-(p-t-butylbenzamido)phenyl)-15-(o-(m-N-imidazolyl)-tyoluamido)phenyl)-2,8,12,18-tetraethyl-3,7,13,17-tetramethyl-porphyrin (27)

m-Toluic acid (10 g, 73.5 mmol) dissolved in nitrobenzene (60 ml) was heated to 125°C. The solution was illuminated with a sun lamp while bromine (11.74 g, 73.5 mmol) was added dropwise. After the addition was complete, (ca. 2 h) the solution was stirred 6 h further at 125°C. The solution was then cooled and poured into petroleum ether (100 ml). The solid was collected and recrystallized from chloroform; m.p. 145-°46°C. α-Bromo-m-toluic acid (1.5 g, 6.98 mmol) and an excess of thionyl chloride (2 ml, 27.4 mmol) in methylene chloride (20 ml) was refluxed under N_2. After the solution had cleared and evolution of gas ceased (ca. 30 min), the excess $SOCl_2$ and CH_2Cl_2 were removed in vacuo to yield the crude acid chloride as a yellow solid.

A mixture of porphyrin 5 (40 mg, 0.0486 mmol) and α-bromo-m-toluic acid chloride (45 mg, 0.193 mmol) in CH_2Cl_2 (60 ml) was refluxed under N_2 for 2 h. The volume of the mixture was reduced to about 20 ml and an excess of sodium imidazolate (90 mg, 1 mmol) in CH_3CN, (20 ml) was added all at once. The mixture was heated to refluxing and the progress of reaction was monitored by TLC. After the reaction was complete, the solution was diluted with water. The organic layer was separated and successively extracted with 5% HCl (100 ml), H_2O (100 ml), saturated $NaHCO_3$(100 ml), H_2O (100 ml), dried over Na_2SO_4 and

evaporated to dryness. The product was purified through a silica gel pad (3 x 15 cm) eluted with 5% MeOH/CH_2Cl_2.

Recrystallization from hexane-CH_2Cl_2, yielded purple flakes, 41.5 mg (84%). ^1H NMR ($CDCl_3$) δ-2.31(s, 2H, pyrrole NH), 0.73(s, 9H, t-butyl), 1.74(m, 2H $ArCH_2$), 4.00(m, 8H, Et), 5.18(s, 1H, IM-H), 6.22(s, 1H, Im-H), 6.25-6.6(m, 8H, Ar), 7.25-8.1(m, 8H, ArNH), 8.96(d, 1H, Ar), 9.08(d, 1H, Ar), 01.29(s, 2H, meso). Anal. Calcd. for $C_{66}H_{68}N_8O_2$ C 78.85, H 6.82, N 11.15; Found C 78.59, H 6.78, N 10.96.

Trans-5-(o-(p-t-butylbenzamido)phenyl)-15-(o-(m-bromotoluamido)-phenyl)-2,8,12,18-tetraethyl-3,7,13,17-tetra-methylporphyrin (26)

A mixture of porphyrin 5 (40 mg, 0.049 mmol) and bromo-m-toluic acid chloride (45 mg, 0.193 mmol) in CH_2Cl_2 (60 ml) was refluxed under N_2 for 2h. The mixture was diluted with water, the organic layer separated, and washed with sat. aqueous $NaHCO_3$, dried and evaporated to dryness. The crude residue was purified on silica columns, eluted with 100% CH_2Cl_2.

Recrystallization from CH_2Cl_2-methanol yielded purple solid, 37 mg (74%) ^1H NMR ($CDCl_3$) δ0.76(s, 9H, t-butyl), 1.73(t, 12H, Me), 2.58(s, 6H, Me), 2.60(s, 6H, Me), 4.0(m, 8H, CH_2), 4.48(s, 2H, $ArCH_2$), 6.23(d, 1H, Ar), 6.47(s, 4H, Ar), 6.74(t, 1H, Ar), 7.40(t, 1H, Ar), 7.45-8.05 (m, 8H, Ar, NH), 9.02(d, 1H, ArH), 9.08(d, 1H, Ar), 10.31(s, 2H, meso).

Tr

8,

a

mg

vo

mg

re

wa

(2

(2(

lay

on

to

The

3%

CH_2

s,

CH_3

1H,

Ar),

1H,

$C_{55}H$

Trans-5-(o-aminophenyl)-15-(o-(m-(-N-imidazolyl)toluamido)phenyl)-2,8,12,18-tetraethyl-3,7,13,17-tetramethylporphyrin (7)

α-Bromo-m-toluic acid chloride (70.8 mg, 0.304 mmol) was added to a methylene chloride (200 ml) solution of the diamino porphyrin 1 (200 mg, 304 mmol). The green solution was refluxed under N_2 for 3 h. The volume was reduced to 1/3 and a solution of sodium imidazolate (500 mg, 55 mmol) in acetonitrile (100 ml) is added. The mixture is refluxed for 2 h. further before evaporated to dryness. The residue was redissolved in CH_2Cl_2 (150 ml), extracted successively with water (2 x 200 ml), 5% HCl (200 ml), H_2O (200 ml), saturated with $NaHCO_3$ (200 ml), and H_2O (200 ml). After drying over Na_2SO_4, the organic layer was evaporated to dryness. The reaction mixture was separated on silica gel columns (4 x 30 cm). The least polar band corresponding to the starting material (64 mg, 32%) was eluted with 100% CH_2Cl_2. The second band which contains the desired porphyrin was eluted with 3% MeOH/CH_2Cl_2. The product was further crystallized from hexane-CH_2Cl_2 to give purple flakes (122 mg, 48%); ^1H NMR (CH_2Cl_2) δ-2.32(br s, 2H, pyyrole NH), 1.72(m, 12H, Et), 2.60(s, 6H, CH_3),2.70(s, 6H, CH_3), 3.22(s, 2H, $ArCH_2$), 3.68(s, 2H, NH_2), 4.02(q, 8H, Et), 5.18(s, 1H, Im-H), 5.64(s, 1H, IM-H), 6.25-6.33(m, 5H, Ar, Im-H), 7.10(d, 1H, Ar), 7.19(t, 1H, Ar), 7.5-7.7(m, 4H, Ar, NH), 7.93(t, 1H, Ar), 8.10(d, 1H, Ar), 8.96(d, 1H Ar), 10.25(s, 2H, meso). Anal. Calcd. for $C_{55}H_{68}N_8O$ C 78.17, H 6.68, N 13.26; Found C 78.24, H 6.80, N 13.07.

Tr

te

w

h

-

4

2

2

Ar

N

Ci

ph

an

NM

CH

1H

6.

7.

8.

Cis

tet

mono

Trans-5-15-bis(o-(m-(-N-imidazoyl)toluamido)phenyl)-2,8,12,18-tetraethyl-3,7,13,17-tetramethylporphyrin (11)

In the above synthesis, the last band eluted with 10% MeOH/CH_2Cl_2 was bis-imidazole porphyrin 11. It was recrystallized from hexane-CH_2Cl_2 to afford purple flakes (37 mg, 12%); ^1H NMR ($CDCl_3$) δ -2.32(s, 2H, pyrrole NH), 1.73(t, 12H, Et), 2.58(s, 12H, CH_3), 3.33(s, 4H, $ArCH_2$), 4.00(q,8H,Et), 5.16(s,2H,IM-H), 5.78(s, 2H, IM-H), 6.30(d, 2H, Ar), 6.40(t, 2H, Ar), 6.52(d, 2H, Ar), 6.60(s, 2H, Ar), 7.57(s, 2H, NH), 7.64(t, 2H Ar), 7.93(t, 2H, Ar), 8.05(d, 2H, Ar), 8.96(d, 2H, Ar), 9.29(s, 2H, meso); Anal. Calcd. for $C_{66}H_{76}N_{10}O_2$; C76.12, H 7.36, N 13.45; Found C 76.05, H 7.21, N13.47.

Cis-5-(o-aminophenyl)-15-(o-(m-(α-N-imidazolyl)toluamido)phenyl)-2,8,12,18-tetrathyl-3,7,13,17-tetramethylporphyrin (8)

This mono-imidazole appended porphyrin was prepared in a manner analogous to the trans isomer using the cis diamino porphyrin 2. ^1H NMR ($CDCl_3$) δ-2.32(s, 2H, pyrrole-NH), 1.75(m, 12H, Et), 2.60(s, 6H, CH_3), 2.97(s, 2H, $ArCH_2$), 3.53(m, 2H, NH_2), 4.03(q, 8H, Et), 4.55(s, 1H, IM-H), 5.33(s, 1H, Im-H), 5.77(s, 1H, IM-H), 6.13(s, 1H, Ar), 6.24(d, 1H, Ar), 6.43(t, 1H, Ar), 6.70(d, 1H, Ar), 7.10(d, 1H, Ar), 7.17(t, 1H, Ar), 7.5-7.7(m, 4H, Ar), 7.92(t, 1H, Ar), 8.14(d, 1H, Ar), 8.93(d, 1H, Ar), 19.27(s, 2H, meso).

Cis-5,15-bis(o-(m-(α-N-imidazoly)toluamido)phenyl)-2,8,12,18-tetraethyl-3,7,13,17-tetramethylporphyrin (12)

This compound was resulted accompanying the preparation of the cis mono-imidazole porphyrin, analogous to the trans system; ^1H NMR

(

C

2

6

8.

Ci

3,

p-

1.

CH

Ar

Ar

Cis

tet

rea

2.5

NH_2

1H,

1H,

Trar

pher

cont

(CH_2Cl_2) δ-2.31(br s, pyrrole NH), 1.71(t, 12H, Et), 2.57(s, 12H, CH_3), 3.53(s, 4H, $ArCH_2$), 3.97(m, 8H, Et), 5.08(s, 2H, IM-H), 5.50(s, 2H, IM-H), 5.84(s, 2H, IM-H), 5.92(s, 2H, Ar), 6.35(d, 2H, Ar), 6.45(t, 2H, Ar), 6.73(d, 2H, Ar), 7.62(t, 2H, Ar), 7.92(t, 2H, Ar), 8.09(d, 2H, Ar), 8.32(s, 2H, NH), 8.90(d, 2H, Ar).

Cis-5,15-bis(o-(m-(α-bromotoluamido))phenyl-2,8,12,18-tetraethyl-3,7,13,17-tetramethylporphyrin

This porphyrin was made in an analogous fashion as the mono p-t-butylbenzamido porphyrin 26. ^1H NMR ($CDCl_3$) δ-2.32(s, 2H, NH), 1.77(t, 12H, Me), 2.62(s, 12H, Me), 3.02(s, 4H, $ArCH_2$), 4.08(q, 8H, CH_2), 6.22(s, 2H, Ar), 6.46(t, 2H, Ar), 6.61(d, 2H, Ar), 6.70(d, 2H, Ar), 7.63(t, 2H, Ar), 7.83(s, 2H, NH), 7.95(m, 4H, Ar), 9.03(d, 2H, Ar), 10.32(s, 2H, meso).

Cis-5-(o-aminophenyl)-15-(o-(m-(α-bromotoluamido))phenyl)-2,8,12,18-tetraethyl-3,7,13,17-tetramethylporphyrin (6)

This α-bromotoluyl porphyrin was isolated from the previous reaction mixture ^1H NMR ($CDCl_3$) δ-2.40(s, 2H, NH), 1.75(m, 12H, Me), 2.58(s, 6H, Me), 2.70(s, 6H, Me), 2.94(s, 2H, $ArCH_2$), 3.66(s, 2H, NH_2), 4.07(m, 8H, CH_2), 6.10(s, 1H, ArH), 6.4-6.8(m, 3H, Ar), 7.09(d, 1H, Ar), 7.18(t, 1H, Ar), 7.5-7.7(m, 4H, Ar), 7.76(s, 1H,NH), 7.90(t, 1H, Ar), 8.01(d, 1H, Ar), 9.00(d, 1H, Ar), 10.27(s, 2H, meso).

Trans-5-(o-acetamidophenyl)-15-o-(m(α-N-imidazolyl)toluamido) phenyl-2,8,12,18-tetraethyl-3,7,13,17-tetramethylporphyrin (43)

To a solution of porphyrin 7 (40 mg, 0.047 mmol) in CH_2Cl (40 ml) containing pyridine (1 ml, 12.4 mmol) was added an excess of acetyl

chloride (0.5 ml, 7 mmol). After stirring 1 h at room temperature, water (100 ml) was added and the mixture stirred 1 h further. The organic layer was separated and washed with 10% HCl, H_2O, sat. aqueous $NaHCO_3$, dried and evaporated to dryness. The crude product was purified on a silica gel column (2% MeOH/CH_2Cl) and recrystallized from hexane-CH_2Cl_2 to yield purple-black crystals (34 mg, 83%). ^1H NMR ($CDCl_3$) δ-2.33(s, 2H, NH), 1.31(s, 3H, MeCO), 1.78(t, 12H,Me), 2.52(s, 6H, Me), 2.58(s, 6H, Me), 3.33(s, 2H, $ArCH_2$), 4.02(m, 8H, CH_2), 5.16(s, 1H, Im-H), 5.78(s, 1H, Im-H), 6.20(s, 1H, Im-H), 6.25-6.55(m, 3H, Ar), 6.60(s, 1H, Ar), 6.87(s, 1H, NH), 7.5-8.1(m, 7H, Ar, NH), 8.79(d, 1H, Ar), 8.96(d, 1H, Ar), 10.30(s, 2H, meso).

Cis-5-(o-acetamidophenyl)-15-o-(m-(α-N-imidazolyl)toluamido) phenyl)-2,8,12,18-tetraethyl-3,7,13,17-tetramethylporphyrin (44)

The cis isomer was made in the same fashion as the trans form except starting with the cis imidazole appended aminoporphyrin 8. ^1H NMR ($CDCl_3$) δ-2.52(s, 2H, NH), 1.38(s, 3H, MeCO), 1.75(m, 12H, Me), 2.50(s, 6H, Me), 2.60(s, 6H, Me), 3.90(s, 2H, $ArCH_2$), 4.00(m, 8H, CH_2), 6.28(d, 1H, Ar), 6.56(s, 1H, NH), 7.10(s, 1H, Im-H), 7.30(s, 1H, Im-H), 7.42(t, 1H, Ar), 7.51(d, 1H, Ar), 7.55(s, 1H, Im-H), 7.64(t, 1H, Ar), 7.8-8.1(m, 4H, Ar), 8.23(d, 1H, Ar), 8.60(m, 2H, NH, Ar), 8.97(d, 1H, Ar), 10.25(s, 2H, meso).

Trans-5-(o-(m-(α-N-imidazolyl)toluamido)phenyl)-15-(o-(3,5-bis (ethoxycarbonyl)benzamido)phenyl)-2,8,12,18-tetraethyl-3,7,13,17-tetra methylporphyrin (32)

A solution of prophyrin 7 (40 ml, 0.0474 mmol) and pyridine (0.5

ml

we

mg

ad

1

mi

suc

100

oil

The

pro

The

HCl,

Crys

58%)

crud

extr

wate

with

satur

gel b

metho

ml, 6.18 mmol) in methylene chloride (20 ml) was added dropwise to a well-stirred solution of 1,3,5-benzenetricarboxylic acid chloride (500 mg, 1.88 mmol) in methylene chloride (40 ml). After completion of the addition (ca. 30 min), the mixture was stirred at room temperature for 1 h. Ethanol (5 ml) was added and the reaction refluxed for 3 h. The mixture was poured into water, the organic layer separated and washed successively 10% HCl (2 x 100 ml), H_2O (100 ml), $NaHCO_3$ (sat aqueous, 100 ml), H_2O, and then dried over Na_2SO_4. After evaporation to a red oil, the product was purified on a silical gel column, (2 x 25 cm). The benzene triester was eluted first with 2% HOAc-CH_2Cl_2. The protonated porphyrin was washed off the column with 5% Et_3N-CH_2Cl_2. The porphyrin containing fraction was extracted successively with 5% HCl, H_2O, $NaHCO_3$, dried over Na_2SO_4 and evaporated to dryness. Crystallization from hexane-CH_2Cl_2 yielded purple granules (30 mg, 58%).

An alternative purification method involved extraction of the crude reaction mixture into 80% phosphoric acid. The acid layer was extracted several times with methylene chloride, then diluted with water and neutralized. The neutralized suspension was back extracted with CH_2Cl_2 and the organic phase was washed with 5% HCl, then H_2O, saturated aqueous $NaHCO_3$. The yield after chromatography on silica gel by this extraction method were generally lower than the first method.

IR: ν_{CO}1670, 1720 cm^{-1}; ^1H NMR ($CDCl_3$) δ-2.30(br s, pyrrole-NH), 0.38(t, 9H, OEt), 1.73(m, 12H, Et), 2.58 (s, 12H, CH_3), 3.28(s, 2H, $ArCH_2$), 3.37(q, 4H, OCH_2CH_3), 4.00(m, 8H, Et), 5.03(s, 1H, IM-H), 5.71(s, 1H, Im-H),6.11(s, 1H, Im-H), 6.23-6.72(m, 4H, Ar), 7.4-8.1(m, 11H, Ar, NH), 8.97(m, 2H, Ar), 10.28(s, 2H, meso); Anal. Calcd. for $C_{68}H_{80}N_8O_6C$ 73.88, H 7.30, N 10.14; Found C 74.02, H 7.43, N 10.10

Trans-5(o-(m-(α-N-imidazolyl)toluamido)phenyl)-15-(o-(3,5-bis (n-butolycarbonyl)benzamido)phenyl)-2,8,12,18-tetraethyl-3,7,13,17-tetramethylporphyrin (33)

This porphyrin was prepared by the above procedure except ethanol was replaced by n-butanol; yield from 7: 63%. ^1H NMR ($CDCl_3$) δ-2.4(br s, 2H, NH), 0.50(t, 6H, Me), 0.77(m, 8H, CH_2), 1.73(m, 12H, Me), 2.60(s, 12H, Me), 3.04(s, 2H, CH_2), 3.34(t, 4H, OCH_2), 4.03(m, 8H, CH_2), 5.06(s, 1H, IM-H), 5.67(s, 1H, IM-H), 6.16(s, 1H, IM-H), 6.2-6.6(m, 8H, Ar), 7.46(d, 2H, Ar), 7.5-8.1(m, 6H, Ar, NH), 8.95(d, 2H, Ar), 10.27(s, 2H, meso)

Trans-5-(o-(m-(α-N-imidazolyl)toluamido)phenyl)-15-(o-(3,5-bis (hydroxymethyl)benzamido)phenyl)2,8,12,18-tetraethyl-3,7,13,17-tetramethylporphyrin (38)

Porphyrin 32 (20 mg, 0.18 mmol) was dissolved in freshly distilled tetrahydrofuran (25 ml). Excess lithium aluminum hydride in THF was added and the reaction stirred for 3 min at room temperature. The reaction was carefully diluted with water (50 ml), followed by CH_2Cl_2 (30 ml). The organic layer was separated and washed with water, brine, and dried over Na_2SO_4. After evaporation, the mixture was

separated on thick layer silica gel plates, the 5% MeOH-CH_2Cl_2. The major band was collected and lypholized from benzene to yield a red powder (13.3 mg, 70%; IR: ν_{CO}1670 cm^{-1},ν_{OH} 3400 cm^{-1}; ^1H NMR ($CDCl_3$)δ -2.4 (br s, 2H, pyrrole NH), 1.75(m, 12H, Et), 2.55(s, 6H, CH_3), 2.59(s, 6H, CH_3), 3.16(s, 4H, $ArCH_2$), 3.25(s, 2H, $ArCH_2$), 3.98(m, 8H, Et), 5.13(s, 1H, Im-H), 5.69(s, 1H, Im-H), 5.92(s, 2H, Ar), 6.1-6.6(m, 6H, Ar), 7.4-8.1(m, 8H, Ar), 8.91(m, 2H, Ar), 10.27(s, 2H, meso).

Trans-5-(o-(m-(α-N-imidazolyl)toluamido)phenyl)-15-(o-(3,5-bis (n-butylaminocarbonyl)benzamido)phenyl)-2,8,12,18-tetraethyl-3,7,13,17-tetramethylporphyrin (34)

This compound was prepared by procedures analogous to that of 3,5-diethyl ester porphyrin 32. The crude diacid chloride was treated with excess n-butylamine and the resultant mixture was refluxed overnight under N_2. After purification by extraction and column chromatography, the amide was crystallized from hexane CH_2Cl_2; 40% yield. ^1H NMR ($CDCl_3$) δ-2.4(br s, 2H, pyrrole-NH), 0.48(t, 6H, Bu-CH_3), 0.75(m, 8H, Bu-CH_2Cl_2), 1.73(m, 12H, Me), 2.58(s, 12H, Me), 3.23(s, 2H, benzyl), 3.34(t, 4H, CH_2O), 4.01(m, 8H, CH_2), 5.06(s, 1H, Im), 5.66(s, 1H, Im), 6.15(s, 1H, Im), 6.28(d, 1H, H), 6.40(t, 1H, H), 6.56(m, 2H, H), 7.4-8.1(m, 11H, Ar, NH), 8.95(m, 2H, Ar), 10.26(s, 2H, meso); Anal. Calcd. for $C_{68}H_{80}N_8O_6$ C 74.58, H 7.82, N 12.08; Found C 74.21, H 7.93, N 11.82.

Trans-5-(o-(m-(α-N-imidazolyl)toluamido)phenyl)-15-(o-(3,5-bis (N,N-diethylaminocarbonyl)benzamido)phenyl)-2,8,12,18-tetraethyl-3,7,13,17-tetramethylporphyrin (35)

This was prepared as described for the diester porphyrin 32. Excess diethyl amine was added to the diacid chloride-porphyrin. After refluxing overnight under N_2 the product was purified as described; yield: 47%. ^1H NMR ($CDCl_3$) δ-2.38(br s, 2H, pyrrole NH), -0.83(br, 6H, NHC_2CH_3), 0.19(br, 6H, NCH_2CH_3), 1.42(br, 4H, NCH2), 1.74(m, 12H, Et), 2.24(br, 4H, NCH_2), 2.56(s, 6H, CH_3), 2.61(s, 6H, CH_3), 3.28(s, 2H, $ArCH_2$), 4.00(m, 8H, Et), 5.10(s, 1H, IM-H), 5.73(s, 1H, Im-H), 6.18(s, 1H, IM-H), 6.23-6.6(m, 6H, Ar), 6.68(s, 1H, Ar), 7.5-8.1(m, 8H, Ar, NH), 8.97(m, 2H, Ar), 10.28(s, 2H, meso).

Trans-5-(o-(m-(α-N-imidazolyl)toluamido)phenyl)-15-(o-(3,5-bis (N,N-di-ipropylaminocarbonyl)benzamido)phenyl)-2,8,12,18-tetraethyl-3,7,13,17-tetramethylporphyrin (36)

This compound was prepared by procedures identical to that for the diethyl analogue 35 except that isopropylamine was used to quench the acid chloride; yield: 55%. ^1H NMR ($CDCl_3$) δ-2.4(br s, 2H, pyrrole-NH), 1.28(d, 12H, i-Pr), 1.72(t, 12H, Me), 2.56(s, 6H, Me), 2.60(s, 6H, Me), 3.22(s, 2H, benzyl), 4.00(m, 8H, CH_2), 4.27(m, 2H, i-Pr), 5.04(s, 1H, Im), 5.65(s, 1H, Im), 6.14(s, 1H, Im), phenyl: 6.30(d, 1H), 6.40(t, 1H), 6.47(s, 2H), 6.54(d 1H), 6.58(s, 1H), 6.68(s, 1H), 7.3-8.2(m, 8H, H, NH), 8.96(d, 1H), 9.03(d, 1H), 10.26(s, 2H, meso).

Trans-5-(o-(m-(α-N-imidazolyl)toluamido)phenyl)-15(o-(3,5-bis (butylthiocarbonyl)benzamido)phenyl)-2,8,12,18-tetraethyl-3,7,13,17-tetramethylporphyrin (37)

This compouond was prepared by procedures identical to that for the ester and analogues 32, 33 except butanethiol was used to quench the acid chloride. After recrystallization from hexane-CH_2Cl_2, yield 71%. ^1H NMR ($CDCl_3$) δ-2.07(br s, 2H, NH), 0.57(t, 6H, Me), 0.78(m, 4H, CH_2), 1.75(m, 20H, Me, CH_2), 2.58(s, 6H, Me), 2.60(s, 6H, Me), 3.10(s, 1H, IM-H), 4.00(m, 8H, CH_2), 4.97(s, 1H, Im-H), 5.50(s, 1H, Im-H), 6.15(s, 1H, IM-H), 6.2-6.6(m, 3H, Ar), 7.16(d, 2H, Ar), 7.38(s, 1H, Ar), 7.65(m, 2H, Ar), 7.7-8.0(m, 4H, Ar, NH), 8.11(d, 1H, Ar), 8.94(d, 1H, Ar), 9.01(d, 1H, Ar), 8.94(d, 1H, Ar), 9.01(d, 1H, Ar), 10.28(s, 2H, meso).

Trans-5,15-bis(o-(3-(N-imidazolyl)propylureido)phenyl)-2,8,12,18-tetraethyl-3,7,13,17-tetramethylporphyrin (17)

To a solution of porphyrin 1 (20 mg, 0.03 mmol) in tetrahydrofuran (30 ml) containing pyridine (1 ml) was added an excess of phosgene in benzene (1 ml, 21 1 mmol/ml). After stirring for 20 min at room temperature, the excess phosgene was removed in vacuo. A solution of excess 3-(N-imidazolyl)propylamine[22](0.5 ml, 517 mmol) in THF (20 ml) was added and the mixture stirred overnight. After removal of solvents, the resultant oil was redisolved in CH_2Cl_2, washed successively with 5% HCl, H_2O, $NaHCO_3$ (sat. aqueous) and dried over Na_2SO_4. The crude product was dried and purified through a silica pad, crystallized from MeOH-CH_2Cl_2 to yield a purple solid (19.2 mg,

8(

12

7.

Tr

ei

bi

mo

9H

2.

5.

NH

9.

Tra

te

8.

met

Aft

org

sat

por

MeO

2.4

Im-

7.84

80%). ^{1}H NMR ($CDCl_3$) δ1.34(t, 4H, CH_2), 1.75(t, 12H, Me), 2.61(s, 12H, Me), 3.19(m, 4H, CH_2, 4.00(q, 8H, CH_2), 6.30(s, 2H, Im-H), 7.43(t, 2H, Ar), 7.82(m, 4H, Ar), 8.57(d, 2H, Ar), 10.31(s, 2H, meso).

Trans-5-(o-(p-t-butylbenzamido)phenyl)-15-(o-(3-(N-imidazolyl)propylureido)phenyl)-2,8,12,18-tetraethyl-3,7,13,17-tetramethylporphyrin (31)

This compound was made in procedures analogous to the bis-imidazolyl propylureido complex except starting with the mono-blocked porphyrin 5. ^{1}H NMR ($CDCl_3$) δ-0.67(m, 2H, CH2), 0.72(s, 9H, t-butyl), 1.70(t, 12H, Et), 1.98(m, 2H, CH_2), 2.17(m, 2H, CH_2), 2.51(s, 6H, CH_3), 2.57(s, 6H, CH_3), 3.96(q, 8H, Et), 4.38(t, 1H, NH), 5.03(s, 1H, Im-H), 5.32(s, 1H, Im-H), 5.38(s, 1H, Im-H), 6.28(s, 1H, NH), 6.44(s, 4H, Ar), 7.36-7.94(m, 7H, Ar, NH), 8.57(d, 1H, Ar), 9.08(d, 1H, Ar), 10.22(s, 2H, meso).

Trans-bis-5,15-(o-(3-(N-imidazolyl)propylamido)phenyl)2,8,12,18-tetraethyl-3,7,13,17-tetramethylporphyrin (15)

This compound was prepared by an analogous procedure as porphyrin 8. The 3-(N-imidazolyl)propionic acid chloride was added to a methylene chloride solution of porphyrin 6 containing triethylamine. After refluxing for 2 h, the mixture was poured into ice water. The organic layer was separated, washed successively with 5% HCl, H_2O, saturated aqueous $NaHCO_3$, and then evaporated to dryness. The crude porphyrin was purified on preparative TLC plates (silica gel, 5% MeOH-CH_2Cl_2). ^{1}H NMR ($CDCl_3$) δ0.84(m, 4H, CH_2), 1.73(t, 12H, Me), 2.45(s, 12H, Me), 3.73(t, 4H, CH_2), 4.02(m, 8H, CH_2), 6.23(s, 2H, Im-H), 6.60(s, 2H, Im-H), 6.93(m, 4H, NH, Im-H), 7.52(t, 2H, Ar), 7.84(t, 4H, Ar), 8.70(d, 2H, Ar), 10.27(s, 2H, meso).

Trans-5(o-(p-t-butylbenzamido)phenyl)-15-(o-(3-(N-imidazolyl) propylamido)phenyl)-2,8,12,18-tetraethyl-3,7,13,17-tetramethylporphyrin(29)

This compound was prepared in procedures analogous to the blocked imidazolyl-butylamido complex 30, except utilizing the corresponding propyl derivative. ^{1}H NMR ($CDCl_3$) δ0.72(s, 9H, t-butyl), 1.73(m, 14H, Et), 2.46(s, 6H, CH_3), 2.58(s, 6H, CH_3), 3.75(t, 2H, CH_2), 4.02(m, 8H, Et), 6.25(s, 1H, Im-H), 6.48(s, 4H, Ar), 6.63(s, 1H, Im-H), 6.85(s, 1H, NH), 7.01(s, 1H, Im-H), 7.56(q, 2H, Ar), 7.90(m, 4H, Ar), 8.0(s, 1H, NH), 8.71(d, 1H, Ar), 9.08(d, 1H, Ar), 10.29(s, 2H, meso).

Trans-bis-5,15-(o-(4-bromobutylamido)phenyl)-2,8,12,18-tetraethyl-3,7,13,17-tetramethylporphyrin (18)

This compound was made in procedures analogous to the alkyl-appended imidazole porphyrins 15, 16. The 4-bromobutyric acid was the result of hydrobromic acid hydrolysis of butyrolactone.[31] Treatment with thionyl chloride produced the acid chloride which was used without further purification. ^{1}H NMR ($CDCl_3$) δ-2.42(s, 2H, NH), 1.46(t, 4H, CH_2), 1.60(m, 4H, CH_2), 1.81(t, 12H, Me), 2.54(s, 12H, Me), 2.86(t, 4H, CH_2), 4.05(q, 8H, CH_2), 6.88(s, 2H, NH), 7.53(t, 2H, Ar), 7.87(m, 4H, Ar), 8.76(d, 2H, Ar), 10.30(s, 2H, meso).

Trans-bis-5,15(o-(N-butyrolactam)phenyl)-2,8,12,18-tetraethyl-3,7,13,17-tetramethylporphyrin (20)

The preceding bromobutylamido porphyrin 18 was treated with excess sodium imidazolate in refluxing dimethylformamide. Chromatography on silica gel revealed a single nonpolar product. ^{1}H NMR ($CDCl_3$) δ

M

A

Tr

to

(2

N-

tr

pr

75

3H

6.

1H,

Tra

ace

por

chl

mal

mix

was

The

extr

with

-2.40(s, 2H, NH), 0.70(q, 4H, CH_2), 1.67(t, 4H, CH_2), 1.74(t, 12H, Me), 2.20(t, 4H, Ch_2), 2.60(s, 12H, Me), 4.02(m, 8H, CH_2), 7.71(m, 2H, Ar), 7.80(d, 4H, Ar), 8.17(d, 2H, Ar), 10.23(s, 2H, meso).

Trans-5-(o-(p-t-butylbenzamido)phenyl)-15-(o-(m-(α-acetylthio) toluamido)phenyl)-2,8,12,18-tetraethyl-3,7,13,17-tetramethylporphyrin (28)

This compound was prepared in procedures analogous to the N-imidazolyl toluamide, except the bromotoluamido porphyrin 26 was treated with an excess of sodium thioacetic acetate. The crude product was separated on silica gel columns (2% MeOH/CH_2Cl_2), yield 75%. ^1H NMR ($CDCl_3$) δ0.78(s, 9H, t-butyl), 1.76(t, 6H Me), 2.35(s, 3H, CH_3CO), 2.59(s, 6H, Me), 2.61(s, 6H, Me), 4.23(s, 2H, $ArCH_2$), 6.2-6.7(m, 4H, Ar), 6.48(s, 4H, Ar), 7.5-8.0(m, 8H, Ar, NH), 9.03(d, 1H, Ar), 9.08(d, 1H, Ar), 10.29(s, 2H, meso).

Trans-5-(o-(m-(α-N-imidazolyl)toluamido)phenyl)-15-(o-(aminocarbonyl-acetamido)Phenyl)-2,8,12,18-tetraethyl-3,7,13,17-tetramethyl-porphyrin (45)

A solution of porphyrin 7 (50 mg, 0.059 mmol) in methylene chloride (30 ml) under N_2 was added to a well stirred solution of malonyl dichloride (0.5 ml, 5.7 mmol) in CH_2Cl_2 (100 ml) and the mixture was refluxed for 2 h. At room temperature, anhydrous ammonia was bubbled through the green solution until the color changed to red. The mixture was then diluted with water (100 ml), separated, and extracted into 80% phosphoric acid (30 ml). The acid layer was washed with CH_2Cl_2 (3 x 100 ml), diluted with water, then neutralized with

1(

co

ar

ge

ga

a

NH

CH_3

1H,

6.5

7.8

7.9

Tra

(t-

tet

Afte

adde

1.7)

3.21

IM-H

1H,

tran

aceta

porp

10% NaOH, and back extracted repeatedly with CH_2Cl_2 (3 x 30 ml). The combined organic phase was washed with water (100 ml), brine (100 ml), and evaporated to dryness. The crude product was purified on silica gel plates, using 2% MeOH-CH_2Cl_2. The second band, the major band, gave the desired porphyrin which was lyophilized from benzene to yield a brown powder (11 mg, 20%). ^1H NMR ($CDCl_3$) δ-3.2(br s, 2H, pyrrole NH), -0.45(br s, 2H, NH_2), 1.5(t, 6H, Et), 1.62(t, 6H,Et), 2.17(s, 6H, CH_3), 2.58(s, 6H, CH_3), 3.27(s, 2H, $ArCH_3$), 3.6-4.0(m, 8H, Et), 5.0(s, 1H, Im-H), 5.65(s, 1H, IM-H), 6.05(s, 1H, Im-H), 6.20(s, 2H, CH_2), 6.50(s, 1H, Ar), 7.3(m, 2H, Ar, NH), 7.6(d, 1H, Ar), 7.70(t, 1H, Ar), 7.80(t, 1H, Ar), 7.96(t, 1H, Ar), 7.40(d, 1H, Ar), 7.64(d, 1H, Ar), 7.94(m, 2H, Ar, NH), 10.0(s, 2H, meso).

Trans-5-(o-(m-(α-N-imidazolyl)toluamido)phenyl-15-(o-(t-butylaminocarbonylacetamido)phenyl)-2,8,12,18-tetraethyl-3,7,13,17-tetramethylporphyrin (46)

This porphyrin was made in an analogue fashion as porphyrin 45. After addition of malonyl dichloride, an excess of t-butylamine was added. ^1H NMR ($CDCl_3$) δ-2.3(br s, pyrrole NH), 0.60(s, 9H, t-butyl), 1.7)t, 12H, Et), 2.34(s, 2H, CH_2), 2.50(s, 6H, CH_3), 2.60(s, 6H, CH_3), 3.21(s, 2H, $ArCH_2$), 4.00(m, 8H, Et), 5.11(s, 1H, Im-H), 5.66(s, 1H, IM-H), 6.0-6.6(m, 6H, Ar, Im-H, NH), 7.3-8.0(m, 8H, Ar, NH), 8.72(d, 1H, NH), 8.95(d, 1H, Ar), 10.27 (s, 2H, meso).

trans-5-(o-(m-(α-n-imidazolyl)toluamido)phenyl)-15-(o-(dimethylamino-acetamido)phenyl)-2,8,12,18-tetraethyl-3,7,13,17-tetamethyl-porphyrin (47)

This porphyrin was made in an analogous fashion as porphyrin 45. ^1H NMR ($CDCl_3$) δ -2.35(br s, pyrrole NH), 1.00(s, 3H, NCH_3), 1.70(t, 12H, Et), 2.08(s, 3H, NCH_3), 2.52(s, 6H, CH_3), 2.59(s, 6H, CH_3), 2.73(s, 2H, $COCH_2$), 3.18(s, 2H, $ArCH_3$), 4.00(m, 8H, Et), 5.14(s, 1H, Im-H), 5.63(s, 1H, Im-H), 6.2-6.6(m, 5H, Ar, Im-H), 7.5-8.0(m, 6H, Ar, NH), 8.2(d, 1H, Ar), 8.7(m, 2H, Ar, NH), 8.96(d, 1H, Ar), 10.27(s, 2H, meso).

Trans-bis-5,15-(o-(m-(α-triethylchloroammonium)toluamido)phenyl)-2,8,12,18-tetraethyl-3,7,13,17-tetramethylporphyrin (21)

A mixture of porphyrin 1 (40 mg, 0.060 mmol) and excess bromo-m-toluic acid chloride (30 mg, 12.8 mmol) in methylene chloride (40 ml) was refluxed under N_2 for 90 min. The mixture was evaporated to dryness and redisolved in acetonitrile (30 ml). Excess triethylamine (3 ml, 32.1 mmol) was added to the green solution and the reaction was stirred at room temperature for 2 h before the mixture was evaporated to dryness. The residue was redissolved in CH_2Cl_2 (30 ml), washed with H_2O (30 ml) and brine (30 ml), and then purified on silica gel plates (10% MeOH-CH_2Cl_2). The porphyrin collected from the most polar band was crystallized from CH_2Cl_2-hexane to yield a purple brown power. ^1H NMR ($CDCl_3$) δ 1.48(s, 18H, Me_3N), 1.76(t, 12H, Me), 2.62(s, 12H, Me), 3.22(s, 4H, $ArCH_2$), 4.05(q, 8H, CH_2), 5.36(s, 6H, Ar), 5.97(s, 2H, Ar), 6.51(s, 2H, Ar), 7.08(m, 2H, NH), 7.73(t, 2H, Ar), 8.00(t, 2H, Ar), 8.04(d, 2H, Ar), 8.86(d, 2H Ar), 10.37(s, 2H, meso).

N

2

E

1H

1H

Ar

Tr

d

te

mak

ami

(CO

2.57

CH_2)

3H,

3H,

9.00

Trans-5-(o-(m-(α-N-imidazolyl)toluamido)phenyl)-15-(o-(m(α-trimethylchloroammonium)toluamido)phenyl)-2,8,12,18-tetraethyl-3,7,1,17-tetramethylporphyrin (41)

This compound was made in procedures analogous to the bis quatenary amines except utilizing the mono imidazole appended porphyrin 7. Yield after recrystallization from CH_2Cl_2-hexane, 71%. ^1H NMR ($CDCl_3$) δ-2.50(br s, 1H, pyrrole NH), -2.37(br s, 1H, pyrrole NH), 0.07(s, 9H, $N(CH_3)_3$), 1.75(m, 12H, Et), 2.42(s, 2H, $ArCH_2$), 2.58(s, 6H, CH_3), 2.63(s, 6H, CH_3), 3.55(s, 2H, $ArCH_2$), 4.04(m, 8H, Et), 4.32(s, 1H, Ar), 5.21(s, 1H, Im-H), 5.98(s, 1H, Im-M), 6.15(s, 1H, Im-H), 6.39(s, 3H, Ar), 6.63(s, 1H, Ar), 6.90(t, 1H, Ar), 7.16(d, 1H, Ar), 7.4(m, 2H, Ar), 7.7(m, 2H, Ar), 7.94(m, 2H, Ar), 8.12(d, 1H, Ar), 8.86(d, 1H, Ar), 8.97(d, 1H, Ar), 10.34(s, 2H, meso).

Trans-5-(o-(m-(α-N-imidazolyl)toluamido)phenyl)-15-(o-(m-(α-dimethylamino)toluamido)phenyl)-2,8,12,18-tetraethyl-3,7,13,17-tetramethylporphyrin (40)

This compound was made in procedures analogous to those used in making the appended quatenary amine 41 except an excess of dimethyl amine was used in the reaction with a α-bromo intermediate. ^1H NMR ($CDCl_3$) δ0.98(s, 6H, Me_2N), 1.74(m, 12H, Me), 2.00(s, 2H, $ArCH_2$), 2.57(s, 6H, Me), 2.61(s, 5H, Me), 3.30(s, 2H, $ArCH_2$), 4.01(m, 8H, CH_2), 5.17(s, 1H, Im-H), 5.74(s, 1H, Im-H), 6.23(s, 1H, Im-H), 6.43(m, 3H, Ar), 6.55(d, 1H, Ar), 6.62(s, 1H, Ar), 6.72(d, 1H, Ar), 7.50(m, 3H, Ar), 7.75(s, 1H, NH), 7.94(m, 3H, Ar, NH), 8.09(d, 1H, Ar), 9.00(m, 2H, Ar), 10.30(s, 2H, meso).

Trans-5(o-(m-(α-N-imidazolyl)toluamido)phenyl)-15-(o-(m-(α-triethylchloroammonium)toluamido(phenyl)-2,8,12,18-tetraethyl-3,7,13,17-tetramethylporphyrin (42)

This compound was made in procedures analogous to those used to make the triethyl ammonium analogue 41, except that triethyl amine was used in the reaction with the bromo intermediate. ^1H NMR ($CDCl_3$) δ -2.40(s, 2H, NH), -0.52(t, 3H, Me), 1.13(q,4H, CH_2), 1.30(t, 6H, Me), 1.65(t, 3H, Me), 1.74(t, 3H, Me), 2.53(s, 6H, Me), 2.58(s, 6H, Me), 3.00(s, 2H, $ArCH_2Im$), 3.27(q, 4H, CH_2), 4.00(m, 8H, CH_2), 4.38(s, 1H, Im-H), 4.66(s, 2H, $ArCH_2N$), 5.13(s, 1H, Im-H), 5.50(s, 1H, Ar), 5.88*s, 1H, Im-H), 6.17(d, 1H, Ar), 6.26(m, 2H, Ar), 6.58(d, 1H, Ar), 6.27(t, 1H, Ar), 7.02(d, 1H, Ar), 7.14(d, 1H, Ar), 7.37(t, 1H, Ar), 7.6-8.1(m, 8H, Ar), 8.86(d, 1H, Ar), 8.97(d, 1H, Ar), 10.27(s, 2H, meso).

5,15-Bis(o-hydroxphenyl)-2,8,12,18-tetraethyl-3,7,13,17-tetramethylporphyrins (22) (23)

4,4'-Diethyl-3,3'-dimethyl-2,2'-dipyrrylmethane (6 gm, 26.1 mmol) and salicylaldehyde (3.2 gm, 26.1 mmol) were dissolved in methanol (300 ml). The solution was cooled to 0°C and deaerated by bubbling with argon for 10 min. Zinc acetate (1 ml sat. MeOH) was added followed by p-toluenesulfonic acid (1.4 gm, 7.4 mmol). The reaction was stirred for 4 h, the solvent was removed in vacuo. The crude porphyrinogen was dissolved in THF (40 ml) and treated with an equal weight of o-chloranil. After stirring for 1 h the solvent was removed in vacuo and the crude solid redissolved in CH_2Cl_2 and precipitated

with methanol-triethyl amine. The porphyrin was collected by filtration and washed with cold methanol. The isomers were purified and separated on silica columns, trans isomer elutes with 100% CH_2Cl_2, the cis isomer requires 10% methanol. Yield after recrystallization from CH_2Cl_2-methanol, 3.6 gm, 39%.

trans isomer (22) ^1H NMR ($CDCl_3$) δ-2.45(s, 2H, NH), 1.78(t, 12H, Me), 2.64(s, 12H, Me), 3.34(d, 2H, OH), 4.03(q, 8H, CH_2), 7.34(m, 4H, Ar), 7.74(m, 4H, Ar), 10.28(s, 2H, meso).

cis isomer (23) ^1H NMR ($CDCl_3$) δ-2.46(br s, 2H, NH), 1.78(t, 12H, Me), 2.64(s, 12H, Me), 3.36(s, 2H, OH), 4.04(q, 8H, CH_2), 7.34(m, 4H, Ar), 7.73(m, 4H, Ar), 10.27(s, 2H, meso).

Trans-5,15-bis(o-(p-t-butylbenzoly)phenyl)-2,8,12,18-tetraethyl-3,7,13,17-tetramethylporphyrin (24)

This compound was made in procedures analogous to those used in generating the corresponding amidoporphyrin 9. ^1H NMR ($CDCl_3$) δ -2.46(s, 2H, NH), 0.72(s, 9H, t-butyl), 1.75(t, 12H, Me), 2.64(s, 12H, Me), 4.01(q, 8H, CH_2), 6.45(d, 2H, Ar), 6.81(d, 2H, Ar), 7.64(m, 2H, Ar), 7.87(m, 2H, Ar), 8.00(m, 4H, Ar), 10.17(s, 2H, meso).

Trans-5,15-bis(o-(m-(α-N-imidazolyl)toluoyl)phenyl)-2,8,12,18-tetraethyl-3,7,13,17-tetramethylporphyrin (25)

This compound was made from the trans diol porphyrin in procedures analogous to those used in generating the corresponding amidoporphyrin 11. ^1H NMR ($CDCl_3$) δ-2.25(br s, 2H, NH), 1.69(t, 12H, Me), 2.24(s, 4H, $ArCH_2$), 2.60(s, 12H, Me), 3.96(m, 8H, CH_2), 4.81(s, 2H, Im-H), 5.10(d, 2H, Ar), 5.96(d, 2H, Ar), 6.17(s, 2H, Im-H), 6.25(s, 2H,

Im-H), 6.42(t, 2H, Ar), 7.00(d, 2H, Ar), 7.76(m, 2H, Ar), 7.91(m, 4H, Ar), 8.23(d, 2H, Ar), 10.12(s, 2H, meso).

CHAPTER 2

THE SYNTHESIS AND CHARACTERIZATION

OF MULTINUCLEAR SYSTEMS DERIVED FROM

DIPHENYL PORPHYRINS

I

t

t

m

d

c

t

i

c

b

m

o

b

c

or

ch

in

be

of

Introduction

Many proteins contain more than one metal center. Often times these metal centers act in concert to achieve the overall function of the enzyme. Examples of metalloproteins containing more than one metal center include: hemocyanin, copper oxidase, superoxide dismutase, and cytochrome oxidase. The interaction of metal centers can also produce interesting characteristics. In cytochrome oxidase, the terminal component of the mitochondrial respiratory chain, studies indicate that an iron and copper center are strongly magnetically coupled. [32,33]

Simple porphyrins would serve as poor models for this and other binuclear systems. Aggregation is difficult to control and mixed metal systems would be impossible to mimic. One method which we and others have employed in the study of these multimetal proteins is binuclear porphyrin systems.[6,19,34-37] These systems incorporate chelating ligands, which are covalently linked to the porphyrin ring.

The creation of one-to-one complexes of either fixed or variable orientation can lead to interesting metal-to-metal interactions and characteristics. Bridging ligands can also be incorporated to investigate the potential of various groups to cause spin coupling between metal centers.

This section describes the design, synthesis, and characterization of several binuclear systems based on diphenyl porphyrins.

Dimers

The design and synthesis of cofacial diporphyrins has received much attention over the past few years. [38-41] The fixed orientation of the two porphyrin rings, over one another, provides an ideal geometry for studying metal-metal interactions. These cofacial porphyrins have found wide use as electrocatalysts for the cathodic reduction of dioxygen to water, a process in principle similar to that performed by cytochrome oxidase.

The general synthesis of previous cofacial diporphyrins has involved the coupling of either two o-amino tetraphenyl porphyrins[38], or two β-substituted porphyrins.[39-41] The yields for the coupling of meso phenyl substituted porphyrins are generally high but the distance between the two rings is inherently large due to the nature of the linkage. β-Substituted porphyrins allow the construction of dimers of varing interplanar distances. The yields of these more versatile systems are invariably lower due to the flopiness of the linkage side chains and their tendency to polymerize.

The smallest chain length for a symmetric dimer constructed from ortho substituted tetraphenyl porphyrins was seven atoms in length[38], while Collman has prepared a β-substituted dimer with a three atom linkage.[41] The ideal system for oxygen reduction so far consists of a four atom dimer (DP-4).

Our system involves a mixed porphyrin dimer, linking a β-substituted diacetic acid porphyrin to the o-amino diphenyl porphyrin system. The orientation of the amines in the cis compound

is ideal for the formation of a dimeric species in high yield. The use of the β-substituted porphyrin allows construction of a dimeric species with an interplanar distance equal to the C_5 dimers. Although this system is larger than the ideal C_4 system, the increase in rigidity obtained by incorporating the diphenyl ring system may lead to a more favorable geometry.

Synthesis

The synthesis of the mixed cofacial porphyrin 50 involved the high dilution coupling of the cis o-amino diphenyl porphyrin 2 and the β-substituted diacetyl chloride 49 in CH_2Cl_2 containing a small amount of triethylamine, Scheme 4. The slow rate of reaction for the ortho amino diphenyl porphyrin allowed the all-at-once addition of equamolar quantities of both components followed by refluxing overnight. Work up of the reaction revealed large amounts of unreacted diamine, indicating that much higher yields could be obtained under optimized conditions.

Metallation of the mixed cofacial diporphyrins proved difficult due to the lower reactivity of the phenyl porphyrin inner protons. The bis cobalt system was obtained by refluxing the free base in dry THF with cobalt acetate. Similar treatment with copper acetate produced only the monometallated adduct. The bis copper complex could only be obtained if copper diamine porphyrins were used in the coupling reaction.

Scheme 4.

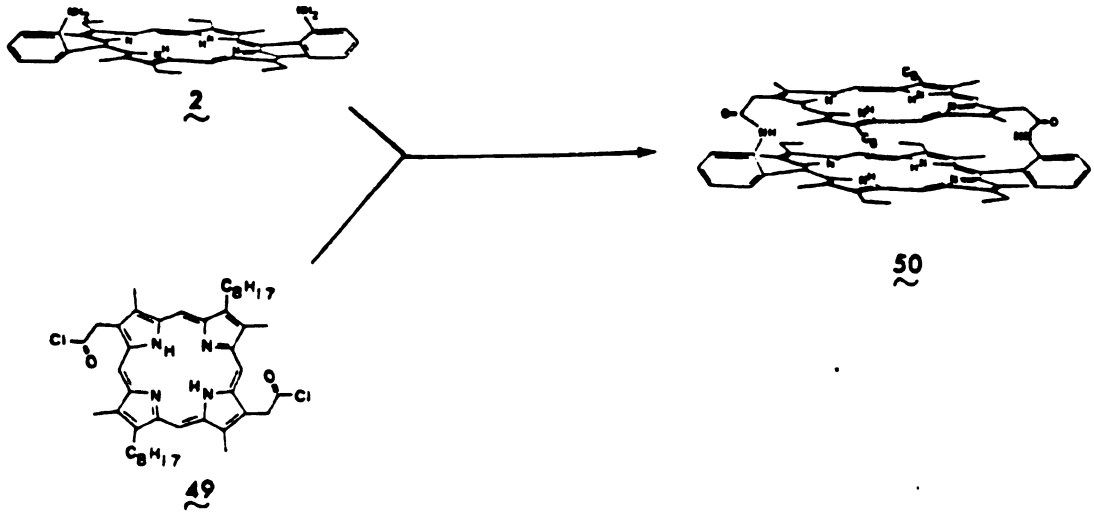

The difference in the acidities of the two porphyrins simplifies the construction of mixed metal systems. The beta-substituted porphyrin can be metallated with standard conditions, e.g., metal acetate/CH_2Cl_2-methanol or acetic acid, without metallating the diphenyl porphyrin.

Absorption Spectra

The absorption spectra, Figure 14, proved valuable in correlating observed results with previously observed trends for cofacial diporphyrins.[38-41] The diphenyl porphyrins exhibit a phyllo type spectra, IV > II> III> I, which is characteristic for mono or di-meso substituted octaalkyl porphyrins. The beta-substituted derivatives

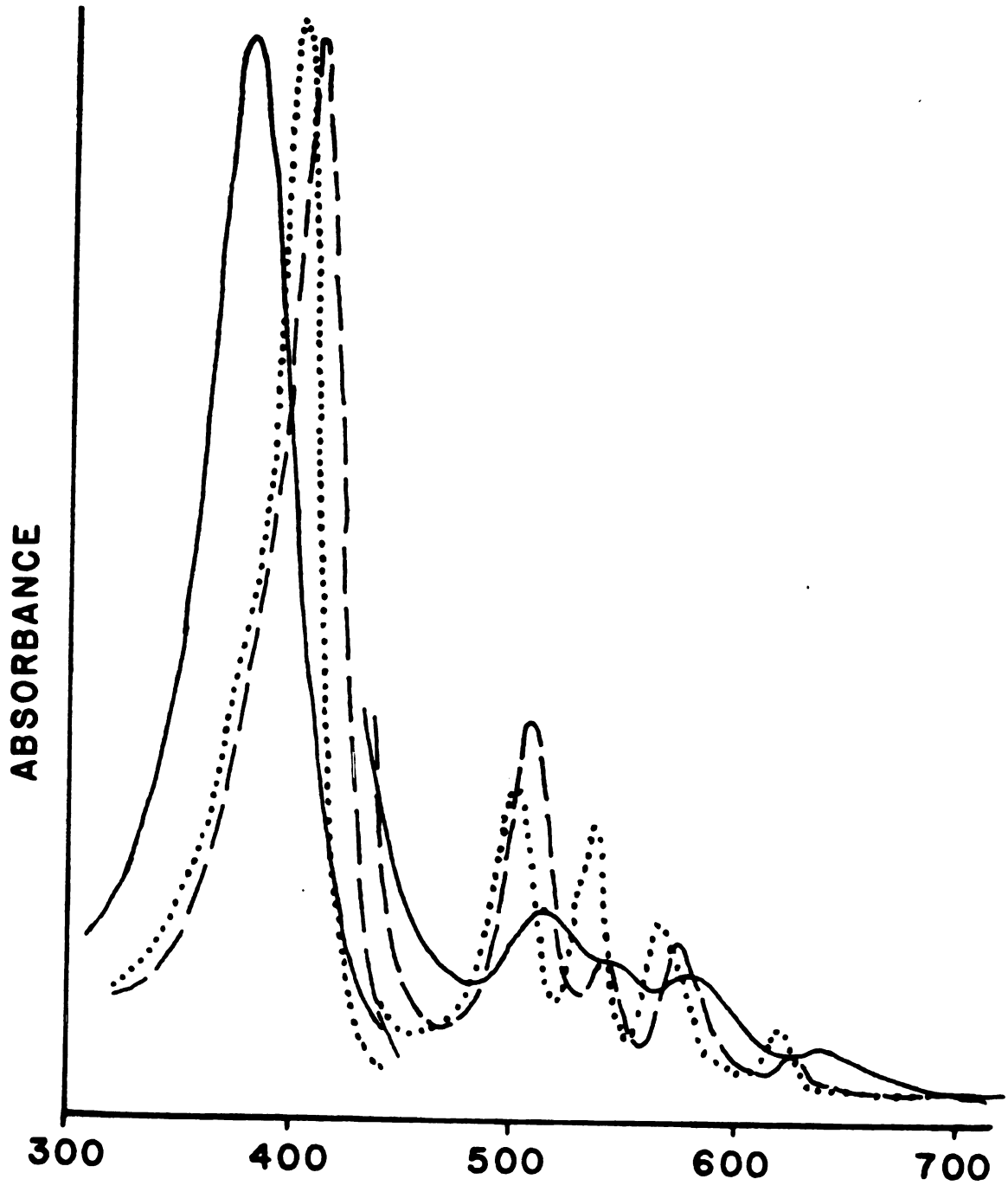

Figure 14. Electronic spectra of C_8 dimethyl ester (49) (....); (amino)$_2$DPE, cis (2) (----); and mixed diporphyrin 50 (——), in CH_2Cl_2.

exhibit the typical etio type spectra, IV> III> II> I. Dimerization was evidenced in the Soret band, representing the π-π*transition, by a blue shift of approximately 20 nm. This shift represents the interaction of the two systems which are held in close proximity. In the visible region the diporphyrin exhibited a slight red shift with band broadening.

^{1}H NMR

As in our previous studies, ^{1}H NMR has proven to be the most powerful tool in verifying the structures of these complex systems. The close proximity of the cofacial porphyrins to one another can cause pronounced shifts in the resonances of nearby protons.

The free base spectrum of the mixed cofacial diporphyrin, Figure 15, indicates the formation of a highly symmetric species. Diporphyrin formation was indicated by the shifts of the phenyl ring protons, the unusual position of the resonances may be due to constraint of the phenyl rings. The inability to form diastereomers in this system was evidenced by the appearance of only three singlets for the meso hydrogens and only four ring methyl resonances. The rigidity of the linkage was indicated by the AA' BB' system corresponding to the α-protons of the acetamide linkage.

The most pronounced feature of the spectrum was the up-field shift of the inner pyrrolic hydrogens. The monomeric diphenyl porphyrin and β-diacid porphyrin show single resonances at -2.5 and -4.0 ppm, respectively, while the dimer exhibited a pair of singlets at -6.4 and -7.7 ppm. the splitting reflected the dissimilarity between the two

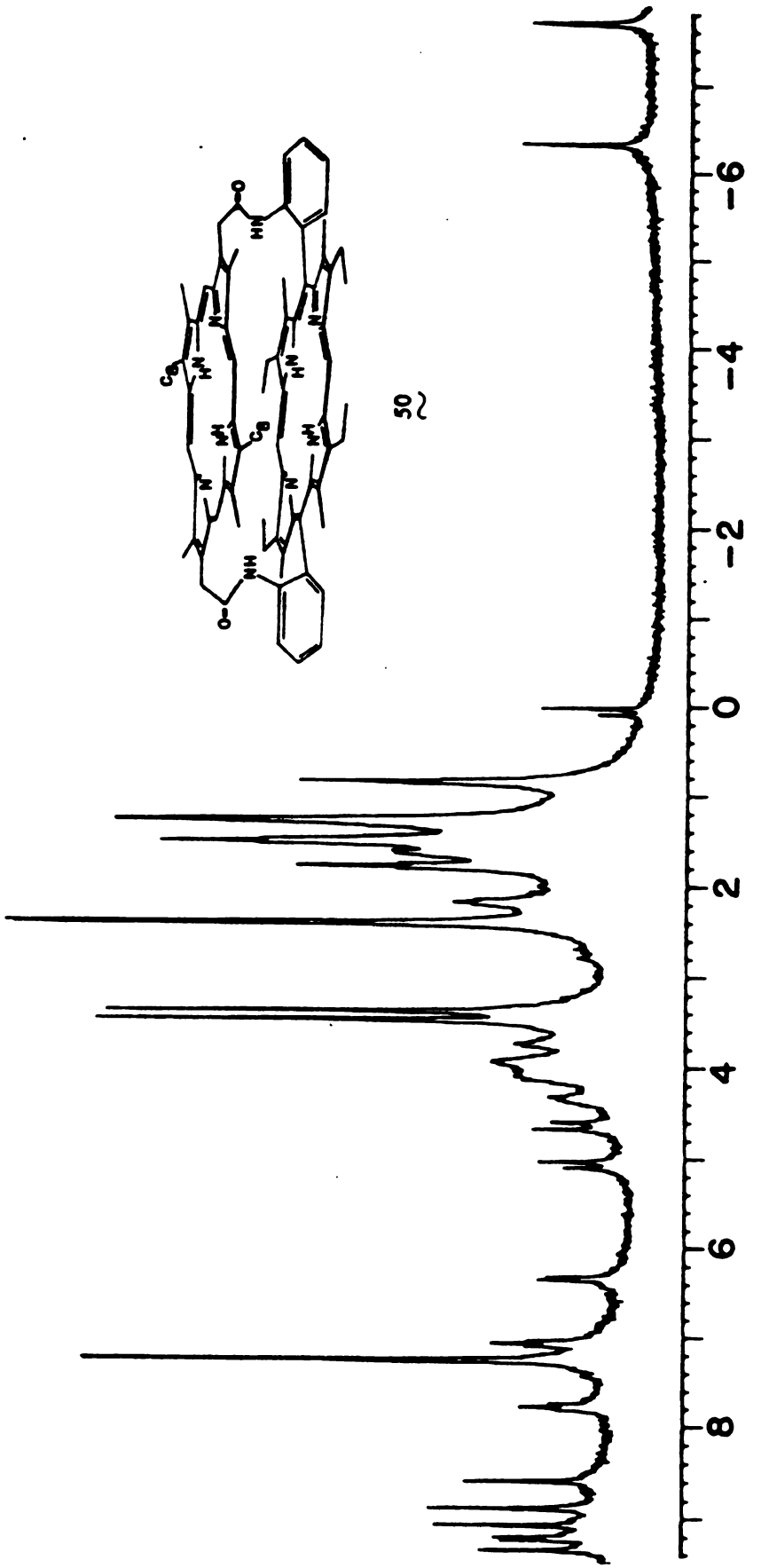

50

Figure 15. 250 MHz ^1H NMR spectrum of mixed diporphyrin 50 in $CDCl_3$.

ring systems and the shift results from interaction of the neighboring system. the size of the shift can be used in determining the interplanar distance between the two rings[40], the closer the proximity, the greater the interaction. The observed shifts indicated an interplanar distance comparable to the DP-4 diporphyrins, assuming that the interaction of the diphenyl porphyrin was the same as for simple B-substituted porphyrins.

ESR, Metal-Metal Interactions

Electron spin resonance was used in the characterization of both copper-copper and cobalt-cobalt complexes of the mixed cofacial diporphyrin. The spectra, measured as toluene-CH_2Cl_2 glasses at 77°K, exhibited features indicative of interaction between the two metal centers.

The spectrum for the bis copper mixed diporphyrin 50, Figure 16, was very different from that of the well characterized monomeric species, Figure 23A. The close proximity of the metal centers in cofacial diporphyrins allows spin interactions to occur, producing for the biscopper complexes a triplet spectrum.

Interactions between the two centers, indicates that the electron exchange was faster than the resonance frequency ($10^{10}s^{-1}$). Each electron would then experience the total spin of the two metal centers, I = 7 for Cu_2^{+2}. The seven hyperfine lines were weakly discernable in the spectrum and were further split by zero field splitting, (D), which arises mainly from electron-electron dipolar interactions. Similar results have been observed by Chang[40] and

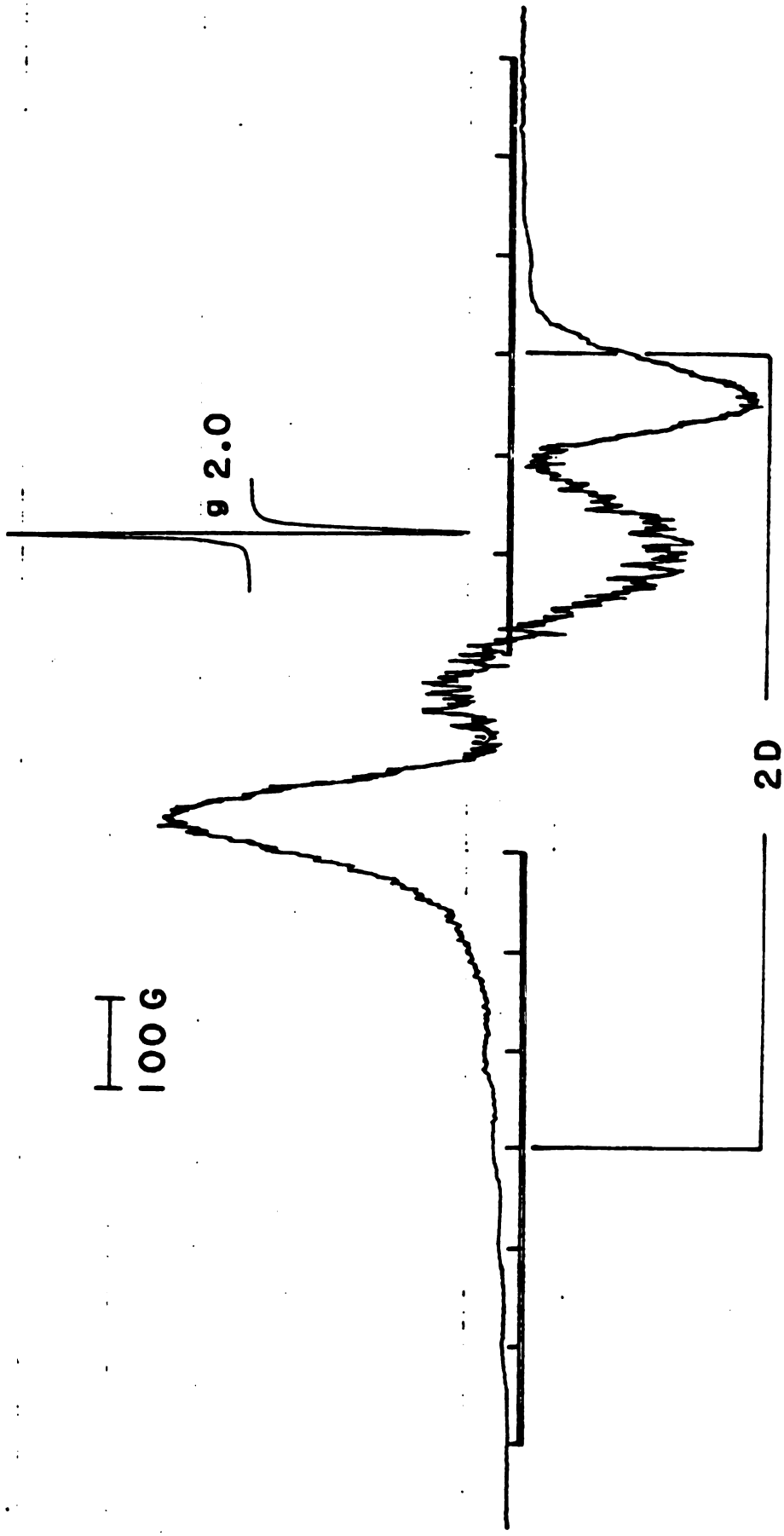

Figure 16. ESR spectrum of Cu(II)-Cu(II) complex of mixed diporphyrin 50 in frozen solution (5% toluene/CH_2Cl_2) at 77°K.

Collman[41], where D has been used to determine the internuclear distance between the two metals. Recent results, however, indicate that the metals tend to assume a slipped orientation in flexible dimers.[41]

The biscobalt (III) complex of the mixed cofacial diporphyrin exhibited no esr signal at 77°K. Reduction with dithionite followed by addition of 1-trityl imidazole produced a weak signal which was enhanced by the addition of iodine, Figure 17. Analogous behavior has been observed with other cobalt cofacial diporphyrins.[40,41]

The initial esr silent species represents the oxidized Co(III)-Co(III) diporphyrin. In the presence of nitrogenous bases, Equation 5, the reduced species binds oxygen to generate a μ-peroxo form which should also be esr silent but was inevitably contaminated with small amounts of the μ-superoxo complex, which can be deliberately formed by oxidation with molecular iodine. The 15 line isotropic spectrum reflects the coupling between the two S = 7/2 centers by the superoxo bridge.

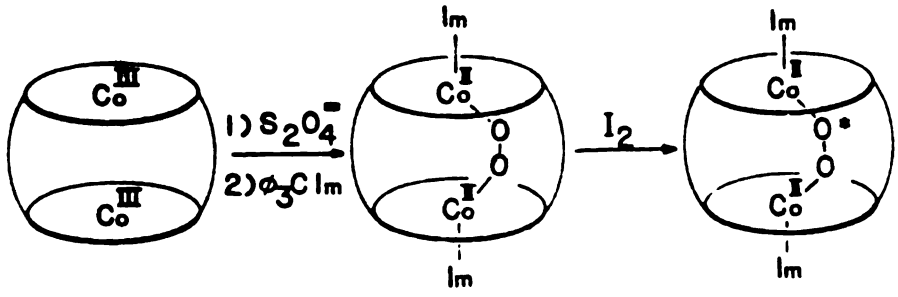

(5)

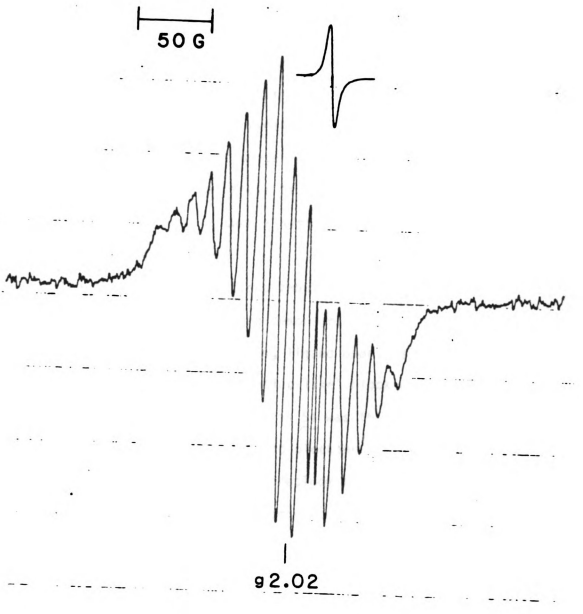

Figure 17. ESR spectrum of dioxygen adduct of the bis cobalt complex of diporphyrin 50 at room temperature after addition of a small amount of I_2.

Porphyrins with Metal-Chelating Appendages

A versatile model for cytochrome oxidase should incorporate several features, most importantly; the ability to hold a copper and an iron center in close proximity. In addition, the model should be stable in the presence of oxygen or hydroxide, e.g., no Fe-O-Fe μ-oxo dimer formation, so that these ligands may serve as possible bridging. In an effort to achieve such a system, several blocked and chelating porphyrins were designed.

The effectiveness of the p-t-butyl phenyl group in preventing μ-oxo dimer formation has been demonstrated. The β-keto amide linkage shoulld also direct a chelating ligand over the porphyrin core in the same fashion as the more "peptide-like" blocking groups (malonyl derivatives). Diphenyl porphyrin 51 was the initial target, incorporating both chelating and blocking groups. The anionic nature of the ligand was utilized to preclude the need of counter ions which might interfere with metal interactions.

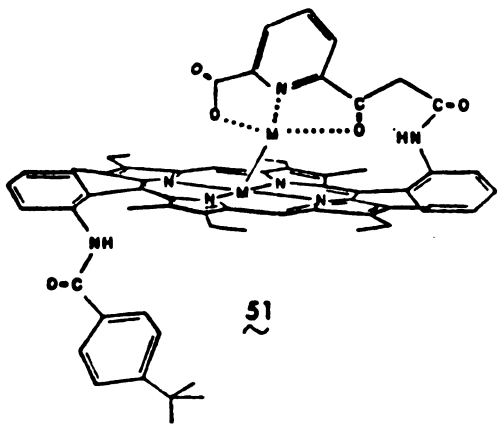

51

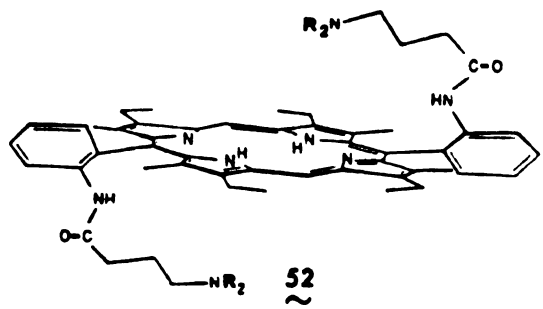

52

R = CH_2CO_2H

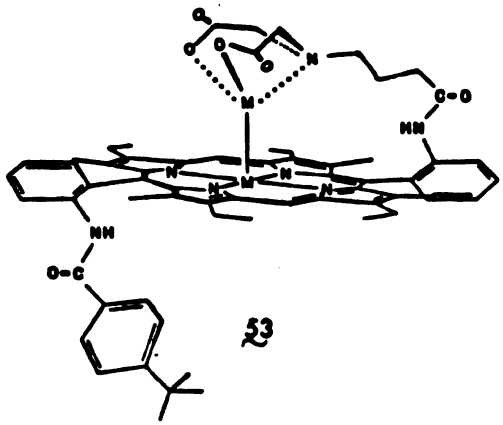

53

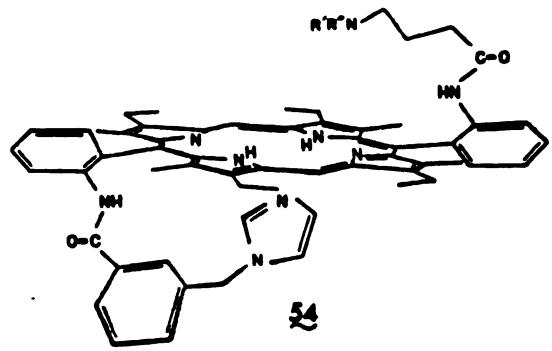

54

$R' = R'' = CH_2CO_2H$

Difficulties encountered in verifying the integrity of the β-keto pyridyl porphyrin led to the development of alternate systems, diphenyl porphyrin 53. The coordination sphere of this system was very similar to EDTA. The butyl amide linkage would be less directed, however, the increased flexibility would allow the two metal centers to achieve an ideal geometry. Three porphyrins utilizing this amino diacetic acid chelate were constructed. Initially a symmetric species capable of coordinating three metals was constructed to develop the synthetic pathway. The ligand was then attached to mono-blocked and imidazole appended systems. The blocked system would prevent μ-oxo dimer formation while the appended system would allow the study of the influence of axial imidazole on promoting spin coupling.

Synthesis

β-Keto Pyridine

The ligand 55 was constructed according to Scheme 5. The mono methyl ester was easily generated from dipicolinic acid by the method of Ooi and Magee.[42] The crude acid chloride, resulting from treatment of the mono acid with thionyl chloride, was converted to the β-keto acid by the method of Van Der Baan.[43] Addition to a solution of lithio bis-trimethylsilyl malonate at dry ice temperatures was followed by careful hydrolysis with sulfuric acid. The mono decarboxylated product was purified by washing with cold ether and crystallization. The product was found to be unstable at room temperature and slowly decomposed.

Scheme 5.

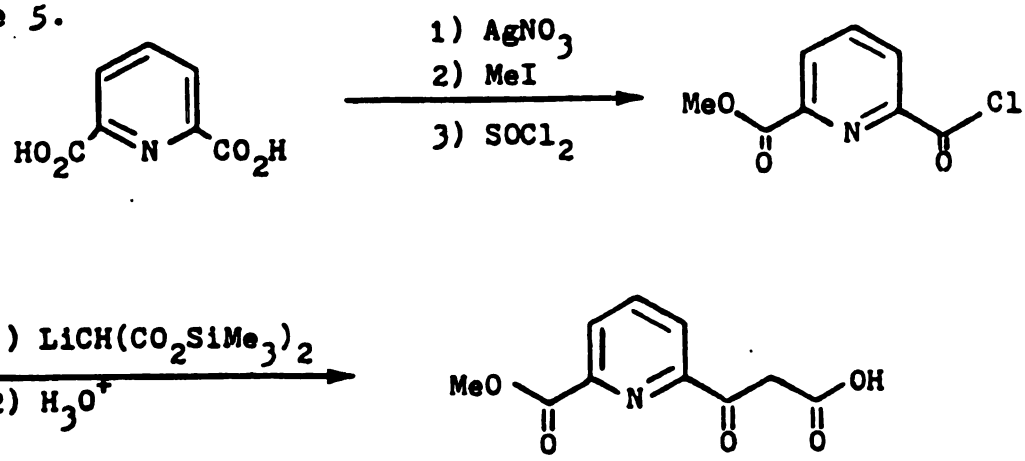

All attempts to generate the acid chloride of the unstable B-keto acid failed, generally resulting in black solutions which probably resulted from rapid ketene formation.

Eventually two routine peptide forming reagents proved successful in coupling the o-amino phenyl porphyrins with the β-keto acid. Dicyclohexylcarbodiimide (DCC) and bis imidazole carbonyl (Im_2CO) were both effective in amide formation, but at different rates. A CH_2Cl_2 solution containing equimolar quantities of DCC, β-keto acid, and porphyrin resulted in quantitative yields after 1h at room temperature. Similar results with Im_2CO would only be obtained if the reaction were allowed to proceed for several days. The effectiveness of DCC was surprising, since others have reported the failure of this reagent in reacting with other o-amino phenyl porphyrins due to steric congestions.[44] We, as well, have not found widespread application of this coupling reagent in diphenyl porphyrins.

The formation of one species by both reagents was indicated by tlc of the free base and zinc complex in a variety of solvents and solid phases. Initial ^1H NMR data showed the presence of a mixture of compounds, which could not be separated. Extensive ^1H NMR studies eventually proved the integrity and the singular nature of the reaction product from both coupling reactions.

The pyridine ester was easily hydrolysized with methanolic sodium hydroxide.

Amino Diacetic Acid

The amino diacetic acid ligand was constructed onto the porphyrin in a stepwise fashion, Scheme 6. Efforts to construct the ligand prior to coupling with the porphyrin failed due to the instability of the tertiary amine. The protected amino butyric acid was linked to the o-amino phenyl porphyrins by a mixed anhydride process using ethyl chloroformate and triethylamine in toluene. The yields of the coupling reaction were routinely low, ca. 35%, however, the only other porphyrin recovered was the starting material.

Initially the carbobenzyloxy (CBz) protected butyroamino acids were used. Their resistance to acid hydrolysis and inconsistent results with catalytic hydrogenation in deprotection led to the use of t-butyloxy carbamide (tBoc) systems.

Purification of reaction mixtures by extraction with 80% phosphoric acid led to premature hydrolysis of the tBoc group. Purification of the very polar free amine was avoided by initial purification of the reaction mixtures on protonated silica columns. Hydrolysis of the purified protected amine proceeds quantitatively in CHl/acetic acid.

The free amines react readily with ethyl bromoacetate in refluxing acetonitrile-CH_2Cl_2 containing a small amount of triethylamine. Short reaction times or lack of base led to isolation of monoesters. Hydrolysis to the diacid was easily achieved with methanolic sodium hydroxide.

Scheme 6.

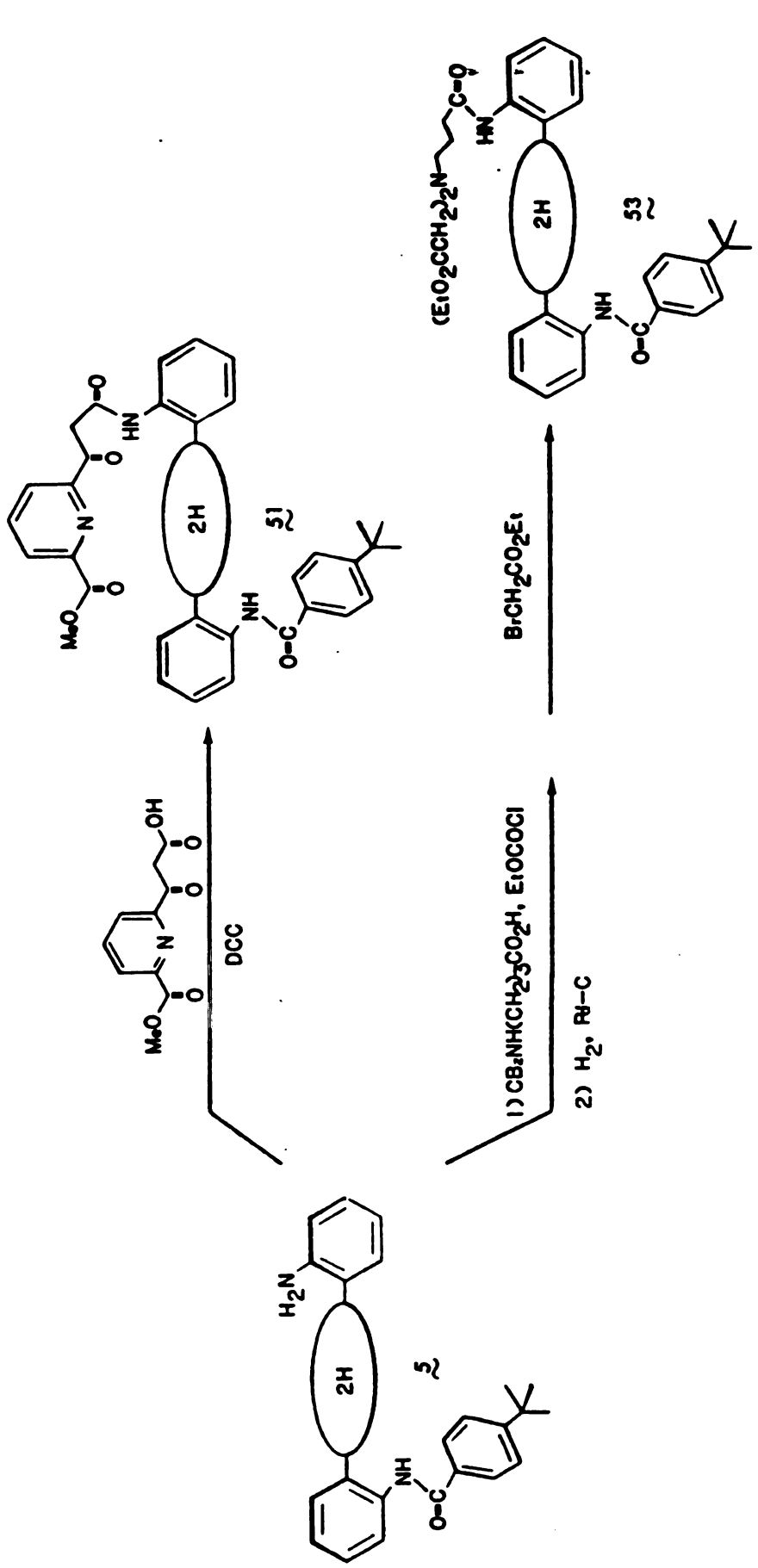

This sequence of reactions led to the formation of the symmetrical tetraacid, 53, which was water soluble, as well as the mono t-butyl benzamide blocking and chelating systems. The trans appended-imidazole was carried out to the free amine stage, however, lack of sufficient material after hydrogenation of the CBz protecting group precluded completion of the synthesis.

Metallation of the systems prior to hydrolysis of the esters produced only the metallo-porphyrin species, as evidenced by epr. Following hydrolysis, the ligands were metallated with copper acetate, which is epr silent due to dimerization.

^{1}H NMR

^{1}H NMR of the free base porphyrins were routinely used to verify the integrity of products and precursors in the reactions leading to protected-chelating porphyrins.

The ^{1}H NMR of the free pyridyl β-keto acid, 55, reveals the presence of enolization by the appearance of vinyl hydrogens, δ6.4 ppm, and the reduced intensity of the α-methylene signal, integration of 1.2 vs. 3 for the methoxy protons. The pyridyl hydrogens appear as a multiplet centered at δ8.0 ppm.

The spectrum of the coupled product in $CDCl_3$ at room temperature showed two species, Figure 18B, a symmetric and an unsymmetric in a ratio of 1:4, respectively. The mixture was indicated by the doubling of all signals, except the ring methyls which point toward the symmetry of the species.

Figure 18. 250 MHz ^{1}H NMR spectra of chelating diphenyl porphyrin 51 in (A) $CDCl_3$ containing trifluoroacetic acid; (B) $CDCl_3$; (C) toluene d_8, all spectra measured at 22°C.

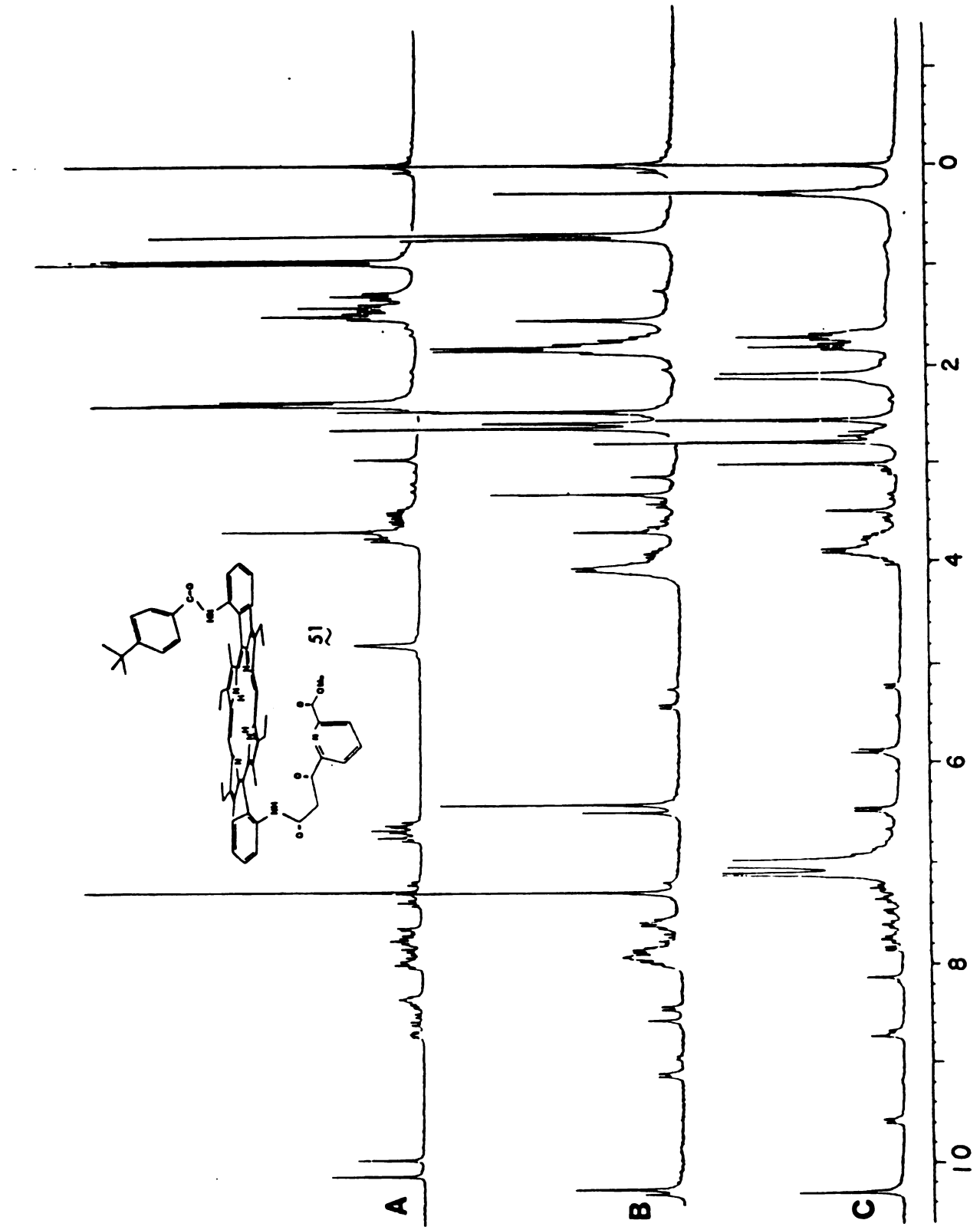
51
A
B
C
0
2
4
6
8
10

After chromatography failed to separate or vary the composition of the mixture, several perturbations were made on the system and the responses were followed by ^1H NMR. The following experiments failed to alter the ratios consistently:

1. Temperature variations, -50 - +50°C.
2. Dilution studies, 20 fold changes.
3. Addition of methanol - d_4.
4. Metallation, Zn, followed by addition of excess imidazole.
5. Protonation, TFA/D_2O.

Eventually the use of toluene-d_8 produced a spectrum reflecting one species, Figure 18C. The AA'BB' quartet observed for the phenyl blocking group was indicative of hindered rotation due to aggregation, as observed previously for the cis bis p-t-butyl benzamide system. Having shown that one species was formed, re-examination of the $CDCl_3$ spectrum revealed identity of the complex. The methyl ester, α-methylene, and enol hydrogens observed in the free ligand were all evident in the coupled complex although at slightly shifted positions. The pyridyl hydrogens are shifted far upfield due to the interaction with the porphyrin ring current. The triplet and doublet of the pyridyl ring, δ3.4 and 3.6 ppm, respectively, shift back downfield to straddle $CDCl_3$ when TFA/D_2O was added to the system, Figure 18A. The changes reflect the disruption of the interaction when both aromatic ring systems become protonated.

The nature of the components of the mixture in $CDCl_3$ are unknown, however, it can be speculated that the highly symmetric species

represents some type of dimeric form. It would be otherwise impossible to explain the high symmetry observed for an unsymmetrical molecule when the ring methyls have always served as extremely sensitive probes.

Amino Diacetic Acid

The high symmetry of the trans tetraacetic acid porphyrin and its precursors simplified assignment of resonances and identification of reaction products, Figure 19. The coupling of the CBz-protected butyroamino acid to trans bis o-amino DPE was indicated by the usual downfield shift of the phenyl protons and the appearance of side chain resonances.

Deprotection of the amine produced large upfield shifts in the side chain resonances. This displacement was due to the coordination of the free amine to the amide NH, exposing the β and α-methylenes to the porphyrin ring current. Evidence for this coordination was also indicated by the corresponding shift of the amide proton during the reaction sequence.

Similar trends were observed in the synthesis of the blocked and imidazole tethered derivatives, Figures 20 and 21. The lack of symmetry in these systems caused splitting of the ring methyls and produced complex patterns in the aromatic region.

The ^{1}H NMR of paramagnetic metallated species, e.g., Cu and Fe, are inherently broadened and offer little structural data. The sensitivity of the isotropic shifts to the spin density of the metal would make the method ideal for probing the interaction between two

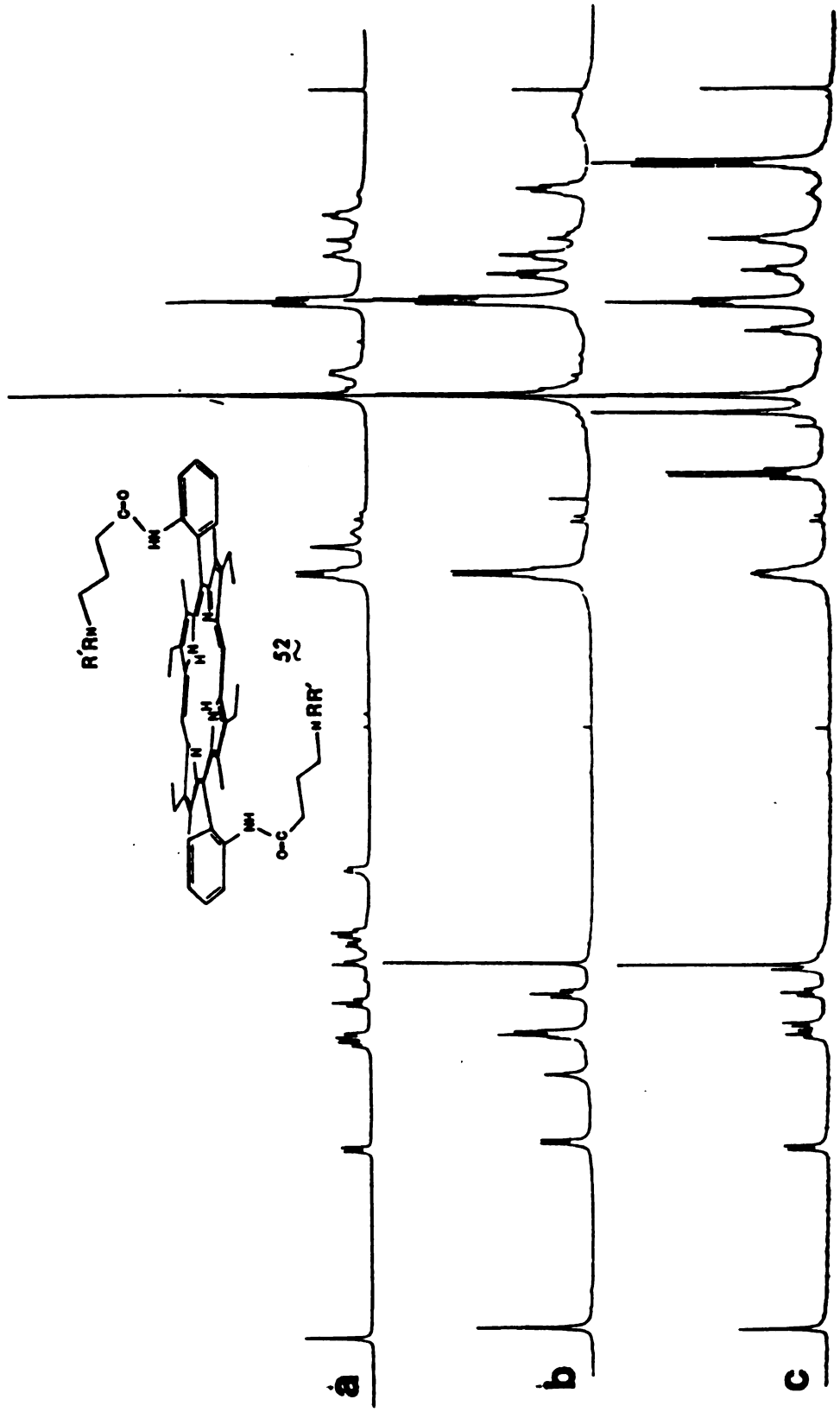

Figure 19. 250 MHz ^{1}H NMR spectra of trinuclear diphenyl porphyrin 52 and precursors, (a) R = H, R' = CBz; (b) R = R' = H; (c) R = R' = CH_2CO_2Et.

Figure 20. 250 MHz ^{1}H NMR spectra of blocked and chelating diphenyl porphyrin 53 and precursors, (A) R = H, R' = tBoc; (B) R = R' = H, (C) R = R' = CH_2CO_2Et.

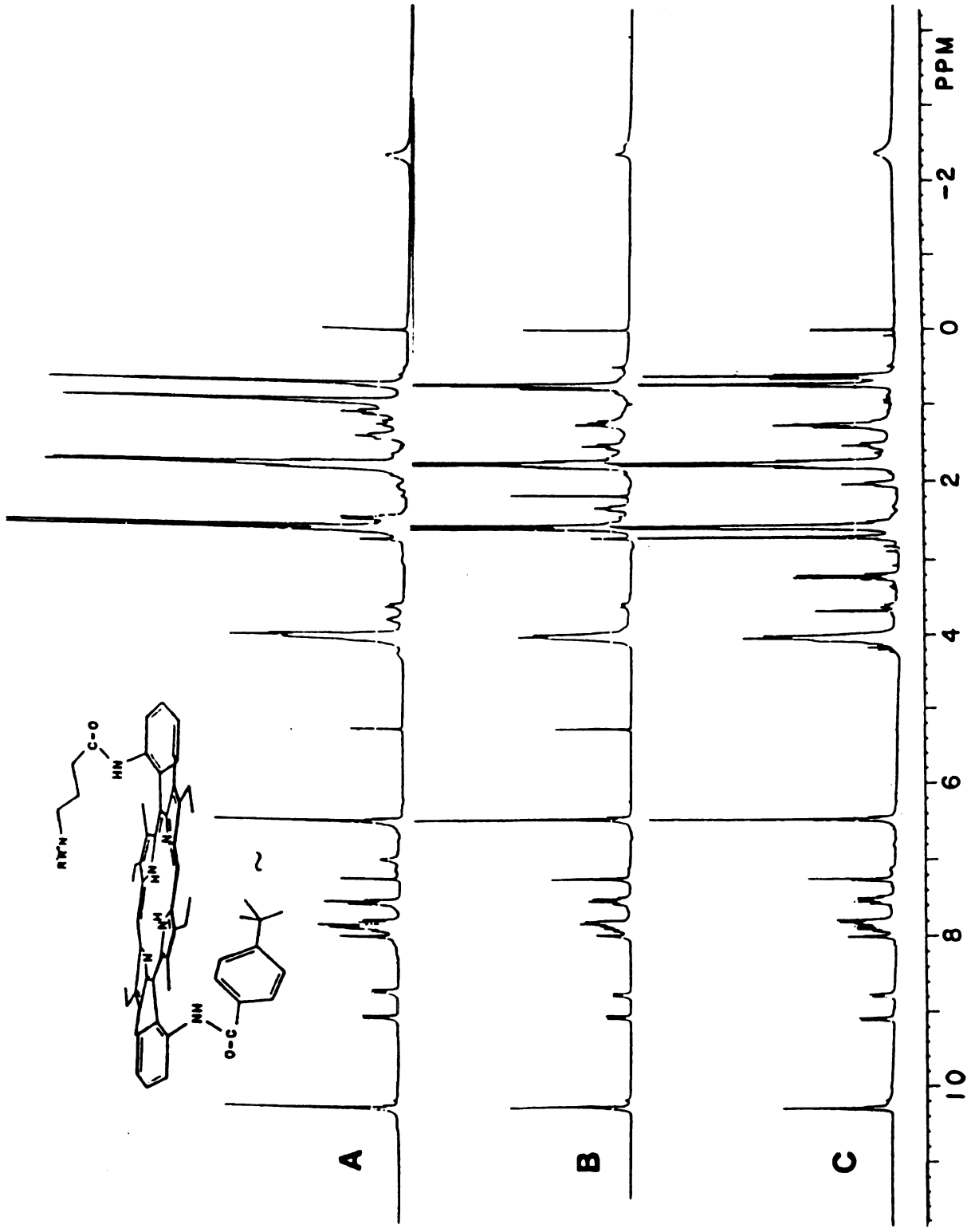
A
B
C
10
8
6
4
2
0
-2
PPM

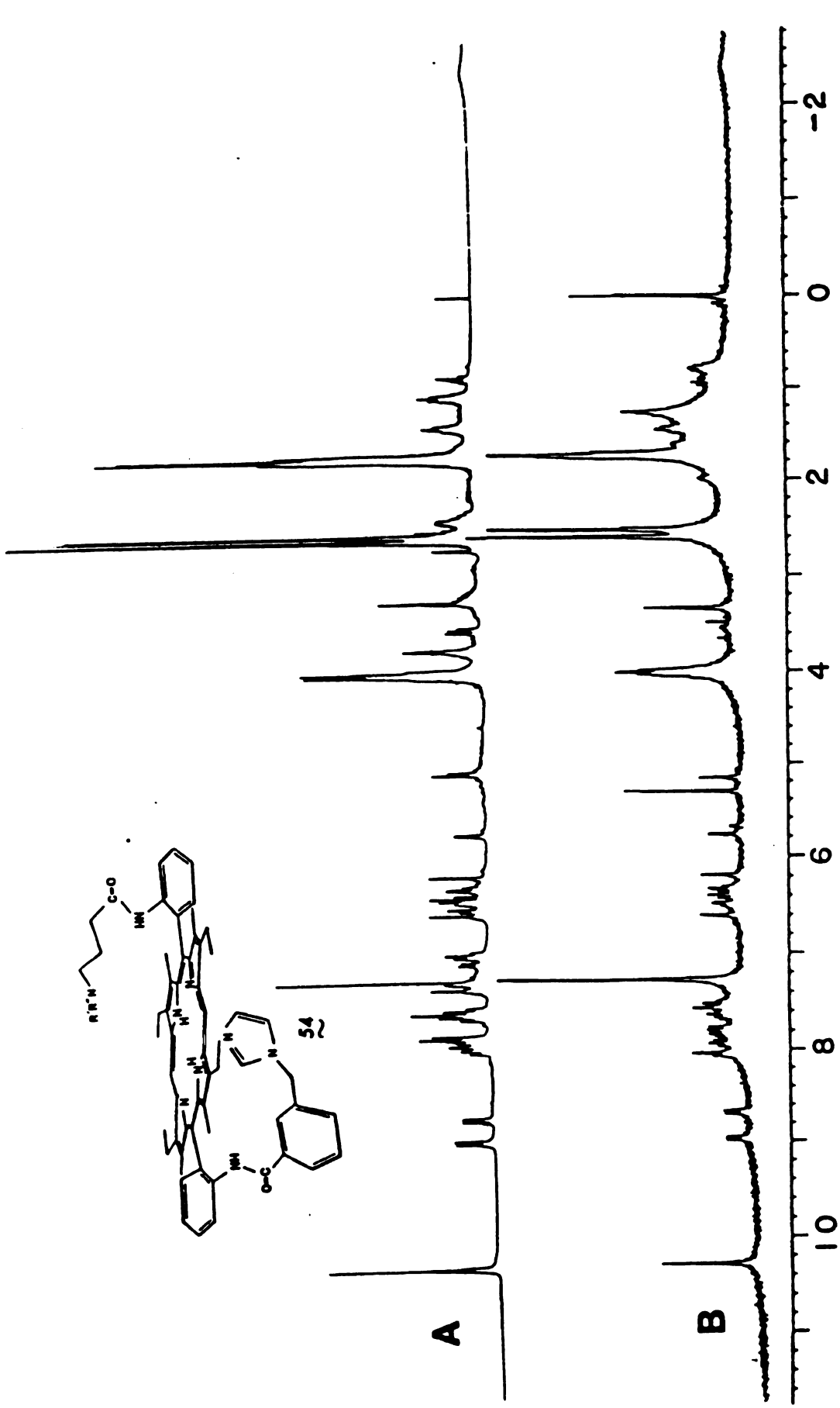

Figure 21. 250 MHz ^{1}H NMR spectra of imidazole appended and chelating diphenyl porphyrin 54 and precursors, (A) R = H, R' = CBz, (B) R = R' = H.

metal centers.[45] Unfortunately, few studies have been performed on mixed metal systems to enable correlation of potential results.

Electronic Spectra, Binuclear Chelating Hemes

The electronic spectra of the chelating systems were dominated by the porphyrin rings. The chelating appendages have little effects on the visible or Soret region of the free base or metallated species, except to provide potential ligands.

Gunter and Mander[6] have used changes in the electronic spectra as evidence for the incorporation of metals into their binuclear diphenyl heme hydroxides. Similar changes were observed for the blocked-chelating ferric hydroxides upon the addition of copper salts, Figure 22. However; similar treatment of non-chelating hemes, e.g., trans bis(p-t-butyl benzamide) DPE ferric hydroxide, produced identical spectral changes. The deviations in the spectra merely reflect the metal catalyzed ligand exchange in hemes and cannot be used to verify metal chelation at the appendages.

ESR - Binuclear Systems

Electron paramagnetic resonance was used to probe the ability of the chelating ligands to bind Cu(II) and investigate possible spin interactions between the two metal centers.

The esr spectra of the bis copper adducts of the β-keto pyridyl and amino diacetic acid protected porphyrins, Figure 23, showed no coupling between the two metal centers. The upper trace represents the spectra of the monomeric copper porphyrin, 53, and the lower trace the effect of adding copper acetate and washing with water. Although

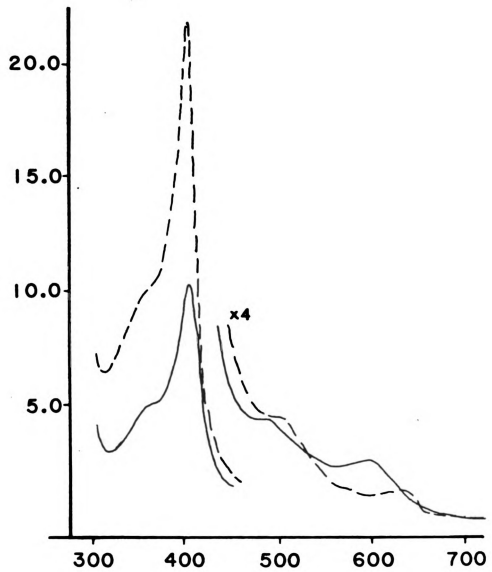

Figure 22. Electronic spectra of the Fe(III)PCl complex of diphenyl porphyrin 53 (——); and the effect of adding Cu(II) acetate to the sample (----).

no coupling was observed, the intensity changes indicated that metallation of the amino-diacetic acid ligand did occur. Similar experiments on the B-keto system produced the same results. The lack of coupling in these blocked systems may reflect the random geometry of the metal centers.

The nature of the chelating ligands were more easily determined using a diamagnetic porphyrin, e.g., zinc or nickel systems. Efforts to use zinc porphyrins in copper chelating reactions resulted in trans metallation, as evidenced by the resulting characteristic Cu(II) porphyrin spectrum. The use of the less labile nickel porphyrins produced the desired results, Figure 24. The uppper trace represents the Ni(II) porphyrin and unmetallated β-keto pyridyl system, 51, the weak signal was probably due to small impurities. Treatment with copper acetate produced the lower trace which shows a typical axial copper spectrum.

The mixed heme-copper complexes were constructed to investigate possible interactions. Treatment of the ferric hydroxide of the protected amino diacetic acid system, 53, with copper acetate produced the binuclear system, Figure 25.

The overlapping Cu signal, g = 2, failed to disappear after numerous washings with water.

Conclusions and Further Work

The utility of the diphenyl porphyrin system in its ability to construct binuclear systems has been demonstrated. Mixed cofacial

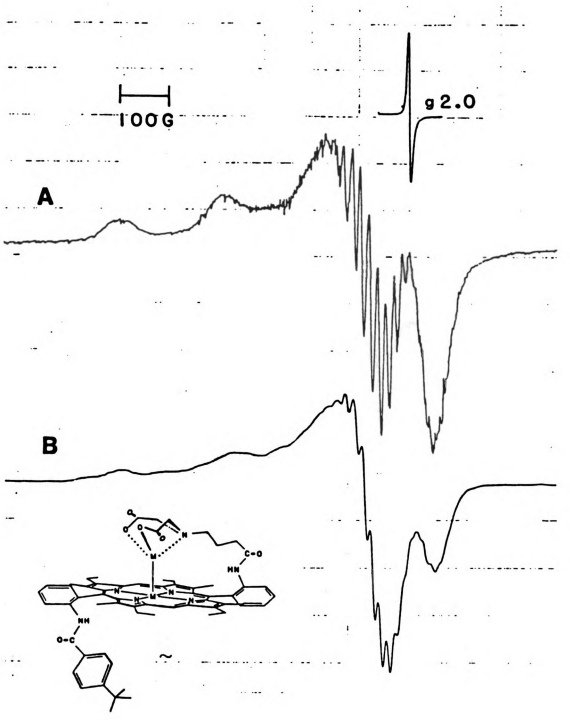

Figure 23. ESR spectra of blocked and chelating diphenyl porphyrin 53. (A) Cu(II) porphyrin-diacid; (B) Cu(II)-Cu(II) complex. Spectra measured in frozen solution (5% toluene/CH_2Cl_2) at 77°K.

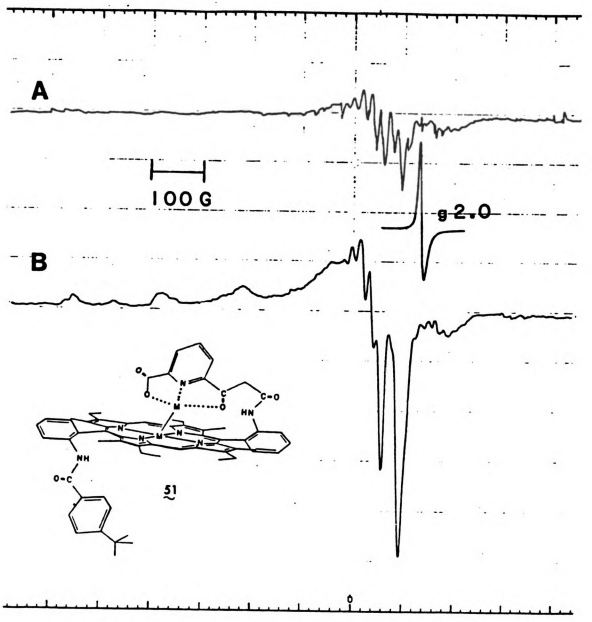

Figure 24. ESR spectra of blocked and chelating diphenyl porphyrin 51, (A) Ni(II) porphyrin-acid; (B) Ni(II) porphyrin Cu(II) complex. Spectra measured in frozen solution (5% toluene/CH_2Cl_2) at 77°K.

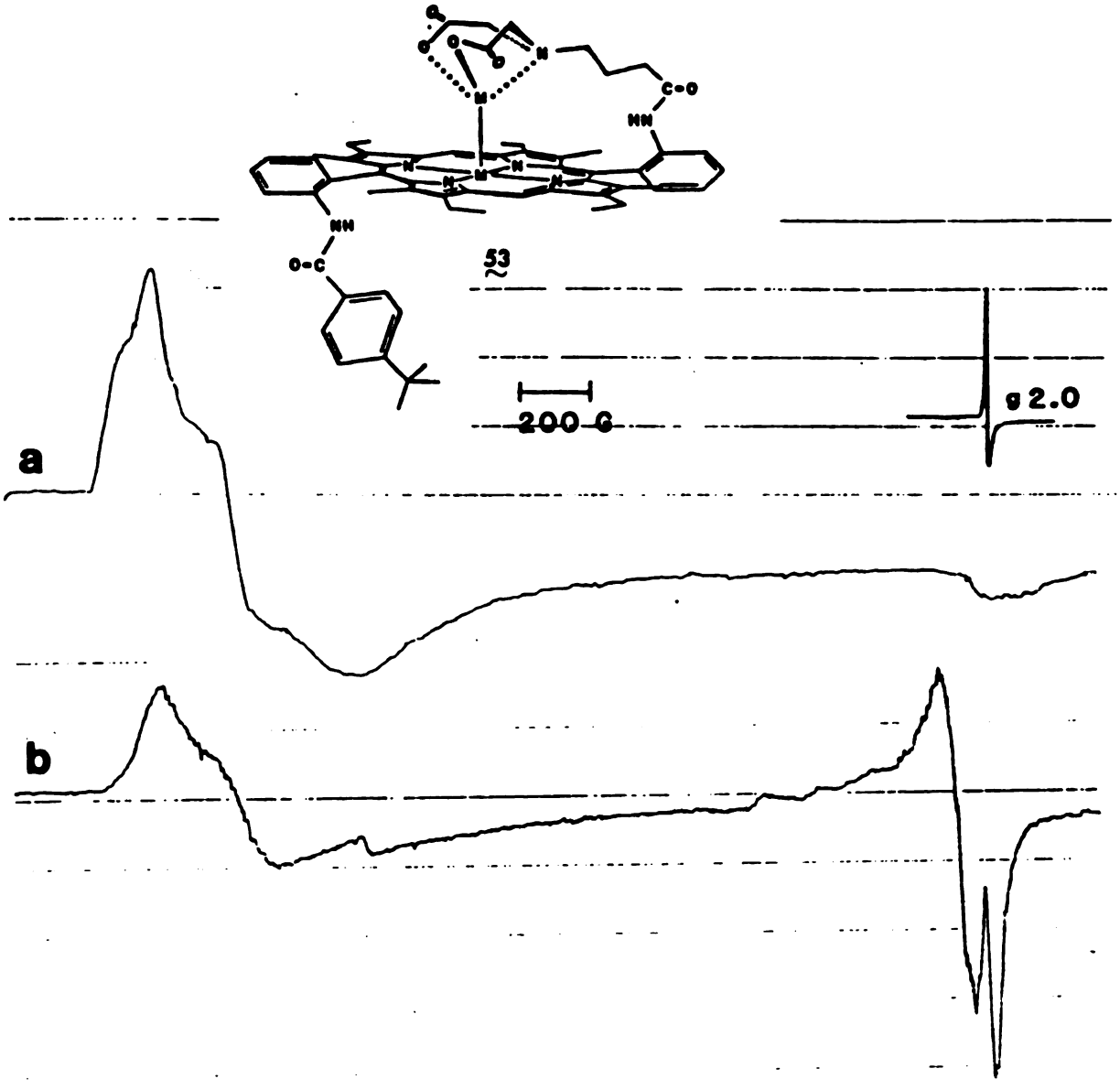

Figure 25. ESR spectra of blocked and chelating diphenyl porphyrin 53, (A) Fe(III)PCl-diacid; (B) Fe(III)PCl-Cu(II) complex. Spectra measured in frozen solution (5% toluene/CH_2Cl_2) at 77°K.

diporphyrins have been constructed in high yield and the bis cobalt complexes of these systems may act as electro catalysts for the cathodic reduction of oxygen to water. This highly rigid system can be exploited further in creating unique inorganic complexes or bio-inorganic models.

The ability to construct non-porphyrin chelating ligands onto these diphenyl porphyrins has also been shown. The exact structure of these systems awaits further characterization. Although no spin coupling was observed in bis copper and iron-copper complexes, the addition of bridging ligands may promote such interaction. The bridging ligands may be added as extraneous species in solution or covalently attached to the porphyrin at the expense of the blocking group. In general, the characterization and exploitation of these multinuclear systems has only just begun.

Experimental (Binuclear Systems)

Mixed Dimer (50)

The C_8 Dimethyl ester (500 mg) was dissolved in formic acid (40 ml) containing hydrochloric acid (3 ml). The solution was refluxed for 2 h before being poured into ice. Extraction with methylene chloride was followed by neutralization. Evaporation gave the crude diacid.

The crude diacid (100 mg) was dissolved in methylene chloride (100 ml) and deareated with nitrogen. Excess oxalyl chloride was added and the mixture was refluxed for 1 h or until tlc after quenching with methanol revealed no acid.

The crude acid chloride, (100 mg of acid) and cis amino diphenyl porphyrin 2 (92 mg) were combined in 2 e of dry methylene chloride containing 2 ml Et_3N. The mixture was refluxed overnight, then quenched with water. After separation, the organic layer was reduced to 100 ml and washed to remove the Et_3N. The solution was then dried over sodium sulfate and eluted through a short silica gel pad with 2% $MeOH/CH_2Cl_2$. Separation on thick layer silica gel plates resulted in 80 mg dimer and 40 mg recovered diamino porphyrin. The nonpolar dimer which does not fluoresce was recrystallized from CH_2Cl_2/MeOH. ^1H NMR ($CDCl_3$) δ-7.71(s, 2H, NH), 1.0-2.2(m, 42H, CH_2, Me), 2.38(s, 6H, Me), 2.40(s, 6H, Me), 3.36(s, 6H, Me), 3.6-4.4(m, 12H, CH_2), 4.61(d, 2H, $-CH_2$), 5.06(d, 2H, CH_2), 6.33(d, 2H, Ar), 7.06(t, 2H, Ar), 7.77(t, 2H, Ar), 8.60(s, 2H, NH), 8.89(s, 2H, meso), 9.06(s, 2H, meso),9.22(d, 2H, Ar), 9.35(s, 2H, meso).

Trans-5,15-bis(o-(N-CBZ-γ-aminobutyramido)phenyl)-2,8,12,18-tetraethyl-3,7,13,17-tetramethylporphyrin (56)

A mixture of CBz-diaminobutyric acid (182 mg, 0.76 mmol) and triethyl amine (78 mg, 0.77 mmol) in dry tolulene (15 ml) was cooled to 0°C under nitrogen. A solution of chloro ethyl formate (82 mg, 76 mmol) in toluene (10 ml) was added dropwise to the cold solution during ca.0.5h; afterward, the mixture was allowed to warm to room temperature for ca. 1h.

Trans-o-diamino porphyrin 1 (74 mg, 0.114 mmol) in dry THF (20 ml) was added dropwise at room temperature. After completing the addition, the mixture was refluxed for 3 h. The solvent was removed

in vacuo and the residue redissolved in CH_2Cl_2 and washed successively with 10% HCl, H_2O, $NaHCO_3$ (sat. aqueous). After evaporation the residue was purified onthick layer silica gel plates eluted with 5% $MeOH/CH_2Cl_2$. The least polar band corresponds to the CBzprotected amine. ^1H NMR ($CDCl_3$) δ-2.33(br s, 2H, NH), 1.05(q, 4H, CH_2),1.40(t, 4H, CH_2), 1.78(t, 12H, Me), 2.35(m, 4H, CH_2), 2.52(s, 12H, Me), 3.67(t, 2H, NH), 3.80(s, 4H, $ArCH_2$), 4.02(q, 8H, CH_2), 6.44(d, 4H, Ar), 6.97(t, 4H, Ar), 7.03(m, 2H, Ar), 7.18(s, 2H, NH), 7.50(t, 2H, Ar), 7.82(m, 4H, Ar), 8.71(d, 2H, Ar), 10.26(s, 2H, meso).

Trans 5,15 bis(o-(γ-aminobutryramido)phenyl)-2,8,12,18-tetraethyl-3,7,13,17-tetramethylporphyrin (57)

The diCBz porphyrin 56 (20 mg) dissolved in formic acid (15 ml) was hydrogenated at 1 atm using Pd/charcoal (5 mg) for 3-5 h. The mixture was diluted with water, neutralized with 10% NaOH and extracted with CH_2Cl_2. The crude product was purified on thick layer silica gel plates with 5% $MeOH/CH_2Cl_2$. ^1H NMR ($CDCl_3$) δ-2.5(br s, 2H, pyrrole NH), -0.05(br, 2H, NH_2), 0.80(m, 4H, CH_2), 1.35(t, 4H, CH_2), 1.52(t, 4H, CH_2), 1.78(t, 12H, Me), 2.54(s, 12H, Me), 4.03(q, 8H, CH_2), 7.49(t, 2H, Ar), 7.82(m, 4H, Ar), 8.15(s, 2H, NH), 8.72(d, 2H, Ar), 10.06(s, 2H, meso).

Trans 5,15 bis(o-(n,N-bis)ethyl acetate)-γ-aminobutyramido)-2,8,12,18-tetraethyl-3,7,13,17-tetramethylporphyrin (52)

A mixture of the diamine 57 (10 mg, 0.022 mmol) and an excess of ethyl bromoacetate in methylene chloride (10 ml) and acetonitrile (10 ml) containing Et_3N (1 ml) was refluxed for 1.5h. Evaporation to

dryness and purification on thick layer plates produced the tetraacetate in 90% yield. ^{1}H NMR ($CDCl_3$) δ-2.4(br s, 2H, NH), 0.63(t, 12H, OEt), 1.29(m, 4H, CH_2), 1.52(t, 4H, CH_2), 1.80(t, 12H, Me), 2.02(t, 4H, CH_2), 2.57(s, 12H, Me), 2.70(s, 8H, CH_2), 3.22(q, 9H, OEt), 4.03(m, 8H, CH_2), 7.09(s, 2H, NH), 7.70(t, 2H, Ar), 7.76(d, 2H, Ar), 7.83(t, 2H, Ar), 8.79(d, 2H, Ar), 10.28(s, 2H, meso).

Trans 5-(o-(α-N-imidazolyl)toluamido)phenyl)-15-(o-(N-CBz- γ-aminobutyramido)pheny)-2,8,12,18-tetraethyl-3,7,13,17-tetramethylporphyrin (60)

This porphyrin was made in the same fashion as the trans bis CBz 56. ^{1}H NMR ($CDCl_3$) δ-2.34(br s, 2H, NH), 1.08(m, 2H, CH_2), 1.42(m, 2H, CH_2), 1.73(m, 12H, Me), 2.38(m, 2H, CH_2), 2.52(s, 6H, Me), 2.58(s, 6H, Me), 3.23(s, 2H, $ArCH_2$), 3.72(s, 2H, $ArCH_2$), 4.00(m, 8H, CH_2), 5.09(s, 1H, Im-H), 5.72(s, 1H, Im-H), 6.2-6.6(m, 5H, Ar, Im-H, NH), 7.5-8.0(m, 7H, Ar, NH), 8.71(d, 1H, Ar), 8.95(d, 1H, Ar), 10.27(s, 2H, meso).

Trans 5-(o-(α-N-imidazolyl)toluamido)phenyl)-15-(o-(γ-aminobutyramido)phenyl)-2,8,12,18-tetraethyl-3,7,13,17-tetramethylporphyrin (61)

The mono CBz α-Im 60 was deprotected according to the previous method to give a trace of this free amine. ^{1}H NMR ($CDCl_3$) δ-2.4(br s, 2H, NH), 1.0-1.6(m, 6H, CH_2), 1.75(m 12H, Me), 2.53(s, 6H, Me), 2.61(s, 6H, Me), 3.32(s, 2H, $ArCH_2$), 4.0(m, 8H, CH_2), 5.16(br s, 2H, NH), 5.77(s, 1H, Im-H), 6.20(s, 1H, Im-H), 6.32(d, 1H, Ar), 6.40(t, 1H, Ar), 6.50(d, 1H, Ar), 6.60(s, 1H, NH), 7.4-8.0(m, 7H, Ar), 8.69(d, 1H, Ar), 8.98(d, 1H, Ar), 10.28(s, 2H, meso).

Trans 5-(o-(α-N-imidazolyl)toluamido)phenyl)-15-(o-(N-tBoc-γ-aminobutyramido)phenyl)-2,8,12,18-tetraethyl-3,7,13,17-tetramethylporphyrin (58)

The mixed anhydride coupling was used involving 155 mg tBoc, 100 mg Et_3N, and 100 mg t-butyl porphyrin 5. Purification was performed on protonated silica columns using 10% acetic acid/CH_2Cl_2 to elute unreacted amino acid. The porphyrins were eluted with 10% methanol/CH_2Cl_2. After washing with 5% NaOH, then purified on thick layer plates to yield: ^1H NMR ($CDCl_3$) δ-2.35(br s, 2H, NH), 0.74(s, 12H, tBu), 0.96(s, 12H, tBoc), 1.10(m, 2H, CH_2), 1.38(t, 2H, CH_2), 1.76(m, 12H, Me), 2.44(m, 2H CH_2), 2.55(s, 6H, Me), 2.59(s, 6H, Me), 4.04(m, 8H, CH_2), 6.48(s, 4H, Ar), 6.97(s, 1H, NH), 7.54(t, 2H, Ar), 7.7-7.9(m, 3H, Ar), 8.0(s, 1H, NH), 8.73(d, 1H, Ar), 9.09(d, 1H, Ar), 10.30(s, 2H, meso).

Trans 5-(o-(p-t-butylbenzamido)phenyl)-15-(o-(γ-aminobutyramido)phenyl)-2,8,12,18-tetraethyl-3,7,13,17-tetramethylporphyrin (59)

The purified tBoc protected porphyrin 58 was dissolved in acetic acid (20 ml) containing HCl (2 ml) and stirred at room temperature for 10 min. Diluted with water, neutralized, and extracted with methylene chloride to give quantitatively 59. ^1H NMR δ-2.35(br s, 2H, NH), 0.74(s, 12H, tBu), 1.24(m, 2H, CH_2), 1.53(t, 2H, CH_2),1.76(m, 12H, Me), 2.31(t, 2H, CH_2), 2.56(s, 6H, Me), 2.59(s, 6H, Me), 4.02(s, 1H, NH), 4.20(m, 8H, CH_2), 6.47(s, 4H, Ar), 7.54(m, 2H, Ar), 7.8-7.9(m, 4H, Ar), 8.00(s, 1H, NH), 8.79(d, 1H, Ar), 9.09(d, 1H, Ar), 10.28(s, 2H, meso).

Trans-5-(o-(p-t-butylbenzamido)phenyl)-15-(o-(N,N bisethylacetate)-γ-aminobutyramido)phenyl)-2,8,12,18-tetraethyl-3,7,13,17-tetramethylporphyrin (53)

The free amine protected porphyrin was treated in the same fashion as the trans diamine 57. ^{1}H NMR ($CDCl_3$) δ-2.37(br s, 2H, NH), 0.63(t, 6H, OEt), 0.74(s, 12H, tBu), 1.27(m, 2H, CH_2), 1.52(t, 2H, CH_2), 1.76(m, 12H, Me), 2.03(t, 2H, CH_2), 2.57(s, 6H, Me), 2.59(s, 6H, Me), 2.71(s, 4H, CH_2), 3.21(q, 4H, OEt), 4.03(m, 8H, CH_2), 6.47(s, 4H, Ar), 7.26(s, 1H, NH), 7.48(m, 2H, Ar), 7.5-7.9(m, 4H, Ar), 8.0(s, 1H, NH), 8.77(d, 1H, Ar), 9.09(d, 1H, Ar), 10.28(s, 2H, meso).

Methyl 2-(β-carboxyl)acetyl-6-carboxylate pyridine (55)

Methyl 2-carboxypyridine-6-carboxylate (2-methyl dipicolinate) was prepared from dipicolinic acid via the silver salt according to Ooi and Magee.[42] The monacid monomethyl ester (3 mg) was suspended in benzene and treated with an excess of thionyl chloride (10 ml). The mixture was stirred at 50°C for 8 h. By the end of this period, all the solids had dissolved. The solution was evaporated to dryness and the resultant acid chloride, m/e 200, was used without further purification.

Methyllithium (28.5 mL, 1.4 M) was added dropwise to a solution of bis(trimethylsilyl)malonate (9.64 gm, 38.9 mmol) in ether (77 ml) under argon at -78°. Following the addition, the solution was allowed to warm to 0°, and the above acid chloride (3.8 gm, 19 mmol) dissolved in THF (40 ml) was added. The solution was stirred for 10 min and a cold solution of aqueous sodium bicarbonate (5%, 20 ml) was added.

The mixture was thoroughly shaken before the aqueous layer separated. It was acidified carefully to pH 2 with cold 4N H_2SO_4, then extracted repeatedly with ether (3 x 100 ml). The organic phase was separated, dried, and evaporated to give the crude keto acid. Decarboxylated impurities (mostly 2-acetylpicolinate) were removed by washing with cold ether. The keto acid was recrystallized from CH_2Cl_2 to give white needles. m.p. 120-121°; ^1H NMR ($CDCl_3$-acetone d_6) δ3.96(s, 3H, OCH_3), 4.20(s, 2H, CH_2), 8.20(m, 4H, pyr.); mass spectrum (70eV) M/e 179(M^+-CO_2), calcd 223.

Trans-5-(o-(p-t-butylbenzamido)phenyl)-15-(o-(methyl 2-β-carboxyl)acetyl-6-carboxylamido)pyridine)phenyl)-2,8,12,18-tetraethyl-3,7,13,17-tetramethylporphyrin (51)

To a solution of porphyrin 5 (20 ml, 0.025 mmol) in CH_2Cl_2 (50 ml) was added an excess of the β-keto acid (22.3 mg, 0.1 mmol) and DCC (20.6 mg, 0.1 mmol). The solution was allowed to stir at room temperature for 3 h or until completion of the reaction as indicated by TLC. Water was added and the organic layer separated, washed successively with 10% HCl, water, 5% NaOH, and dried. After evaporation, the crude solid was recrystallized from CH_2Cl_2-hexane to afford a red powder, yield 23 mg, 94%. m.p. 250°C. ^1H NMR (toluene d_8) δ-3.1(br s, 1H, NH), -2.1(br s, 1H, NH), 0.28(s, 9H, t-Bu), 1.70(t, 6H, Me), 2.54(s, 6H, Me), 2.77(s, 6H, Me), 3.00(s, 3H, OMe), 3.08(t, 1H py), 3.50(s, 2H, CH_2), 3.58(d 1H, pyl), 3.80(m, 8H, CH_2), 5.21(d, 1H, py), 5.87(d, 2H, Ar), 6.46(d, 2H, Ar), 7.23(t, 1H, Ar), 7.35(t, 1H, Ar), 7.48((d, 1H, Ar), 7.60(t, 1H, Ar), 7.74(t, 1H, Ar),

7.82(d, 1H, Ar), 8.12(s, 1H, NH), 8.68(d, 1H, Ar), 8.72(s, 1H, NH), 9.57(d, 1H, Ar), 10.29(s, 2H, meso). Anal. Calcd. for $C_{68}H_{80}N_8O_6$C, H 6.58, N 9.55; found C 76.11, H 6.38, N 9.32

CHAPTER 3

THE SYNTHESIS AND CHARACTERIZATION OF SIMPLE AND DERIVATIZED GEMINAL ALKYLATED HYDROPORPHYRINS

Introduction

Hydroporphyrins, porphyrins which are partially reduced, occur in a wide variety of proteins and enzymes. Chlorins (62), (dihydroporphyrins) and bacteriochlorins (63),(tetrahydroporphyrins) have been studied extensively due to the presence of their magnesium complexes as the essential chromophoric units in the photosynthesis of algae, plants, and bacteria.[45] Isobacteriochlorins (64), compounds with adjacent rings reduced, have only recently been found in nature [46] and hence have been studied less extensively. The iron complex, siroheme (65), has been found to be the binding and active site of several assimilatory and dissimilatory sulfite and nitrite reductases.[46,47] The demetallated form, sirohydrochlorin, has also been identified as a key intermediate in the biosynthesis of Vitamin B_{12}[48-50], a corrin.

The scarcity of naturally occurring material promotes the use of model systems of comparable oxidation state in determining why nature has utilized these reduced systems. Hydroporphyrins, as the name

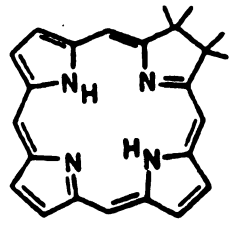

62

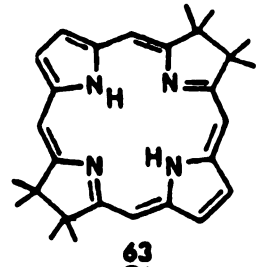

63

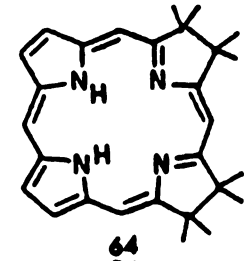

64

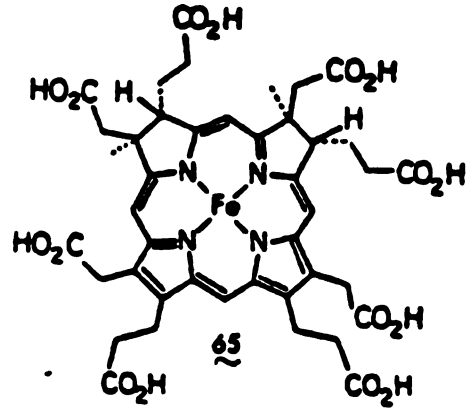

65

implies, result from hydrogenation of the porphyrin macrocycle. The di and tetrahydro derivatives can be generated by a variety of reductive techniques[51] on porphyrins and metalloporphyrins, including: catalytic hydrogenation, diimide, and dissolving metal. These hydro-derivatives undergo facile dehydrogenation to the more unsaturated chlorins and porphyrins.[52] This instability to mild oxidizing agents is characteristic of most naturally occurring chlorins and bacteriochlorins. However, several chlorins and siroheme are stabilized by alkylation.

We have devised a method for constructing gem-di-alkylated hydro-porphyrins such as siroheme and the chlorin, heme d[53-57], which are resistant to mild oxidation. This route has led to the synthesis of both simple and more complex models of the hydroporphyrin family. The characterization of these systems will hopefully help in understanding what special competence these reduced systems have which is required to perform their unique function in nature.

Oxidation-Reduction

Inhoffen and coworkers[58] initially synthesized oxo-analogues of hydroporphyrins by the oxidation of octaethylporphyrin (OEP). The geminal ketones produced were isolated and fully characterized by visible and ^{1}H NMR. We have modified their procedures to maximize the formation of these key intermediates by a similar reaction sequence.[59] The reaction involved oxidation of the peripheral double bonds to form vicinal diols which rearrange in the presence of acid to form geminal alkylated ketones of varying substitution patterns. A fully symmetrical species, such as OEP, will produce one monoketone, six diketones,

and four triketones, Scheme 7. An isophlorin, 72, resulting from the oxidation of trans methine positions, was also isolated. The yield of each component reflects the degree of steric congestion generated by geminal alkylation.

Isolation of the ketones from the complex mixtures involved separation on numerous silica and alumina plates and columns. The crude mixture was initially separated into two fractions using a silica column. The first fraction was eluted with 25% CH_2Cl_2/hexane until the eluent became green, signaling the second fraction. Each fraction was further separated on plates or columns until components were pure by visible spectroscopy. Almost all ketones can be purified to the point of producing crystals from CH_3OH/CH_2Cl_2. The 2, 3 diketone (68), however, was always contaminated by triketones and purification could only be achieved by decomposition of the impurities. The triketone was found to react more rapidly with alkyl lithiums, resulting in isolation of pure diketone after chromatography.

The ketones serve as poor models to naturally occurring hydroporphyrins, due to the dominance of the carbonyls which are in conjugation with the aromatic ring system, but are versatile intermediates in the construction of model systems. Simple systems can be constructed by the reduction of the carbonyls to alkyls or hydrogens.

Our initial studies on these reduce systems involved alkylation of the ketones with alkyl lithiums and reduction of the resulting benzylic type alcohols. These sterically hindered alcohols were resistant to reduction and readily eliminated to the exo-methylene

Scheme 7.

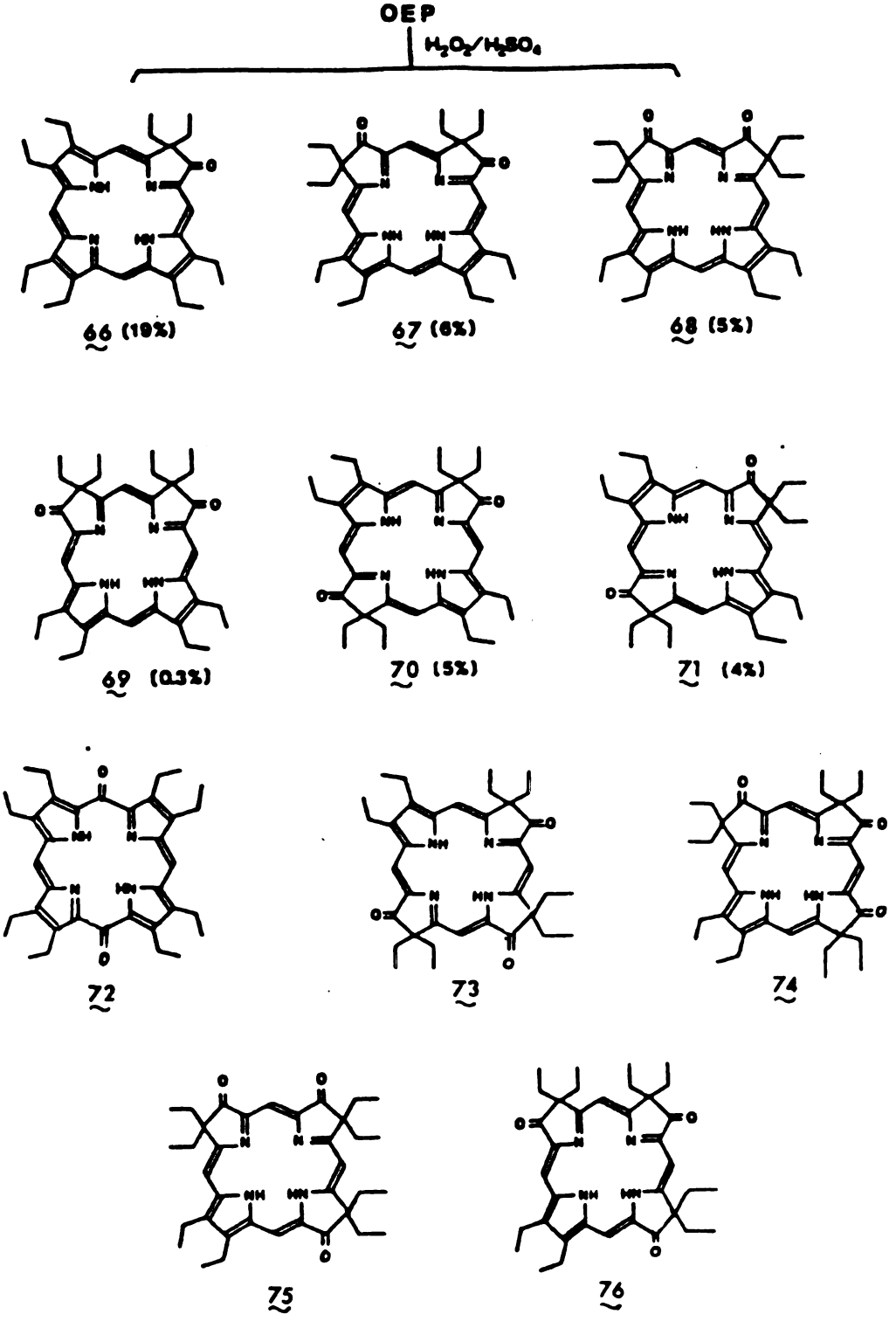

compounds which extend the conjugated system. The reduction of the methylene can be achieved in low yields with catalytic hydrogenation. Alternatively, the alkene or alcohol can be reduced in good yields by a modification of the reductive alkylation procedure developed by MacDonald[60] for alkylating pyrroles.

The reagent, which should be freshly prepared, is composed of a mixture of hydriodic acid, acetic acid, and hypophosphorous acid in a 10:10:1 ratio, respectively. This mixture was added to an acetic acid solution of the alcohol containing a small amount of ascorbic acid. The reaction was warmed to 60° for a few minutes, and then was quenched by diluting with water. This method has found general success in the reduction of chlorin and isobacteriochlorin benzylic-type alcohols, Equations 6, 7, however, failed to reduce the corresponding bacteriochlorins.

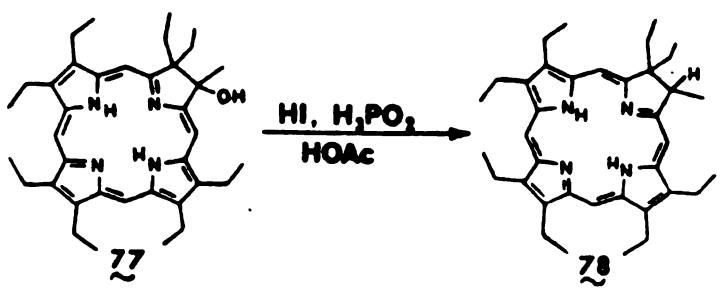

77 78 (6)

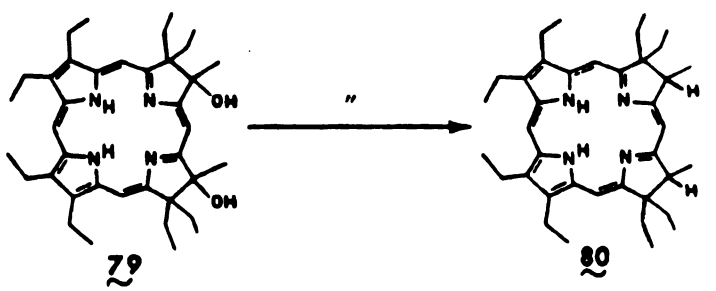

79 80 (7)

The bacteriochlorins represent that least acidic and stable of the reduced porphyrin series. Treatment of their benzylic-type alcohols with the hydriodic acid reagent produced the corresponding alkenes

initially, which decomposed after longer reaction times. Catalytic hydrogenation of the alkenes produced small amounts of the reduced species, as evidenced by visible spectroscopy, however isolation of small quantities of the unstable material proved difficult.

The only method found to be effective in the formation of the reduced species was diimide reduction of the alkene, Equation 8. This reduction, which was also employed by Whitlock and Oester[61] to produce hydroporphyrins from tetraphenyl porphyrins, involves the gradual generation of diimide. Tosyl hydrazide was added portion wise to a pyridine solution of the porphyrin containing potassium carbonate. The competing disporportionation was impeded by maintaining a low concentration of diimide. Progress of the reaction was easily monitored by visible spectra of the reaction mixture. Purification of the light sensitive reduced species was carried out in the dark on an alumina column to yield the reduced species in good yield.

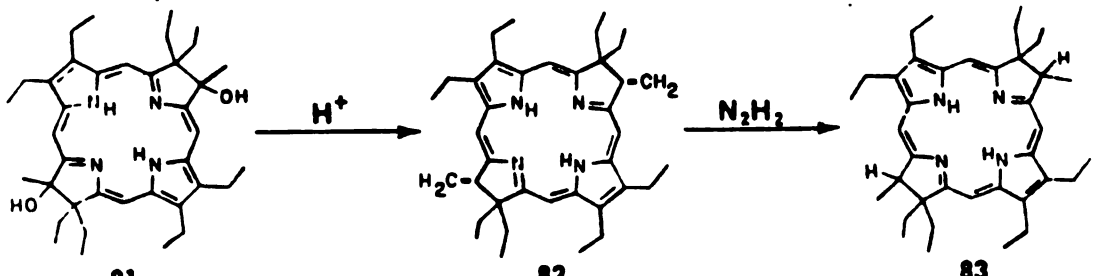

81 82 83 (8)

Ligand Appended Systems

In an effort to study the binding properties of hydroporphyrin-type heme systems, several derivatized hydroporphyrins were designed and constructed. The use of covalently linked imidazoles allows the kinetic study of O_2 and CO binding to reduced hemes. The high local concentration of ligand also allows the study of mixed ligand systems

not possible with unappended porphyrins.

Attempts to utilize the benzylic-type alcohols, 77, in ester couplings failed due to facile elimination, again, owing to thesteric congestion. The alcohol 86, resulting from lithium aluminum hydride reduction of the ketone, cannot eliminate exo to the porphyrin ring, however, coupling reactions only resulted in complex mixtures which may be due to initial isochlorin formation.[62]

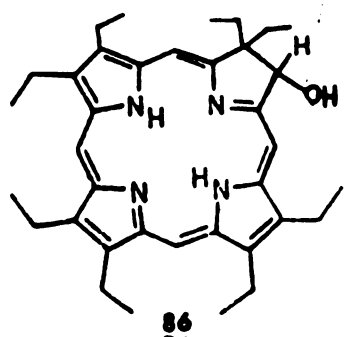

86

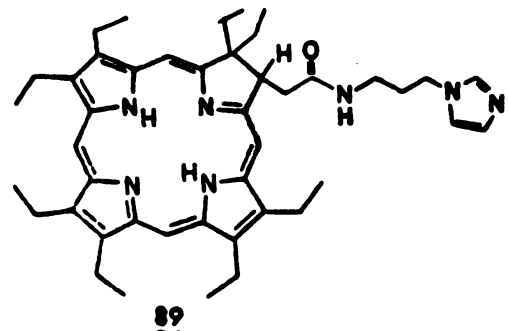

89

Our initial route to chlorins with appended imidazoles involved the treatment of the ketone with the lithium enolate of ethyl acetate to produce the chlorin hydroxy ester, 87, which was easily reduced with the hydriodic acid reagent. Hydrolysis to the acid, 88, was

The low yields associated with hydrolysis and acid chloride formation led to the study of alternate techniques in attachment of the side chain. Utilization of the lithium dianion of the acetyl derivative of 4(N-imidazolyl)butyl amine produced low yields, as did the use of the lithium enolate of the N(isopropyl), N(acetyl) derivative. Wittig reactions involving the generation of the unstable yield of ethyl-β-triphenyl phosphonium proprionate in the presence of the zinc mono ketone also proved unsuccessful.

Eventually the step-wise synthesis was modified to eliminate the

rigorous treatment of the chlorin nucleus, Scheme 8. The ester chlorin was readily reduced with lithium aluminum hydride to produce the corresponding alcohol, 91, in quantitative yield. The alcohol was easily coupled with a variety of imidazolyl acid chlorides to create imidazole appended chlorins, 92-96, of varying chain length.

Scheme 8.

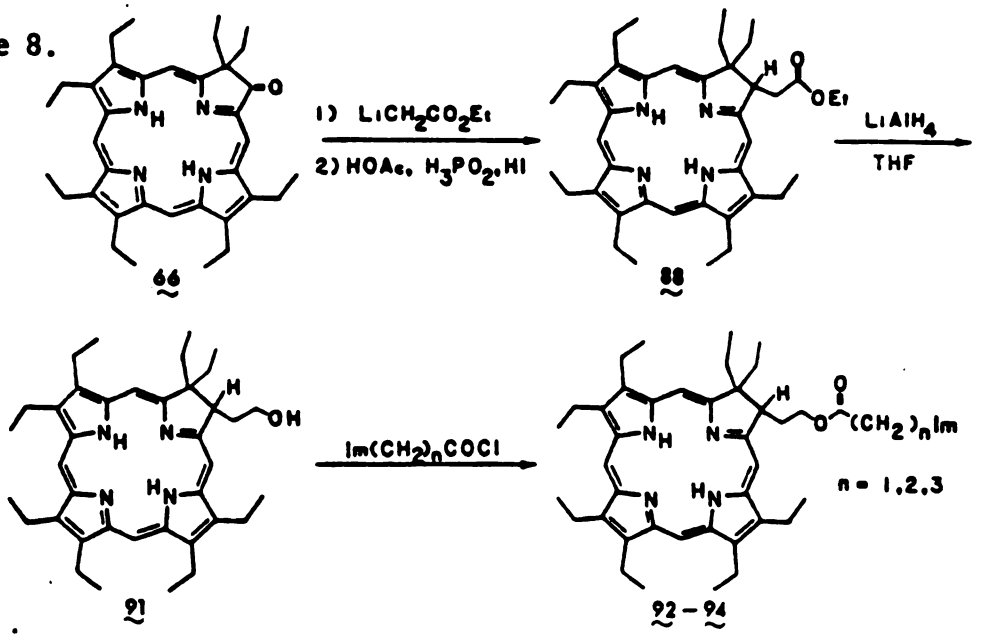

66 88 91 92-94

Derivatized isobacteriochlorins have also been synthesized by a similar route, Scheme 9. Monoalkylation of the 2, 3 diketone (68) was achieved by the dropwise addition of methyllithium to an ethereal solution of the ketone at room temperature. Usually an excess of methyllithium was required to initially destroy the triketone impurities which seem to react faster than the corresponding diketone. Careful monitoring by TLC results in a statistical mixture of mono-, di-, and unalkylated diketone.

Scheme 9.

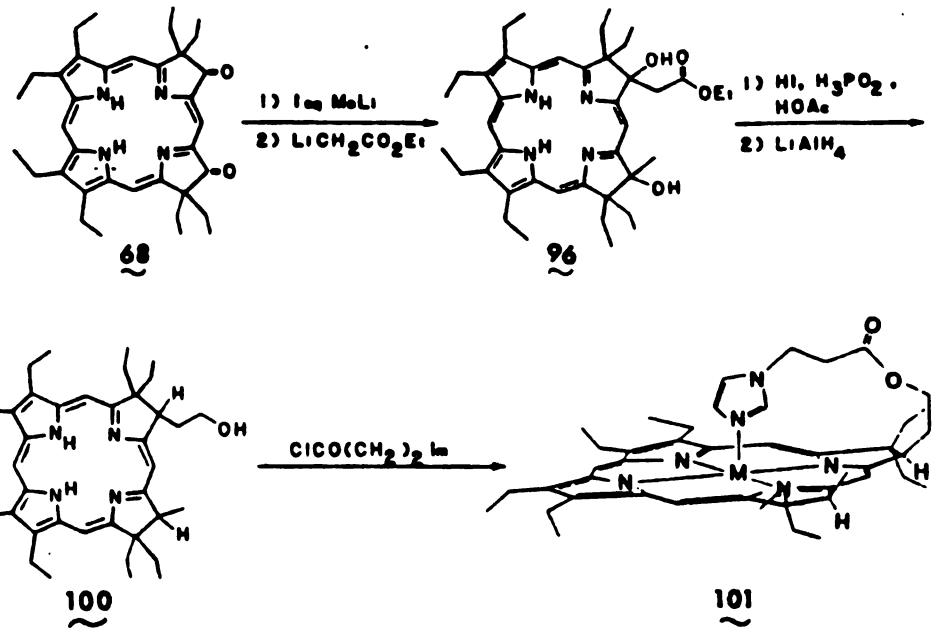

68 96 100 101

Separation of the mono alkylated species, 95, followed by treatment with excess ethyl lithio acetate produced the dissimilarly substituted diol, 96. The diol was unstable to light and air and should be reduced soon after formation, alternatively, the sterically congested intermediate can be stabilized by treatment with mesyl chloride to yield the eliminated species, 97. The diol or alkene was reduced with the hydriodic acid reagent to produce either the mono- or di-reduced species. Analysis of the mono reduction products, 98, indicate that the methyl substituted benzylic-type alcohol was reduced initially, followed sluggishly by the ester alcohol. The strongly hydrogen bonded beta hydroxy ester system was evident in the IR and ^1H NMR spectra. The coordinated carbonyl appears at 1700 cm^{-1} and the hydroxyl at 3480 cm^{-1} in the mono reduced species, while the doubly reduced system shows the free carbonyl at 1760 cm^{-1} and no hydroxyl absorption. In the ^1H NMR the methylene of the rigid β-hydroxy ethyl acetate, Figure 26, appears as an aa'bb' system and as a simple quartet in the fully reduced system.

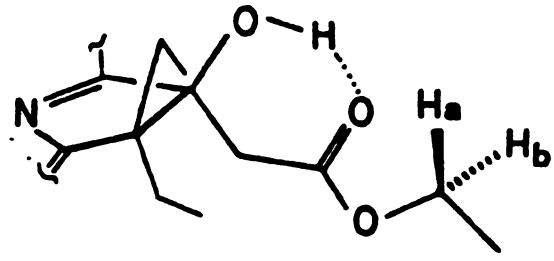

Figure 26. Hydrogen bonding in chlorin and isobacteriochlorin ethyl acetate-alcohols.

The fully reduced system was then treated with lithium aluminum hydride to yield the primary alcohol. 100, which readily coupled with acid chloride imidazoles.

Absorption Spectra

The visible spectra of reduced porphyrins have been well characterized and were routinely used in the identification of ring systems. In general, chlorins have a narrow red band around 650 nm and a Soret three times as intense. Bacteriochlorins have an intense signal around 700 nm and a split Soret. Isobacteriochlorins are characterized by multiple bands in the Soret region and a series of four bands on increasing intensity followed by a weak band around 640 nm. Table 8 lists the visible spectra of some of the model hydroporphyrin systems which were constructed.

The dominance of the carbonyls in conjugation with the system for the geminal ketones was most evident in the visible spectra, Figure 27 through 29, which contain features not present in the alkylated species. Following alkylation, changes on the substituents of the pyrroline ring produced only small shifts in the visible spectra due to the insulating effect of the reduced ring on the residual conjugated system. Alkene formation, which extends

Table 8 Electronic Spectral Data for Selected Hydroporphyrins

Geminal Octaethyl Chlorins

H, CH_3	(78)	647(0.26)[a]		491(0.07)		391(1.0)		
OH, CH_3	(77)	645(0.24)		492(0.07)		391(1.0)		
OH, CH_2CO_2Et	(87)	646(0.28)		496(0.07)		393(1.0)		
H, amide Im	(89)							
free base		644(0.25)		495(0.08)		397(1.0)		
Zn		620(0.26)	575(0.04)	512(0.03)		411(1.0)		
CH_2	(85)	655(0.24)	600(0.04)	533(0.15)	503(0.11)	399(1.0)		

Geminal Bacteriochlorins

2, 6 diketone	(70)		687(0.56)		549(0.05)	513(0.03)	409(1.0)	400(0.83)	
2, 5 diketone	(71)		671(0.21)		549(0.06)	513(0.05)	420(1.0)	399(0.52)	
2, 6(OH, CH_3)$_2$	(81)								
cis		726(0.39)		497(0.16)	467(0.06)	440(0.03)	375(1.0)	350(0.79)	
trans		719(0.43)		497(0.15)	466(0.06)	438(0.04)	374(1.0)	350(0.79)	
$(CH_2)_2$	(83)	738(0.76)	700(0.06)	520(0.06)	487(0.10)	465(0.02)	407(1.0)	384(0.72)	
(H, CH_3)$_2$	(84)	729(0.70)	692(0.07)	493(0.15)	464(0.06)	405(0.10)	375(1.0)	347(0.88)	

Geminal Isobacteriochlorins

2,3 monoketone, OH, CH_3	(95)		639(0.17)	595(0.14)	551(0.08)	519(0.07)	433(0.74)	411(1.0)	
(OH, CH_3)$_2$	(79)	633(0.07)	585(0.25)	544(0.16)	515(0.10)	408(0.39)	385(0.82)	376(1.0)	360(0.61)
(H, CH_3)$_2$	(80)	634(0.03)	589(0.40)	546(0.24)	511(0.12)	400(0.52)	384(0.91)	371(1.0)	358(0.79)

[a] Wavelength in nm; extinction coefficients relative to Soret in parentheses.

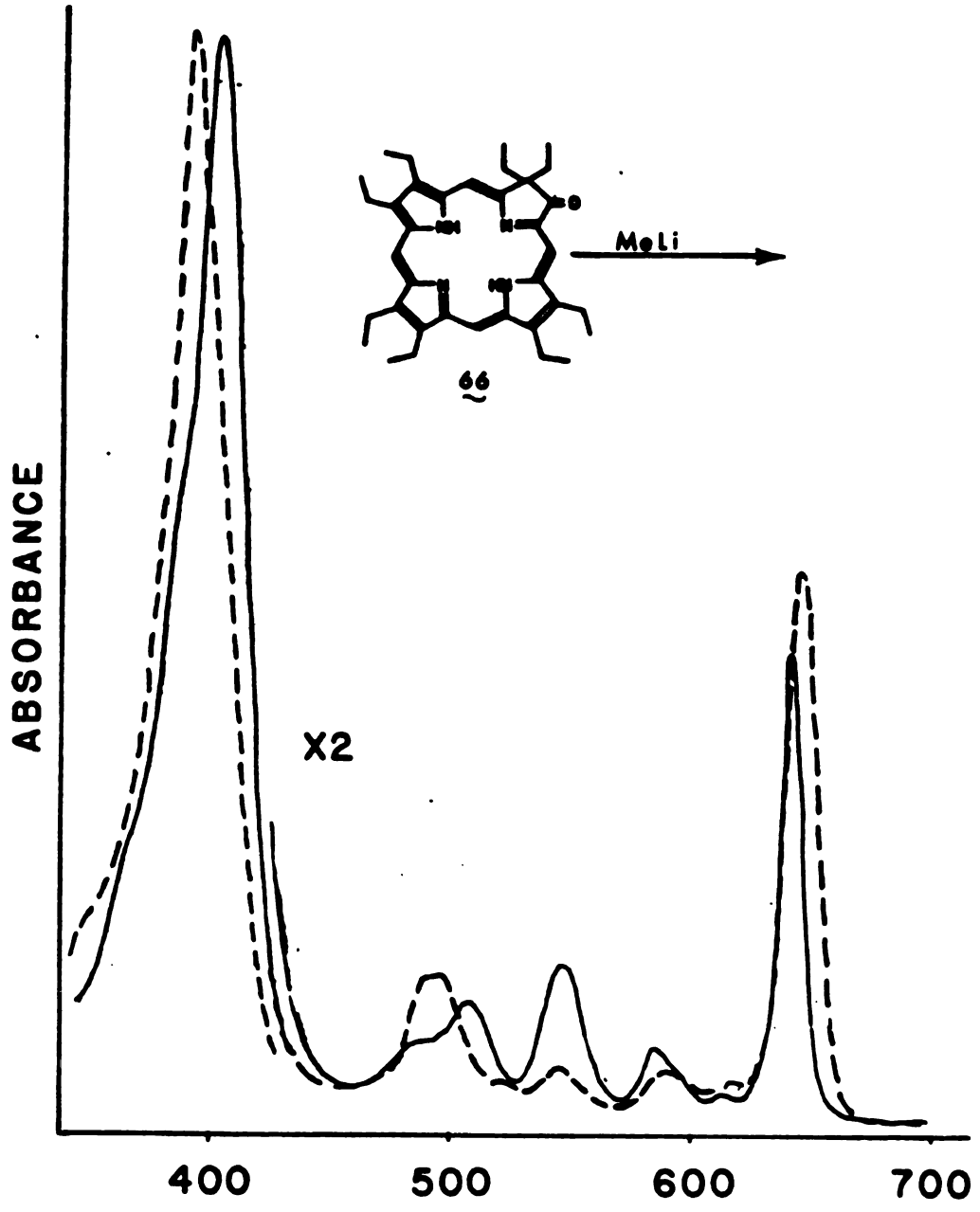

Figure 27. Electronic spectra of monoketone 66 (———); and methyl chlorin alcohol 77 (----).

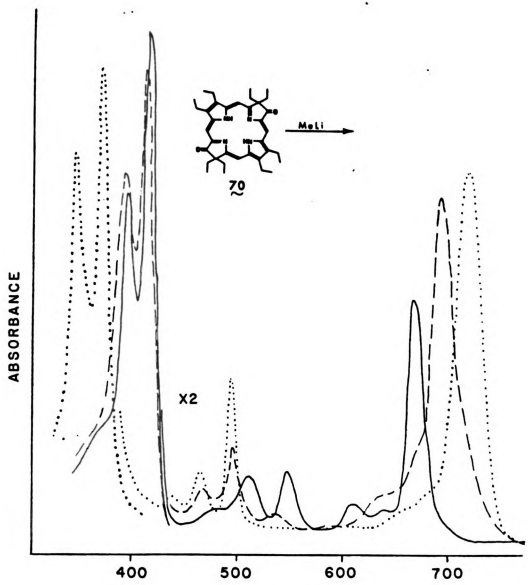

Figure 28. Electronic spectra of 2,6 diketone 70 (_____); and alkylated products; mono alkylated (- - - -); bis alkylated bacteriochlorin 81 (....).

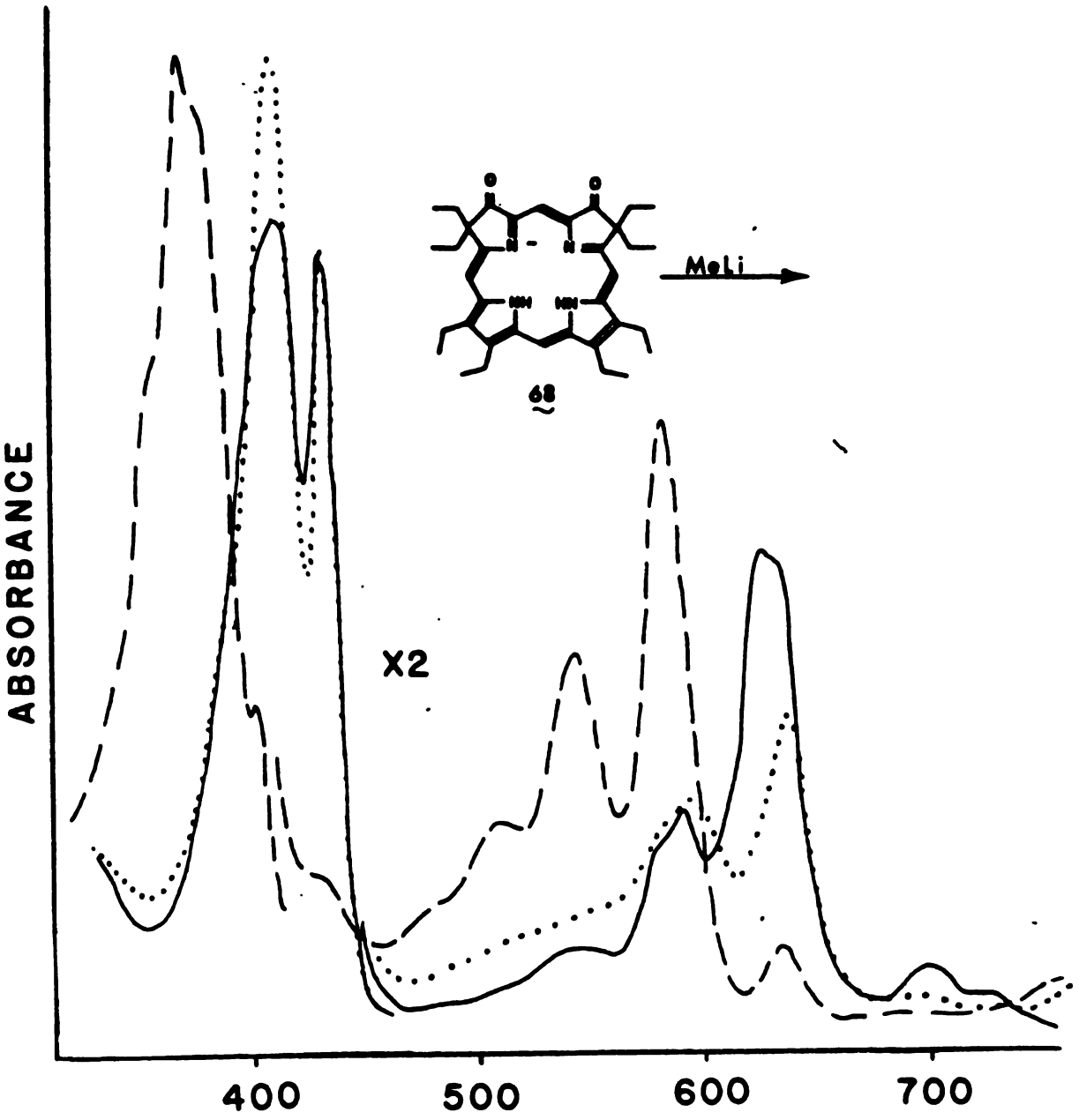

Figure 29. Electronic spectra of 2,3 diketone 68 (——); and alkylated products; mono alkylated isobacteriochlorin 95 (....); bis alkylated isobacteriochlorin 79 (----).

conjugation, results in an overall blue shift compared to the alcohols. The elimination of diasteriomers also produces a narrowing of peaks.

The absorption spectra also revealed the instability of bacteriochlorins, Figure 30, which shows the effect of subdued room light on the chromophore, T 1/2 = 20 min. Attempts to regenerate the chromophore by addition of reducing agents failed.

The similarity of band maxima and overall spectral features of these geminal alkylated systems and naturally occurring chromophores demonstrates the viability of using these compounds as models.

^{1}H NMR

Although the visible spectra served useful in monitoring the substitution of geminal alkylated hydroporphyrins, NMR was generally used as structural proof. In addition, side chain modifications could only be observed in the ^{1}H NMR.

The ^{1}H NMR of geminal dialkylated hydroporphyrins are generally not complex due to the high degree of symmetry in these models. The reduced ring current associated with saturation of peripheral double bonds was most evident in the upfield shift of neighboring meso hydrogens and the downfield shift of inner pyrrole hydrogens. In chlor ins, two methines are adjacent to a pyrroline ring and are shifted upfield. All four methines are shifted in bacteriochlorins, while isobacteriochlorins have the most complex pattern due to the distribution of reduced rings.

The geminal ketones and exo-methylene compounds show a high degree of symmetry corresponding to the rigidity and planarity of the

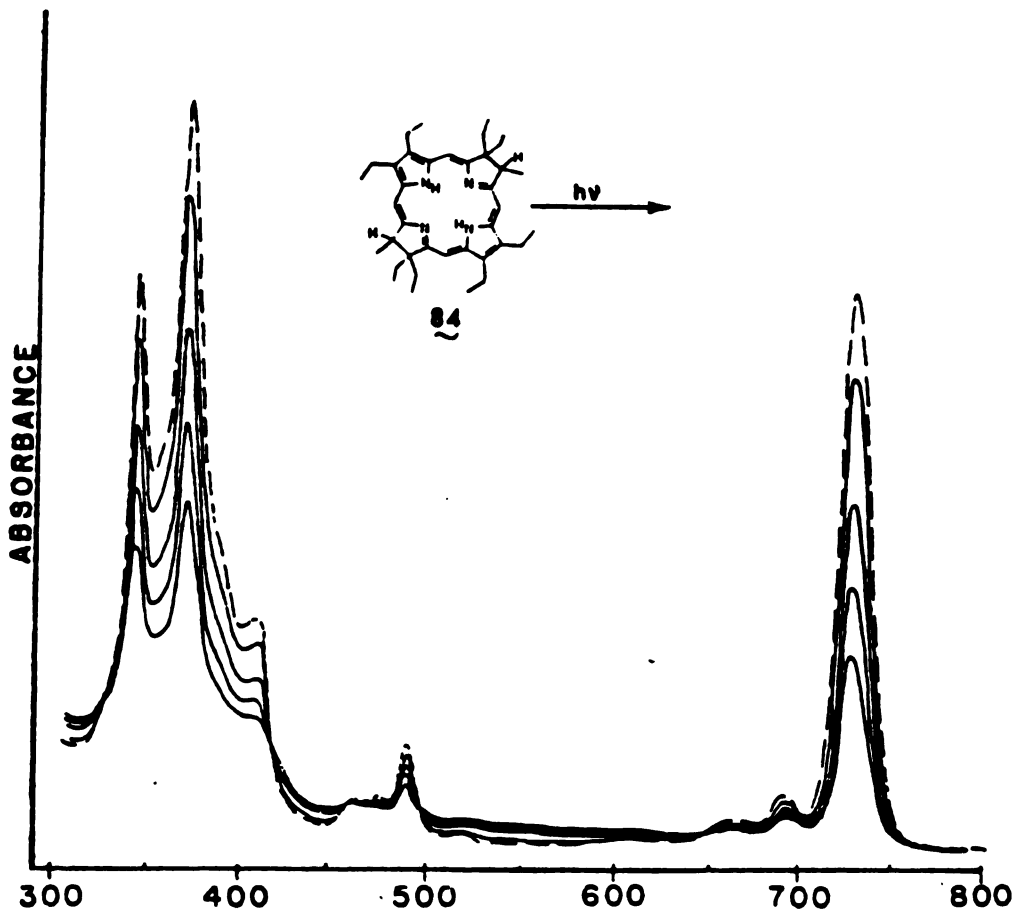

Figure 30. Electronic spectra of reduced 2,6 bacteriochlorin 84 (----); and effect of exposure to light (——).

partially reduced ring. Figure 31. The planarity of the exo-methylene bacteriochlorin, 85, analogous to bacteriochlorophyll b[63], has been shown by x-ray analysis, Figure 32, and may be important in the aggregation of these chromophores during photosynthetic processes.[45]

Alkylation of the ketone or reduction of the methylene generates chiral centers which reduce the overall symmetry of the molecule, as evidenced by the non equivalence of geminal ethyl groups. The diastereotopic nature of cis and trans bacteriochlorin diols was easily determined by NMR, Figure 33. The isolated isomers possessed different spectra due to retnetion or destruction of symmetry following alkylation. The addition of acid to the samples produced the same protonated intermediates, which after work up yielded identical alkenes.

Reduction of the alcohol or alkene was easily determined by the appearance of the pyrroline hydrogen, ca. δ 3-4 ppm and the splitting of the geminal alkyl substituent. The prochiral nature of the ethyl hydroxy ester has already been discussed. The attachmeent of imidazole side chains was easily determined by the appearance of imidazole hydrogens. The integrity of these species was verified in the same fashion as the diphenyl porphyrins. The addition of trifluoroacetic acid results in coulombic repulsion of the protonated species, Figure 34 and zinc incorporation causes coordination, Figure 35, both causing the expected changes in side chain and imidazole hydrogen resonances.

The ^{1}H NMR of the ligated species proved extremely concentration dependent due to severe aggregation, Figure 36. In general, the

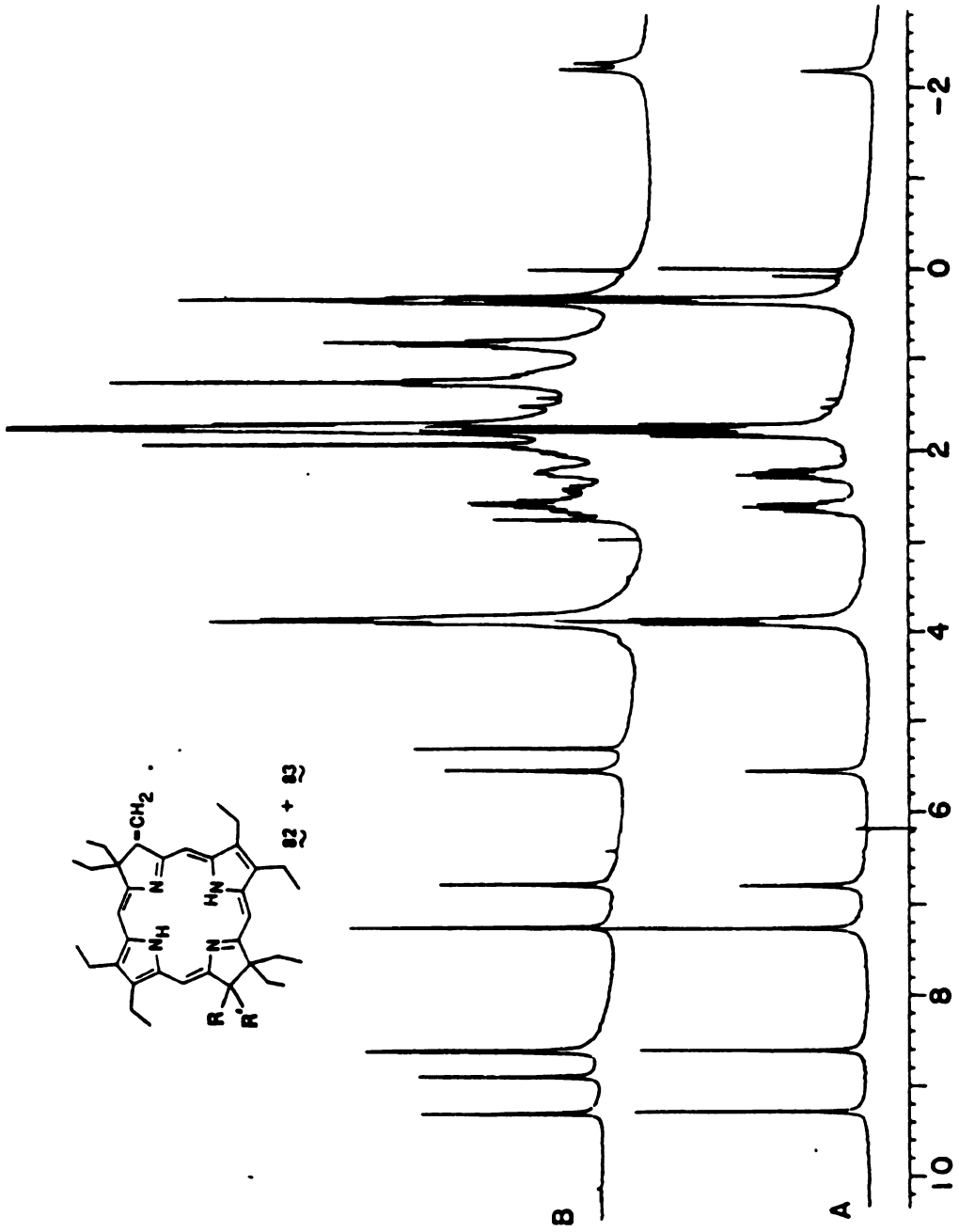

Figure 31. ^{1}H NMR spectra of methylene bacteriochlorins; (A) (R, R') = CH_2 (83); (B) R = CH_3, R' = OH (82).

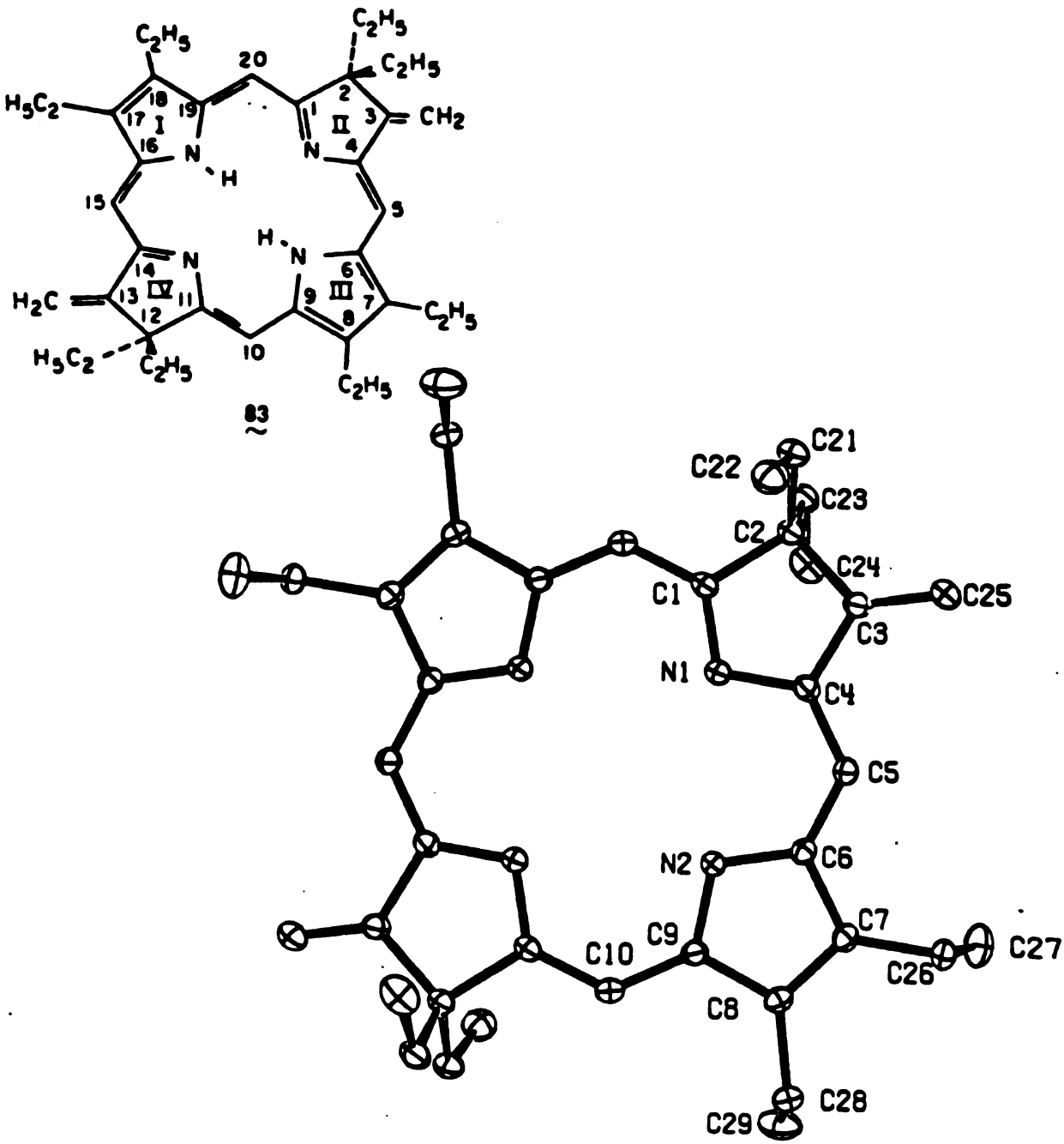

Figure 32. ORTEP representation of 2,6 dimethylene bacteriochlorin 83.

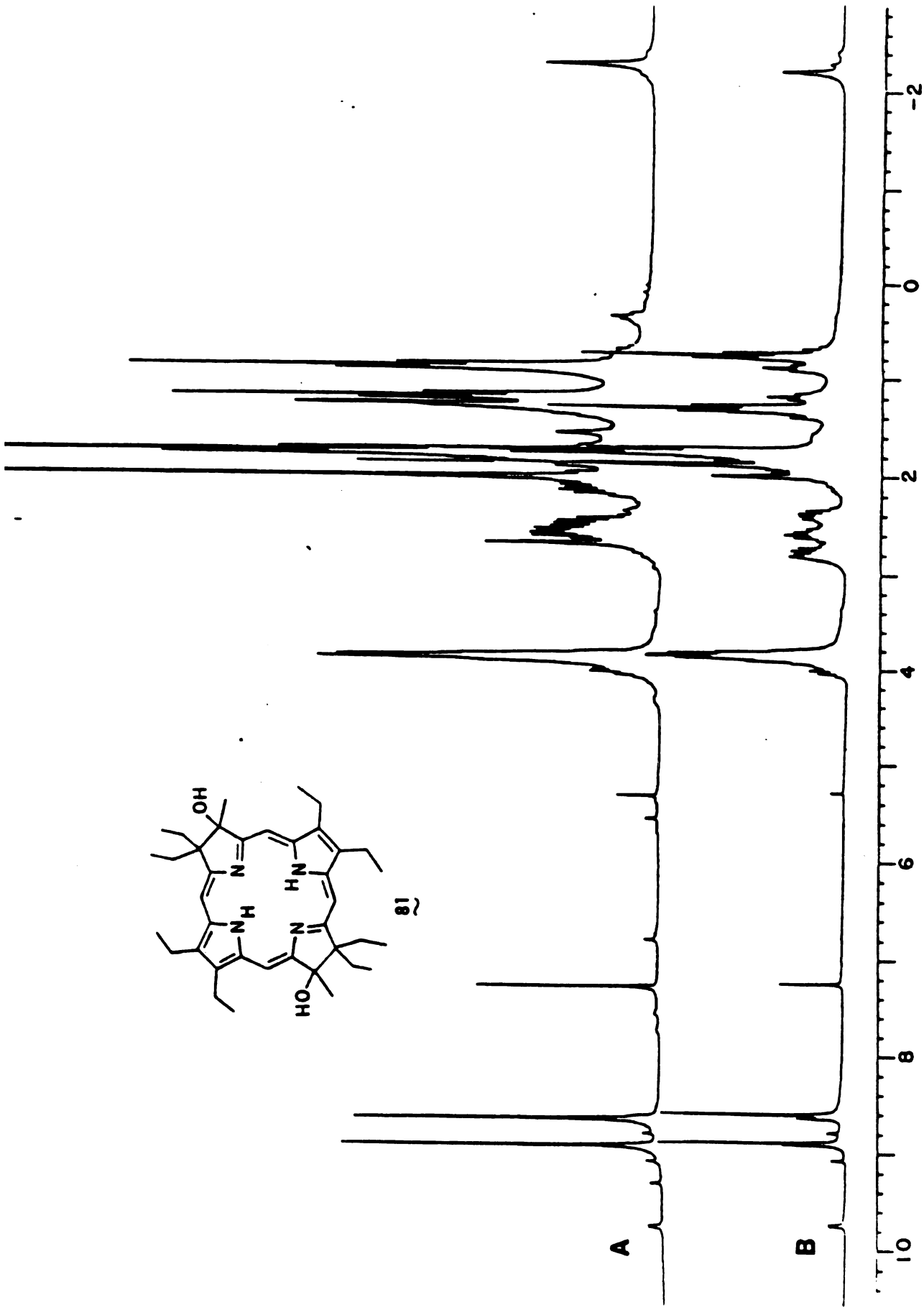

Figure 33. ^{1}H NMR spectra of diasteriomeric 2,6 dimethyl gemini octaethylbacteriochlorin alcohols (81); (A) trans; (B) cis.

Figure 34. ^{1}H NMR spectra of imidazole appended chlorin 93; (A) in $CDCl_3$; (B) $CDCl_3$-TFA.

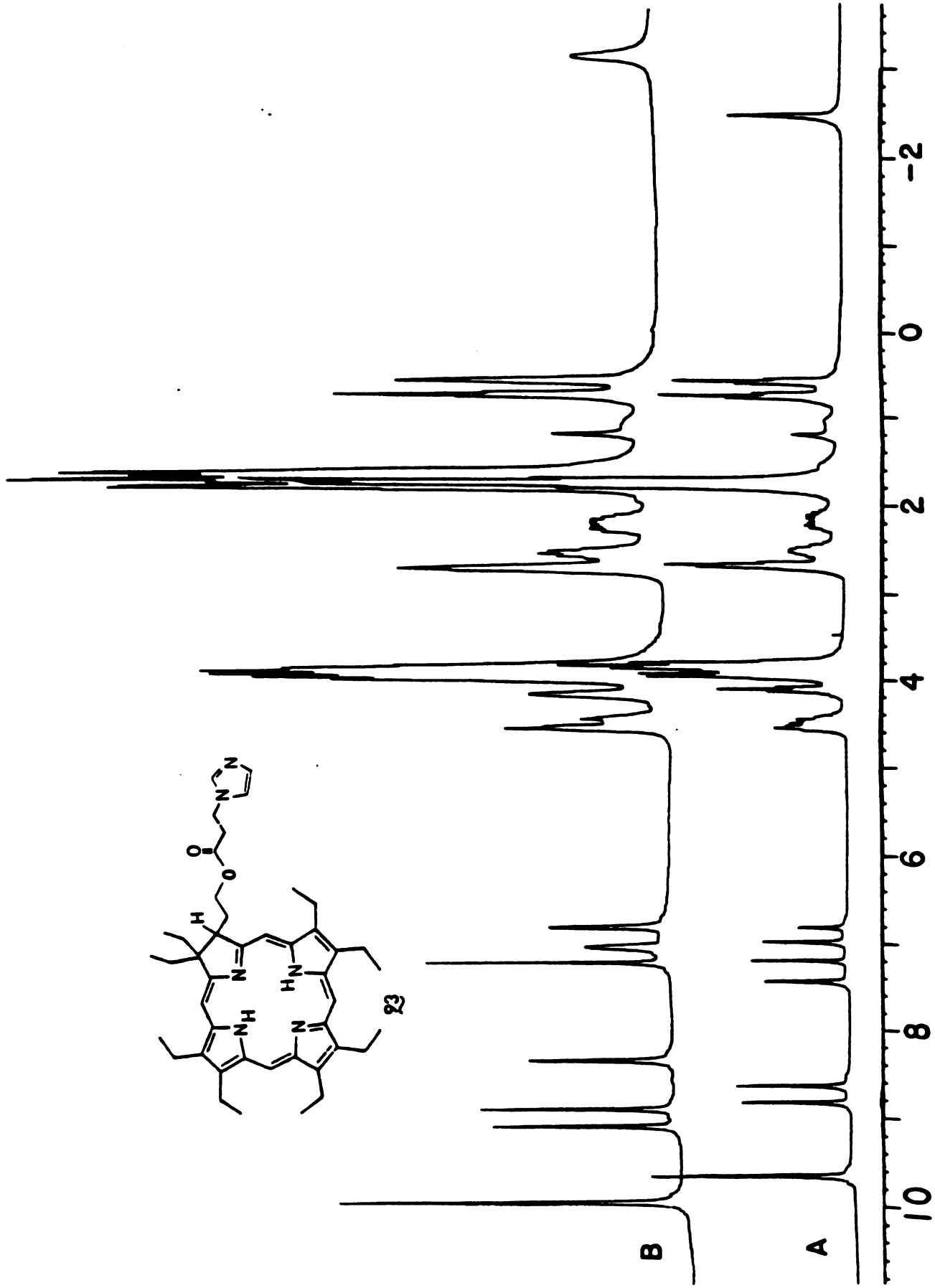
B
A
10
8
6
4
2
0
-2
23

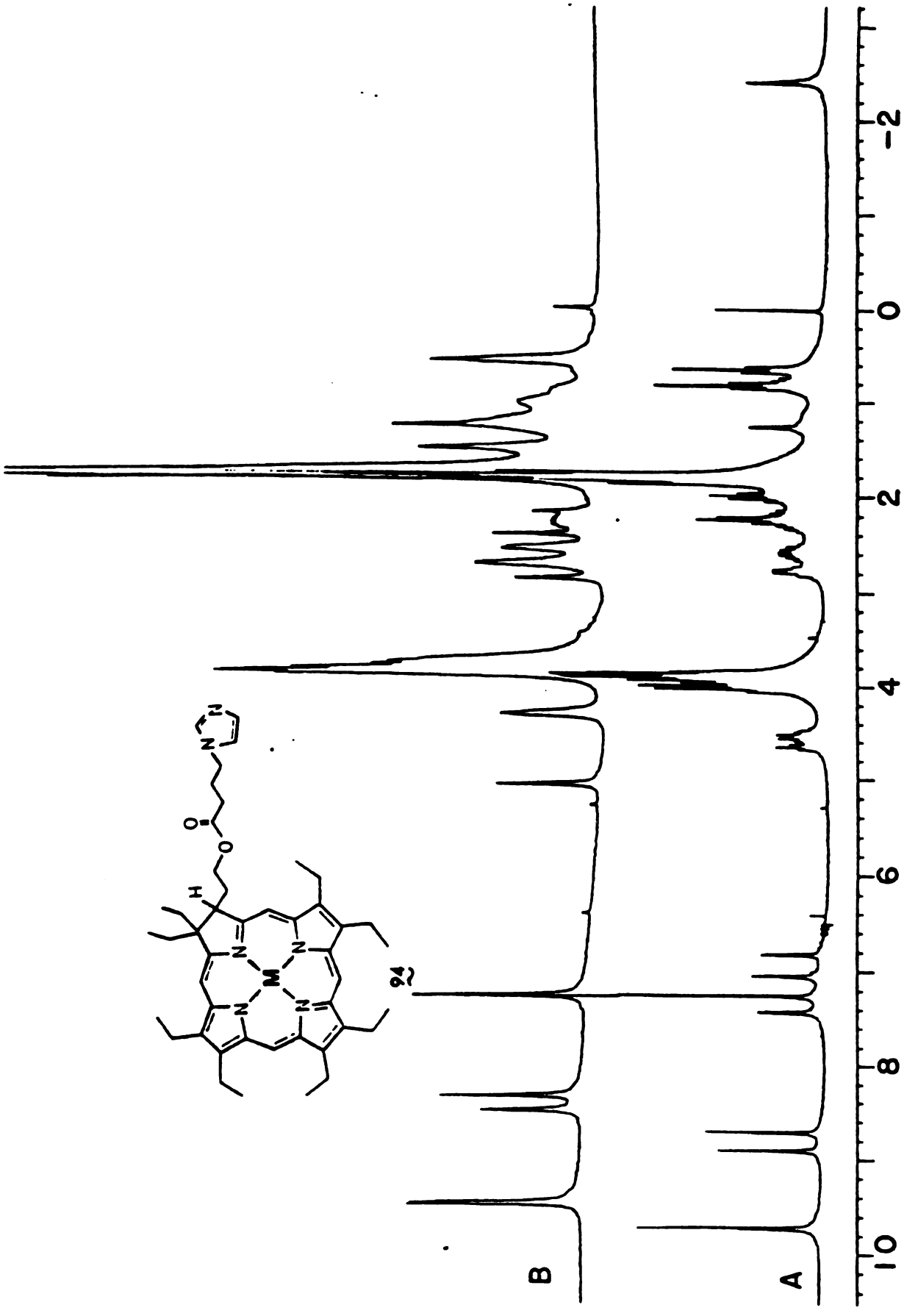

Figure 35. ^{1}H NMR spectra of imidazole appended chlorin 94; (A) free base, M = 2H; (B) M = Zn.

Figure 36. ^{1}H NMR spectra of appended chlorin 89 showing affect of increasing dilution, lowest trace most concentrated.

overall features of spectra are more important than absolute chemical shifts.

Cyclic Voltammetry

Cyclic voltammetric measurements reveal the redox potentials for the reduced system and the effect of metal incorporation. The redox properties of hydroporphyrins are important due to the possible redox role of the macrocycle itself in mult-electron enzymatic reductions as well as the role of cation radicals in photosynthetic systems.[45] The redox potentials of geminal alkylated hydroporphyrins are listed in Table 9.

All free base porphyrins and hydroporphyrins exhibit the same three step redox curve, but at distinctly different potentials, Figure 37. These include the successive formation of mono and dication radicals at oxidizing potentials and the formation of a mono anion radical at reducing potentials.

The oxidation potential for the formation of the mono cation radical for geminal alkylated hydroporphyrins follows the same order as other reduced series[64]; bacteriochlorin < isobacteriochlorin < chlorin < porphyrin. The greater the degree of saturation, the easier it is to abstract an electron from the π system.

Dihydro and tetrahydro-porphyrins of TPP and OEP generally oxidize at high potentials to more highly oxidized macrocyles.[65] The geminal alkylated hydroporphyrins are resitant to this dehydrogenation as evidenced by the lack of decomposition even after numerous scans.

The effect of substituents on the pyrroline ring was generally small, the alcohol, acetate, and methylene derivatives show little shift in the chlorins, and only about 50 mV increase in oxidation

Table 9 Redox Characteristics of Hydroporphyrins

		ring - ring$^+$		ring - ring$^-$
		0/1+	1+/2+	0/1-
OEP		0.83[a]		-1.45
Chlorins				
OH, CH_3	(77)	0.58	----	-1.45
OAc, CH_3		0.57	1.18	-1.52
H, CH_3	(78)	0.58	1.19	-1.50
CH_2	(85)	0.59	1.18	-1.47
Bacteriochlorins				
2, 5 OH, CH_3		0.33	1.01	-1.43
OAc, CH_3		0.30	0.97	-1.46
2, 6 OH, CH_3	(81)	0.30	0.96	-1.42
H, CH_3	(84)	0.26	0.97	-1.53
CH_2	(83)	0.32	1.03	-1.50
Isobacteriochlorins				
2, 3 OH, CH_3	(79)	0.38	1.02	
OAc, CH_3		0.37	0.95	
H, CH_3	(80)	0.33	0.92	
CH_2		0.38	1.02	
Chlorin - Imidazole				
free base	(89)	0.56	1.16	-1.46
Zinc		0.30	0.76	1.13
Tetraphenyl				
TPP		1.06	1.35	-1.29
TPC		0.88	1.17	-1.33
Zn TPC		0.58	0.92	
TPBC		0.43	0.92	-1.29

[a] Spectra run in CH_2Cl_2 using $(Bu)_4NClO_4$ as the supporting electrolyte and SCE as reference electrode.

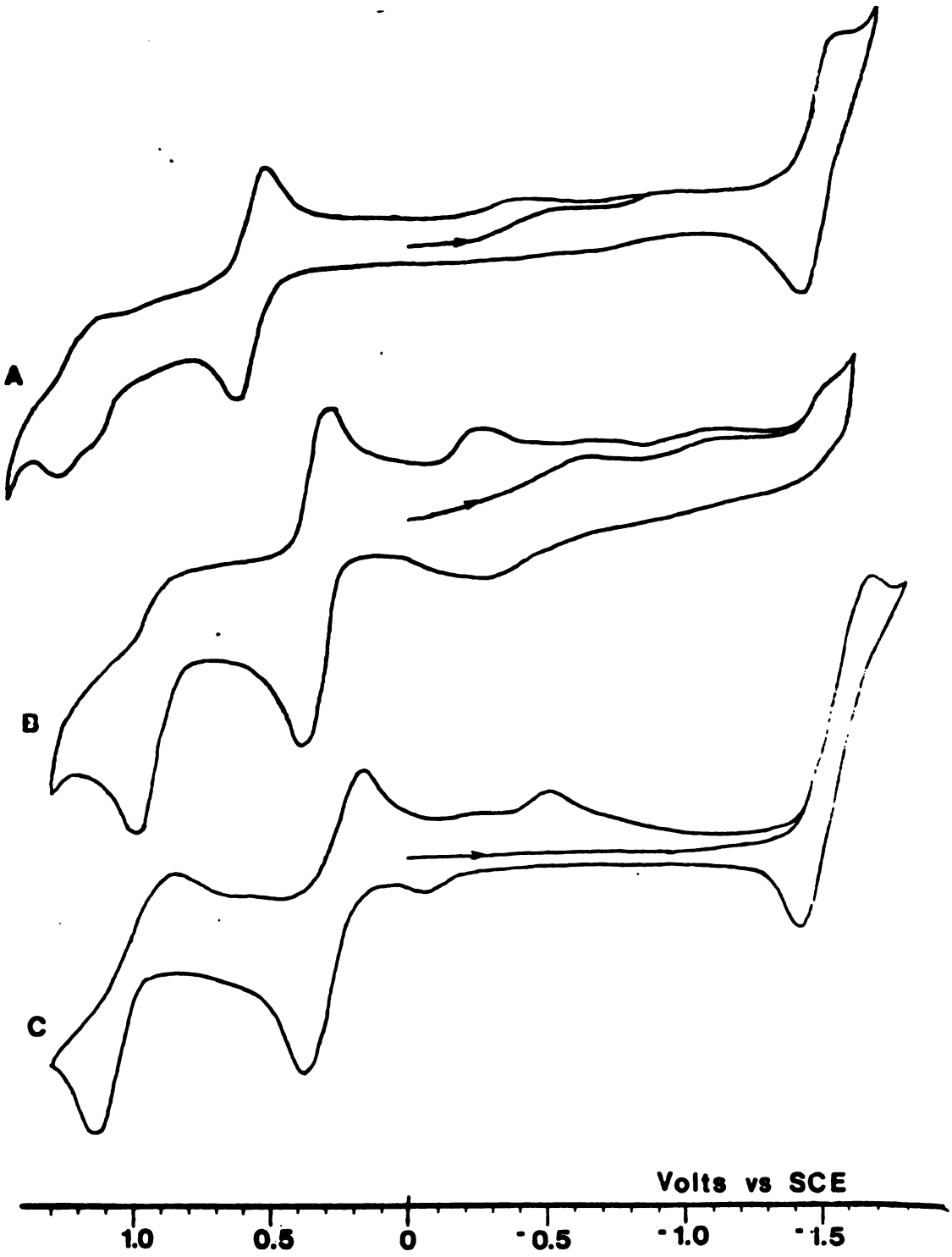

Figure 37. Cyclic voltammograms of gemini alkylated hydroporphyrins derived from OEP; (A) chlorin 78; (B) isobacteriochlorin 80; (C) bacteriochlorin 84. Spectra measured in CH_2Cl_2 with $(Bu)_4NClO_4$ as supporting electrolyte.

potential for the reduced bacterio and isobacteriochlorins. Little variations were also observed in the oxidation potential of configurational isomers. The 2,6 and 2,5 bacteriochlorins showed only a 25 mV difference, the latter being more difficult to oxidize.

Zinc incorporation increases electron density of the ring, making it easier to oxidize. The free base of imidazole appended chlorins was 250 mV more difficult to oxidize than the corresponding zinc complex. A similar trend in the incorporation of zinc into bacteriochlorins would produce a species which had an oxidation potential of 0V. or less vs S.C.E. The metallated species would easily photooxidize to the cation radical which may account for its instability and the difficulty encountered in generating it.

Metal Insertion and Coordination Studies

The lower acidity of reduced porphyrins hinders the incorporation of metals.[52] Geminal alkylated chlorins and isobacteriochlorins can be metallated by standard conditions using longer reaction times. Similar treatment of unstabilized hydroporphyrins would lead to partially dehydrogenated products. Efforts to insert metals into the least acidic hydroporphyrin, bacteriochlorins, failed.

Bacteriochlorins of TPP have been metallated, however, no model studying involving β-substituted bacteriochlorins has been reported. Metallation of the naturally occurring bacteriopheophytin requires special techniques and the yields are inevitably low.[69] In nature the metals are incorporated before the rings are reduced. Efforts to use the zinc diketones in alkylation only produced demetallated diols.

The inability to metallate these model bacteriochlorins limits their study, however, the free bases have provided information on the structure and reactivity of bacteriochlorins.

The O_2 and CO binding constants for the imidazole appended ferrous chlorins and isobacteriochlorins have been reported elsewhere.[64d,8a] Rates indicate that the presence of the fifth ligand, imidazole, outweighs any electronic effect due to the reduction of the ring system.

The zinc derivatives of the tailed chlorins exhibit unusual epr properties. The cation radical of the zinc complex exhibits two signals at room temperature but only one at reduced temperature. As the chain length was shortened, the temperature at which the two signals coalesce rises. These observations imply the presence of two species at room temperature and only one at reduced temperatures. The two species may be either inter- and intra-molecularly bound species, or two types of intramolecularly bound systems, Figure 38. As the temperature was reduced, the more stable species was formed, representing the intramolecularly bound species of least strain. More detailed discussion of these results will appear elsewhere.[66]

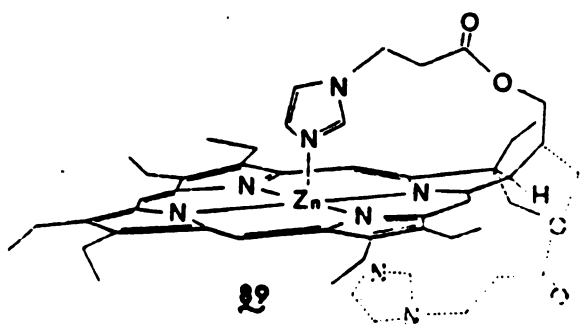

89

Figure 38. Possible orientations for intramolecular coordination in the zinc complex of appended chlorin 89.

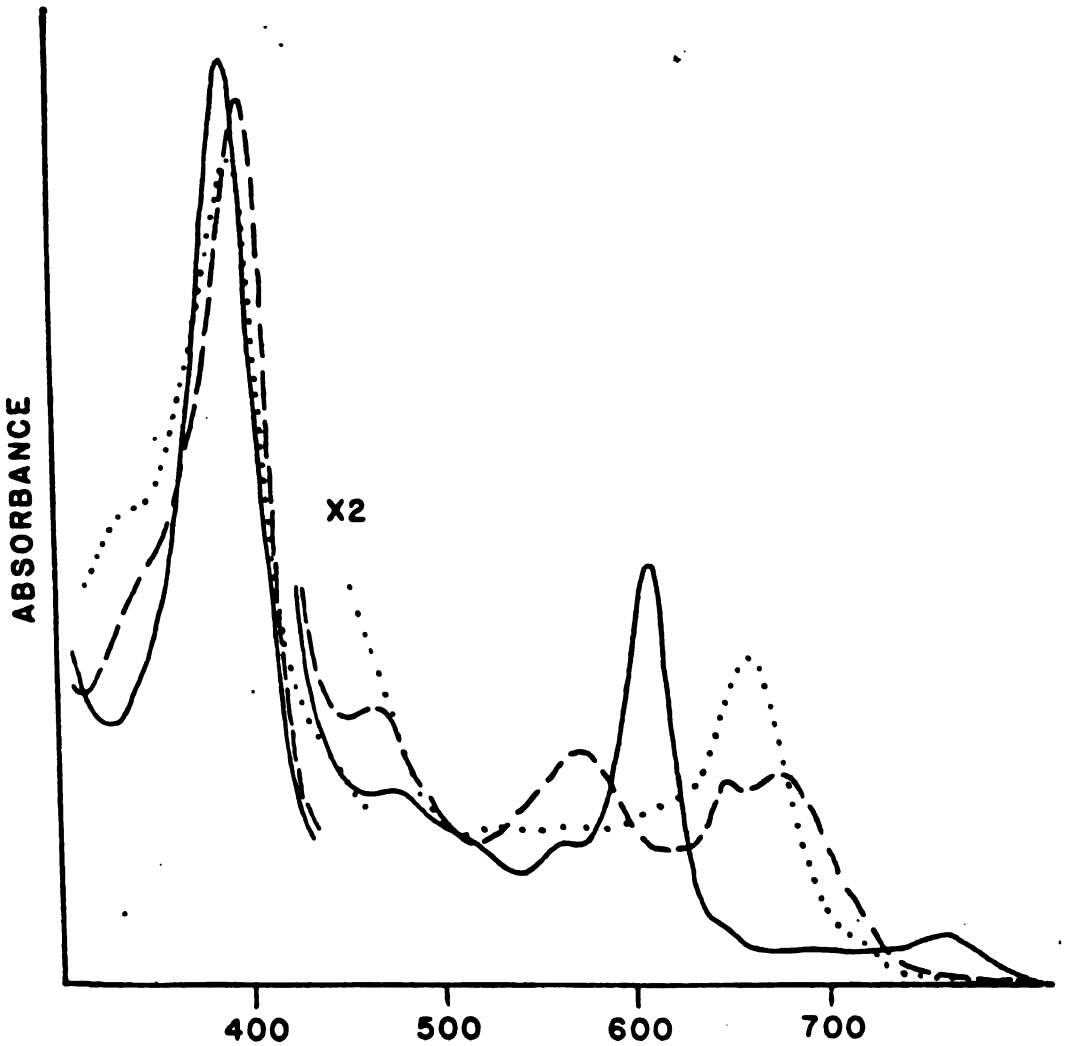

Figure 39. Electronic spectra of the ferric chloride complex of methyl octaethylchlorin 78 (____); effect of adding Et_3N or 25% aq. NaOH (----); effect of adding $(Bu)_4NOH$ (....).

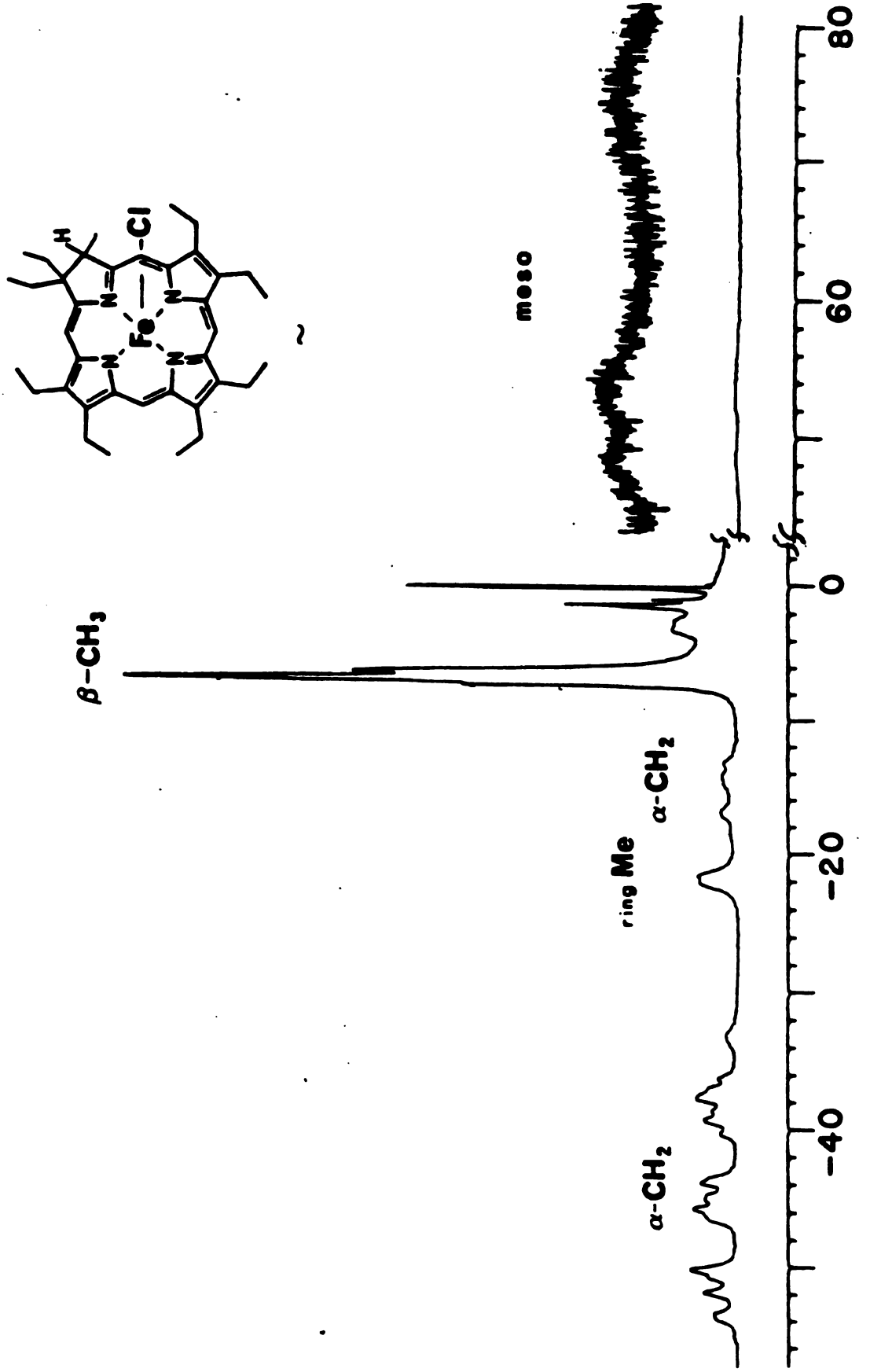

Figure 40. ^{1}H NMR spectrum of paramagnetic ferric chloride complex of methyl octaethylchlorin 78.

Ferric Hydroporphyrins, Alkaline Form

During the course of O_2 and CO binding studies on iron hydroporphyrins, it was observed that the base treatment of ferric hydroporphyrin-type hemes produced a species which was dependent on base strength. Dilute or concentrated hydroxide, triethylamine, and tetrabutylammonium hydroxide all produced unique species, as evident by the visible spectra, Figure 39. In addition, it was observed that electrochemical oxidation produced the same species as aqueous hydroxide. This behavior was reminiscent of hydroxide formation in protected hemes, as ferrous hemes will react with oxygen to generate ferric hydroxides. The ability of unhindered iron hydroporphyrins to stabilize hydroxide formation was unexpected and may be important in species which utilize iron hydroporphyrins and oxygen.

NMR analysis of ferric hydroporphyrins and other unprotected hemes indicate that a transient alkaline form can be generated and the it is of high symmetry. The existance of few studies on ferric hydroporphyrin-type hemes, due to their instability, make correlations difficult.[67] The spectra of these systems are generally complex and assignments limited by the presence of diasteriosomers and magnetic inequivalences. The ^1H NMR of the ferric chloride form of methyl geminal octaethylchlorin, 78, Figure 40, reveals the complex nature of reduced hemes.

Treatment of the ferric chloride with basic deuterium oxide generated initially the alkaline form, Figures 41 and 42, which gradually converted to the μ-oxo dimer. This final form was

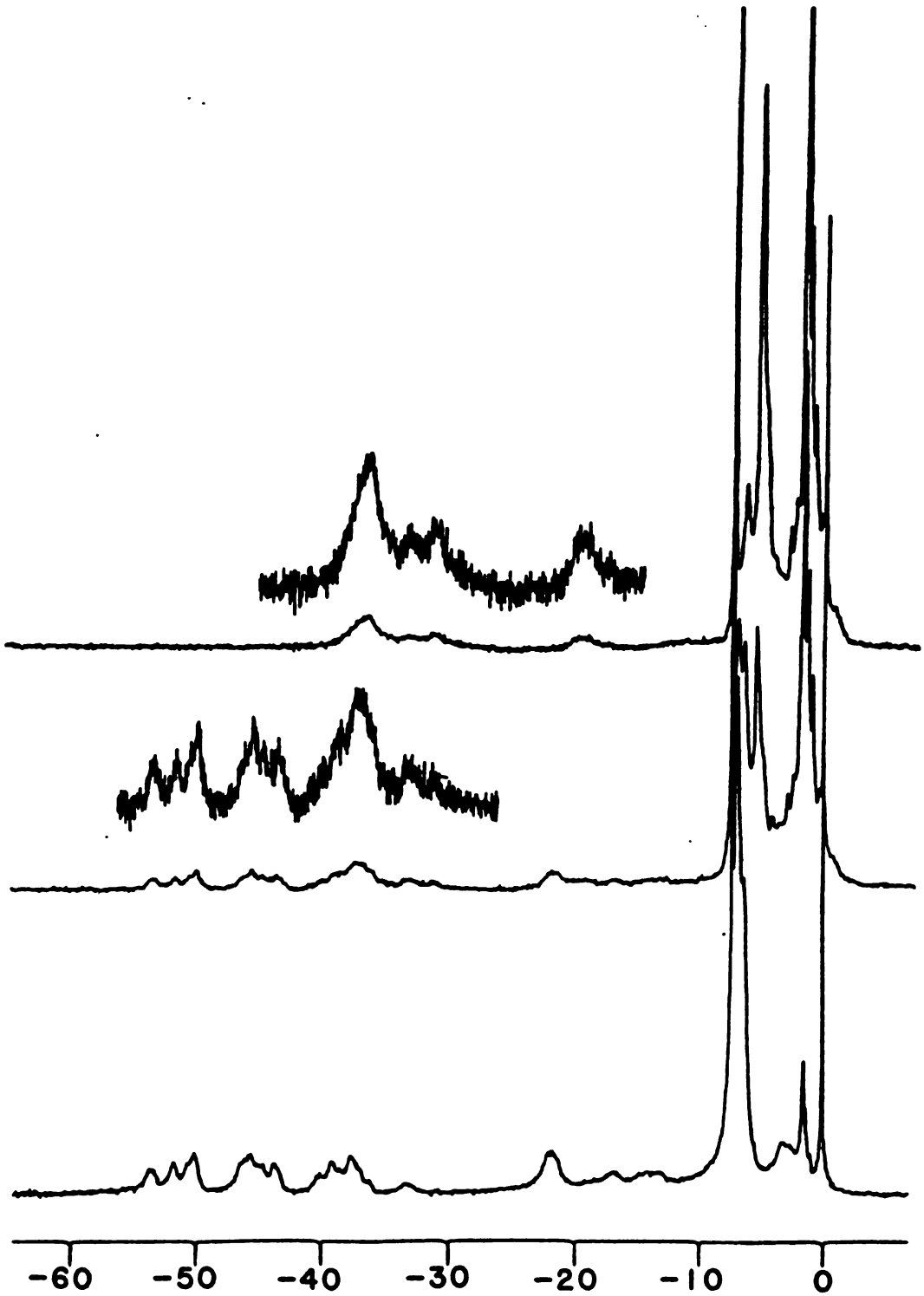

Figure 41. ^{1}H NMR spectra monitoring the addition and reaction of OD^-/D_2O to Fe(III)Cl complex of chlorin 78. (A) Fe(III)Cl, no base; (B) 10 min after addition of base; (C) 20 min after addition, complete conversion to alkaline form.

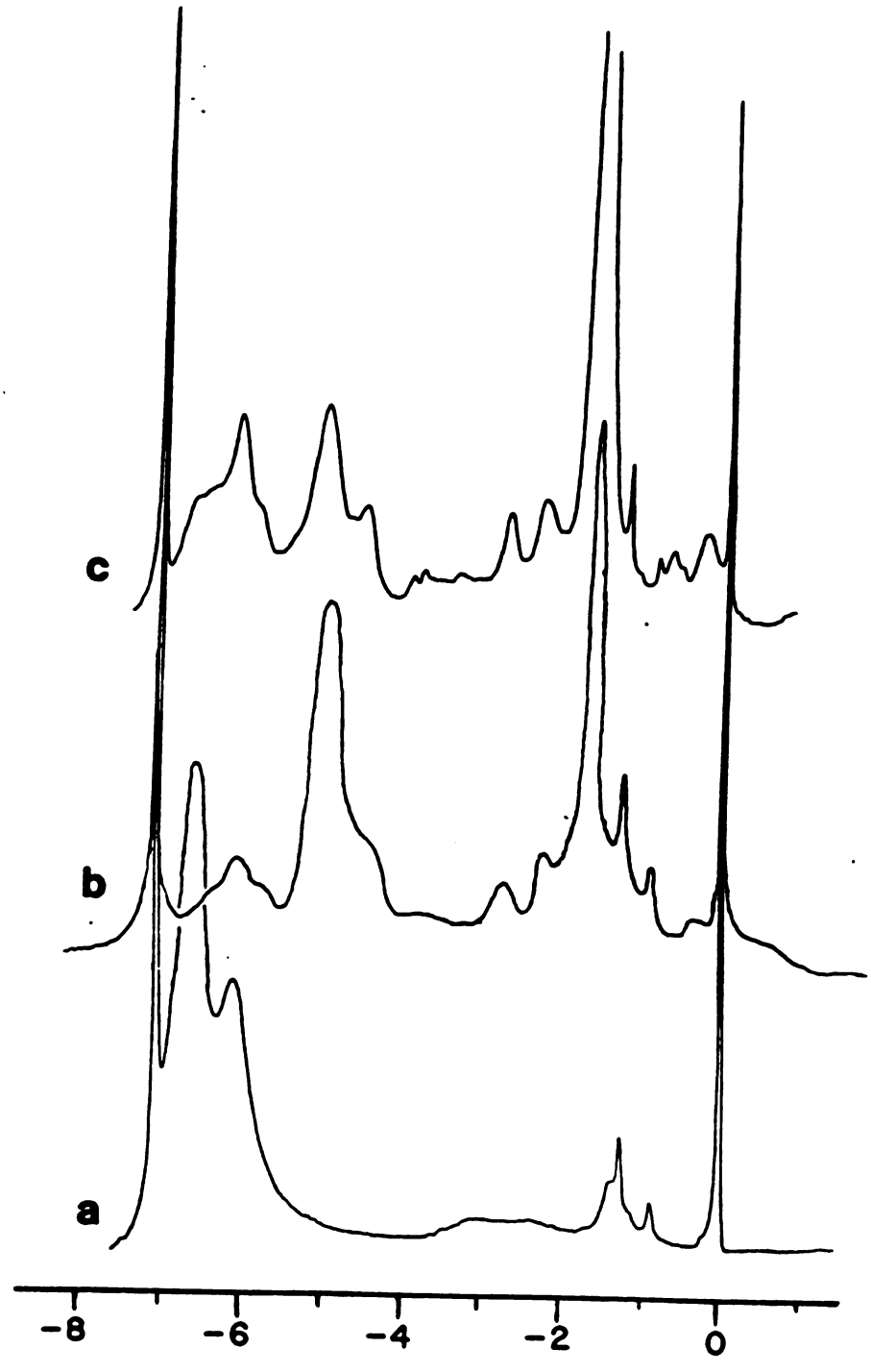

Figure 42. Comparison of ^{1}H NMR spectra of FE(III) complexes of chlorin 78; (A) chloride; (B) "alkaline form"; (C) μ-oxodimer.

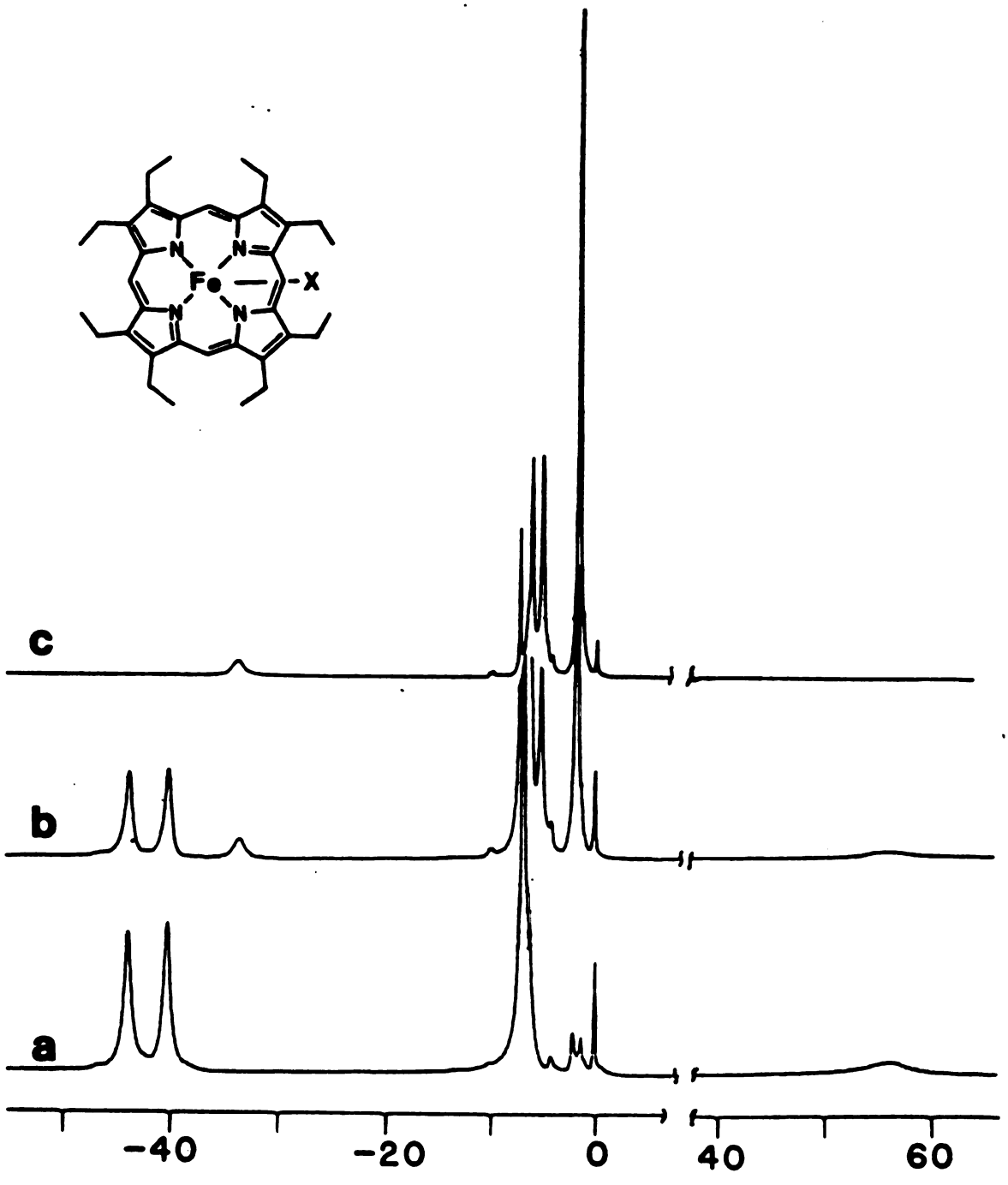

Figure 43. ^1H NMR spectra monitoring the addition and reaction of OD^-/D_2O to Fe(III)Cl complex of octaethylporphyrin. (A) Fe(III)Cl; no base; (B) 10 min after the addition of base; (C) completion of reaction, μ-oxo dimer.

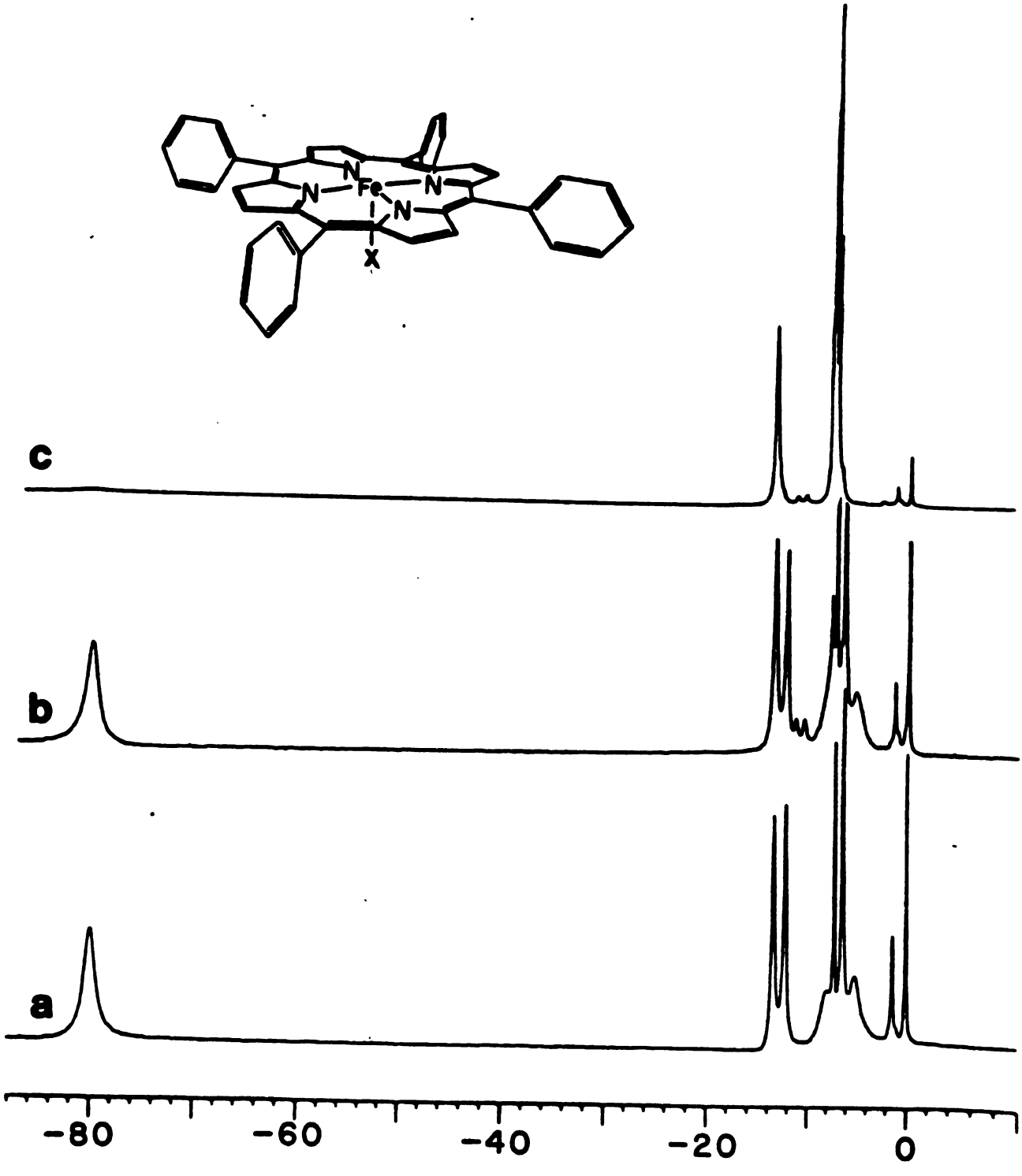

Figure 44. ^1H NMR spectra monitoring the addition and reaction of OD^-/D_2O to Fe(III)Cl complex of tetraphenyl porphyrin. (A) Fe(III)Cl, no base; (B) 10 min after addition of base; (C) completion of reaction, μ-oxo dimer.

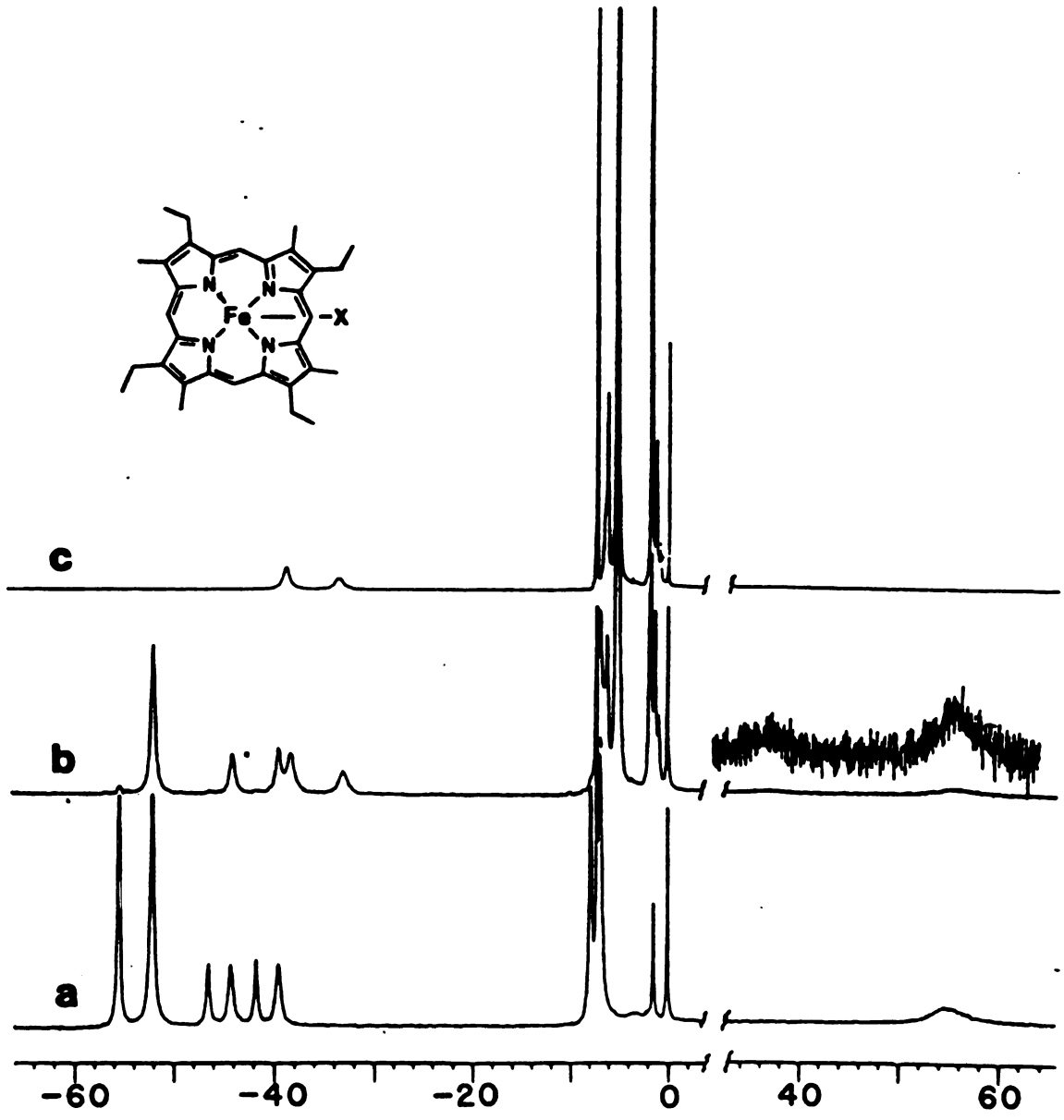

Figure 45. ^1H NMR spectra monitoring the addition and reaction of D^-/D_2O to Fe(III)Cl complex of etioporphyrin. (A) Fe(III)Cl, no base; (B) 10 min after addition of base; (C) completion of reaction, μ-oxo dimer.

identical to that generated by elution through alumina. The high symmetry of the alkaline and chloride forms was evidenced by the broad singlet and shoulder corresponding to the α-methylenes which appear as a doublet in the μ-oxodimer. The alkaline form was also characterized by the low field resonances for the other ring substituents.

Similar treatment of OEP and TPP produced only the strongly antiferromagnetically coupled μ-oxo dimer, Figures 43 and 44. Etio porphyrin, which is of lower symmetry, produced a transient species, Figure 45. The high symmetry of this species was indicated by the ring methyl resonances which appear as a doublet in the chloride form and as a low field singlet in the alkaline form. The μ-oxo dimer of this porphyrin shows only meso hydrogens in the low field region.

The high symmetry of the alkaline form may be accounted for by bis-hydroxy type species, or coordination of water as the sixth ligand. Hydrogen bonding, Figure 46, can create an extremely symmetric species.

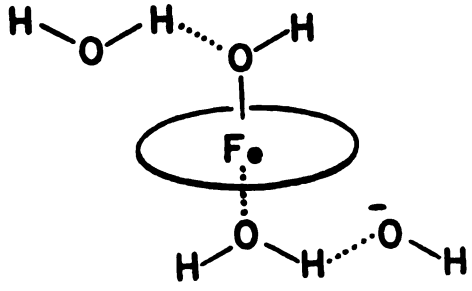

Figure 46. Possible structure of highly symmetrical ferric hydroxides.

The reduced rates in μ-oxo dimer formation for hydroporphyrin-type hemes, may be attributed to the well documented increased flexibility of the hydroporphyrin skeleton. Affinity for weak ligands, e.g., H_2O, is strongly dependent on the flexibility of the core in allowing the metal center to expand.[68] Coordination of these weak ligands reduces the availability of free binding sites which may be necessary in μ-oxo dimer formation.

Experimental

OEP Oxidation

Octaethyl porphyrin (1 gm) dissolved in sulfuric acid (100 ml) was cooled to 0°C in an ice bath. Hydrogen peroxide (18 ml, 3%) was added dropwise at such a rate that the temperature did not exceed 15°. After completing the addition (ca. 15 min) the reaction was stirred 10 min further in the ice bath followed by 15 min removed from the bath. The reaction was then quenched by pouring into water (250 ml) containing sodium acetate (100 gm).

The crude solid was collected by filtration and redissolved in methylene chloride (500 ml). The solution was washed with water and 5% NaOH, separated, dried, and evaporated to dryness. The crude product was chromatographed on a silica column 2 x 12 in (Baker 3405). The first fraction was collected with hexane/CH_2Cl_2 (40:60) until the eluent became green. The second fraction was eluted with 100% CH_2Cl_2 until the eluent no longer appeared green.

The initial fraction was purified further on a series of columns and plates to yield pure ketones which can be recrystallilzed from

CH_2Cl_2/methanol. The mono ketone 66 and 2, 6 diketone, 70, were best separated using an activated alumina column with 1:1 hexane-CH_2Cl_2. The isomeric bacteriochlorins, 2,5 and 2,6 were separated by fractional recrystallization, the 2,5 isomer, 71, was slightly more soluble in methanol. The oxophlorin, 72, and unreacted octaethylporphyrin, due to low solubility, tend to persist as small impurities in all fractions. The 1,4 diketone, 69, which occurs in the lowest yield due to steric congestion, was extremely difficult to isolate from the 2,5 diketone, 71. To obtain the alkylated species it was easiest to alkylate the mixture and separate the isomeric alcohols which show a greater difference in retention rates than the ketones.

The second fraction contains the remaining two isobacteriochlorin ketones and triketone impurities. The 2,4 diketone, 67, were separated from the triketone by a series of columns or plates. Alternatively, if recrystallization from methylene chloride-methanol was slow, the diketone plates can be manually separated from the triketone needles. Purification of the 2,3 diketone, 68, was extremely difficult, if pure diketone was needed the best route was degradation of the triketone impurities with methyl lithium.

All of the ketones isolated were characterized by visible and ^1H NMR spectra and correlated well with previously published values.[58]

Methylation of Ketones

The ketone was dissolved in ether or THF and treated with an excess of methyllithium. After a few minutes the reaction mixture was quenched with water. The organic layer was separated, dried, and

evaporated to dryness. Purification was easily achieved using silica columns in subdued light. Separation of diasteriomeric diols was easily obtained but was unnecessary due to isomerization during reduction.

Methyl Gemini Octaethylchlorin Alcohol (77)

^{1}H NMR ($CDCl_3$)δ-2.58(s, 2H, NH), 0.71(t, 3H, CH_3), 0.97(t, 3H, CH_3), 1.80(m, 18H, CH_3), 2.10(s, 3H, CH_3), 2.30(m, 2H, CH_2), 2.60(m, 2H, CH_2), 4.02(m, 12H, CH_2), 6.52(s, 1H, OH), 8.77(s, 1H, meso), 9.18(s, 1H, meso), 9.75(s, 1H, meso); Mass Spectrum (70 eV), 566 (M+), calcd. 566.

2,6-Dimethyl Gemini Octaethylbacteriochlorin Diol (81)

Trans

^{1}H NMR ($CDCl_3$) δ-2.31(s, 2H, NH), 0.88(t, 6H, CH_3), 1.18(t, 6H, CH_3), 1.74(t, 12H, CH_3), 1.98(s, 6H, CH_3), 2.1(m, 4H, CH_2), 2.53(m, 4H, CH_2), 2.64(s, 2H, OH), 3.85(m, 8H, CH_2), 8.62(s, 2H, meso), 8.89(s, 2H, meso); Mass Spectrum (70 eV) 562 (M+), calcd. 598.

Cis

^{1}H NMR ($CDCl_3$) δ-2.33(s, 2H, NH), 0.75(t, 6H, CH_3), 1.30(t, 6H, CH_3), 1.74(t, 12H, CH_3), 1.87(s, 6H, CH_3), 2.37-2.75(m, 8H, CH_2), 3.83(m, 8H, CH_2), 8.56(s, 2H, meso), 8.88(s, 2H, meso); Mass Spectrum (70 eV) 562 (M+), calcd. 562.

2,3 Dimethyl Gemini Octaethyl Isobacteriochlorin Diol (79)

^{1}H NMR ($CDCl_3$) δ0.86(t, 6H, CH_3), 1.27(t, 6H, CH_3), 1.68(m, 12H, CH_3), 1.90(s, 6H, CH_3), 2.48(m, 8H, CH_2), 3.69(m, 8H, CH_2), 5.70(s, 2H, OH), 7.12(s, 1H, meso), 7.31(s, 1H, meso), 7.33(s, 1H, meso), 8.52(s, 1H, meso). Mass Spectrum (70 eV) 598 (M+), calcd 598.

Dehydration of Alcohols

The alcohol was dissolved in dry CH_2Cl_2 containing triethylamine. Methanesulfonyl chloride was added dropwise until the reaction was judged complete by tlc. Water was added and the organic layer separated and washed successively with; 10% HCl, H_2O, and saturated $NaHCO_3$. After drying the product was purified through a silica pad.

Alternatively, the chlorin and bacteriochlorin alcohols may be eliminated by simply washing with strong acid. A methylene chloride solution of the chlorin and bacteriochlorin required 25% and 15% HCl, respectively.

Methylene Gemini Octaethylchlorin (85)

^1H NMR ($CDCl_3$) δ-2.50(s, 2H, NH), 0.36(t, 6H, CH_3), 1.85(m, 18H, CH_3), 2.34(m, 2H, CH_2), 2.70(m, 2H, CH_2), 4.00(m, 12H, CH_2), 5.65(s, 1H, vinyl H), 6.97(s, 1H, vinyl H), 8.80(s, 1H, meso), 9.50(s, 2H, meso), 9.78(s, 2H, meso); Mass Spectrum (70 eV) 548 (M+), calcd. 548.

2-Methylene-6-ol Geminal Octaethylbacteriochlorin (82)

^1H NMR ($CDCl_3$) δ-2.23(s, 2H, NH), -2.20(s, 1H, NH), 0.37(t, 6H, CH_3), 0.85(m, 3H, CH_3), 1.29(t, 3H, CH_3), 1.75(m, 12H, CH_3), 1.94(s, 3H, CH_3), 2.0-2.7(m, 8H, CH_2), 2.76(s, 1H, OH), 3.88(m, 8H, CH_2), 5.53(s, 1H, vinyl H), 6.80(s, 1H, vinyl H), 8.62(s, 2H, meso), 8.86(s, 1H, meso), 9.31(s, 1H, meso).

2,6 Dimethylene Gemini Octaethylbacteriochlorin (79)

^1H NMR ($CDCl_3$) δ-2.20(s, 2H, NH), 0.35(t, 12H, CH_3), 1.77(m, 12H, CH_3), 2.24(m, 4H, CH_2), 2.59(m, 4H, CH_2), 3.87(m, 8H, CH_2), 5.59(s, 2H, vinyl H), 6.78(s, 2H, vinyl H), 8.60(s, 2H, meso), 9.27(s, 2H, meso). Mass Spectrum (70 eV) 562 (M+), calcd 562.

Reduction by $HI-HP_3O_2-HOAc$

Hydriodic acid (5 ml, 56.7%) was cooled to 0° in an ice bath, glacial acetic acid (5 ml) was added dropwise, followed by hypophosphorous acid (1 ml, 50%). The solution should obtain a yellow cast which gradually fades. The reagent should be stored at reduced temperature and was effective for several days.

The methylene or alcohol (50 mg) was dissolved in acetic acid (20 ml) containing ascorbic acid (50 mg). An excess of the freshly prepared reducing solution (0.5 ml) was added and the mixture warmed to 60° for ca. 3-5 min. After cooling, the mixture was diluted with water and extracted with CH_2Cl_2. The organic layer was separated and washed with dilute base and water, dried and evaporated to dryness. The products were purified through a silica gel column to yield the reduced species, yield ca. 75%.

Methyl Gemini Octaethyl Chlorin (78)

^1H NMR ($CDCl_3$) δ-2.2(s, 2H, NH), 0.44(t, 3H, CH_3), 0.97(t, 3H, CH_3), 1.78(m, 18H, CH_3), 2.10(d, 3H, CH_3), 2.48(m, 4H, CH_2), 3.92(m, 12H, CH_2), 4.73(q, 1H, ring H), 8.71(s, 1H, meso), 8.87(s, 1H, meso), 9.69(s, 2H, meso); Mass Spectrum (70 eV) 551 (M+), calcd. 550.

2,3 Dimethyl Gemini Octaethyl Isobacteriochlorin (80)

^1H NMR ($CDCl_3$) δ0.72(t, 6H, CH_3), 0.90(t, 6H, CH_3), 1.42(m, 12H, CH_3), 1.60(d, 3H, CH_3), 1.93(m, 8H, CH_2), 3.26(m, 8H, CH_2), 3.80(q, 2H, ring H), 6.70(s, 1H, meso), 7.15(s, 2H, meso), 8.38(s, 1H, meso); Mass Spectrum (70 eV) 566, calcd. 566.

Diimide Reduction

The dimethylene and reduced bacteriochlorins were handled in the dark due to their extreme instability to light. 2,6 Dimethylene gemini octaethylbacteriochlorin, 83, (100 mg), tosyl hydrazide (66 mg) and potassium carbonate (218 mg) were dissolved in pyridine (10 ml). The mixture was purged of oxygen and heated with stirring to 105°C. After two hours additional tosyl hydrazide (66 mg) was added, the addition was repeated every two hours until the visible spectra indicated completion of the reduction. After 17 hours the ratio of reduced to methylene compounds was 7:1 according to the intensity of the Sorets.

Upon completion of the reaction, benzene and water were added to the mixture. The solution was then digested 1 h on a steam bath, then cooled. The organic layer was separated and washed with 3N HCl, water, and sat. bicarbonate. Concentration, chromatograph on a silica gel column, and recrystallization from hexane/CH_2Cl_2 yields shiny green flakes.

2,6-Dimethyl Gemini Octaethylbacteriochlorin (84)

^1H NMR ($CDCl_3$) δ-2.25(s, 2H, NH), 0.590.941.73(m, 12H, CH_3), 1.99(t, 6H, CH_3), 2.08-2.46(m, 8H, CH_2), 3.82(q, 8H, CH_2), 4.57(m, 2H ring H), 8.52(s, 2H, meso), 8.67(s, 2H, meso). Mass Spectrum (70 eV) 566 (M+), calcd 566.

Lithium Aluminum Hydride Reduction of Ketones

The ketone was dissolved in dry THF and an excess of $LiAlH_4$/THF was added. The reaction was quenched by the slow addition of water. Alcohols were purified on a silica gel pad.

Hydro Gemini Octaethylchlorin Alcohol (86)

^{1}H NMR ($CDCl_3$) δ-2.57(s, 2H, NH), 0.72(t, 3H, CH_3), 0.96(t, 3H, CH_3), 1.80(m, 18H, CH_3), 2.29(m, 2H, CH_2), 2.57(m, 3H, CH_2, ring H), 3.88(m, 12H, CH_2), 6.52(s, 1H, OH), 8.77(s, 1H, meso), 9.18(s, 1H, meso), 9.75(s, 1H, meso), 9.76(s, 1H, meso); Mass Spectrum (70 eV) 562 (M+), calcd 562.

Ethyl Acetate Gemini Octaethylchlorin Alcohol (87)

To freshly distilled hexane (5 ml) under argon and cooled to 0° was added methyllithium (7.6 ml, 1.4 M) followed by diisopropylamine (1.4 ml). The reaction mixture was allowed to warm to room temperature and stirred 10 min further. The solvents were removed in vacuo, producing a white, flakey solid. Dry THF (10 ml) was introduced, after the lithium salts have dissolved the solution was cooled to -78°. Ethyl acetate (0.97 ml) was added dropwise and the mixture stirred for 5 min. A solution of monoketone, 66, (120 mg) in THF (50 ml) was added through a cannula, and the mixture stirred 5 min at -78° before allowing to warm to room temperature. After 10 min, the reaction was quenched with saturated aqueous ammonium acetate. The organic layers were separated, washed with water, and dried over sodium sulfate. The alcohol was purified through a silica gel pad, yield ca. 85%. ^{1}H NMR ($CDCl_3$) δ-2.38(s, 2H, NH), 0.36(t, 3H, CH_3), 0.59(t, 3H, CH_3), 1.60(t, 3H, ester CH_3), 1.80(m, 18H, CH_3), 2.4(m, 1H, CH_2), 2.67(m, 1H, CH_2), 2.62(d, 1H, ester CH_2), 3.09(m, 1H, CH_2), 3.25(d, 1H, ester CH_2), 3.68(m, 1H, CH_2), 3.93(m, 12H, CH_2), 6.22(s, 1H, OH), 8.71(s, 1H, meso), 8.95(s, 1H, meso), 9.70(s, 1H, meso),

9.72(s, 1H, meso); Mass Spectrum (70 eV), 638 (M+), calcd. 638, IR(KBr) ν_{co} 1780.

Ethyl Acetate Gemini Octaethylchlorin, Reduced (88)

The chlorin alcohol 87 was reduced in the same manner as the simple chlorin 77, yield, 80%. ^{1}H NMR ($CDCl_3$) δ-2.46(s, 2H, NH), 0.40(t, 3H, CH_3), 0.97(t, 3H, CH_3), 1.40(t, 3H, ester CH_3), 1.80(m, 18H, CH_3), 2.15(m, 1H, CH_2), 2.40(m, 2H, CH_2), 2.65(m, 1H, CH_2), 3.50(m, 2H, CH_2), 3.7-4.1(m, 12H, CH_2), 4.44(q, 2H, ester CH_2), 5.29(t, 1H, ring H), 8.73(s, 1H, meso), 8.88(s, 1H, meso), 9.73(s, 2H, meso); Mass Spectrum (70 eV) 622 (M+), calcd. 622; IR(KBr) co 1760.

Amide Linked Imidazole Chlorin (89)

The ester (30 mg) 88 was dissolved in CH_2Cl_2 (10 ml) and diluted with methanol (20 ml). Methanolic sodium hydroxide (5 ml, 5%) was added and the mixture allowed to stand overnight.

The next day the solution was diluted with CH_2Cl_2 and water, the organic layer separated and dried. The crude acid was dissolved in dry CH_2Cl_2 (20 ml) and refluxed with oxalyl chloride (1 ml). After 20 min, the solvent and excess oxalyl chloride were removed in vacuo. The residue was redissolved in CH_2Cl_2 (10 ml) and treated with 3-(N-imidazolyl)propylamine and refluxed 1 h. Extraction and chromatography produced the tailed chlorin, yield 50%. ^{1}H NMR ($CDCl_3$) -2.5(br s, 2H, NH), 0.67(t, 3H, CH_3), 0.90(t, 3H, CH_3), 1.75(m, 18H, CH_2), 2.0-2.8(m, 8H, CH_2), 2.9-3.4(m, 6H, CH_2), 3.9(m, 12H, CH_2), 5.12(t, 1H, ring H), 5.51(t, 1H, NH), 6.21(s, 1H, Im-H), 6.56(s, 1H, Im-H), 7.05(s, 1H, Im-H), 8.73(s, 1H, meso), 8.85(s, 1H, meso),

9.67(s, 1H, meso), 9.69(s, 1H, meso); Mass Spectrum (70 eV) 702 (M+), calcd 702.

3-(1-Imidazolyl)propylamine

Acrylonitrile (20 gm, 0.38 mol) was heated to 75°C and imidazole (13.6 gm, 0.2 mol) was added in small portions. The mixture was heated to 90° and stirred for 3 h. After cooling, the mixture was evaporated to dryness and the residual oil dissolved in methanol (100 ml). The solution was decolorized with activated charcoal, and concentrated to yield the 1-(β-cyanoethyl)imidazole.

The nitrile (18 gm), dissolved in methanol saturated with ammonia, was hydrogenated with W-7 Raney-nickel catalyst (50 psi) for 4 h. The solution was flushed with nitrogen and filtered. Treatment with activated charcoal and concentration produced a sticky yellow oil. The oil was purified by bulb to bulb distillation (200°, 4 mm Hg) to yield a colorless oil. ^{1}H NMR ($CDCl_3$) δ 2.03(q, 2H, CH_2), 3.07(t, 2H, CH_2), 4.05(t, 2H, CH_2), 6.80(s, 1H, Im-H), 6.94(s, 1H, Im-H), 7.45(s, 1H, Im-H); Mass Spectrum (70 eV), 126 (M+), calcd 125.

Ethanol Gemini Octaethylchlorin (91)

The ester chlorin, 88, was dissolved in THF and treated with an excess of lithium aluminum hydride/THF. After 3 min the reaction was quenched by the careful addition of water. Extraction with CH_2Cl_2 and chromatography through a silica pad produced the corresponding alcohol in >90% yields. ^{1}H NMR ($CDCl_3$) δ -2.40(s, 2H, NH), 0.61(t, 3H, CH_3), 0.83(s, 3H, CH_3), 1.79(m, 18H, CH_3), 2.22(m, 2H, CH_2), 2.56(m, 2H, CH_2), 2.72(q, 2H, CH_2), 3.95(m, 14H, CH_2), 4.72(t, 1H, ring H),

8.70(s, 1H, meso), 8.95(s, 1H, meso), 9.70(s, 2H, meso); Mass spectrum (70 ev) 580 (m+), calcd. 580.

Ester linked imidazole chlorins

The chlorin alcohol 91 was dissolved in CH_2Cl_2 and treated with an excess of the imidazole-acid chlorides. The mixture was refluxed for 2 h, diluted with water, extracted with CH_2Cl_2 and washed with dilute acid, base, and water. Chromatography on thick layer silica gel plates (5% methanol/CH_2Cl_2) produced the tailed chlorins in high yields (70-80%). The products were recrystallized from methanol/CH_2Cl_2 to yield shiny green flakes.

Ester Linked Imidazole Chlorins, n=1 (92)

^{1}H NMR ($CDCl_3$) δ-2.40(s, 2H, NH), 0.75(t, 3H, CH_3), 0.80(t, 3H, CH_3), 1.83(m, 18H, CH_3), 2.12(m, 2H, CH_2), 2.32(m, 2H, CH_2), 2.50(m, 2H, CH_2), 2.70(m, 2H, CH_2), 3.95(m, 12H, CH_2), 4.56(s, 2H, CH_2Im), 4.60(m, 3H, ring H, CH_2O), 6.84(s, 1H, Im-H), 7.08(s, 1H, Im-H), 7.43(s, 1H, Im-H), 8.71(s, 1H, meso), 8.87(s, 1H, meso), 9.70(s, 2H, meso); Mass Spectrum (70 eV), 688 (M+), calcd. 688.

n=2 (93)

^{1}H NMR ($CDCl_3$) δ-2.42(s, 2H, NH), 0.63(t, 3H, CH_3), 0.81(t, 3H, CH_3), 1.77(m, 18H, CH_3), 2.23(m, 2H, CH_2), 2.56(m, 2H, CH_2), 2.71(m, 4H, CH_2), 3.96(m, 12H, CH_2), 4.15(t, 2H, CH_2Im), 4.54(m, 3H, CH_2O, ring H), 6.85(s, 1H, Im-H), 7.00(s, 1H, Im-H), 7.48(s, 1H, Im-H), 8.68(s, 1H, meso), 8.87(s, 1H, meso), 9.70(s, 2H, meso); Mass Spectrum (70 eV), 702 (M+), calcd. 702.

n=3 (94)

^{1}H NMR ($CDCl_3$) δ-2.41(s, 2H, NH), 0.65(t, 3H, CH_3), 0.82(t, 3H, CH_3), 1.80(m, 18H, CH_3), 1.96(m, 4H, CH_2), 2.2(m, 4H, CH_2), 2.57(m, 2H, CH_2), 2.76(m, 2H, CH_2), 3.94(m, 14H, CH_2), 4.6(m, 3H, ring H, CH_2Im), 6.80(s, 1H, Im-H), 7.03(s, 1H, Im-H), 7.43(s, 1H, Im-H), 8.70(s, 1H, meso), 8.89(s, 1H, meso), 9.70(s, 2H, meso); Mass Spectrum (70 eV), 716 (M+), calcd. 716.

3-methyl,4-keto Gemini Octaethylisobacteriochlorin Alcohol (95)

Methyllithium (1.6 M ether) was added dropwise at room temperature to a THF solution of 2,3 diketone 63 (50 mg). The reaction was monitored by tlc, the mono alkylated species appears blue-green and was of intermediate polarity. The red diol was the most polar species formed. The reaction was quenched with saturated aqueous ammonium acetate after a statistical distribution of the alkylated products were observed. Ether extraction and separation on a silica gel column produced the mono alkylated species, with yields dependent on triketone impurities. ^{1}H NMR ($CDCl_3$) δ0.50(t, 6H, CH_3), 0.86(t, 3H, CH_3), 1.27(t, 3H, CH_3), 1.68(m, 12H, CH_3), 1.90(s, 3H, CH_3), 2.48(m, 8H, CH_2), 2.70(s, 1H, OH), 3.69(m, 8H, CH_2), 8.09(s, 1H, meso), 8.31(s, 1H, meso), 8.43(s, 1H, meso), 9.23(s, 1H, meso).

3-Methyl, 4-Ethyl Acetate Gemini Octaethylisobacteriochlorin Diol (96)

The mono alkylated IBC 95 was alkylated in the same fashion as the monoketone 66 with $LiCH_2CO_2Et$. ^{1}H NMR ($CDCl_3$) δ0.61(t, 3H, CH_3), 0.89(t, 3H, CH_3), 0.96(t, 3H, ester CH_3), 1.04(t, 3H, CH_3), 1.34(t, 3H, CH_3), 1.48(m, 12H, CH_3), 1.88(s, 3H, CH_3), 2.14(m, 6H, CH_3), 2.53(d, 1H, ester CH_2), 2.91(d, 1H, ester CH_2), 3.31(t, 3H, CH_3),

3.91(m, 1H, CH_2), 4.07(m, 1H, CH_2), 5.71(s, 1H, OH), 7.11(s, 1H, meso), 7.30(s, 1H, meso), 7.32(s, 1H, meso), 8.49(s, 1H, meso); Mass Spectrum (70 eV), 670 (M+), calcd. 670.

3-Methyl, 4-Ethyl Acetate, Gemini OEIBC, Reduced

The isobacteriochlorin diol 96 was reduced by the usual procedure using the hydriodic acid reagent.

Mono Alcohol (98)

^{1}H NMR ($CDCl_3$) δ0.59(t, 3H, CH_3), 0.85(t, 3H, CH_3), 0.93(t, 6H, CH_3), 1.35(t, 3H, CH_3), 1.49(m, 12H, CH_3), 1.67(d, 3H, CH_3), 2.0(m, 8H, CH_2), 2.50(d, 1H, ester CH_2), 2.92(d, 1H, ester CH_2), 3.29(m, 8H, CH_2), 3.9(m, 3H, CH_2, ring H), 5.73(s, 1H, OH), 6.86(s, 1H, meso), 7.19(s, 1H, meso), 7.21(s, 1H, meso), 8.43(s, 1H, meso); Mass Spectrum (70 eV), 654 (M+), calcd. 654.

3-Methyl 4-Ethanol Gemini OEIBC (100)

The isobacteriochlorin ester, 99, was reduced by lithium aluminum hydride in the same manner as the chlorin ester, 88, to yield the corresponding primary alcohol. ^{1}H NMR ($CDCl_3$) δ0.55(t, 3H, CH_3), 0.90(m, 6H, CH_3), 1.30(t, 3H, CH_3), 1.40(m, 12H, CH_3), 1.63(d, 3H, CH_3), 1.70-2.5(m, 5H, OH, CH_2), 3.20(m, 8H, CH_2), 3.70(m, 3H, ring H, CH_2), 6.94(s, 1H, meso), 7.08(s, 1H, meso), 7.17(s, 1H, meso), 8.33(s, 1H, meso).

Ester-linded Imidazole Geminal Isobacteriochlorin (101)

The isobacteriochlorin alcohol, 100, was dissolved in CH_2Cl_2 and treated with an excess of (N-imidazolyl) propionyl chloride dissolved in acetonitrile. The mixture was refluxed 2 h under argon then

diluted with water. Separation of the organic layer and washing with acid and base produced the crude product. Purification was performed on thick layer silica gel plates (5% methanol/CH_2Cl_2). ^1H NMR ($CDCl_3$) 0.50(t, 3H, CH_3), 0.78(m, 6H, CH_3), 1.22(t, 3H, CH_3), 1.40(m, 12H, CH_3), 1.63(d, 3H, CH_3), 1.8-2.5(m, 4H, CH_2), 3.2(m, 8H, CH_2), 3.70(t, 2H, CH_2O), 3.80(t, 2H, CH_2Im), 3.91(m, 1H, ring H), 6.47(s, 1H, Im-H), 6.57(s, 1H, Im-H), 6.83(s, 1H, meso), 6.85(s, 1H, meso), 7.15(s, 1H, meso), 7.21(s, 1H, meso), 8.35(s, 1H, meso). Mass Spectrum (70 eV), 718 (M+), calcd. 718.

2-(N-Imidazolyl)acetyl Chloride

Ethyl bromoacetate (16 mg, 100 mmol) was slowly added to an acetone (100 ml) solution of imidazole (6.8 gm, 100 mmol) containing sodium carbonate (10.6 gm, 100 mmol). The reaction, which was initially vigorous, was refluxed for 4 h. After cooling, the salts were filtered off, and the solvent and excess bromo ester removed in vacuo. The crude oil was dissolved in CH_2Cl_2 and washed with water and saturated aqueous sodium bicarbonate. After drying the crude solid was recrystallized from hexane/CH_2Cl_2.

The ester (1 gm) was dissolved in acetic acid (20 ml) containing hydrochloric acid (1 ml). After refluxing under argon for 1 h, the solvent was removed in vacuo to yield the crude acid.

The crude acid was dissolved in acetonitrile and purged of oxygen. Excess oxalyl chloride was added and the mixture refluxed until the evolution of SO_2 ceased, ca. 1 h. Removal of excess oxalyl chloride and solvents on the pump produced an off white solid which was used

without further purification. Ester; ^{1}H NMR ($CDCl_3$) δ1.56(t, 3H, CH_3), 4.44(q, 2H, CH_2), 4.90(s, 2H, CH_2), 7.13(s, 1H, Im-H), 7.23(s, 1H, Im-H), 7.66(s, 1H, Im-H); Mass Spectrum (70 eV), 154 (M+), calcd. 154.

3-(N-Imidazolyl) Proprionic Acid

Imidazole (6.8 gm, 0.1 mmol) and excess methyl acrylate (17.2 gm, 0.2 mmol) were dissolved in ether (50 ml). The mixture was refluxed for 3 h. The excess acrylate and ether were removed in vacuo to yield a yellow oil. Unreacted imidazole was removed by cooling the sample and filtering. The acid and acid chloride were formed in the same manner as the acetic acid analogue. ^{1}H NMR($CDCl_3$) δ2.79(t, 2H, CH_2), 3.70(s, 3H, OCH_3), 4.28(t, 2H, CH_2), 6.92(s, 1H, Im-H), 7.03(s, 1H, Im-H), 7.50(s, 1H, Im-H); Mass Spectrum acid (70 eV), 140 (M+), calcd. 140.

4-(N-Imidazolyl) Butyric Acid

4-Bromobutyronitrile (8.3 gm, 51 mmol) and excess sodium imidazolate (8.9 gm, 100 mmol) were dissolved in dry THF under argon. The mixture was stirred 24 h at room temperature. The salts were filtered and a yellow oil resulted after evaporation.

The crude imidazolyl butyronitrile was added to a saturated aqueos potassium hydroxide solution (16 gm, 6 ml H_2O). Enough ethanol was added to obtain a homogeneous solution, and the mixture refluxed for 5 h. After cooling to room temperature, HBr (48%) was added dropwise until a pH of 4 was obtained. The salts were filtered off and the filtrate evaporated to yield a sticky yellow solid. The acid was

washed several times with methanol to finally yield a yellow solid containing a small amount of KBr.

The acid chloride was generated in the same fashion as the acetic acid derivative. ^{1}H NMR ($CDCl_3$) δ 1.62(m, 2H, CH_2), 1.80(m, 2H, CH_2), 3.70(t, 2H, CH_2), 6.68(s, 1H, Im-H), 6.81(s, 1H, Im-H), 7.34(s, 1H, Im-H); Mass Spectrum (70 eV), 154 (M+), calcd. 154.

Wittig Reaction on Chlorin Ketones

Triphenylphosphine (36.2 gm, 0.14 mol) and ethyl β-bromo proprionate (25 gm, 0.14 mol) were heated on a steam bath under nitrogen for 1 h. After cooling the crude salt was recrystallized from chloroform-ethanol, 20-1, diluted with ether.

A portion of the dry phosphonium salt (32 mg, 0.072 mmol) and zinc monoketone 66 (30 mg, 0.049 mmol) were dissolved in THF-DMSO (15 ml, 1-1). The solution was added to dry sodium hydride (20 mg, 0.8 mmol) under nitrogen at 0°C. After stirring for 1 h, the solution was allowed to warm to room temperature and stirred 19 h further. Dilution with water was followed by extraction with CH_2Cl_2. The organic layer was separated, washed with 15% HCl, H_2O, and sat. aqueous $NaHCO_3$, dried and evaporated to dryness. The crude product was purified on thick layer alumina plates, 1% MeOH/CH_2Cl_2. The third major band corresponds to the desired chlorin 90, yield ca. 10%. ^{1}H NMR ($CDCl_3$) δ -2.50(s, 2H, pyrrole NH), 0.38(t, 3H, Me), 0.86(m, 2H, $-CH_2$), 1.80(m, 24H, Me), 2.72(q, 2H, OCH_2), 4.0(m, 16H, CH_2), 6.80(s, 1H, CH), 9.04(s, 1H, meso), 9.81(s, 2H, meso), 9.98(s, 1H, meso).

APPENDIX

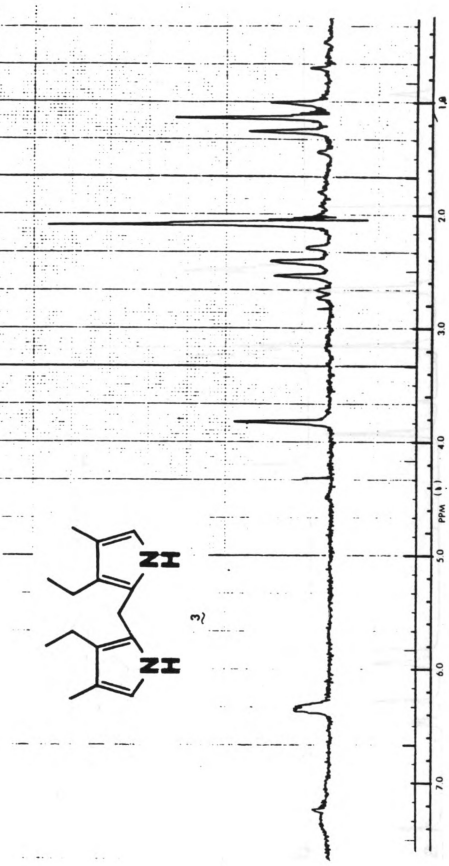

Figure A1. 60 MHz ^1H NMR spectrum of 4,4'-diethyl-3,3'-dimethyl-2,2'-dipyrrylmethane (3).

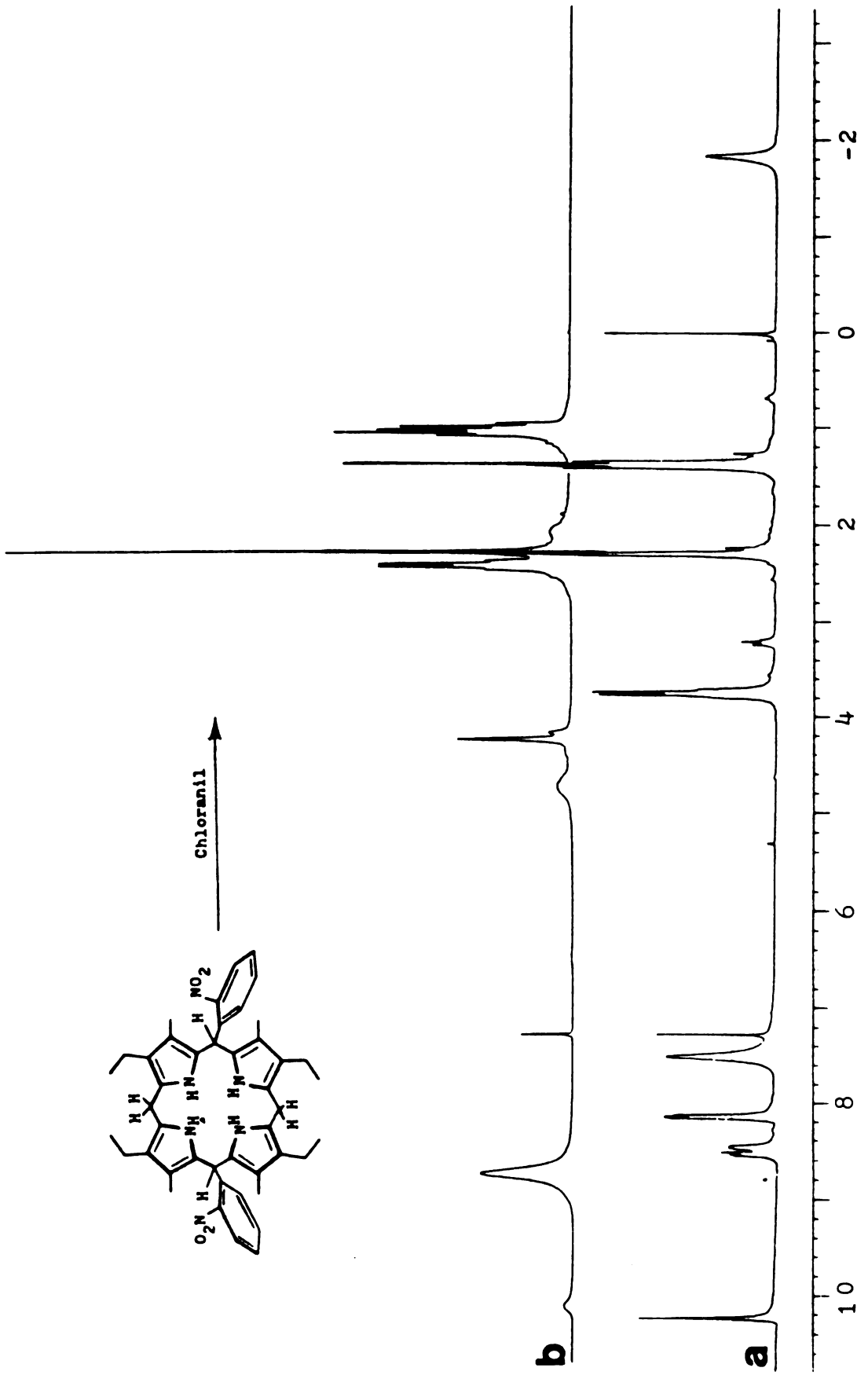

Figure A2. 250 MHz ^{1}H NMR spectra of (a) $(nitro)_2DPE$ (4); (b) $(nitro)_2DP$ etioporphyrinogen.

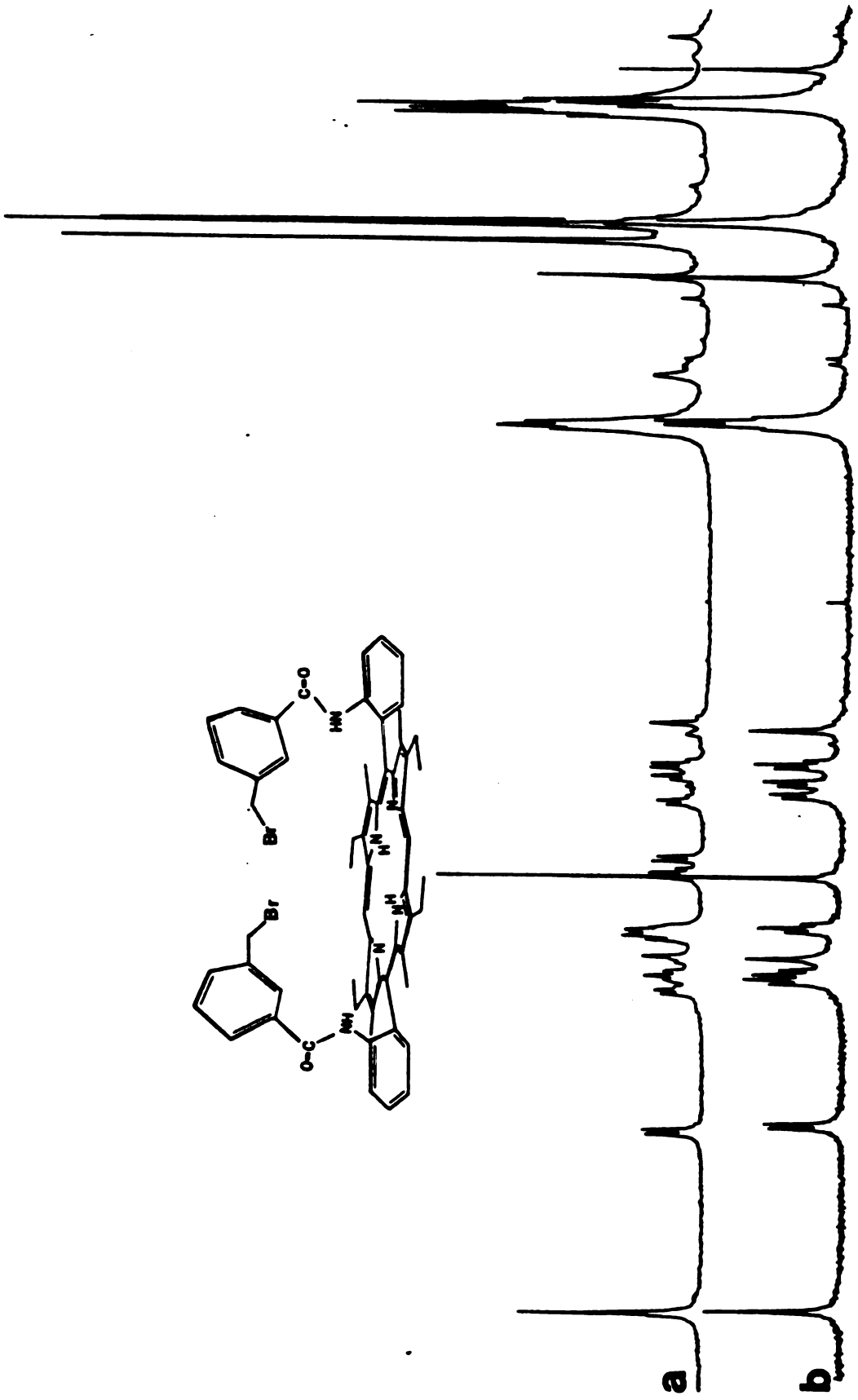

Figure A3. 250 MHz ^1H NMR spectra of (a) (amino),(m-$BrCH_2$benzamide)DPE, cis (6); (b) (m-$BrCH_2$benzamide)$_2$DPE, cis.

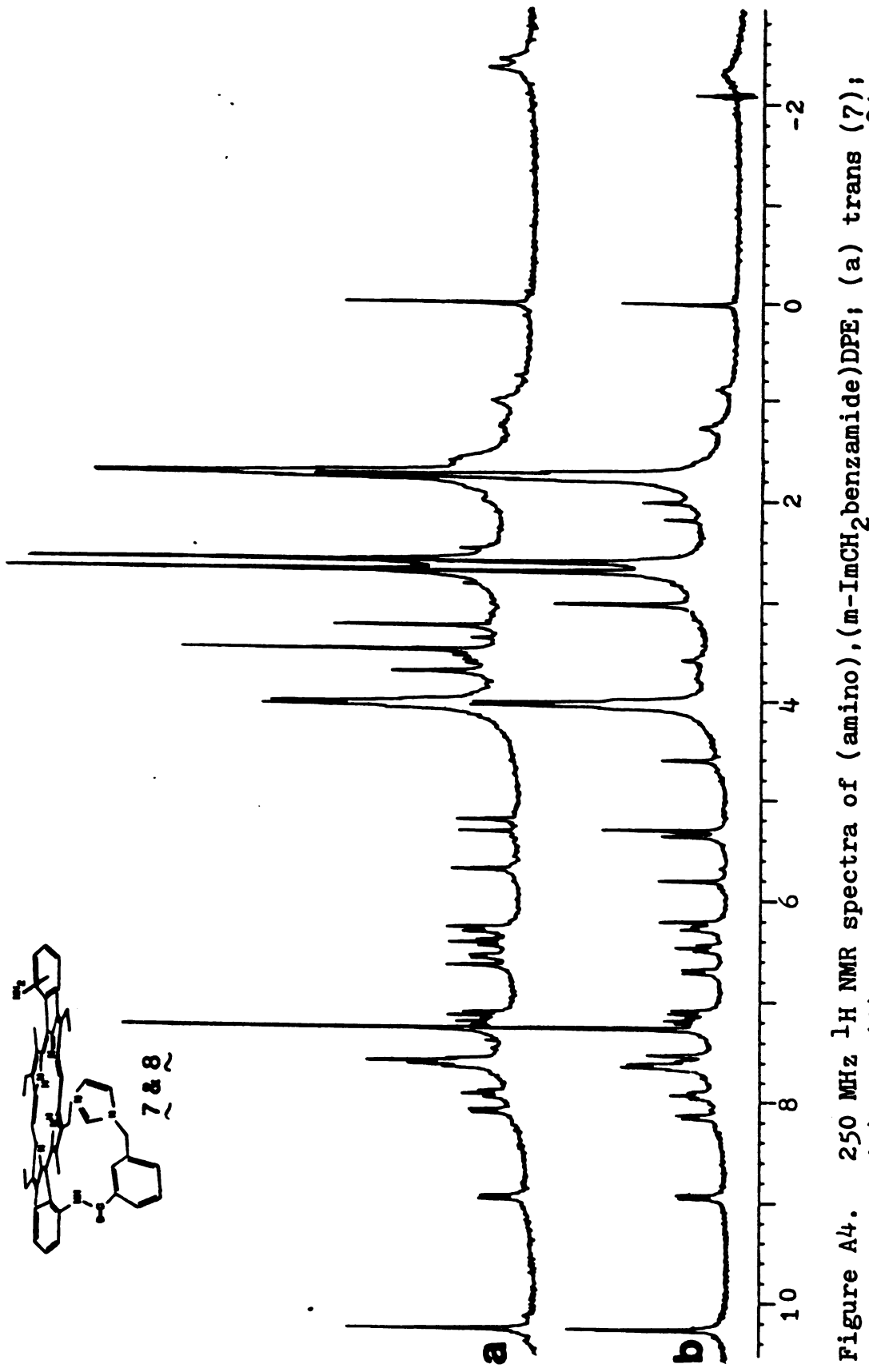

Figure A4. 250 MHz ^1H NMR spectra of (amino),(m-ImCH_2benzamide)DPE; (a) trans (7); (b) cis (8).

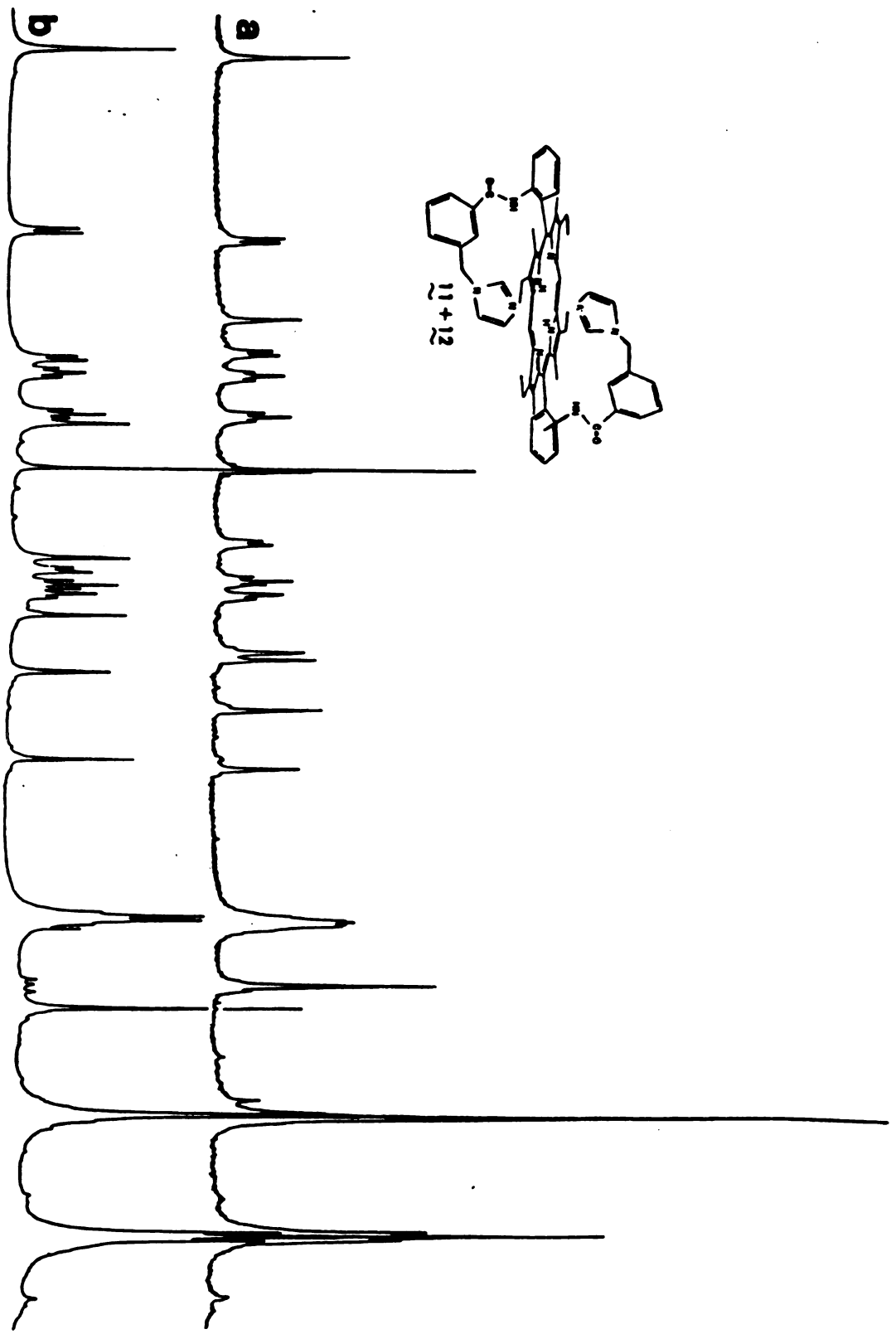

Figure A5. 250 MHz ^1H NMR spectra of (m-$ImCH_2$benzamide)$_2$DPE; (a) cis (12); (b) trans (11).

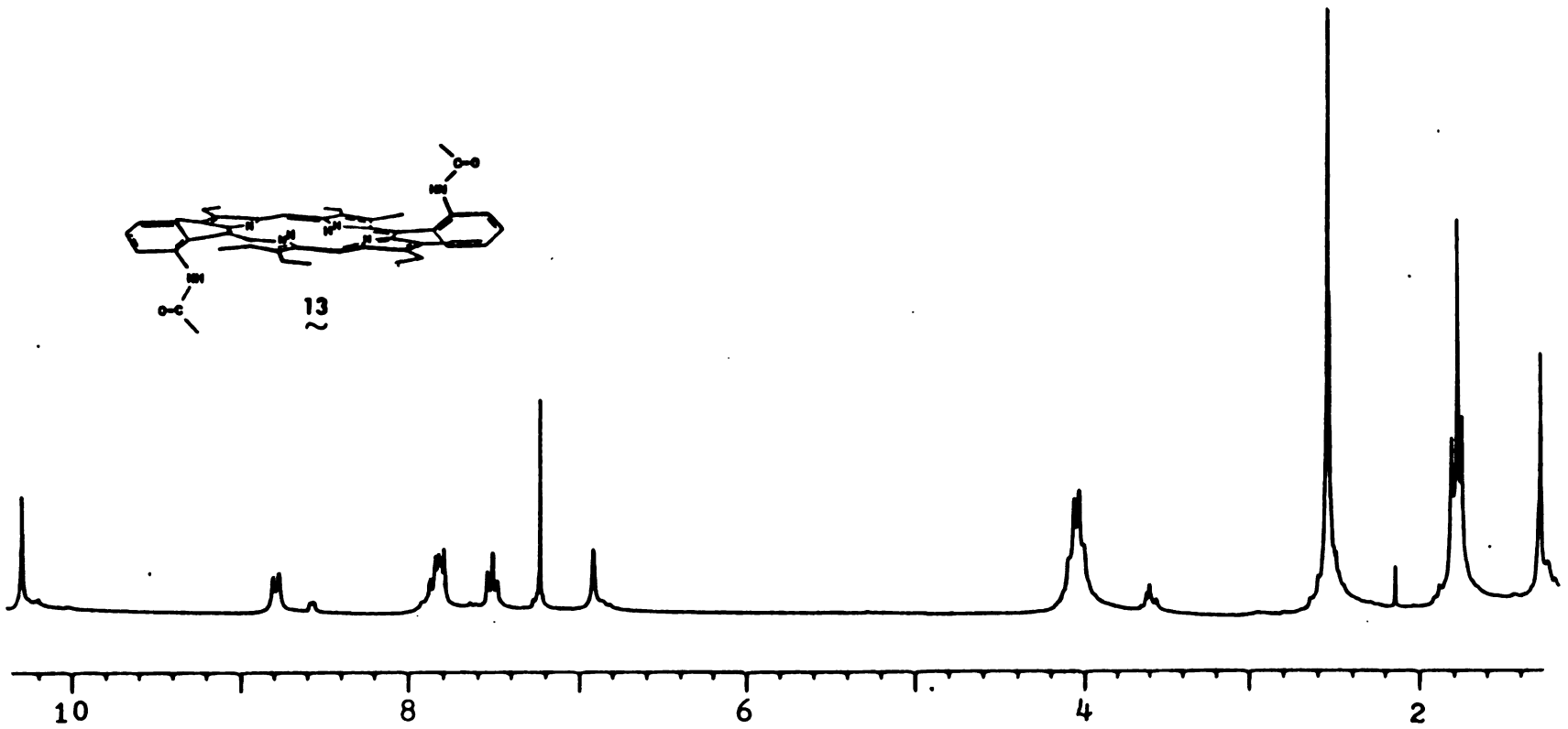

Figure A6. 250 MHz ^{1}H NMR spectrum of (acetamide)$_2$DPE, trans (13).

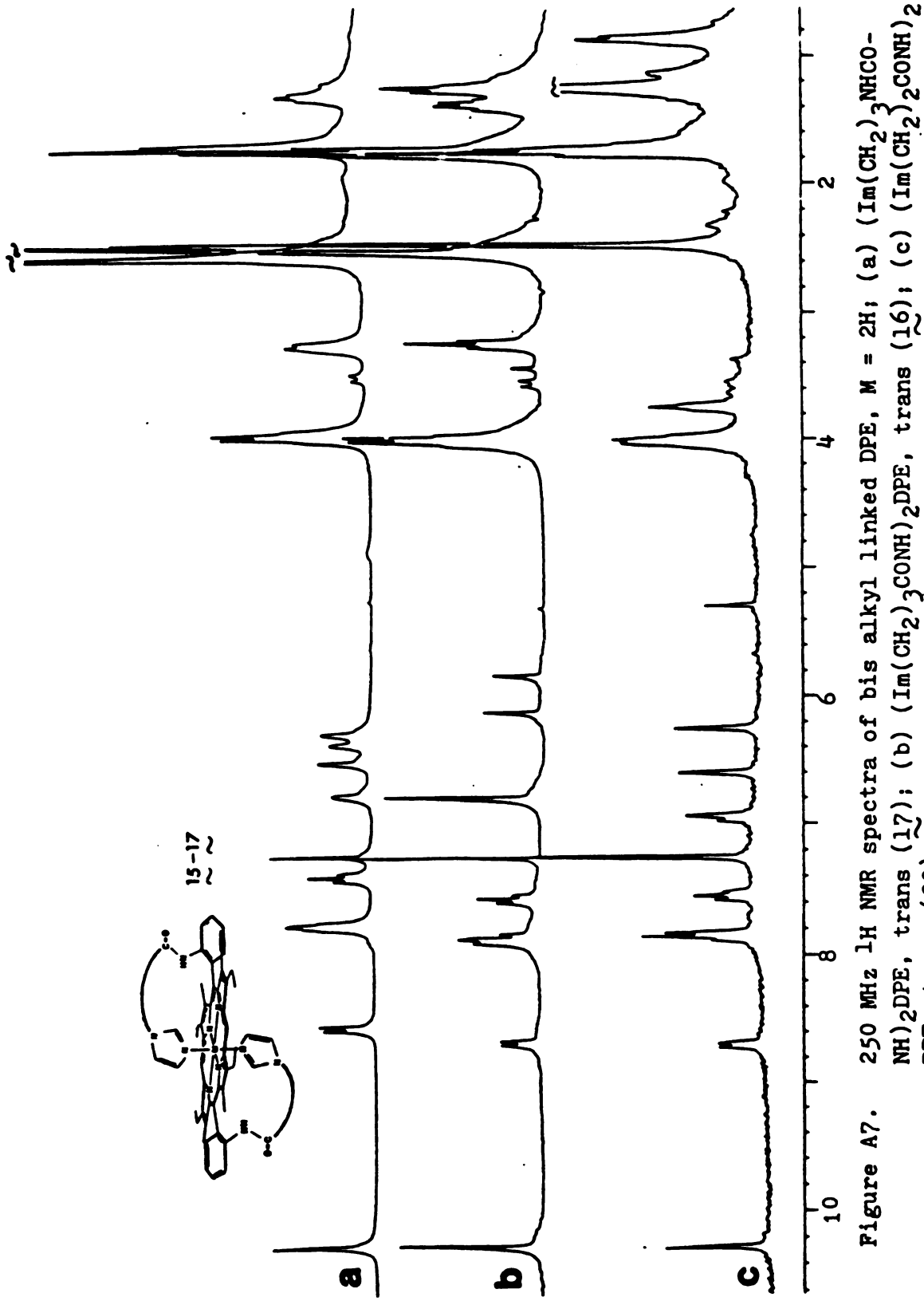

Figure A7. 250 MHz ^1H NMR spectra of bis alkyl linked DPE, M = 2H; (a) $(Im(CH_2)_3NHCO-NH)_2DPE$, trans (17); (b) $(Im(CH_2)_3CONH)_2DPE$, trans (16); (c) $(Im(CH_2)_2CONH)_2$ DPE, trans (20).

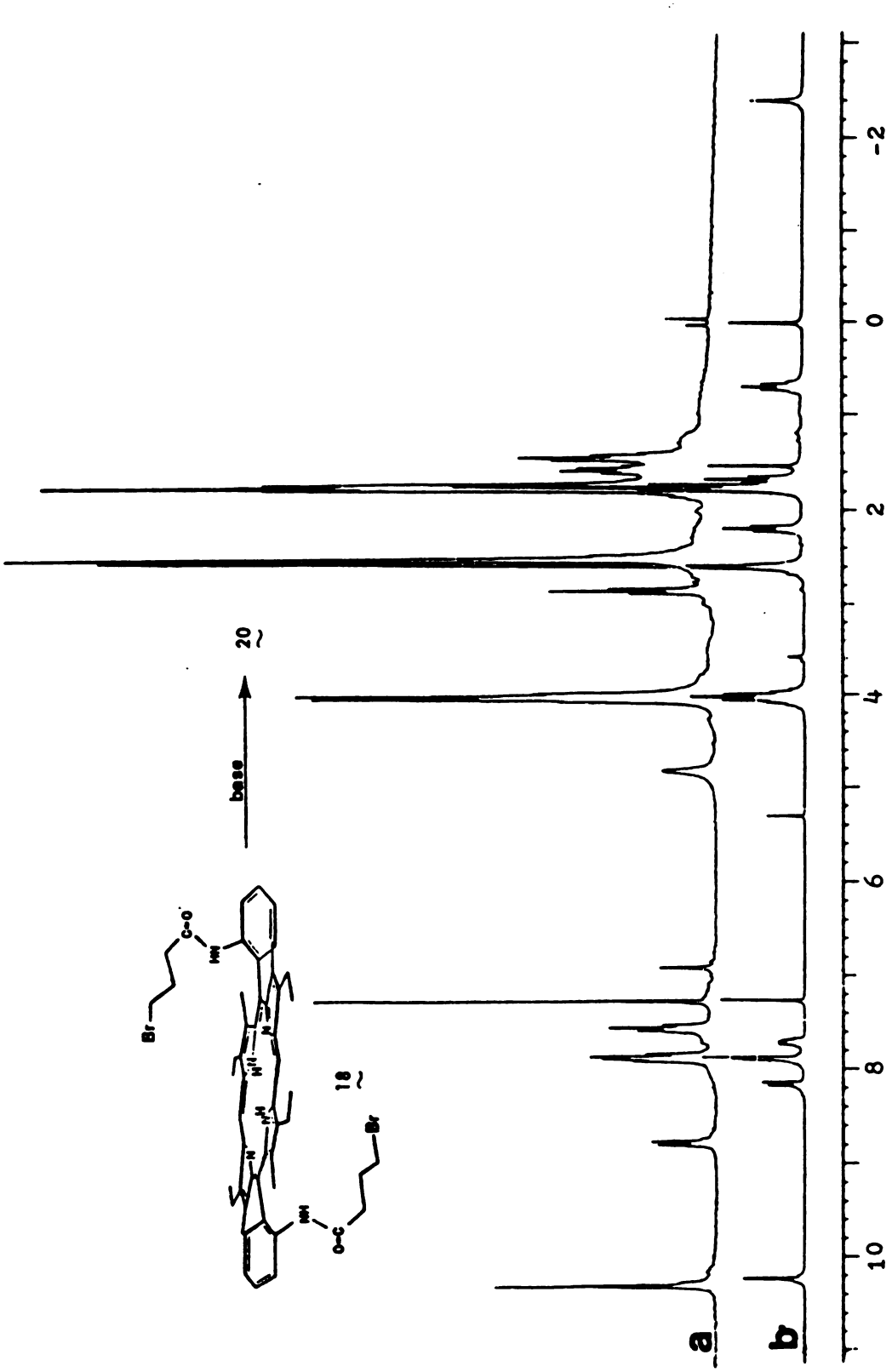

Figure A8. 250 MHz ^1H NMR spectra of (a) $(Br(CH_2)_3CONH)_2DPE$, trans (18); (b) lactam $((CH_2)_3CONH)_2DPE$, trans (20).

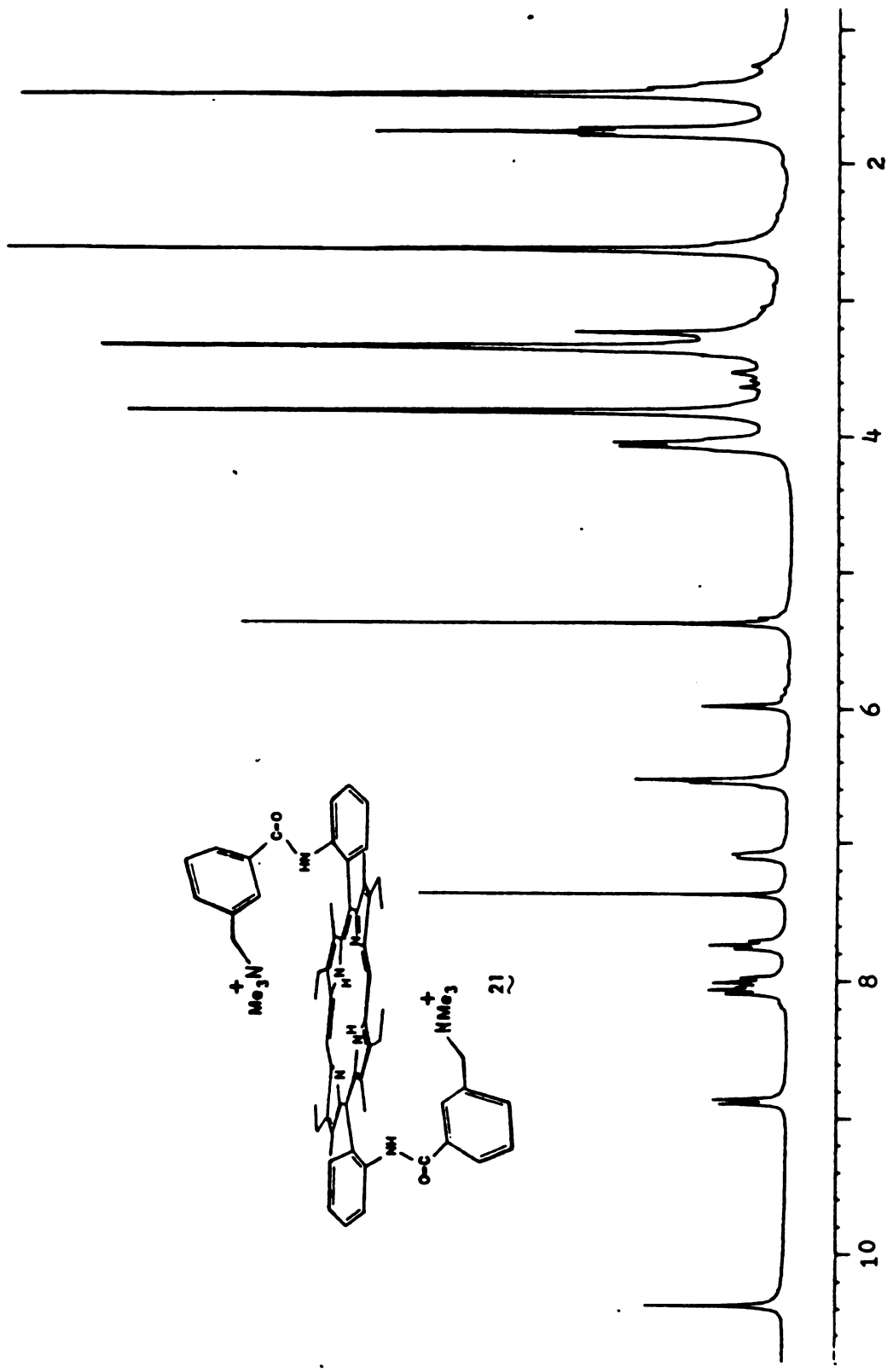

Figure A9. 250 MHz ^1H NMR spectrum of (m-$NMe_3^+CH_2$benzamide)$_2$DPE, trans (21).

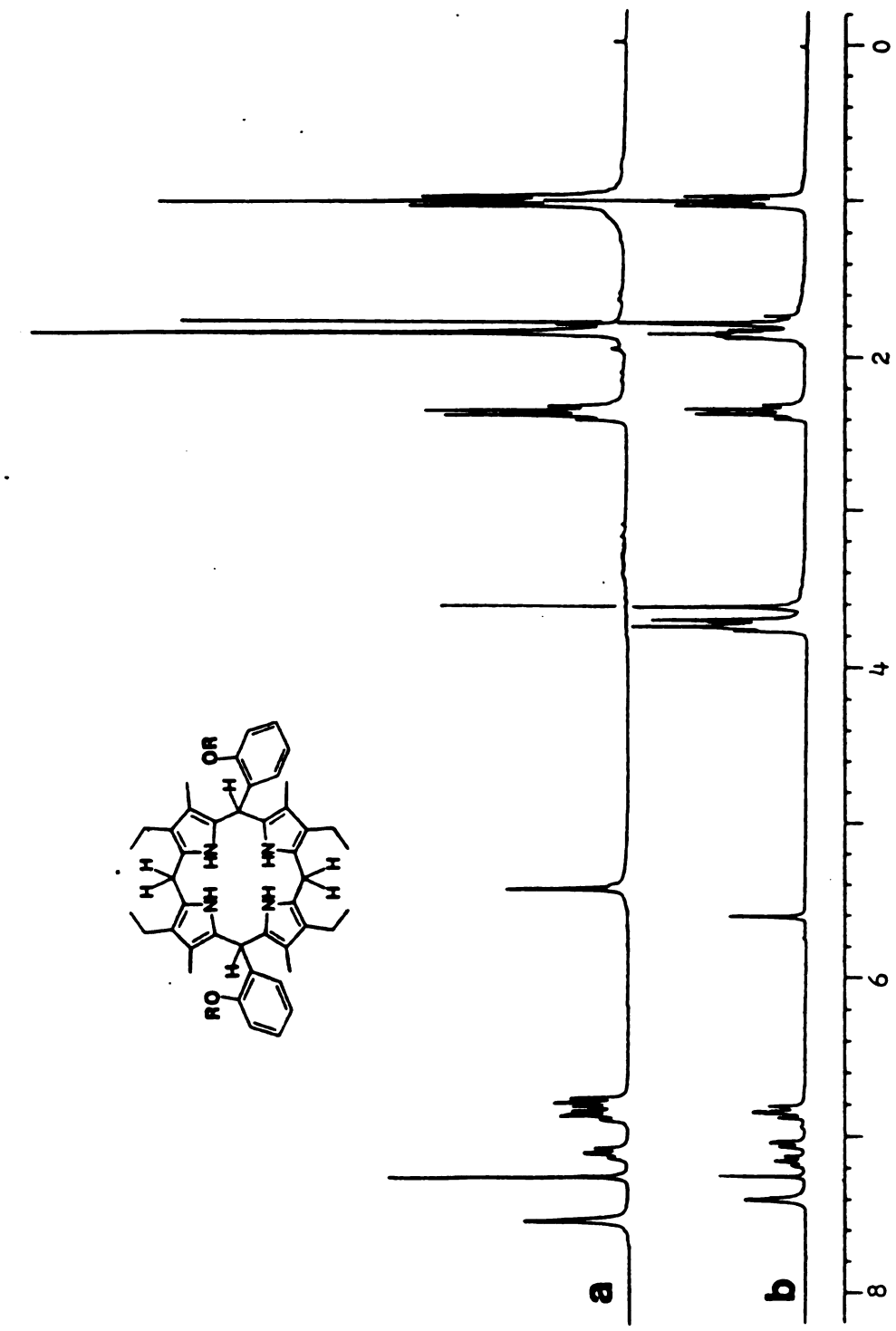

Figure A10. 250 MHz ^1H NMR spectra of phenolic porphyrinogens; (a) R = Me; (b) R = H.

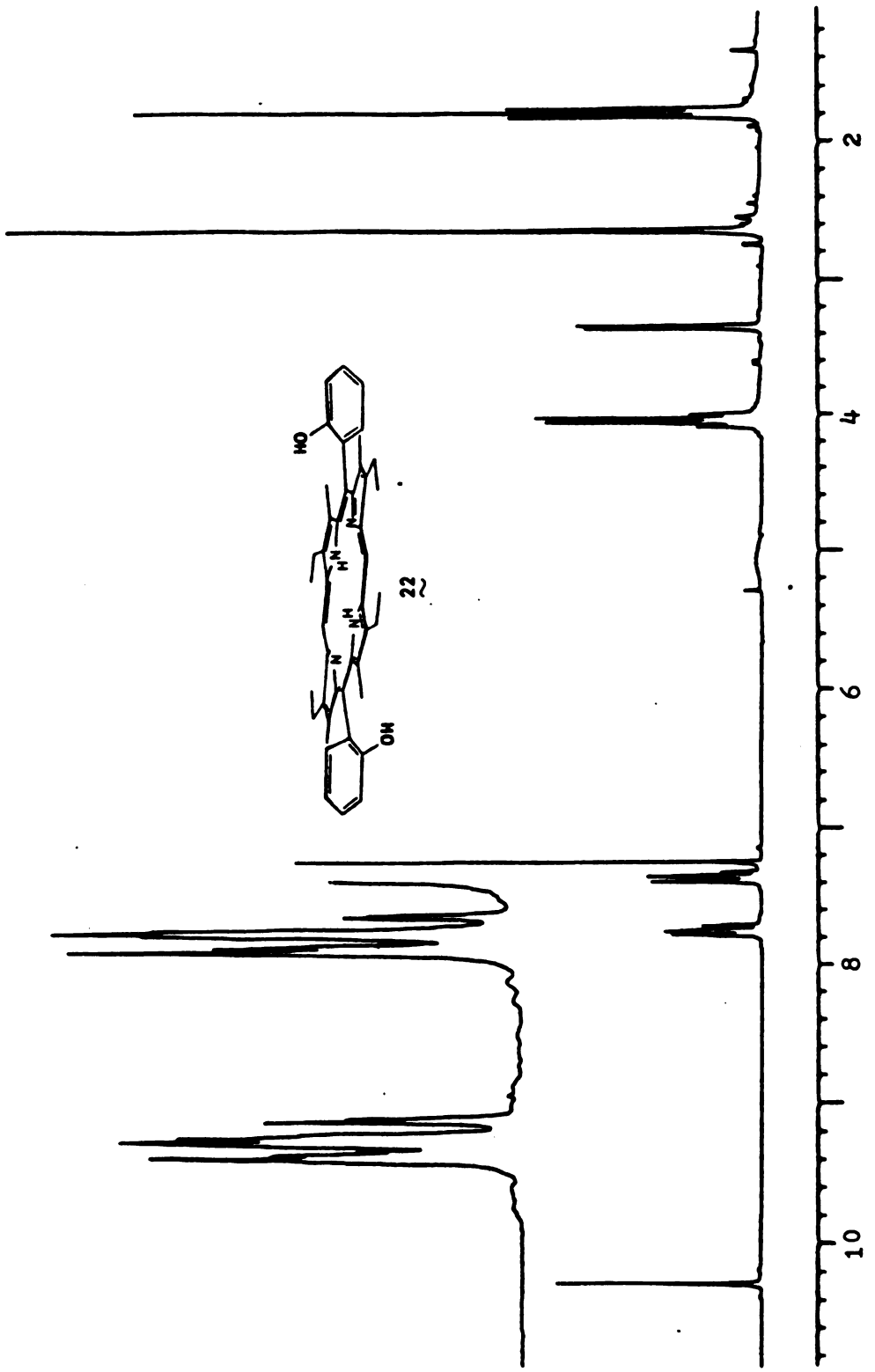

Figure All. 250 MHz ^1H NMR spectrum of (hydroxy)$_2$DPE, trans (22).

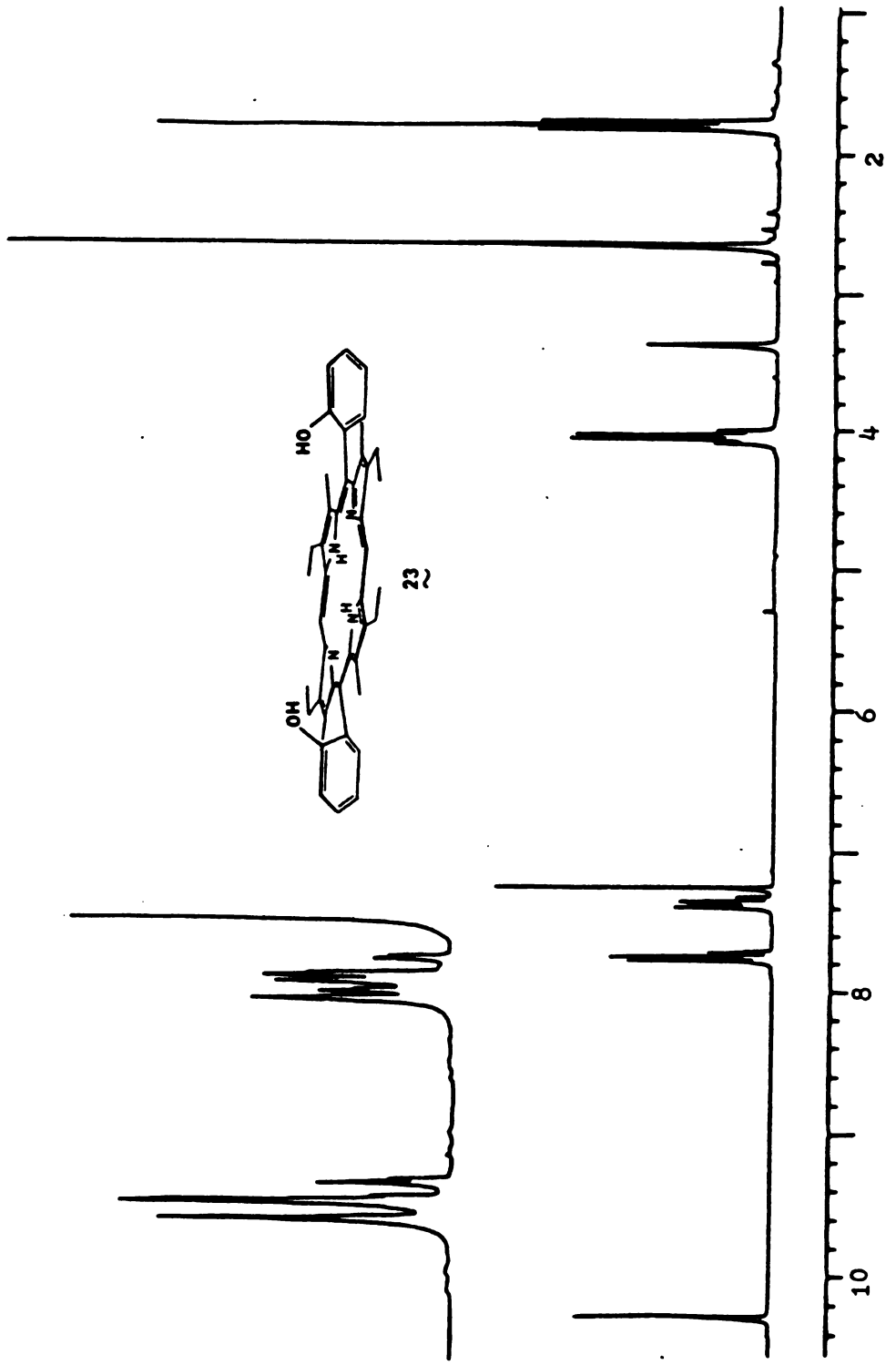

Figure A12. 250 MHz ^{1}H NMR spectrum of (hydroxy)$_2$DPE, cis (23).

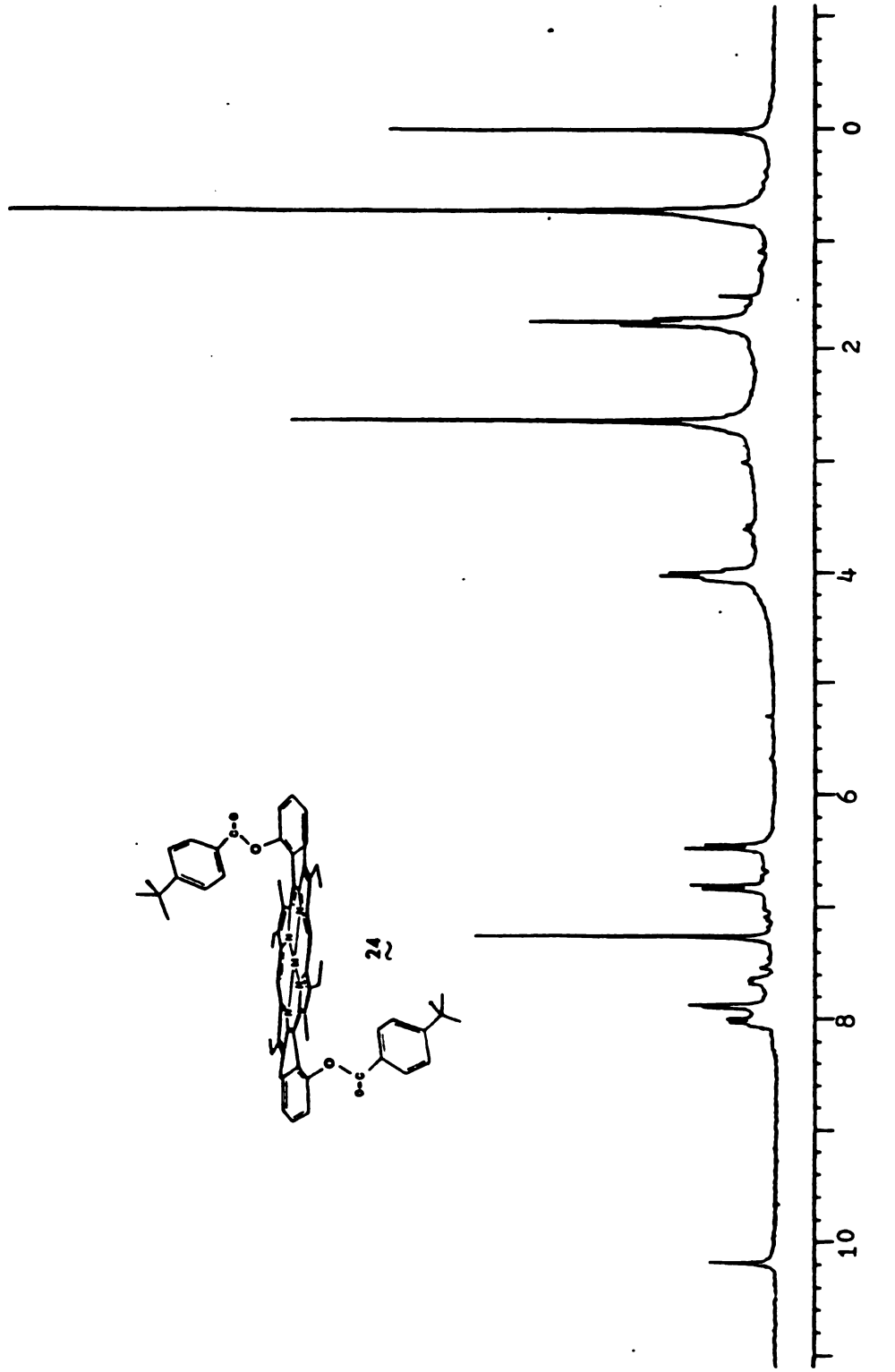

Figure A13. 250 MHz ^1H NMR spectrum of (p-tBu-benzoate)$_2$DPE, trans (24).

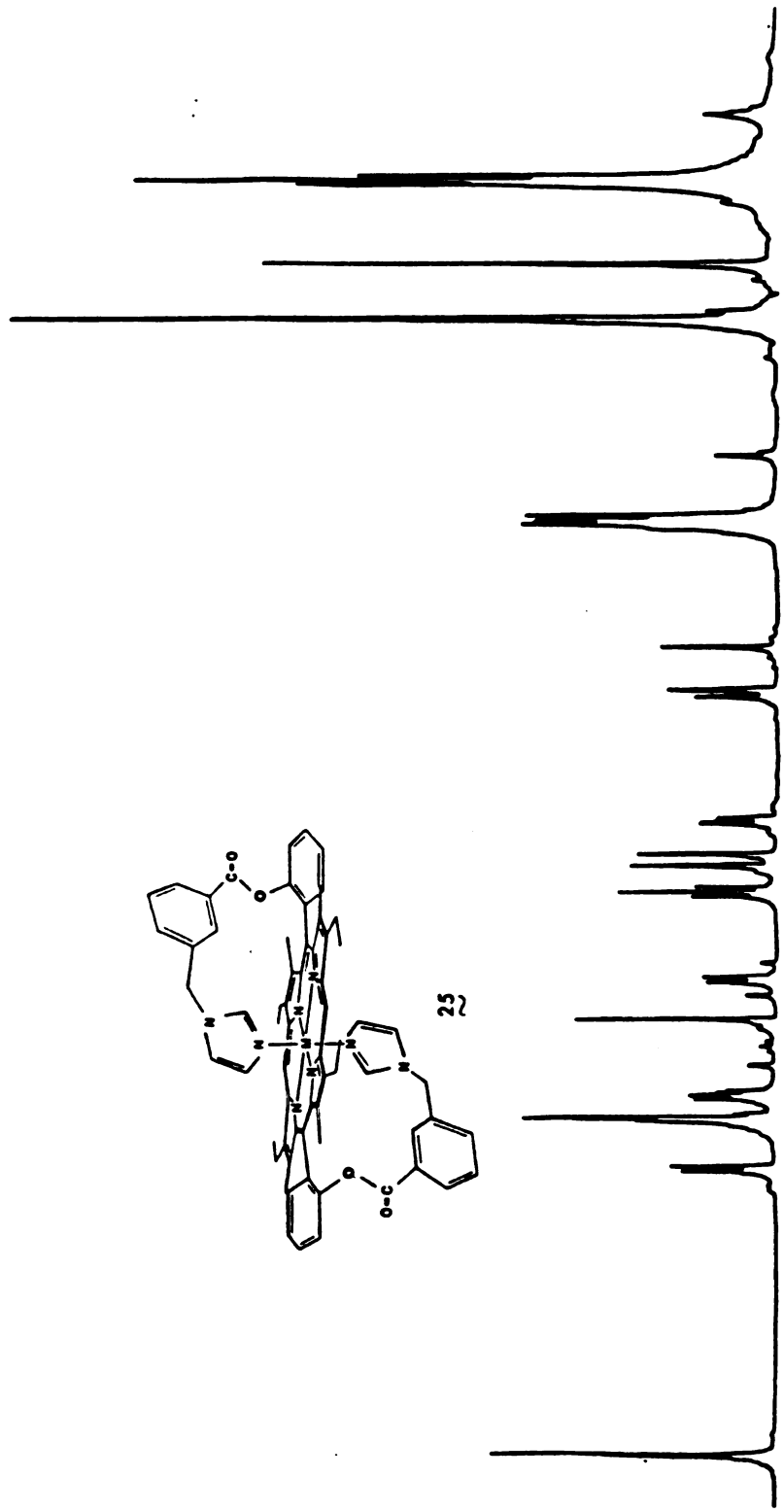

25

Figure A14. 250 MHz ^1H NMR spectrum of (m-ImCH_2benzoate)$_2$DPE, trans, M = 2H (25).

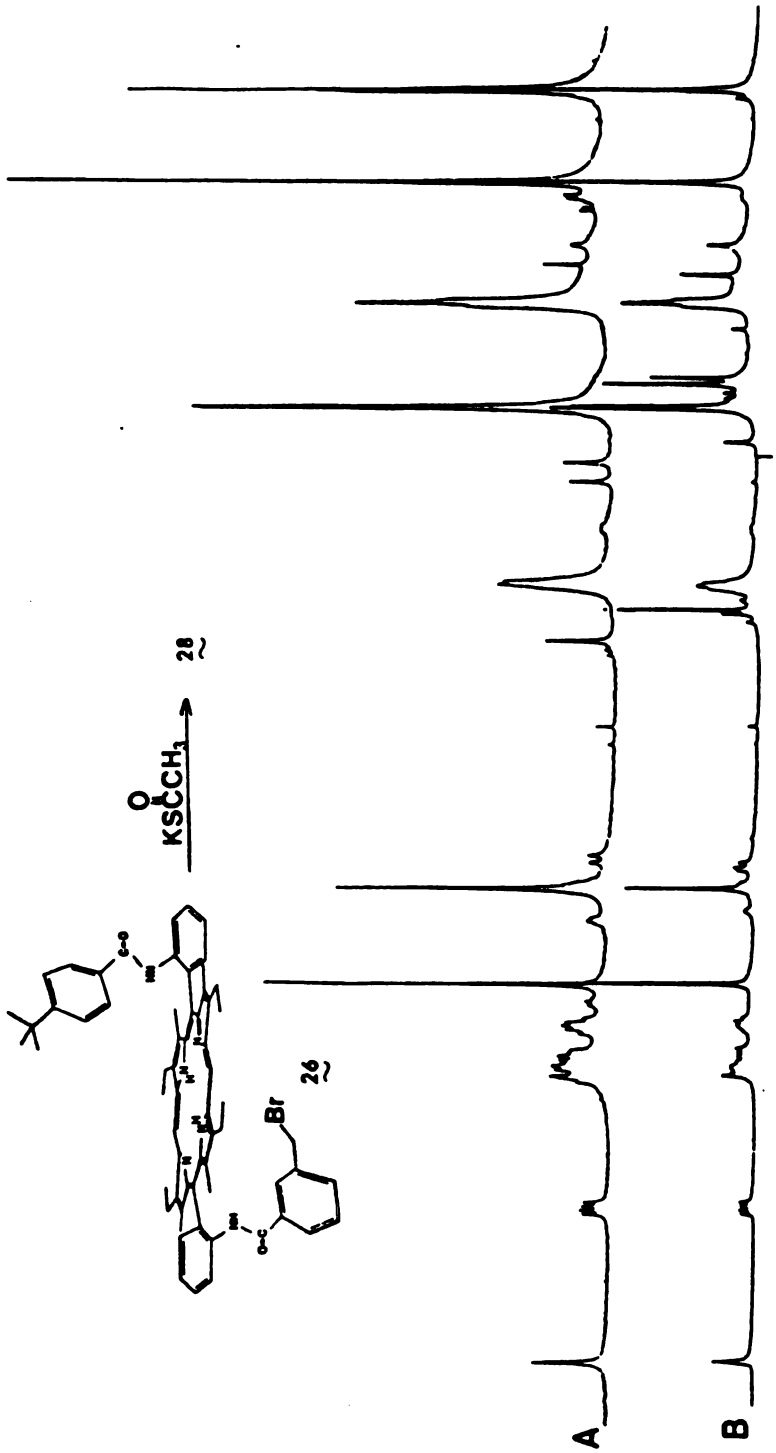

Figure A15. 250 MHz ^{1}H NMR spectra of (a) (m-$BrCH_2$benzamide),(p-tBu-benzamide)DPE, trans (26); (b) (m-$AcSCH_2$benzamide),(p-tBu-benzamide)DPE, trans (28).

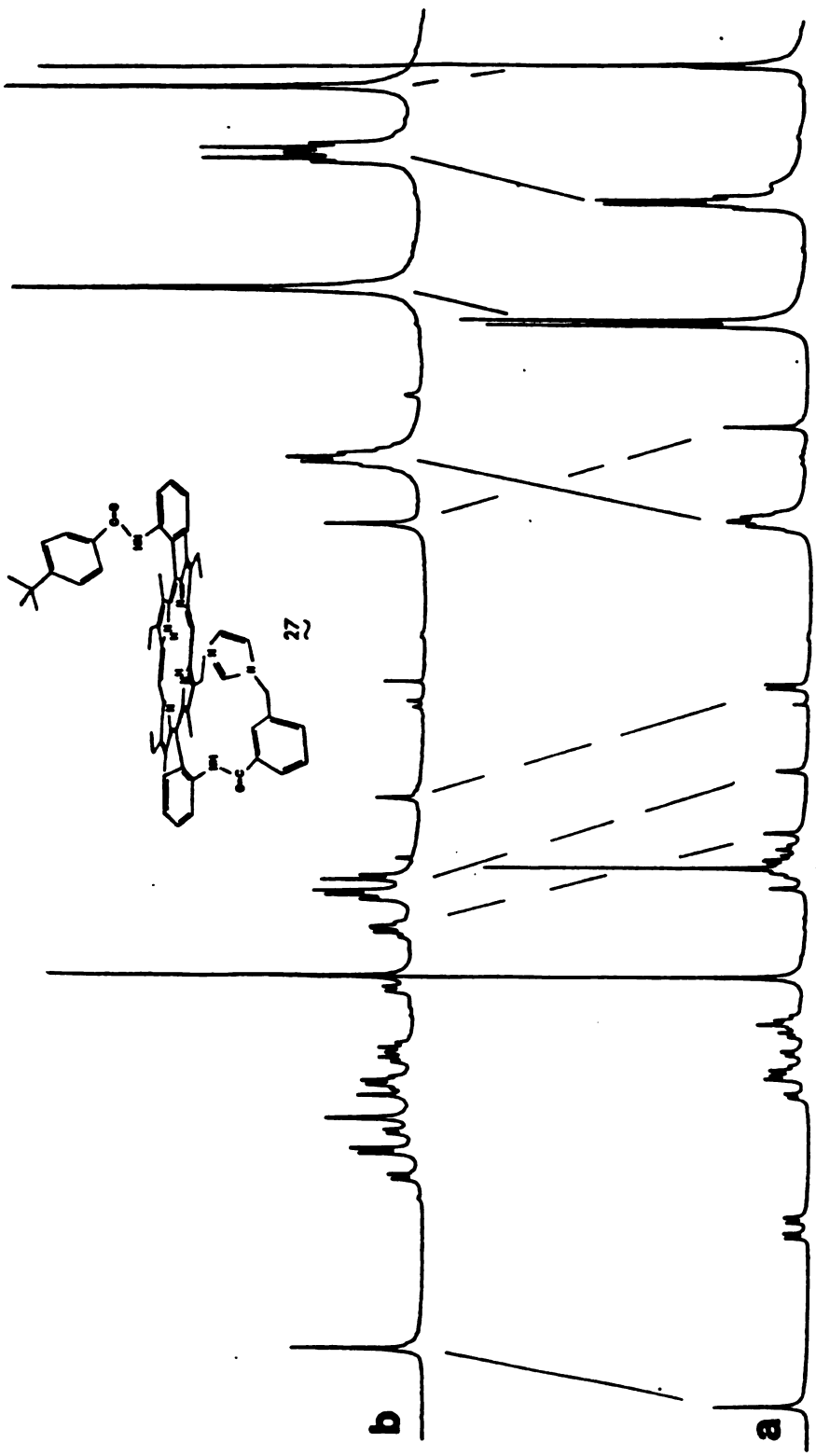

Figure A16. 250 MHz ^1H NMR spectra of (p-tBu-benzamide),(m-ImCH_2benzamide)DPE, trans (27) in (a) $CDCl_3$, (b) $CDCl_3$ + TFA.

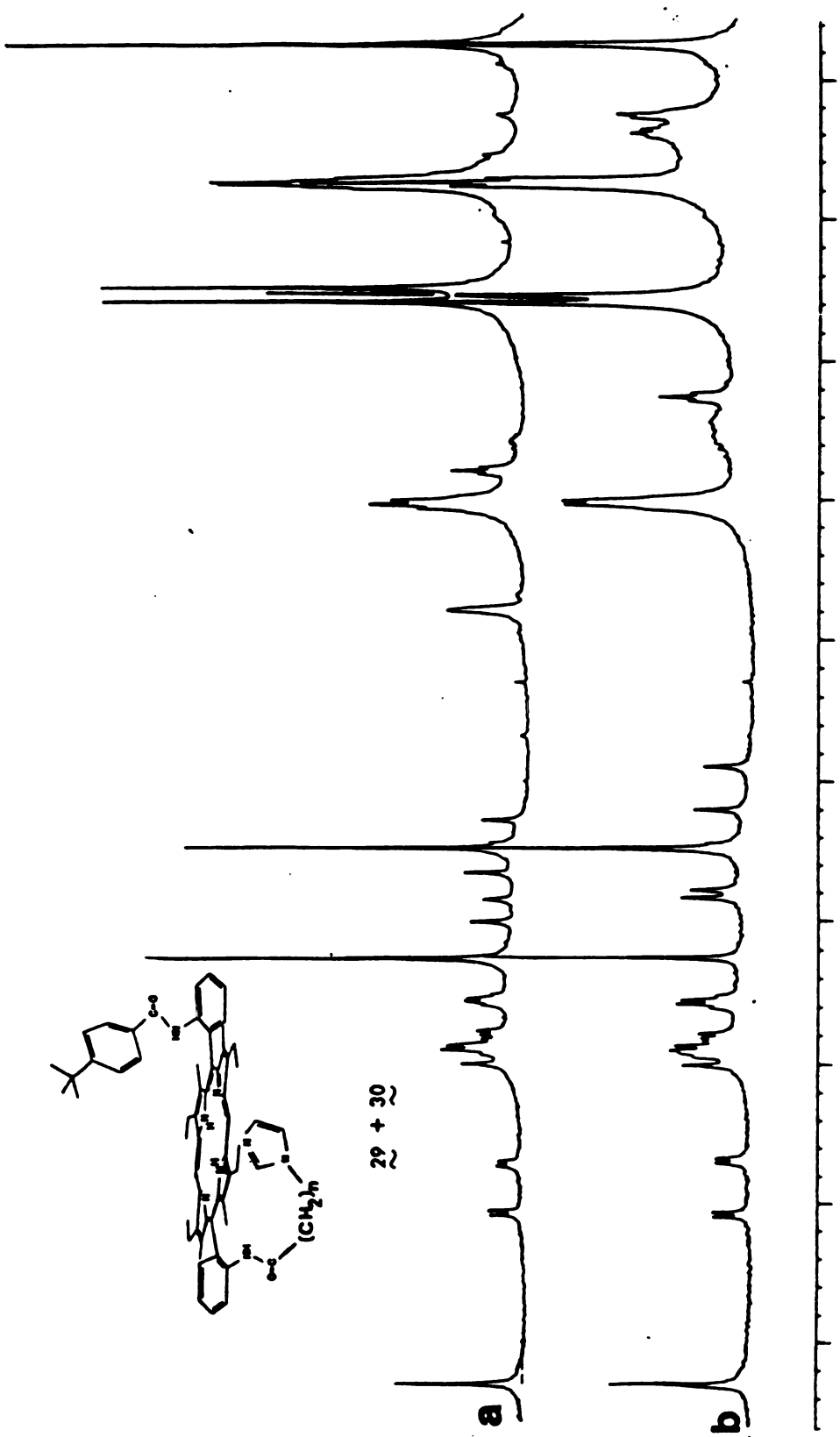

Figure A17. 250 MHz ^1H NMR spectra of (a) (p-tBu-benzamide),$(Im(CH_2)_2CONH)DPE$, trans (29); (b)(p-tBu-benzamide),$(Im(CH_2)_3CONH)DPE$, trans (30).

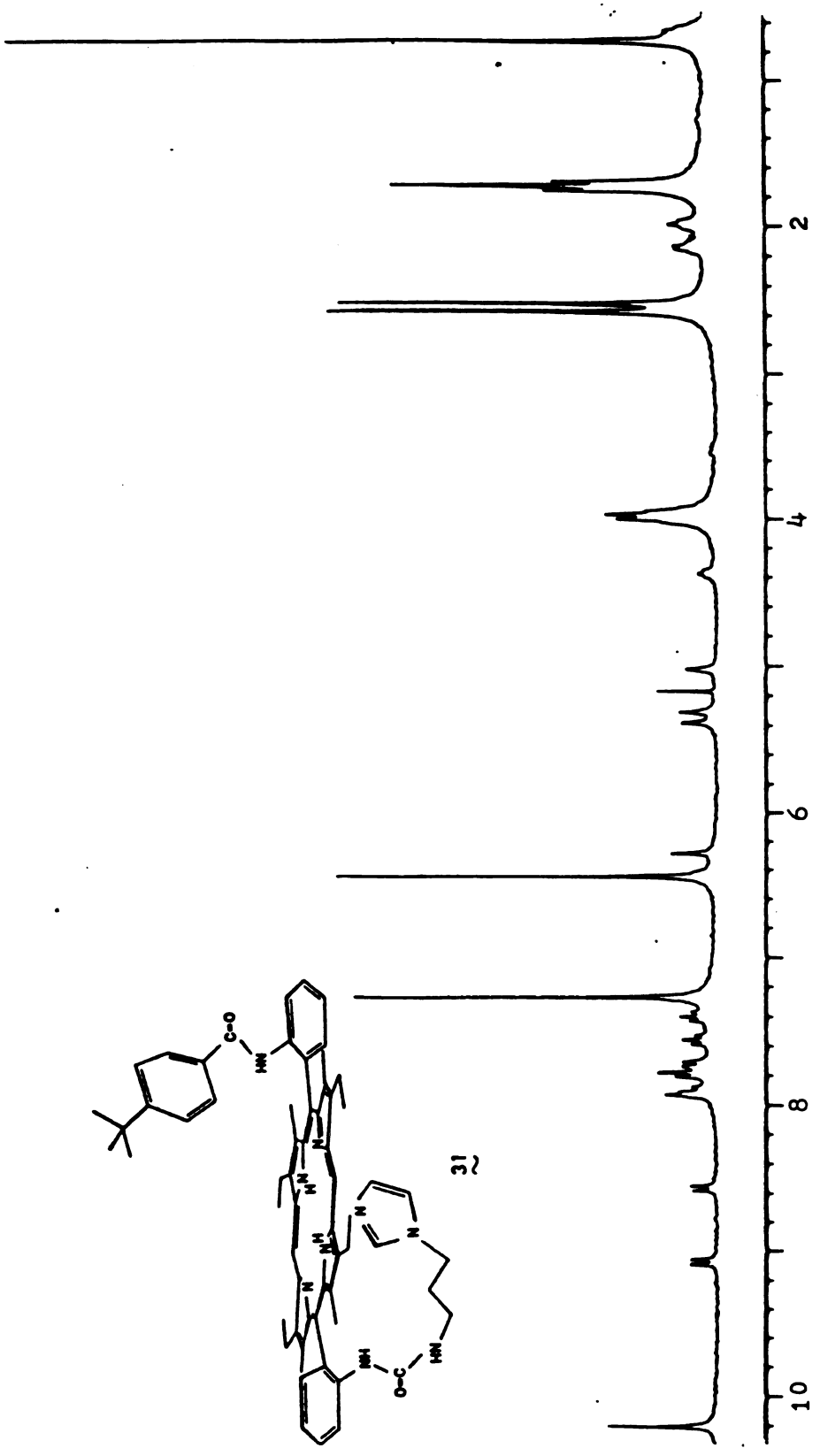

31

Figure A18. 250 MHz ^1H NMR spectrum of (p-tBu-benzamide),$(Im(CH_2)_3NHCONH)DPE$, trans (31).

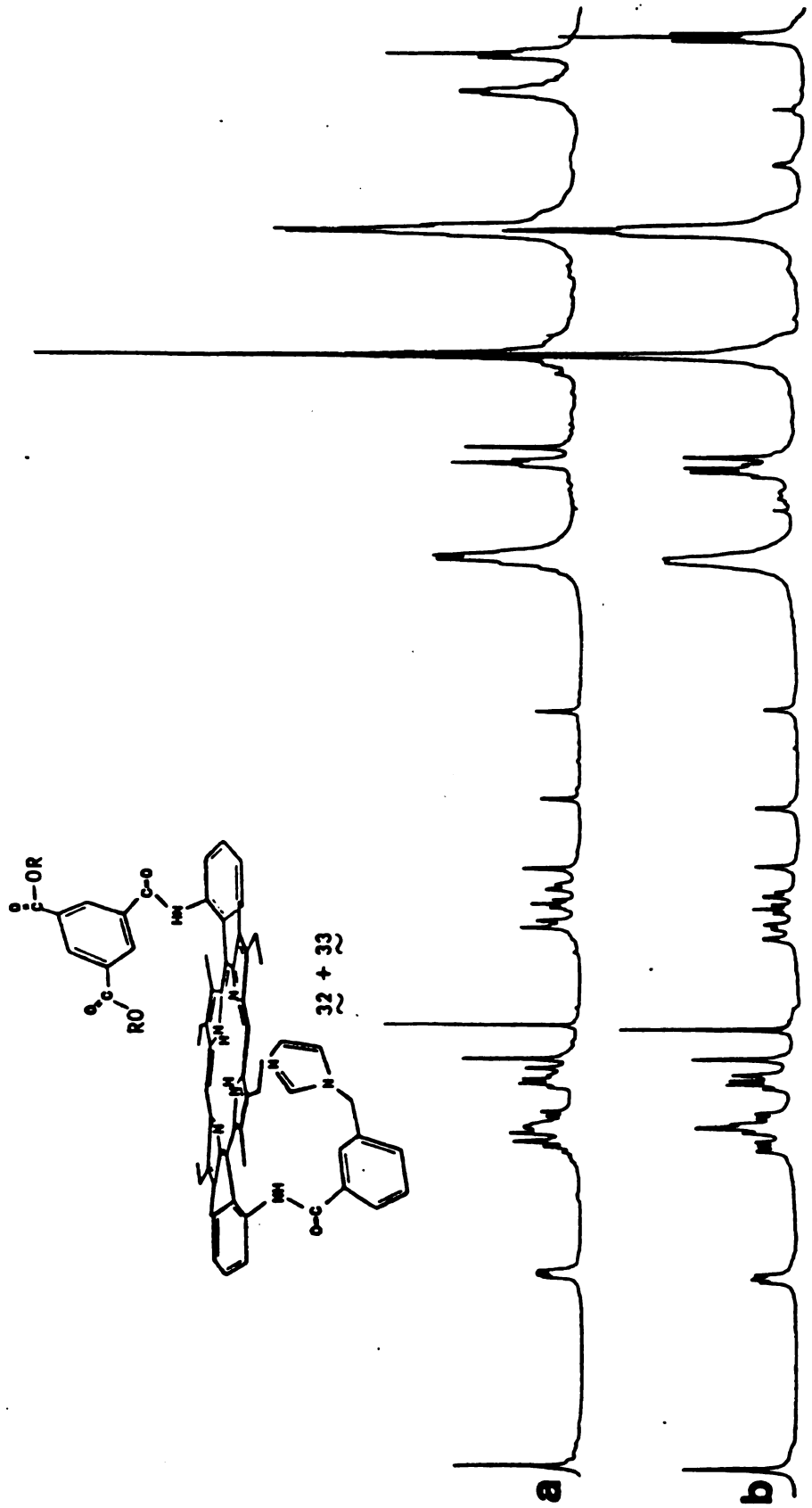

Figure A19. 250MHz ^{1}H NMR spectra of trans blocked (m-ImCH_2benzamide)DPE; (a) R = n-Bu (34); (b) R = Et (32).

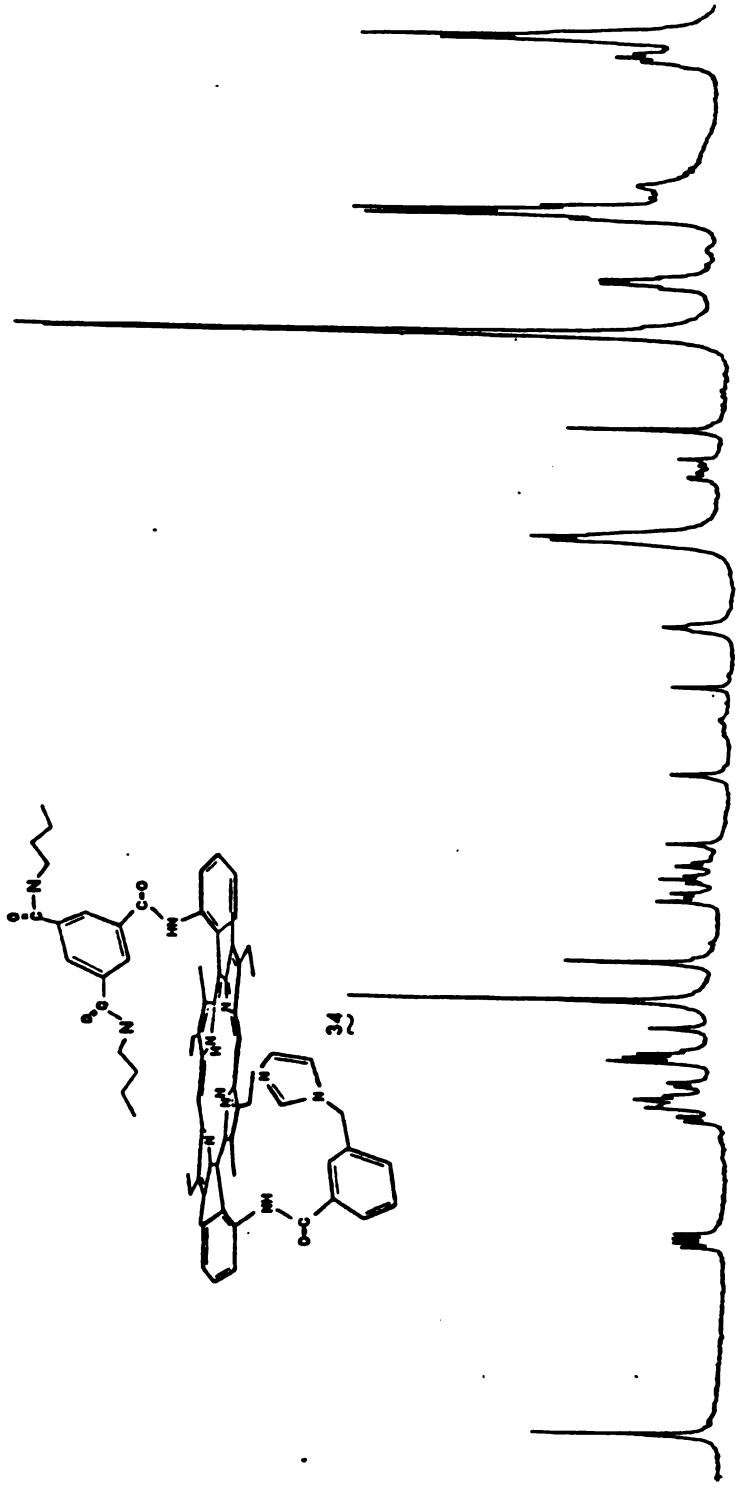

Figure A20. 250 MHz ^1H NMR spectrum of (3,5(CONH-nBu)$_2$benzamide),(m-ImCH$_2$-benzamide)DPE, trans (34).

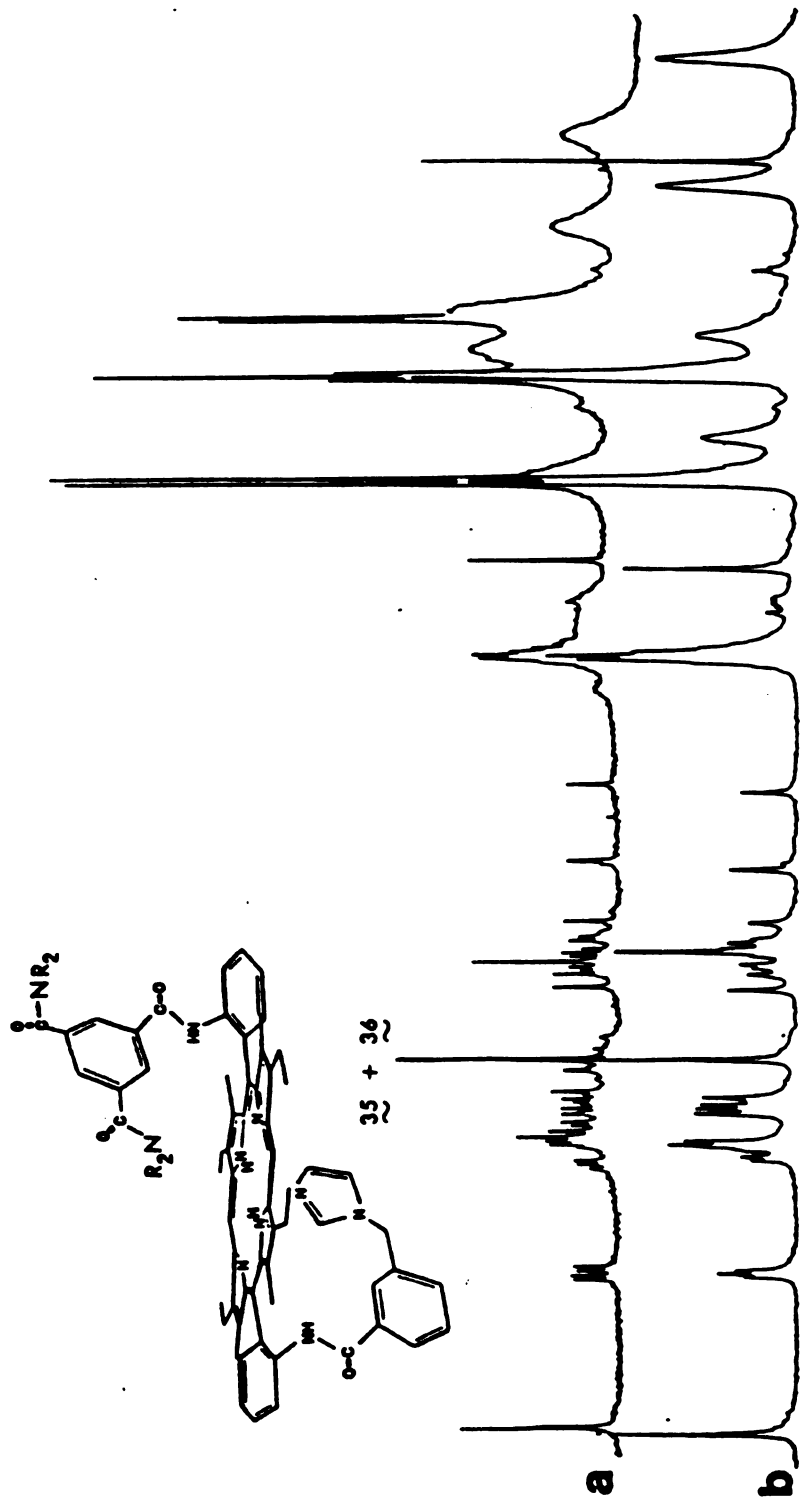

Figure A21. 250 MHz ^1H NMR spectra of trans benzamide blocked (m-ImCH_2benzamide) DPE; (a) R = iPr (36); (b) R = Et (35).

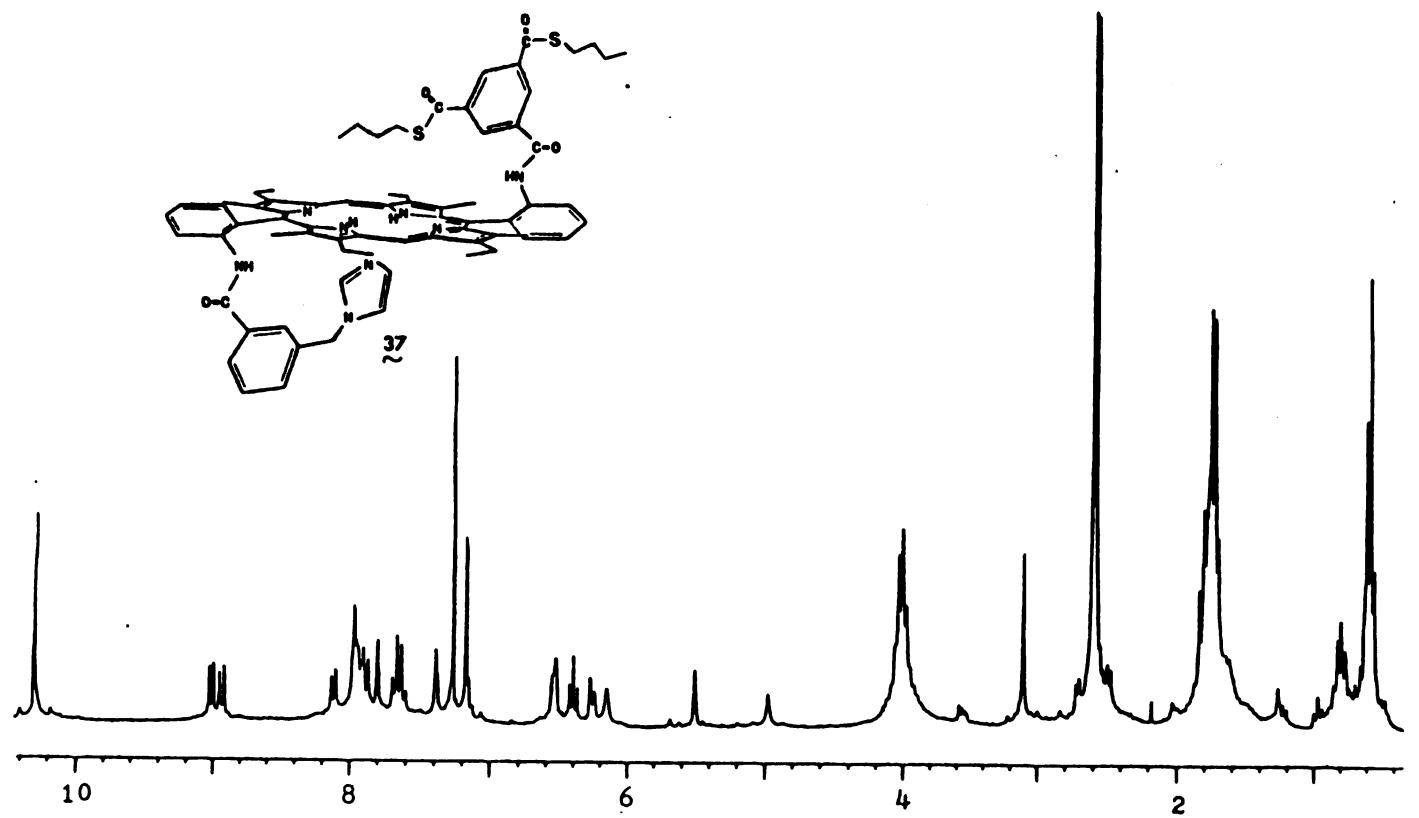

Figure A22. 250 MHz ^{1}H NMR spectrum of (3, 5(COS-nBu)$_2$benzamide),(m-ImCH$_2$-benzamide)DPE, trans (37).

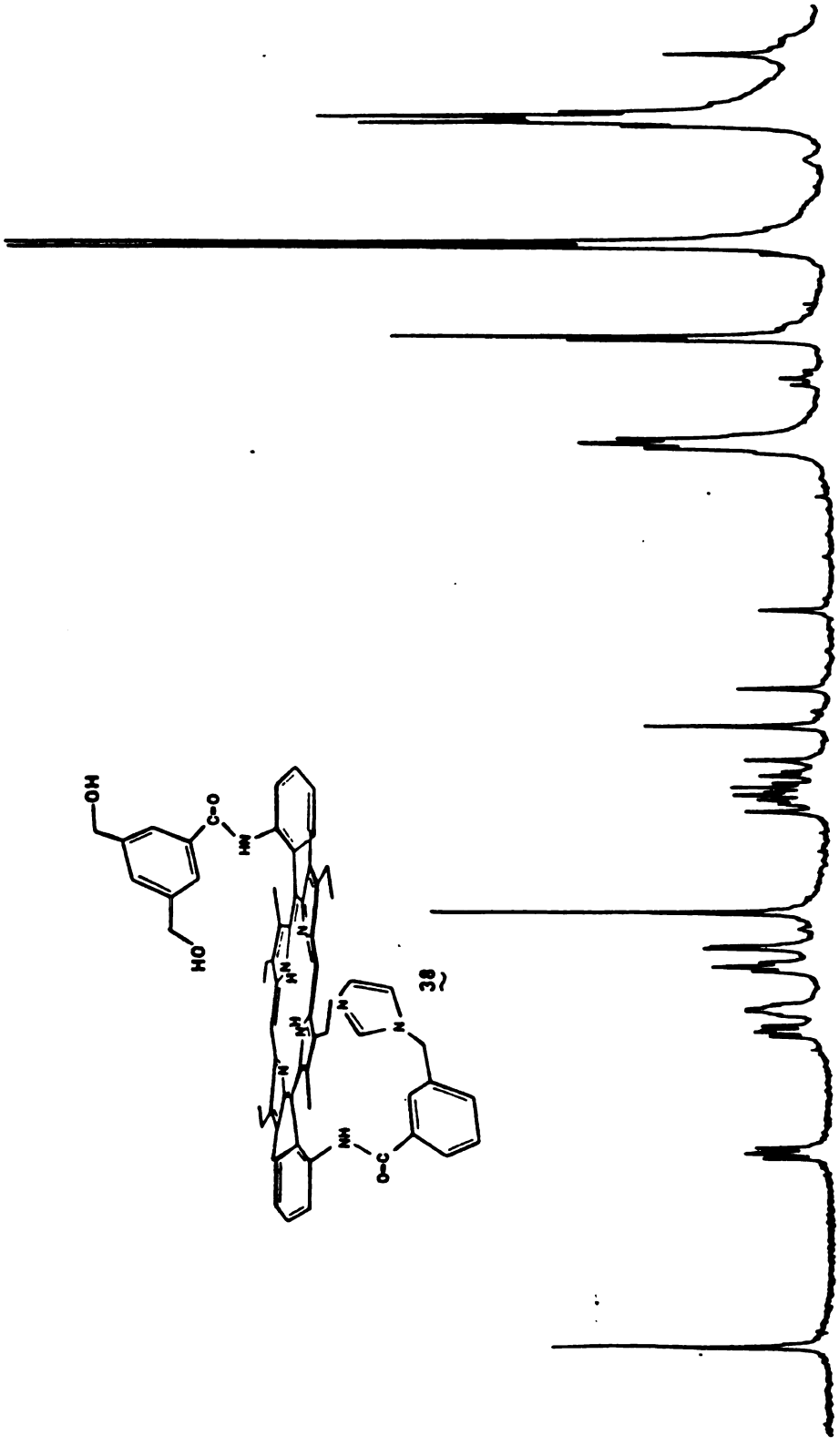

Figure A23. 250 MHz ^1H NMR spectrum of (3,5(CH_2OH)$_2$benzamide),(m-ImCH_2benzamide)DPE, trans (38).

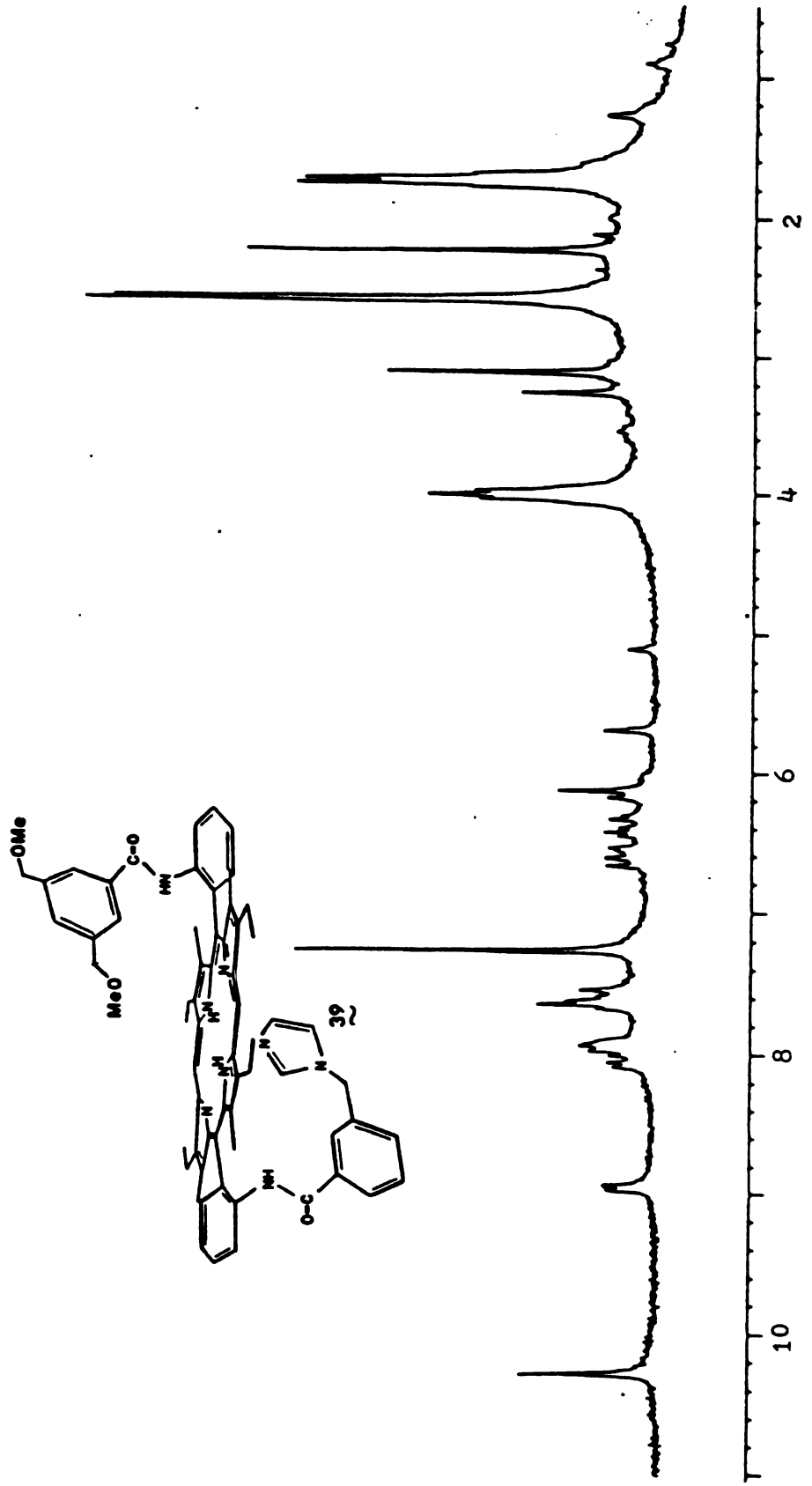

Figure A24. 250 MHz ^1H NMR spectrum of (3,5($CH_2OMe)_2$benzamide),(m-ImCH_2-benzamide)DPE, trans (39).

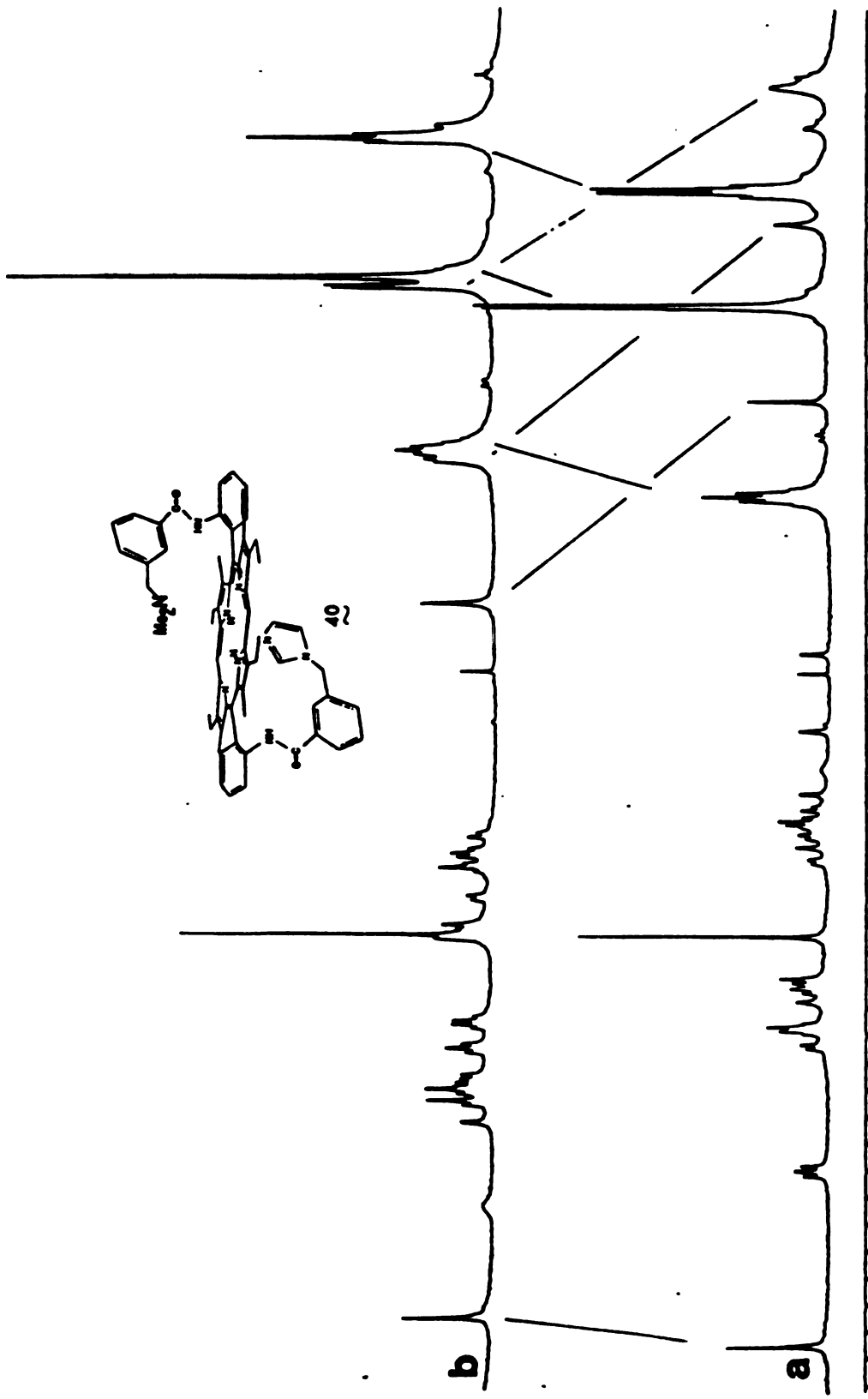

Figure A25. 250 MHz ^1H NMR spectra of (m-NMe_2CH_2benzamide),(m-$ImCH_2$benzamide)DPE, trans (40); in (a) $CDCl_3$; (b) $CDCl_3$ + TFA.

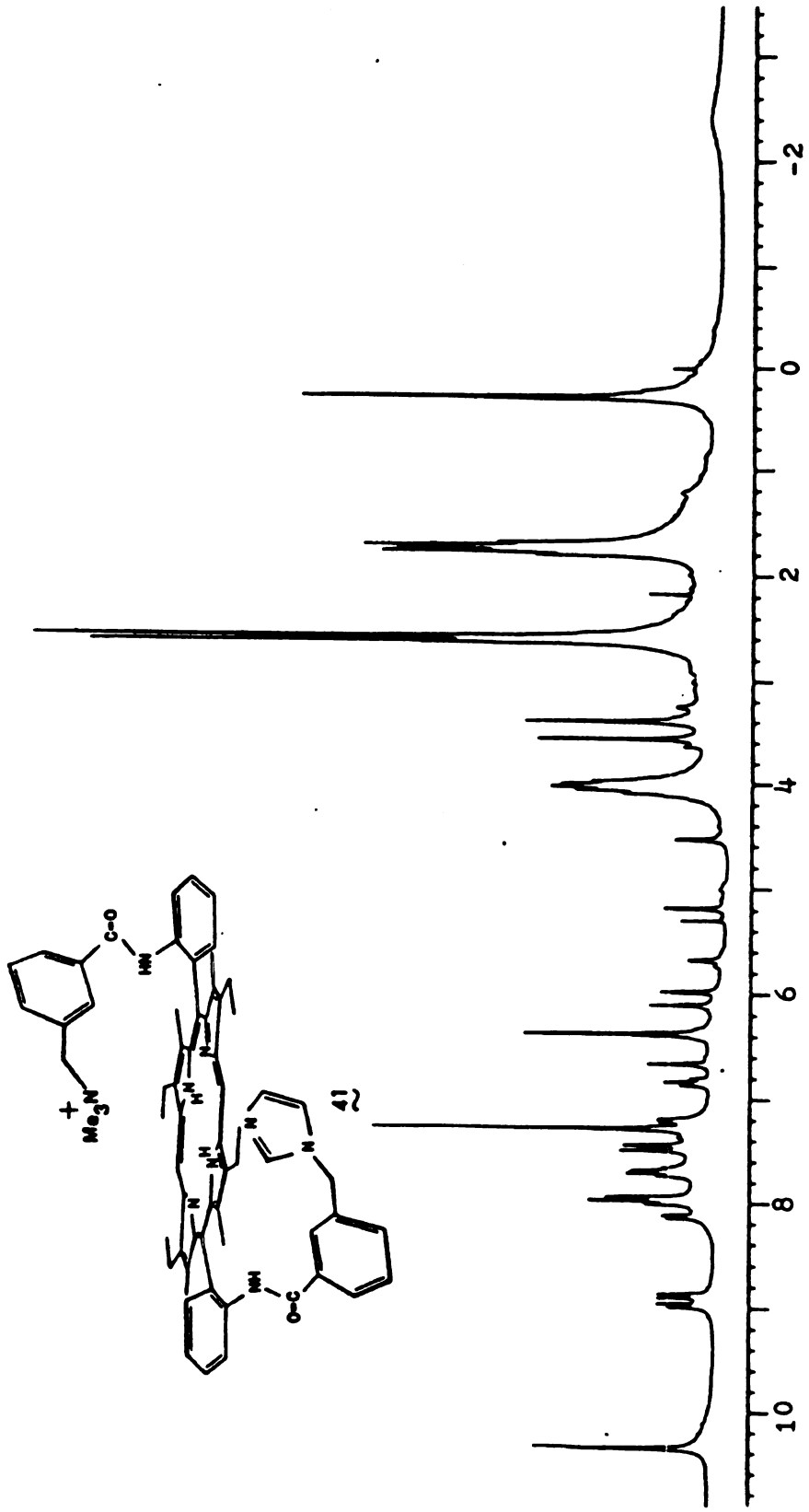

Figure A26. 250 MHz ^1H NMR spectrum of (m-$NMe_3^+CH_2$benzamide),(m-$ImCH_2$-benzamide)DPE, trans (41).

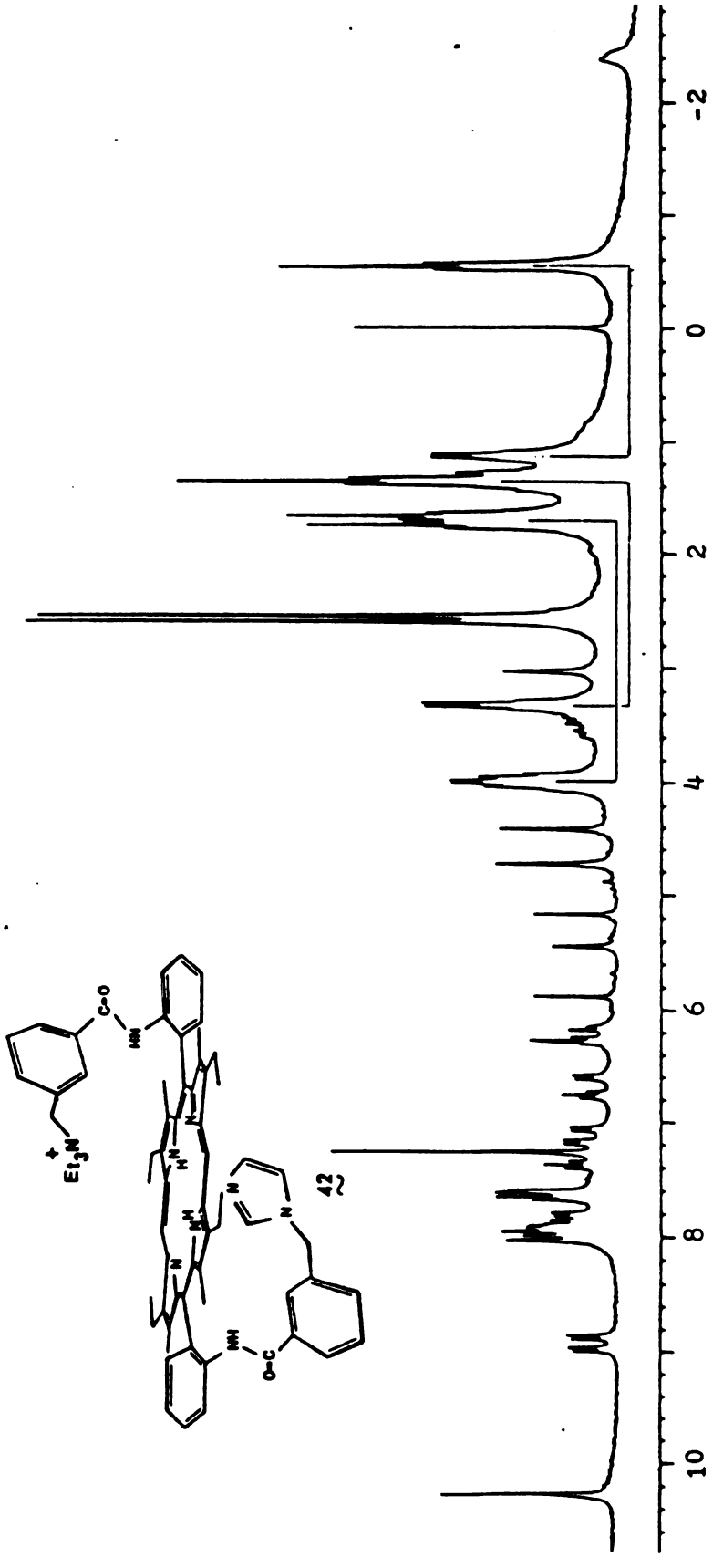

Figure A27. 250 MHz ^{1}H NMR spectrum of (m-$NEt_3^+CH_2$benzamide),(m-$ImCH_2$benzamide)DPE, trans (42).

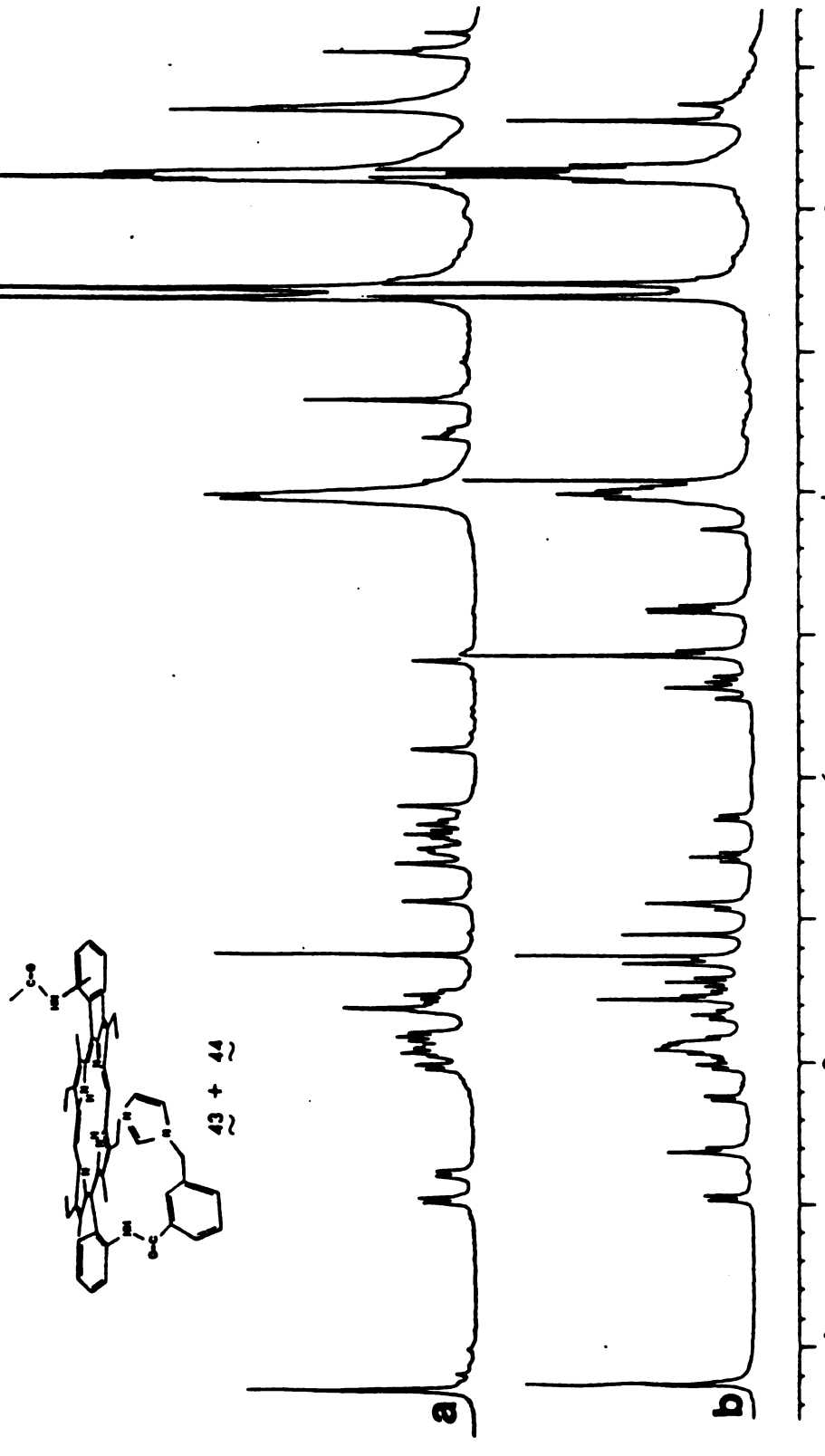

Figure A28. 250 MHz ^1H NMR spectra of (acetamide),(m-ImCH_2benzamide)DPE, (a) trans (43); (b) cis (44).

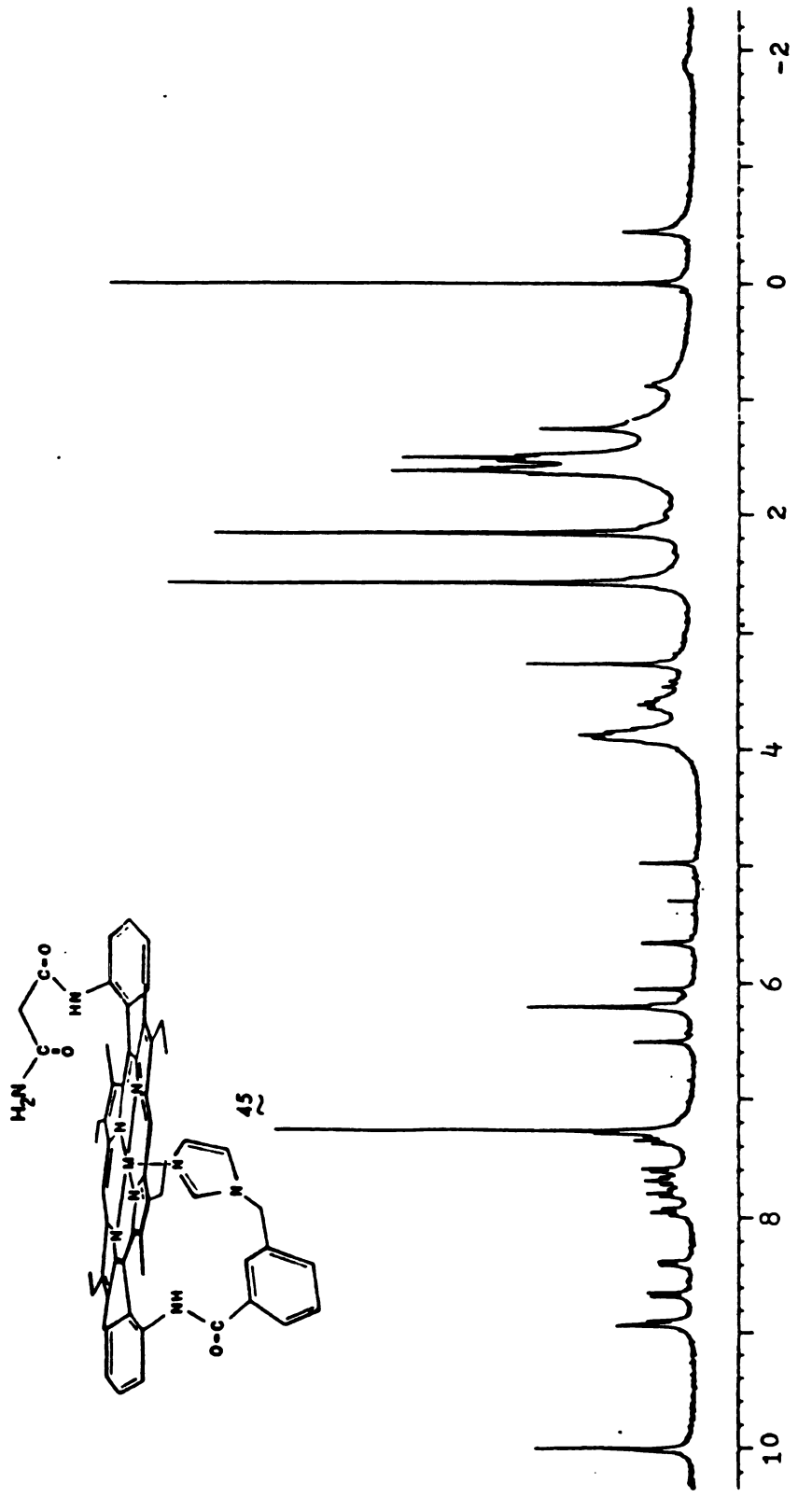

Figure A29. 250 MHz ^1H NMR spectrum of malonamide blocked, imidazole appended DPE 45.

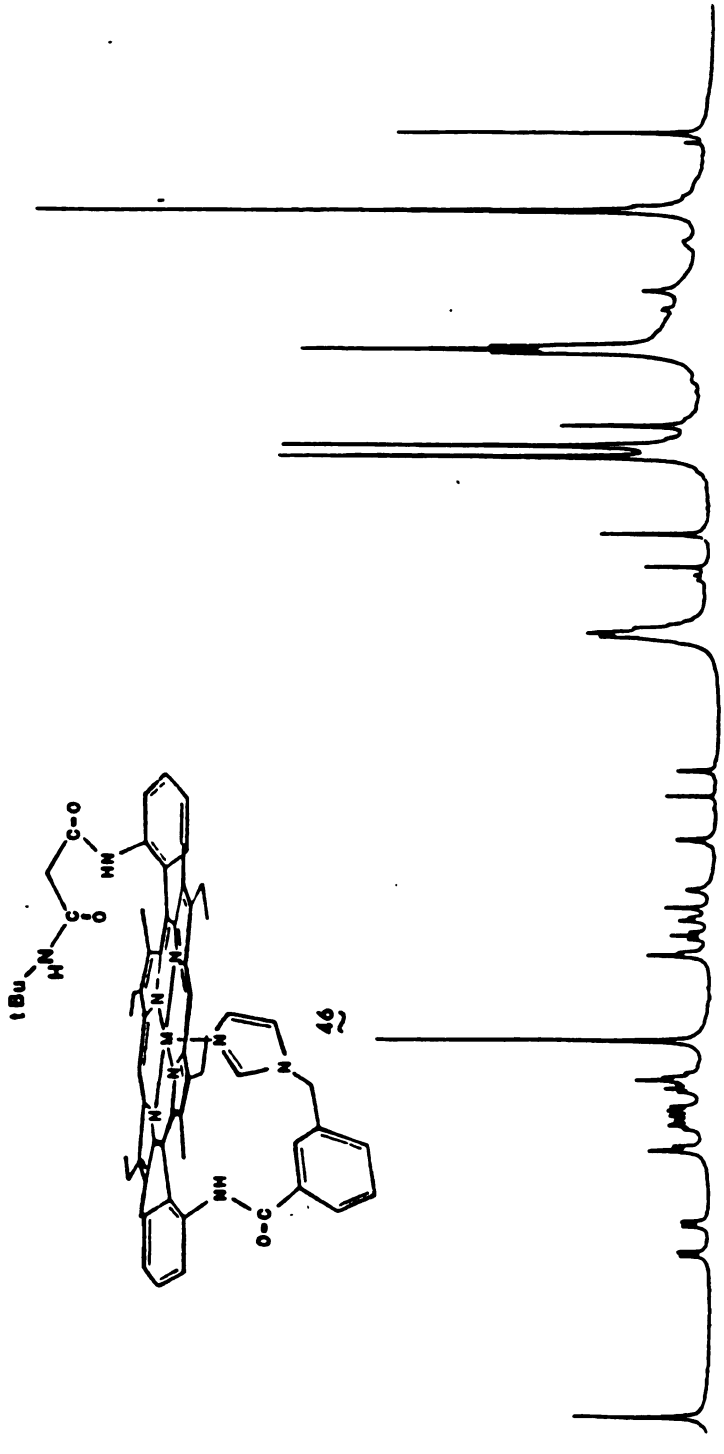

Figure A30. 250 MHz ^1H NMR spectrum of tBu-malonamide blocked, imidazole appended DPE 46.

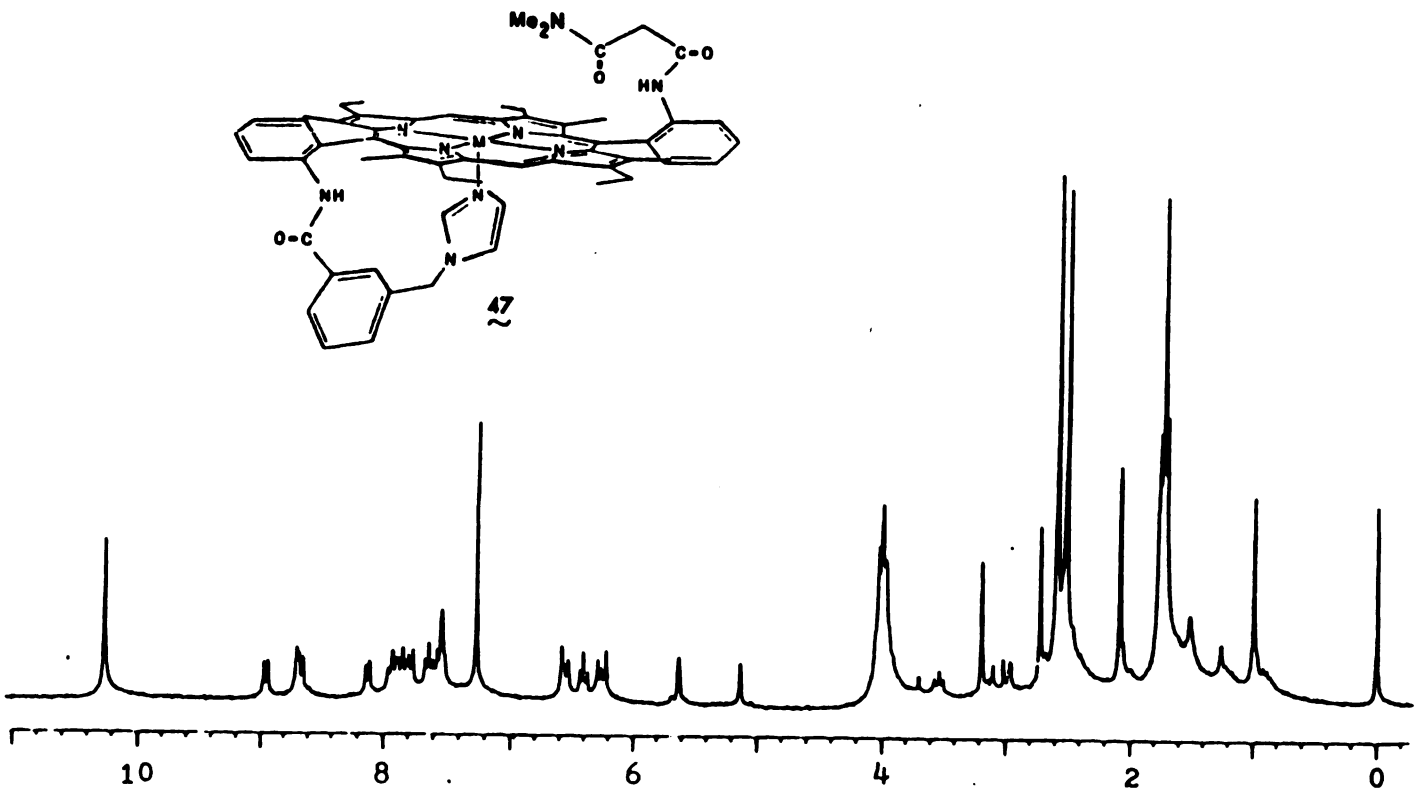

Figure A31. 250 MHz ^{1}H NMR spectrum of dimethyl malonamide blocked, imidazole appended DPE 47.

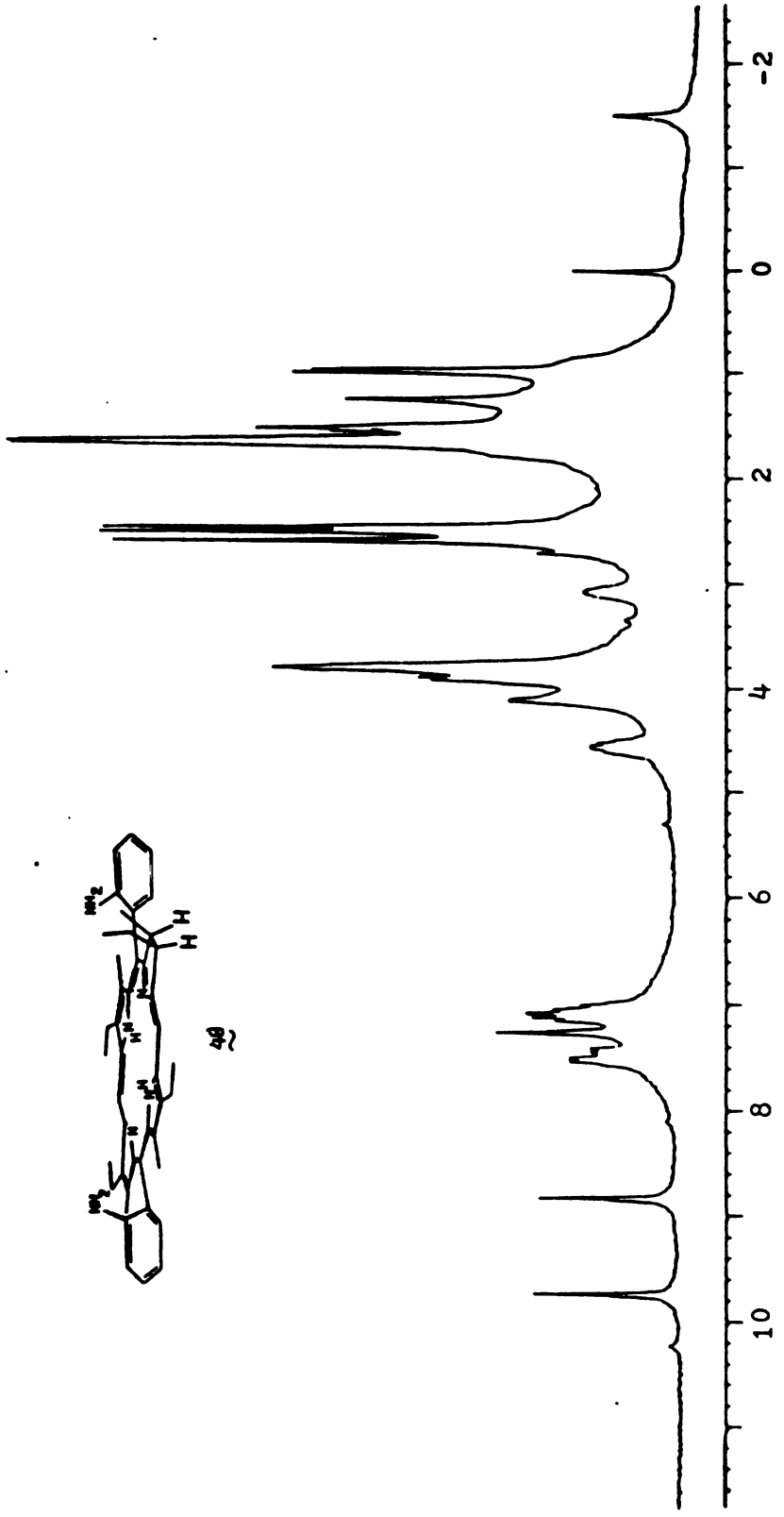

Figure A32. 250 MHz ^1H NMR spectrum of (amino)$_2$DP etiochlorin, cis (48).

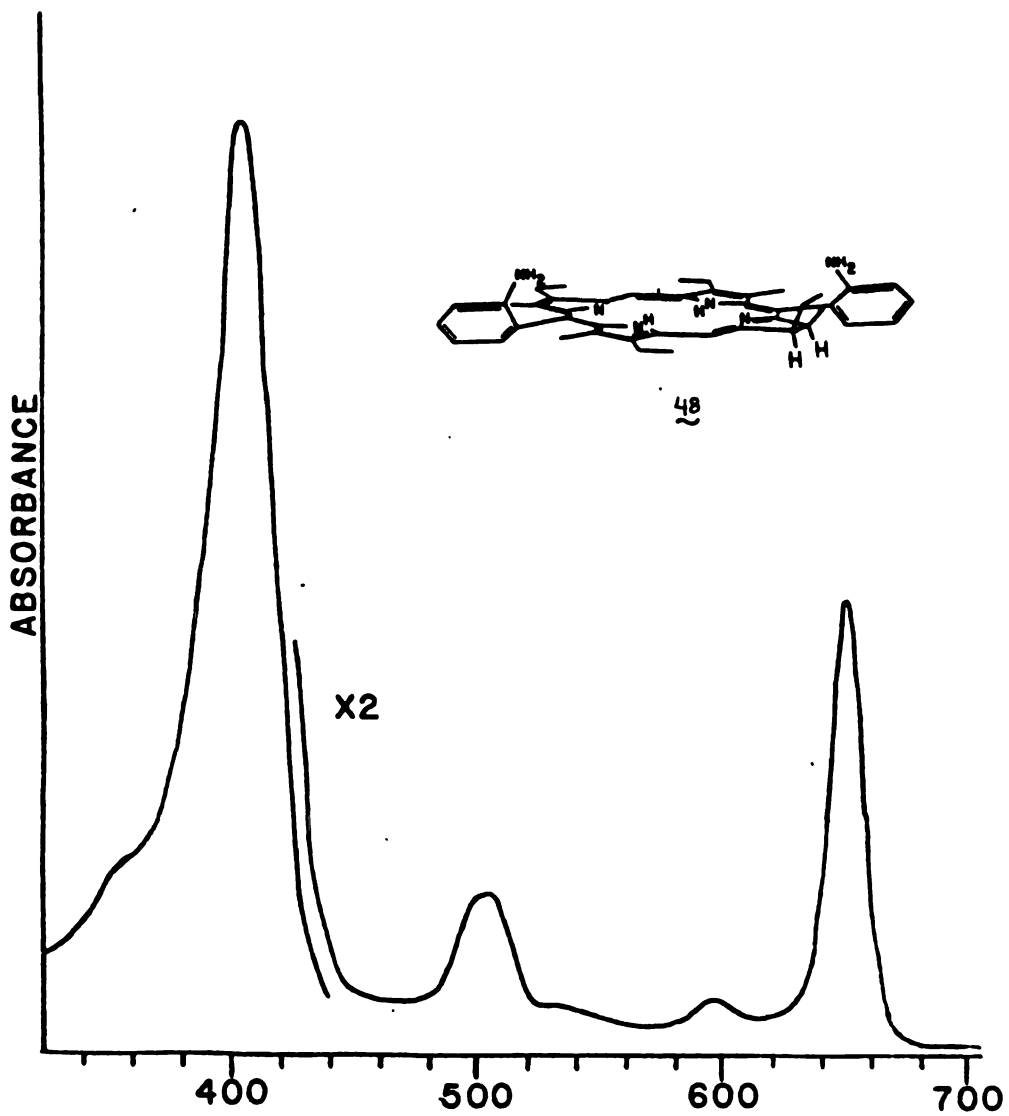

Figure A33. Electronic spectrum of (amino)$_2$DP etiochlorin, cis (48).

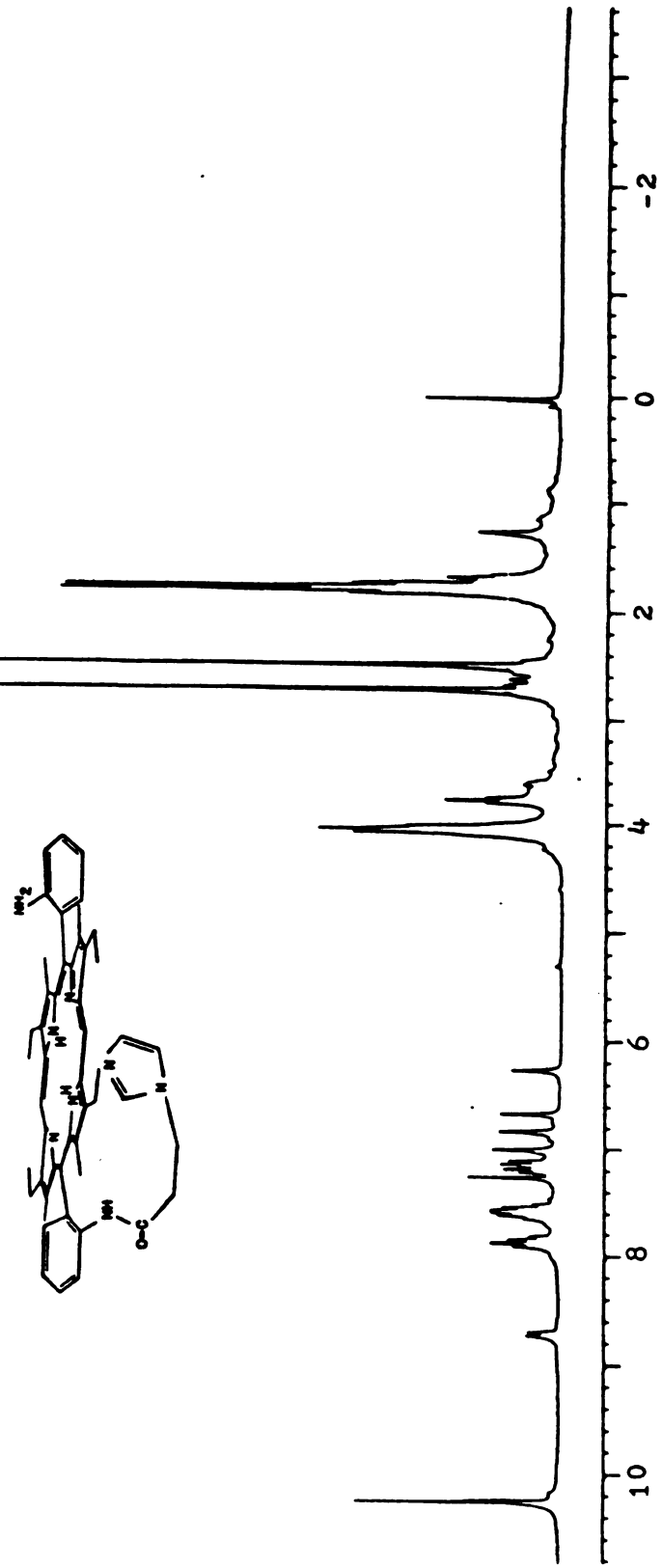

Figure A34. 250 MHz ^{1}H NMR spectrum of (amino),$(Im(CH_2)_2CONH)DPE$, trans.

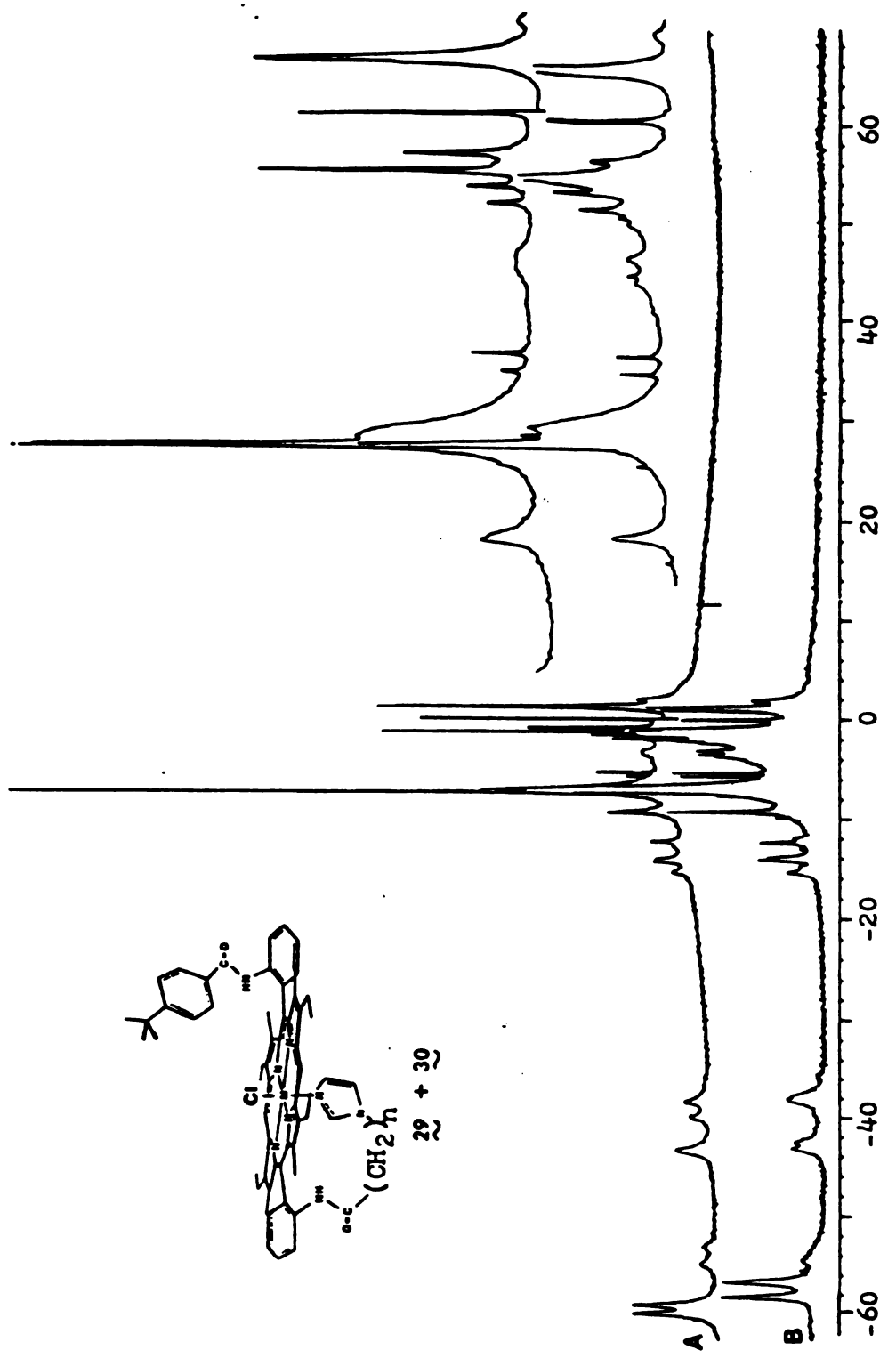

Figure A35. 250 MHz ^1H NMR spectra of the Fe(III)PCl complexes of alkyl appended imidazole DPE; (a) n = 3 (30); (b) n = 2 (29).

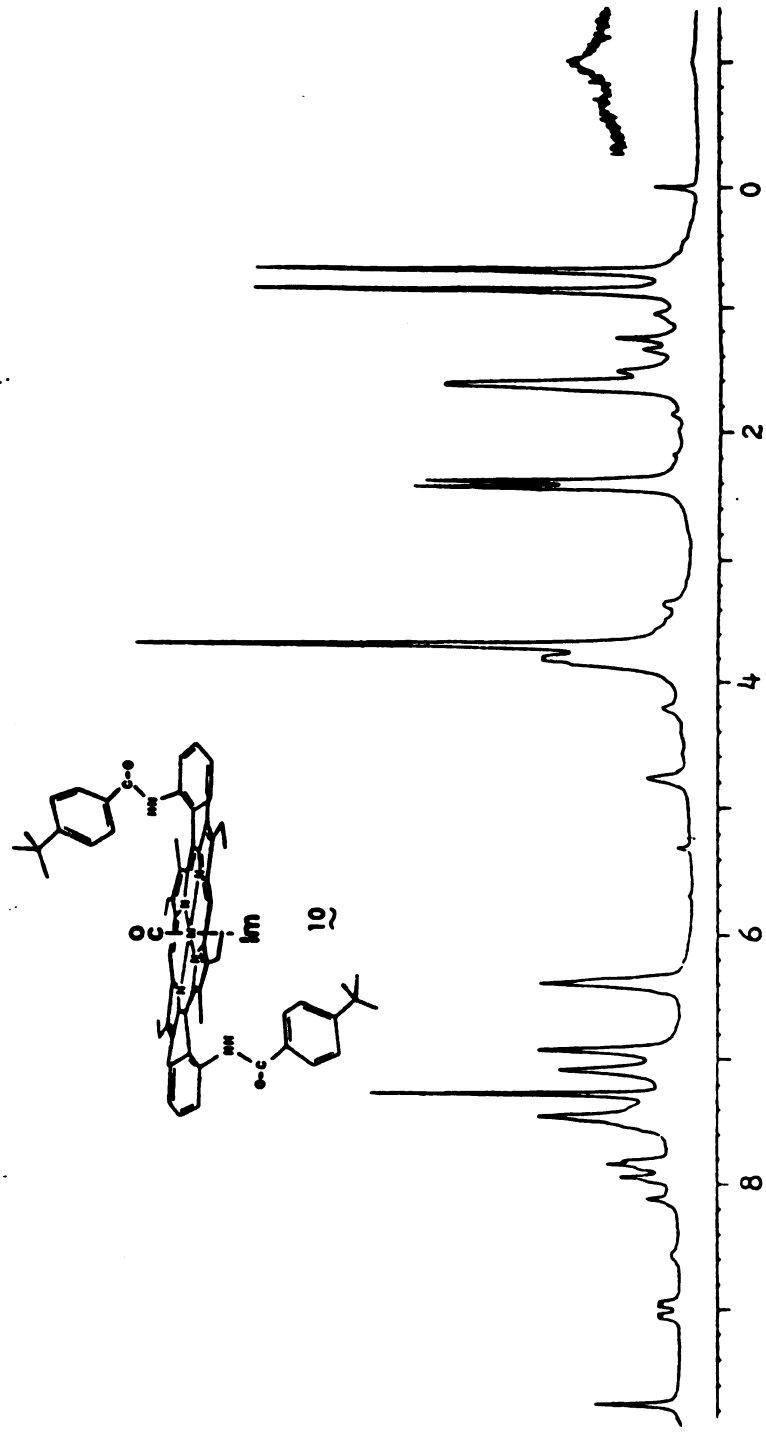

Figure A36. 250 MHz ^1H NMR spectrum of the Fe(II)PImCO complex of doubly protected DPE 10.

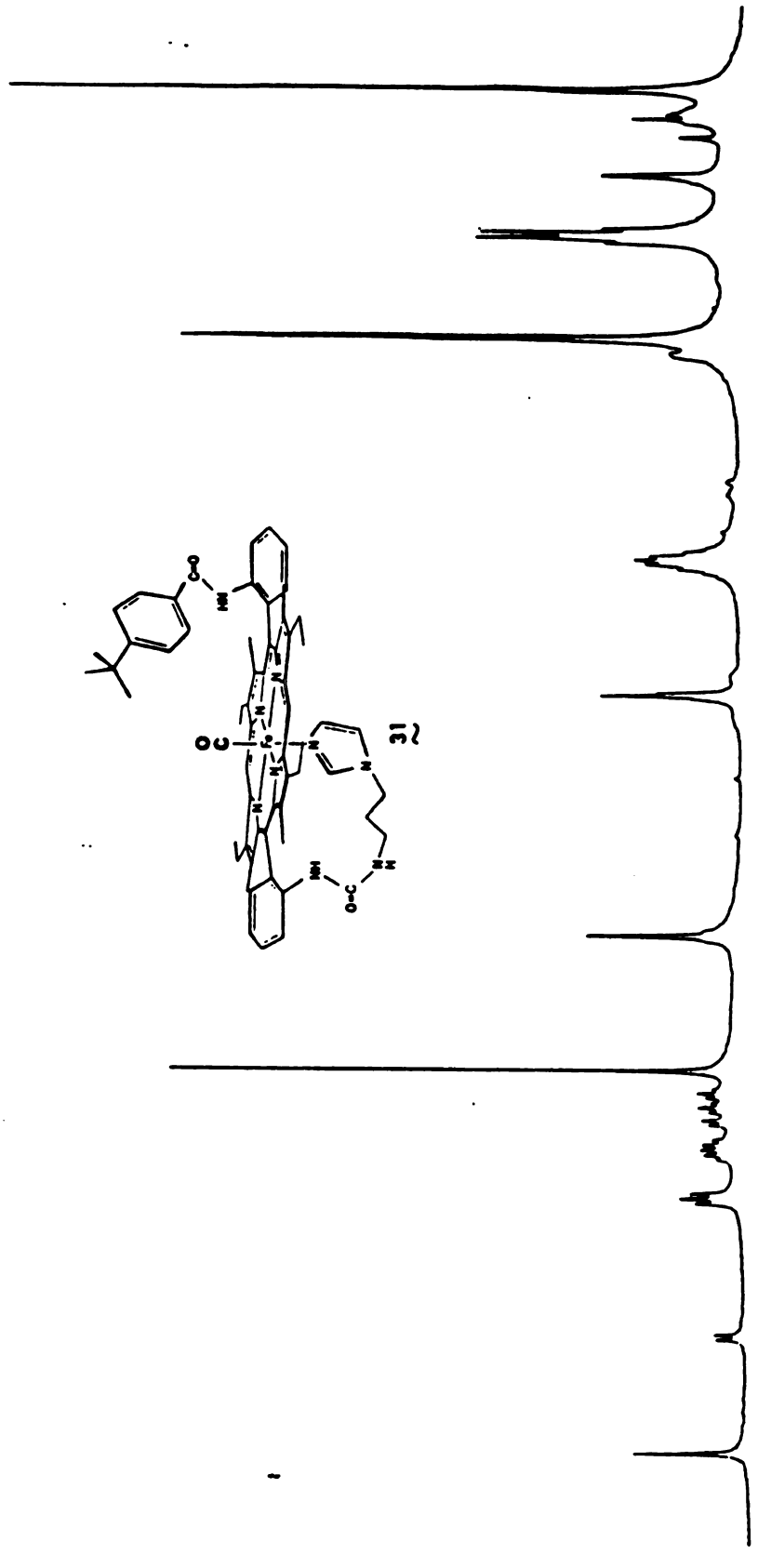

Figure A37. 250 MHz ^{1}H NMR spectrum of the Fe(II)PImCO complex of imidazole appended DPE 31.

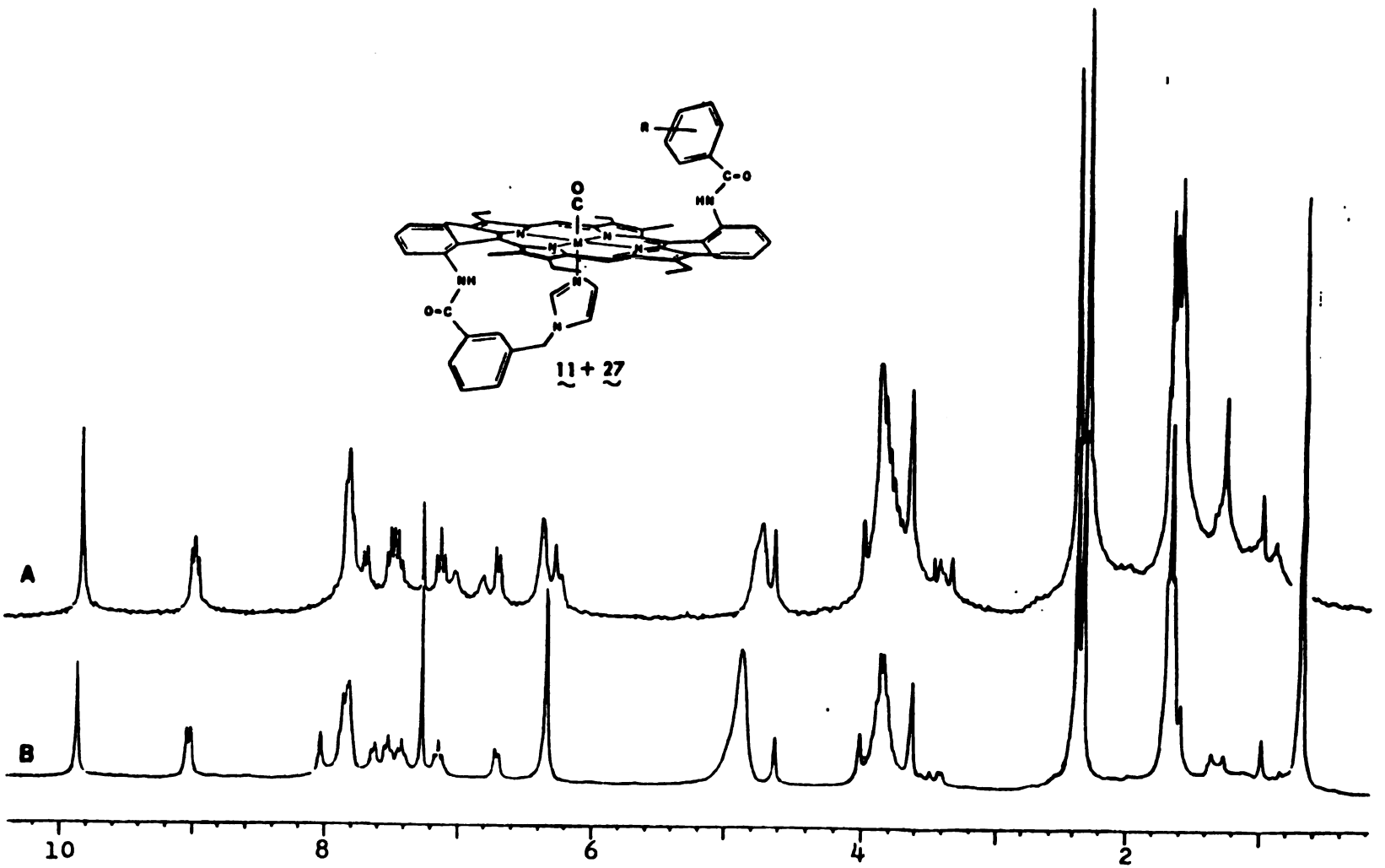

11 + 27

Figure A38. 250 MHz ^{1}H NMR spectra of the Fe(II)PImCO complexes of imidazole appended DPE; (A) R = m-ImCH_2 (11); (B) R = p-tBu (27).

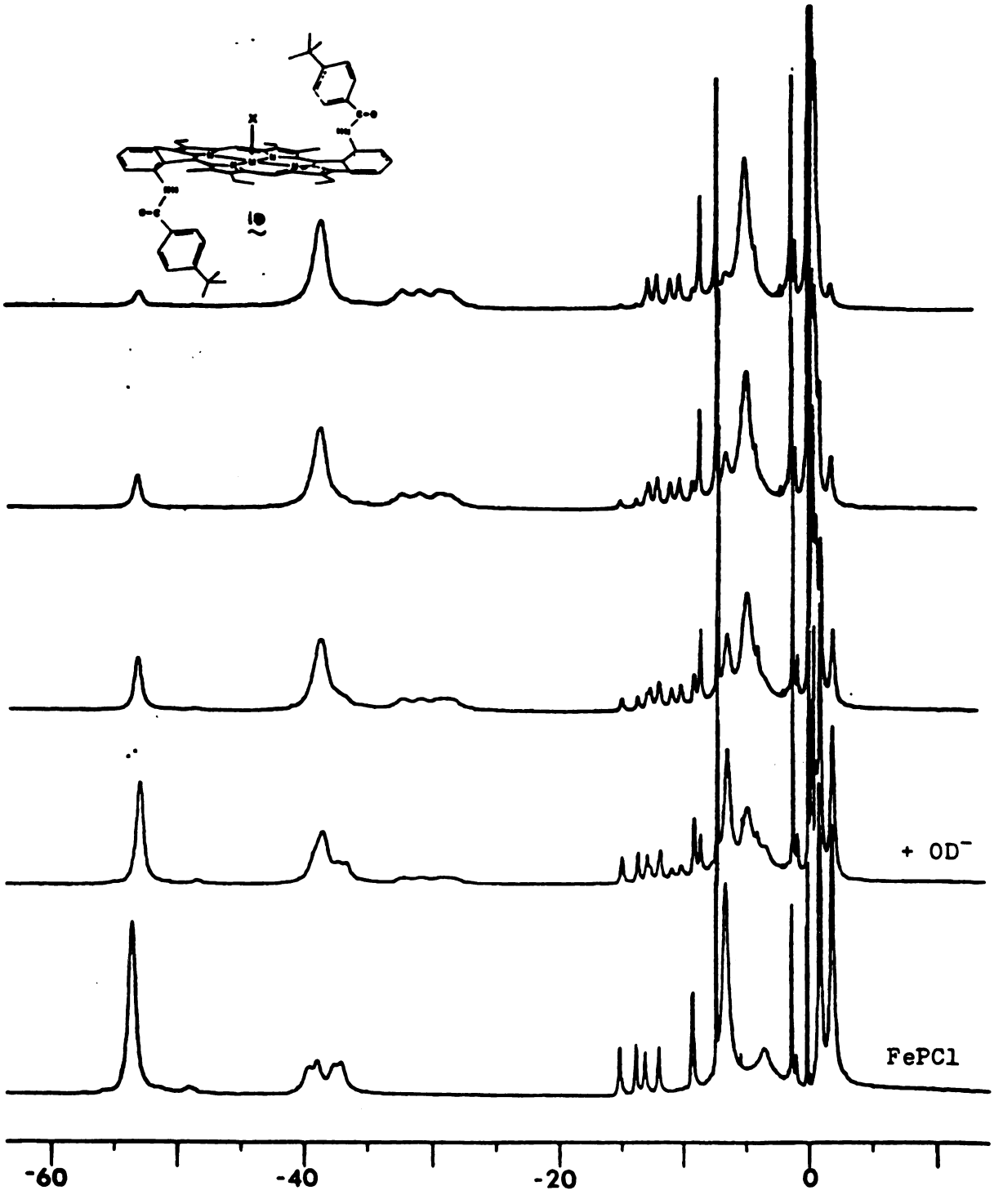

Figure A39. ^{1}H NMR spectra monitoring the conversion of Fe(III)PCl to Fe(III)POH in DPE 10.

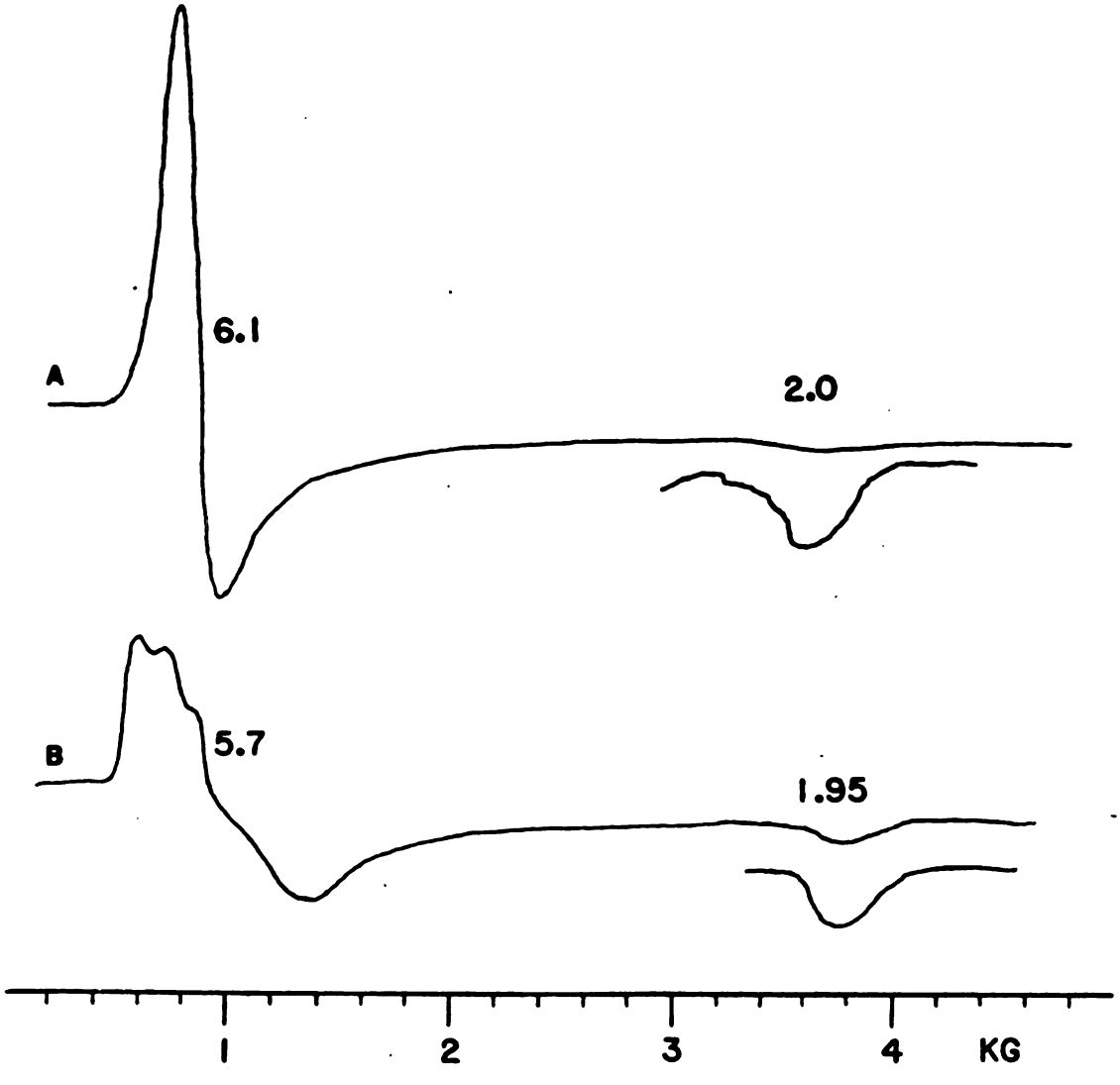

Figure A40. ESR spectra of Fe(III) complexes of DPE 10; (A) FePCl; (B) FePOH. 77°K in CH_2Cl_2.

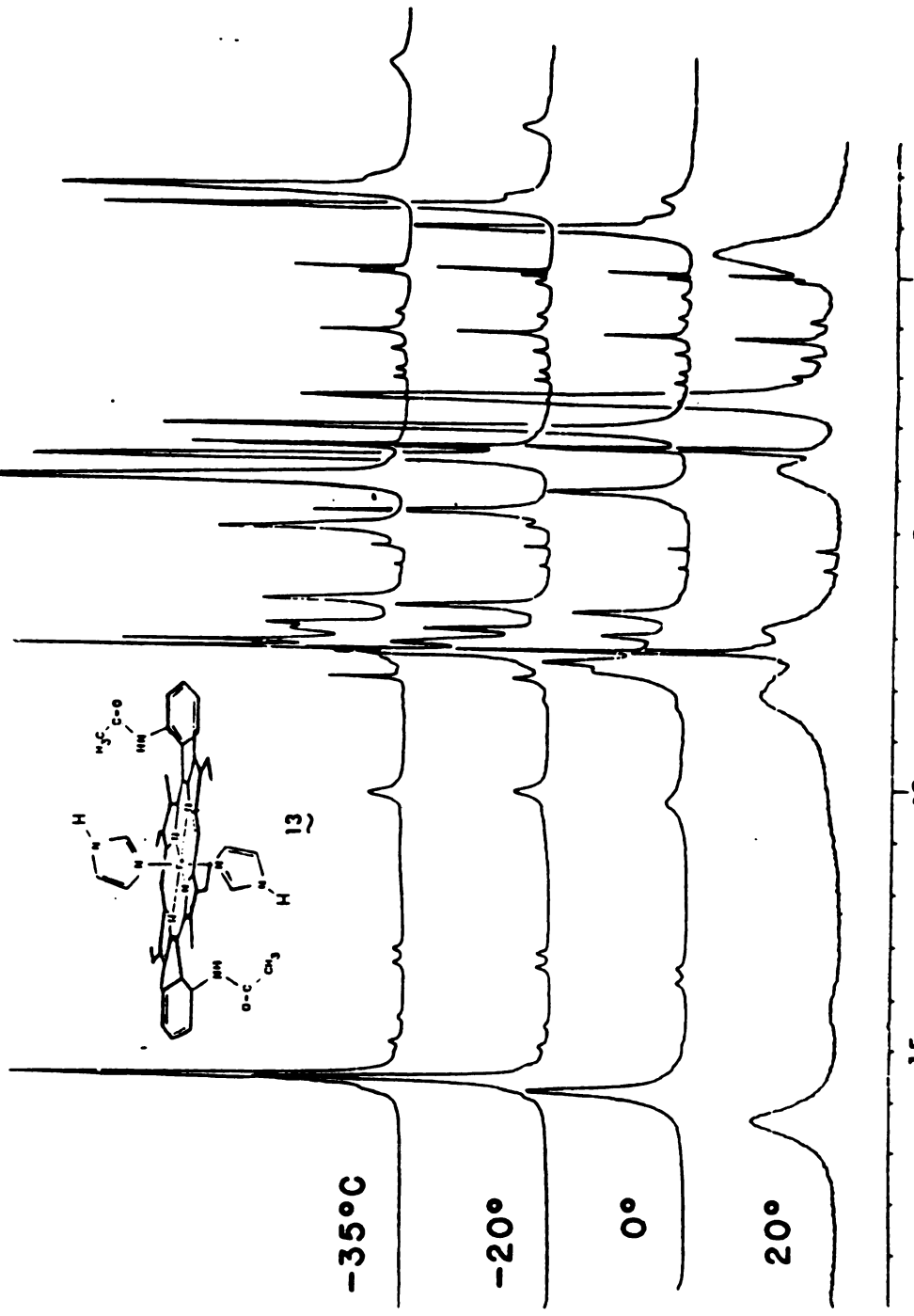

Figure A41. Temperature dependant ^{1}H NMR spectra of the Fe(III)PIm$_2$Cl complex of DPE 13.

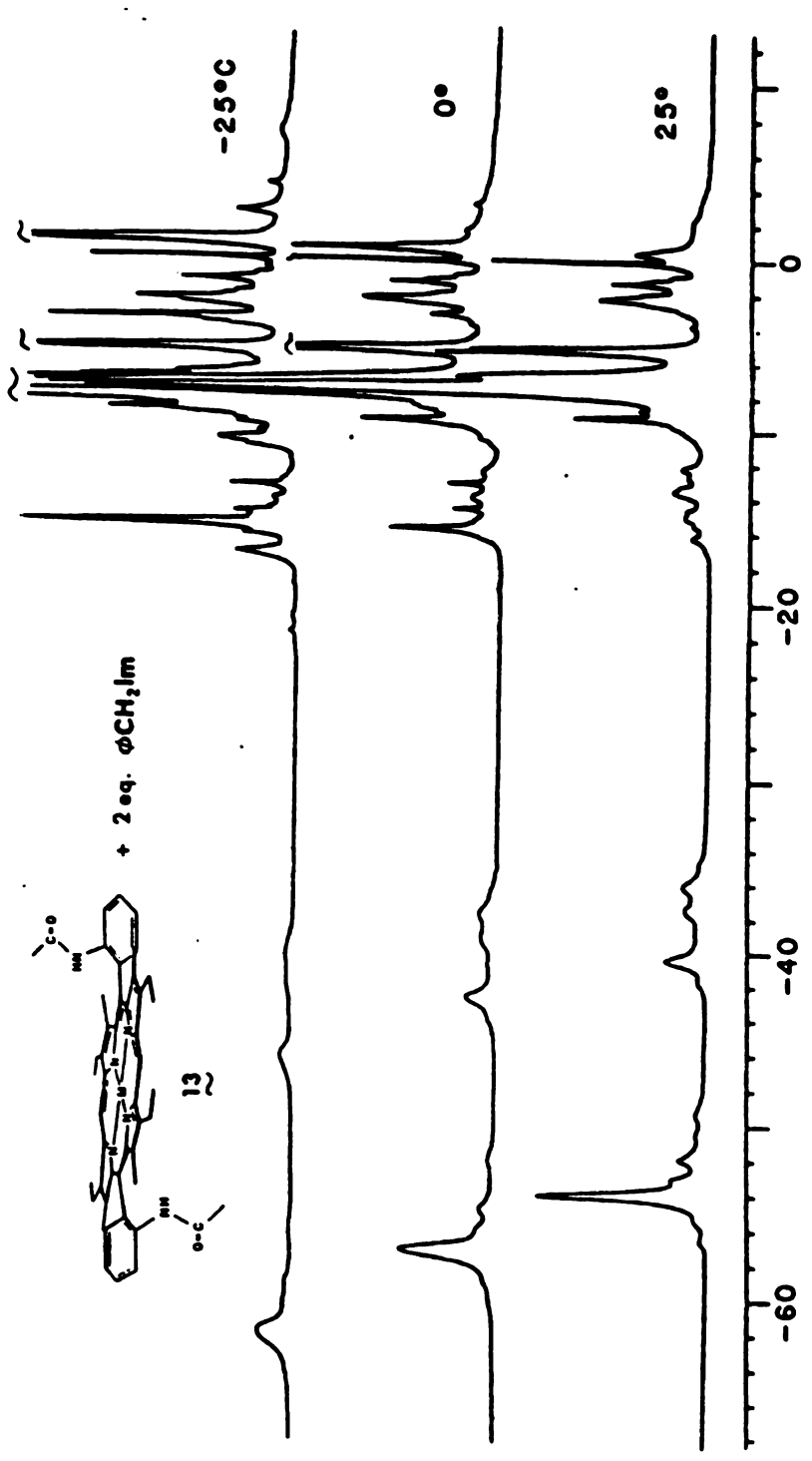

Figure A42. Temperature dependant ^1H NMR spectrum of the Fe(III)P(benzyl Im)$_2$Cl complex of DPE 13.

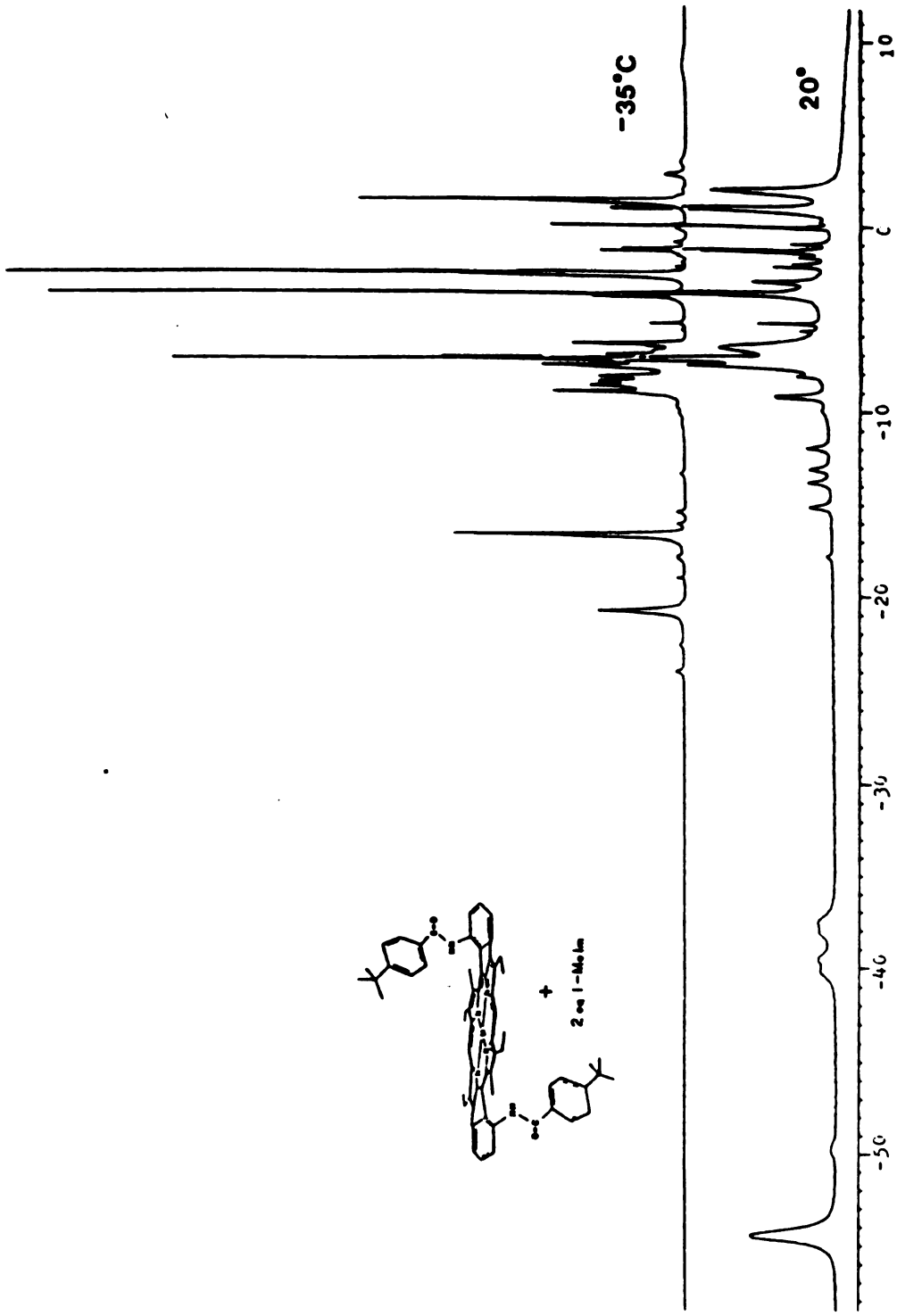

Figure A43. Temperature dependant ^1H NMR spectra of the Fe(III)P(1-MeIm)$_2$Cl complex of DPE 10.

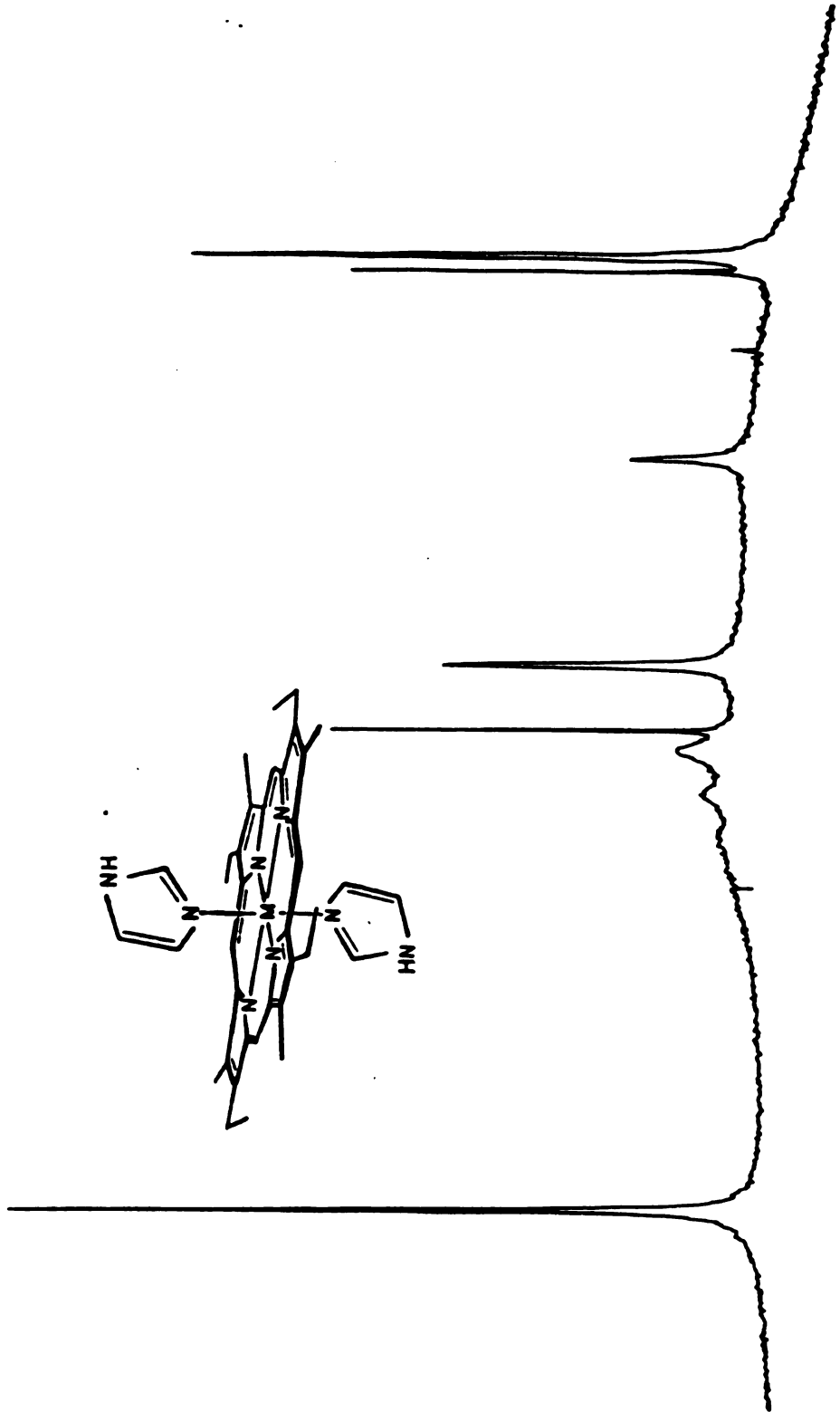

Figure A44. Room temperature ^1H NMR spectrum of the Fe(III)PIm$_2$Cl complex of etioporphyrin II.

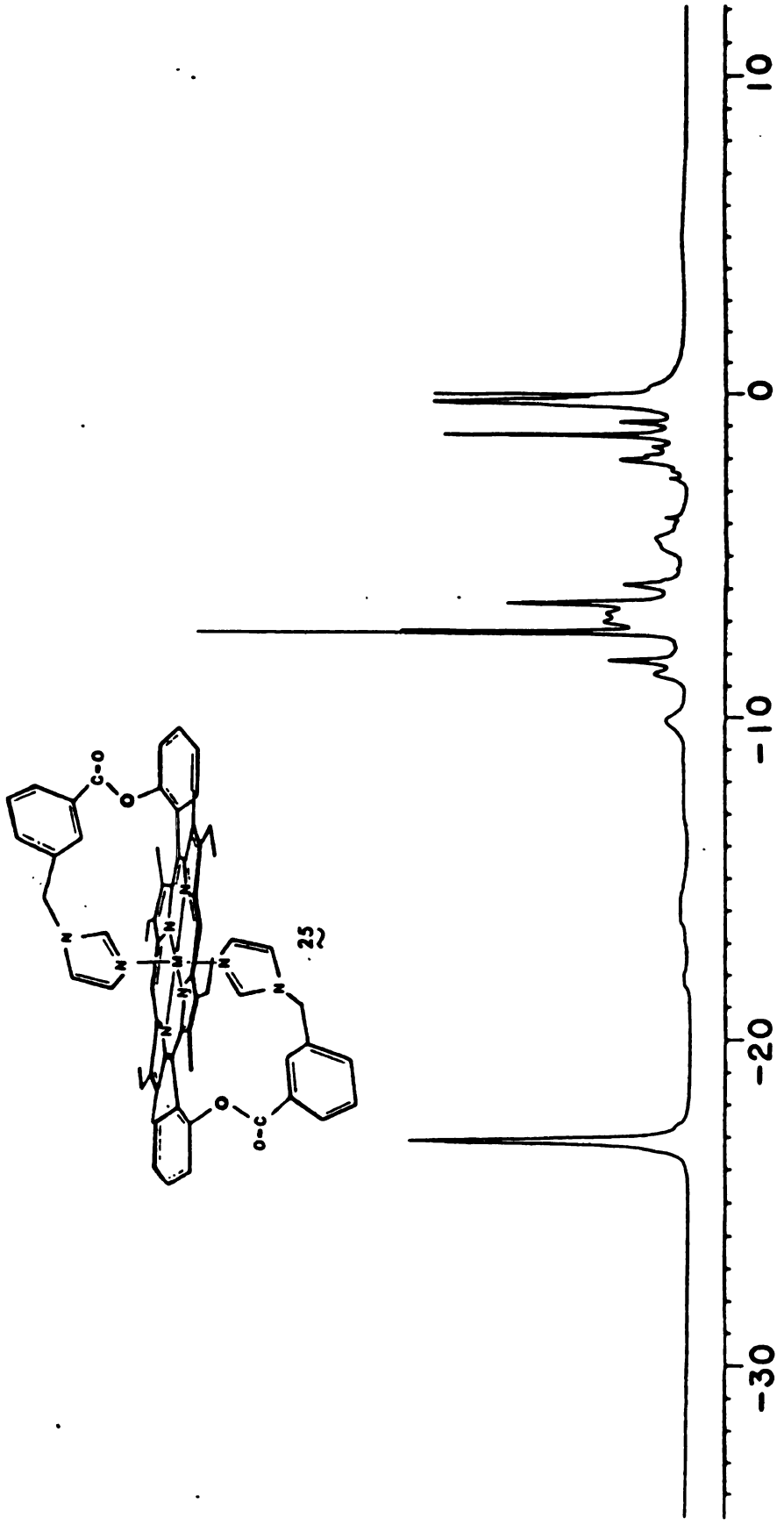

Figure A45. Room temperature ^1H NMR spectrum of the Fe(III)PIm_2Cl complex of $(m\text{-}ImCH_2benzamide)_2DPE$, trans (25).

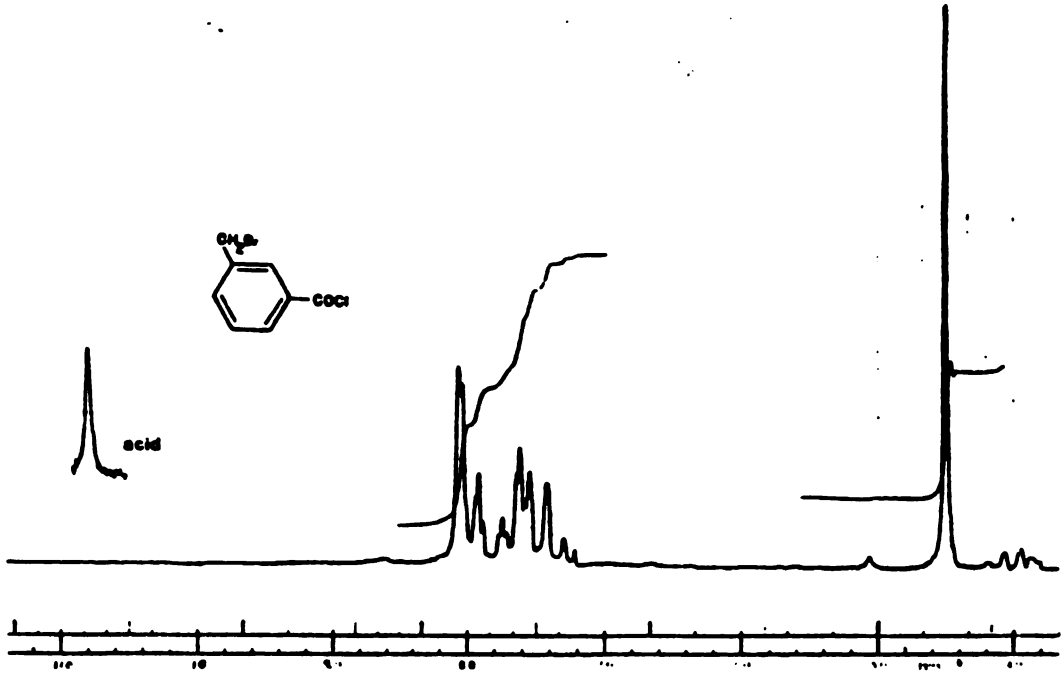

Figure A46. 60 MHz ^1H NMR spectrum of m-(α-bromo)toluoyl chloride.

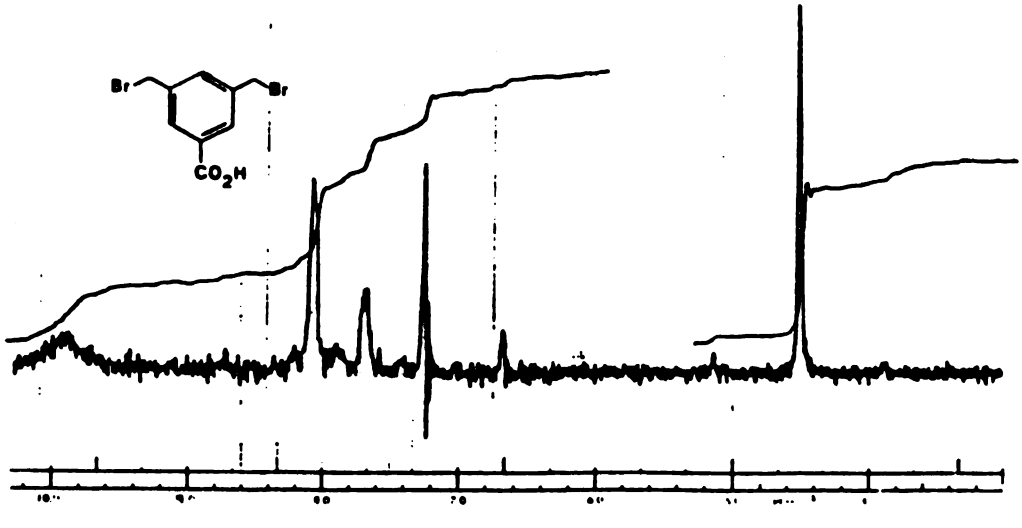

Figure A47. 60 MHz ^1H NMR spectrum of 3,5 $(BrCH_2)_2$-benzoic acid.

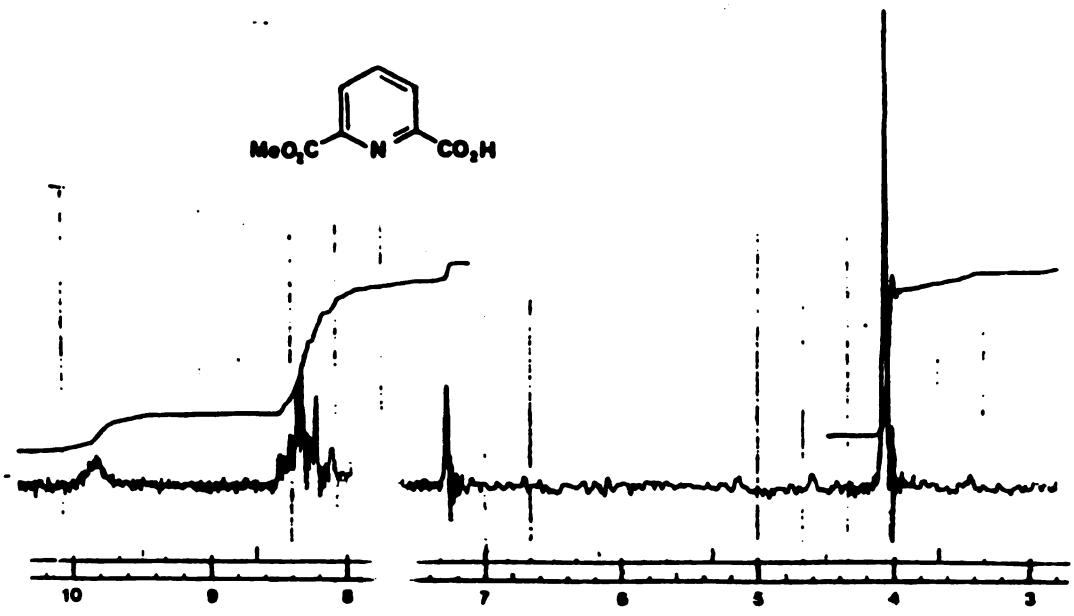

Figure A48. 60 MHz ^{1}H NMR spectrum of the monomethyl ester of dipicolinic acid.

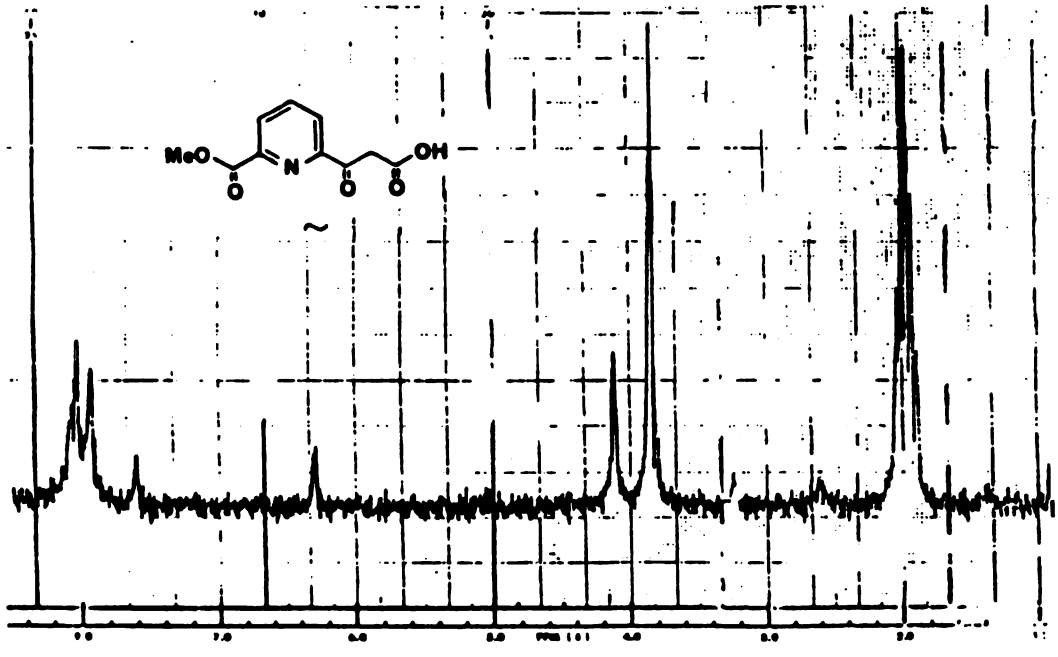

Figure A49. 60 MHz ^{1}H NMR spectrum of methyl 2-(β-carboxyl)acetylpyridine-6-carboxylate.

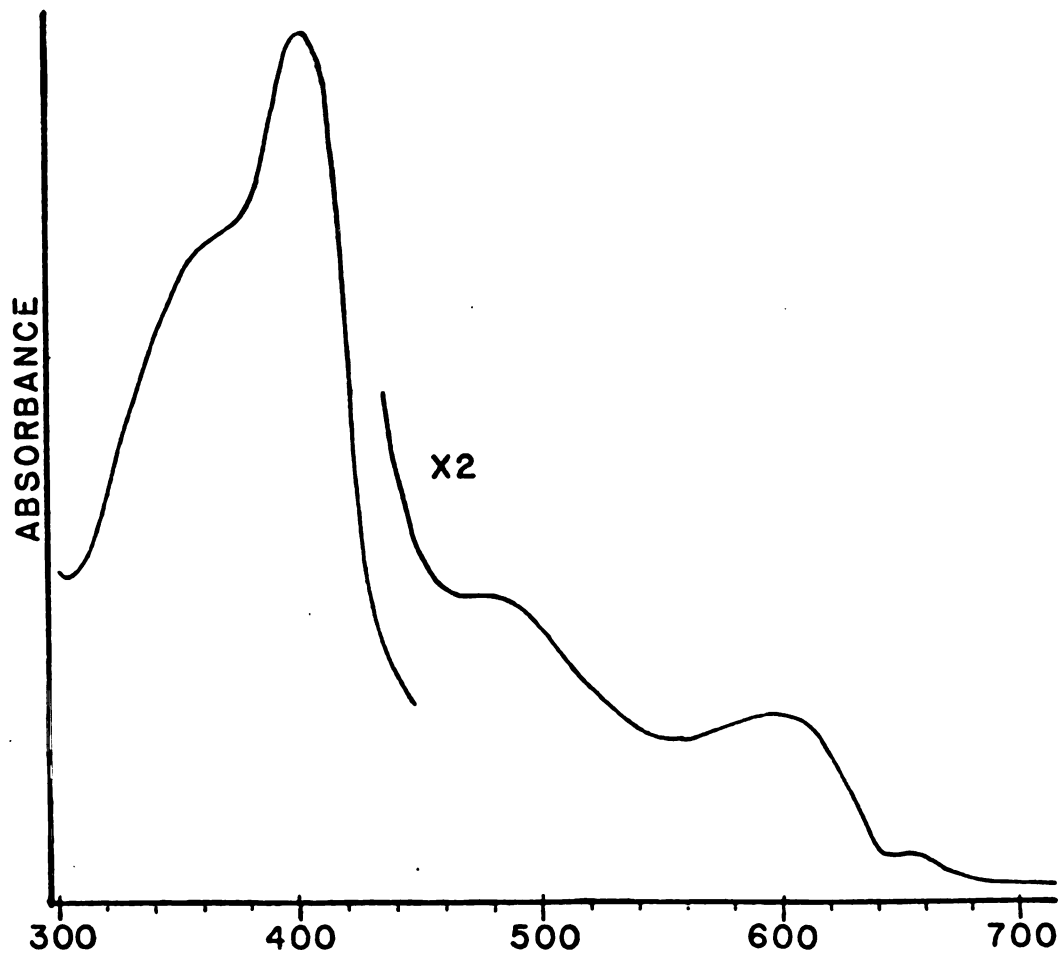

Figure A50. Electronic spectrum of the Fe(III)POH complex of bis aminodiacetic acid DPE 52 in water.

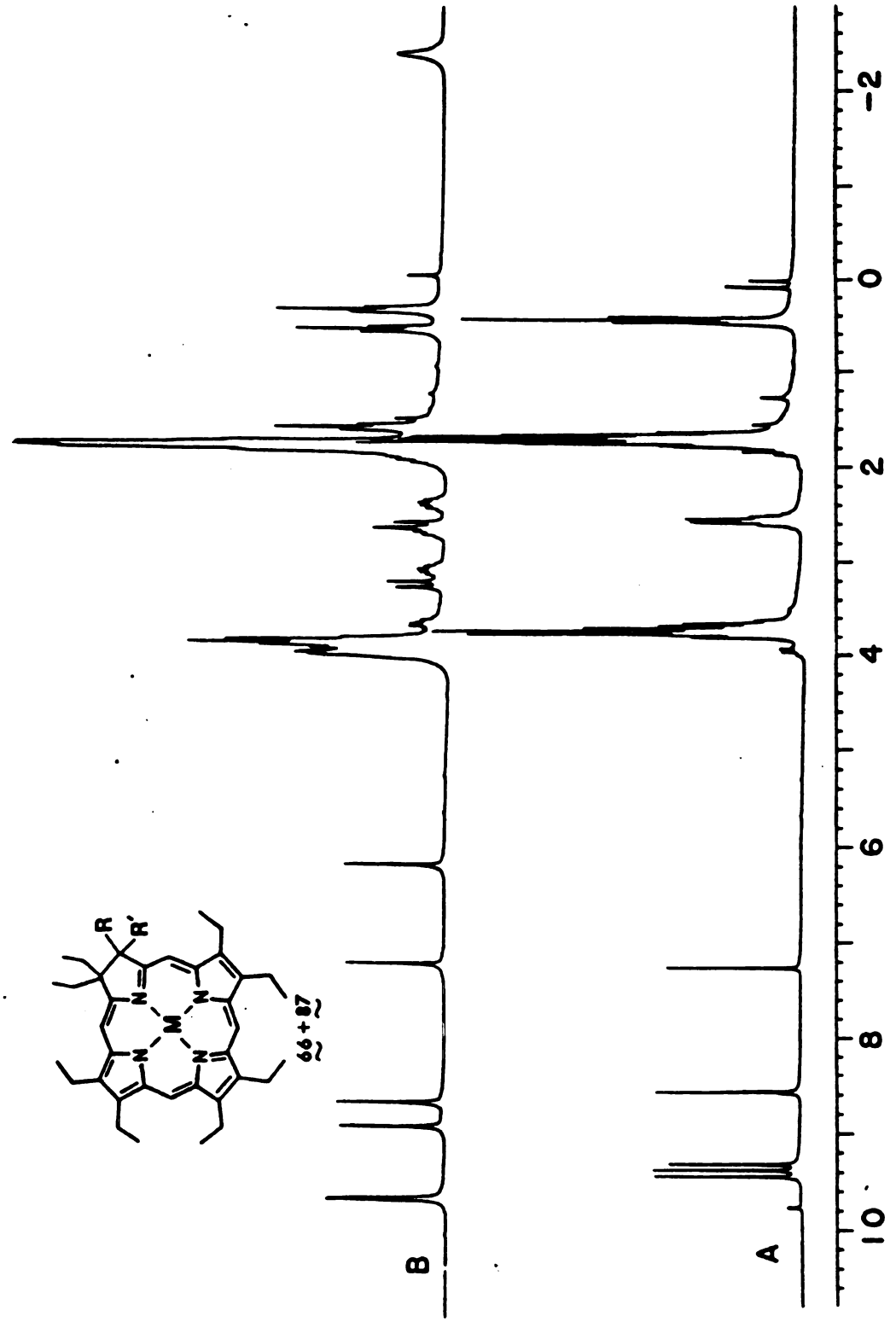

Figure A51. 250 MHz ^1H NMR spectra of (a) (R, R') = O, monoketone 66; (b) R = CH_2CO_2Et, R' = OH, chlorin 87.

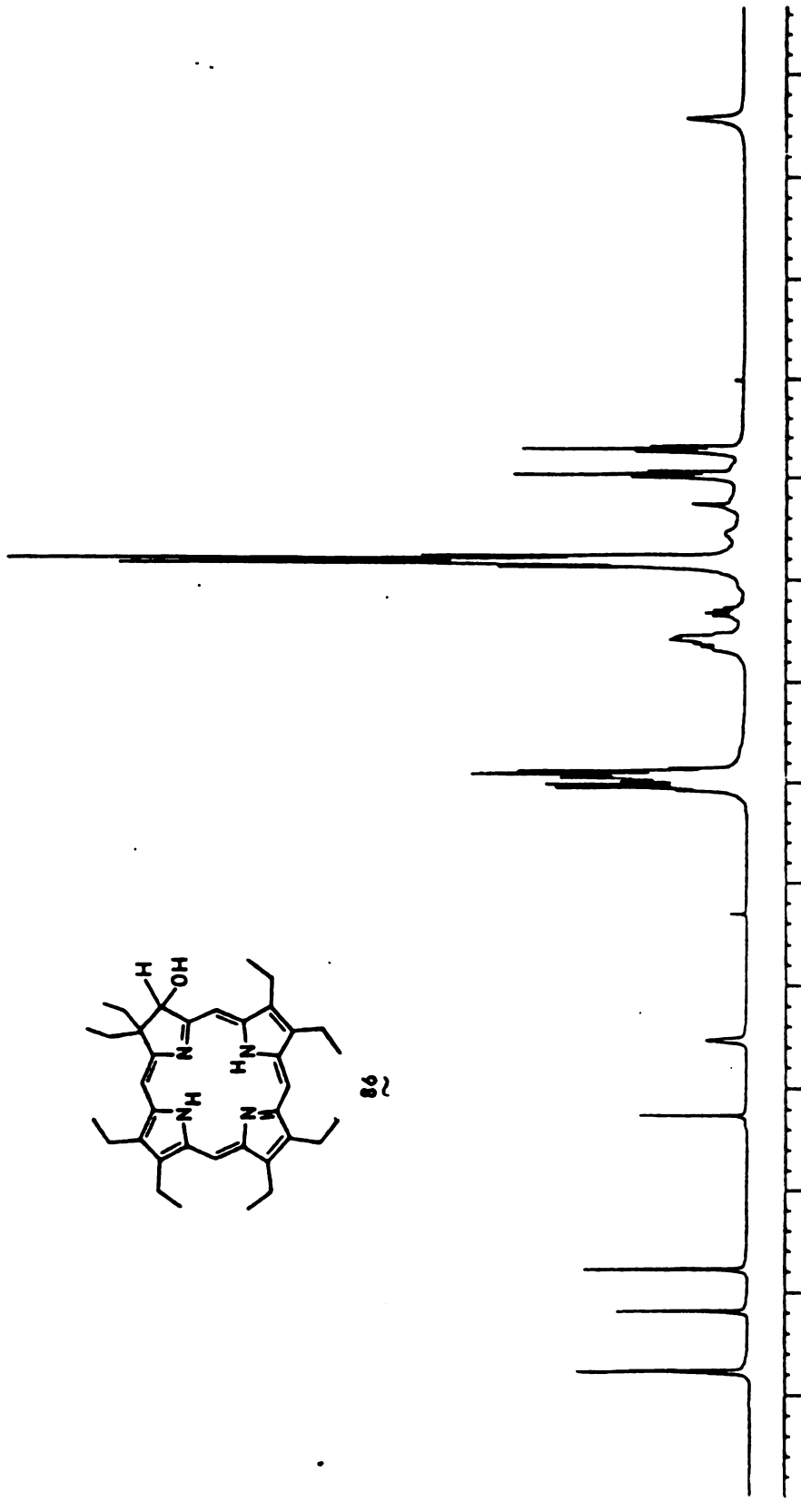

86

Figure A52. 250 MHz ^1H NMR spectrum of alkylated chlorin 86.

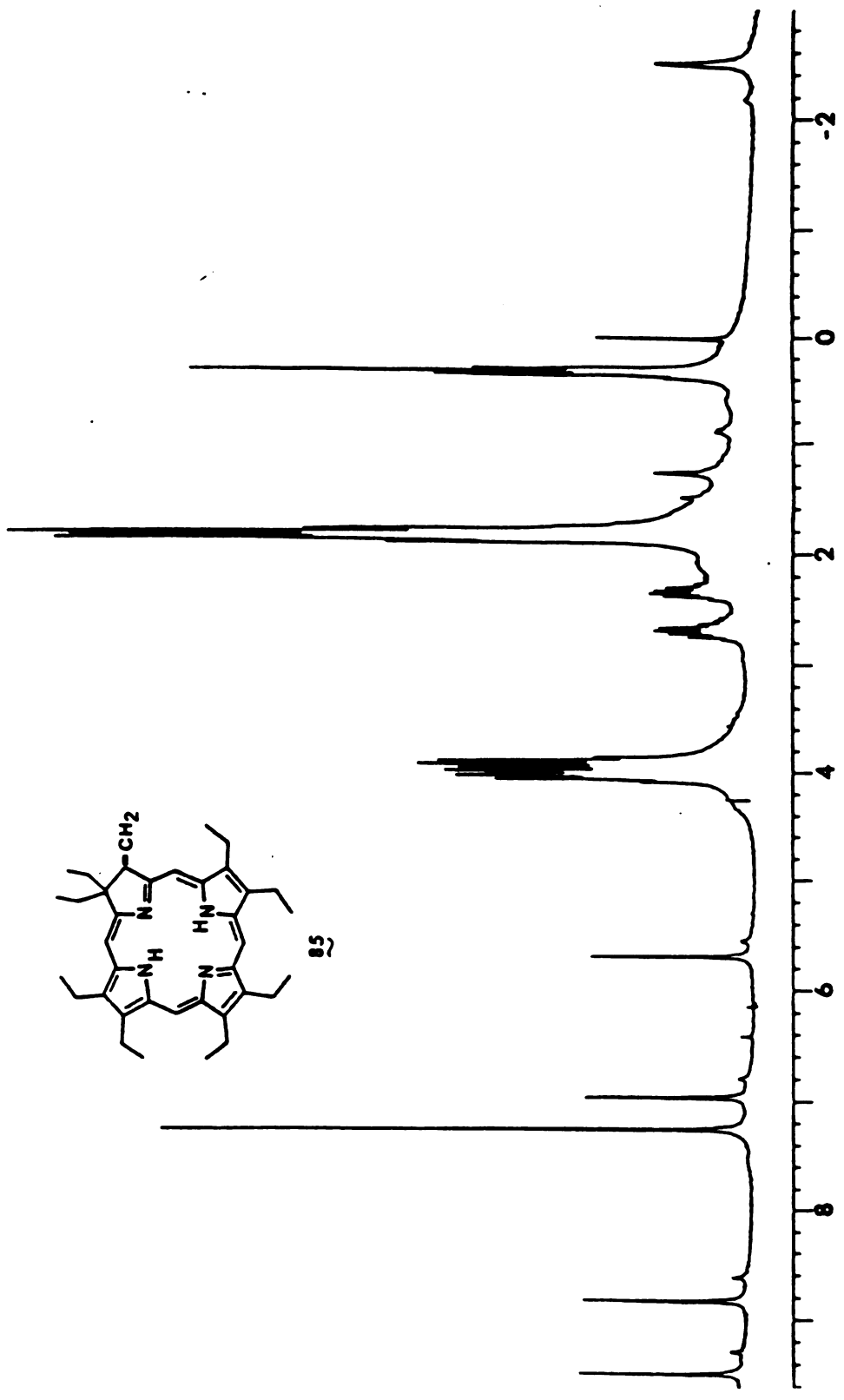

Figure A53. 250 MHz ^{1}H NMR spectrum of methylene alkylated chlorin 85.

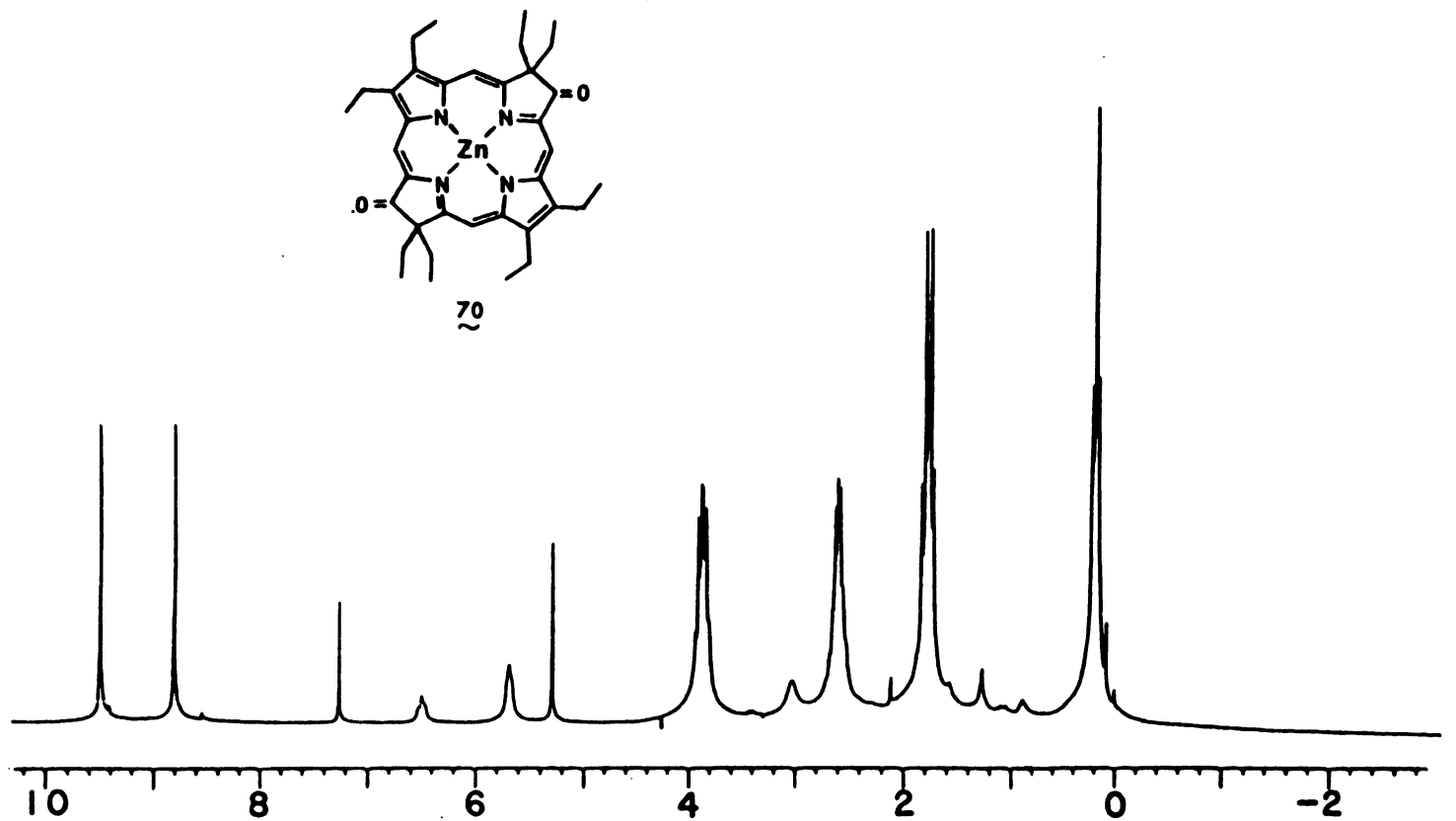

70

Figure A54. 250 MHz ^{1}H NMR spectrum of the zinc complex of 2, 6 diketone 70.

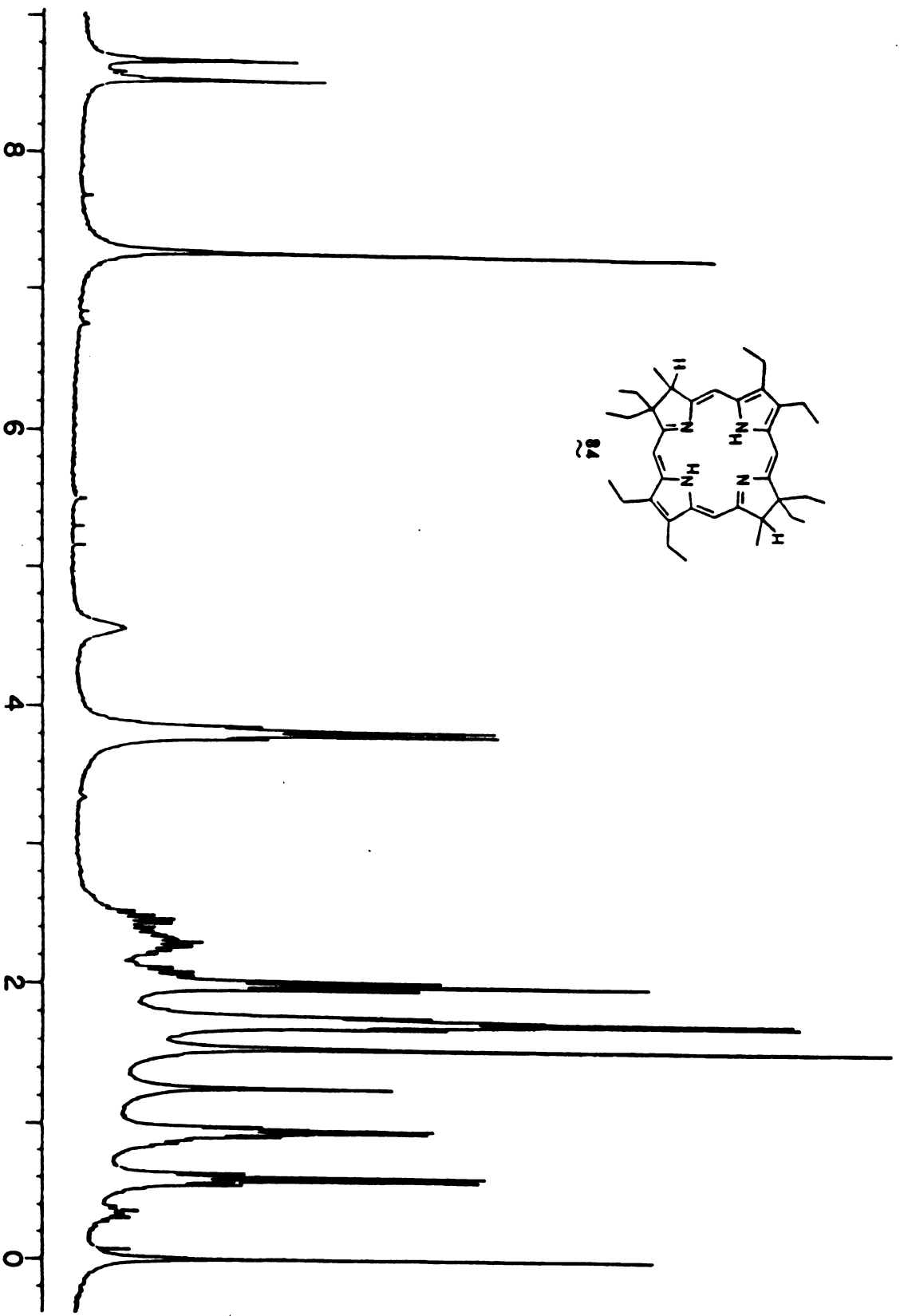

Figure A55. 250 MHz ^1H NMR spectrum of alkylated bacteriochlorin 85.

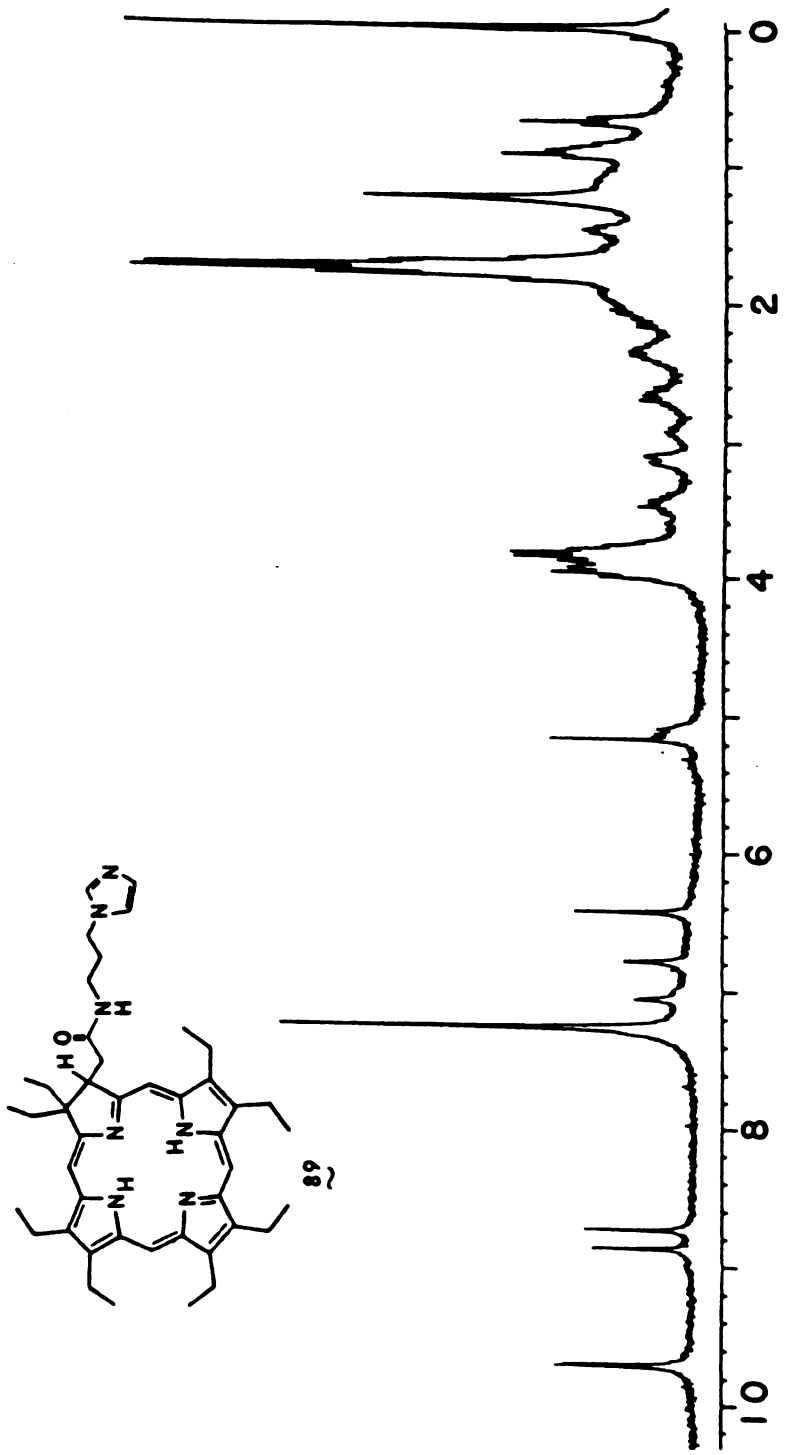

Figure A56. 250 MHz ^{1}H NMR spectrum of amide linked imidazole chlorin 89.

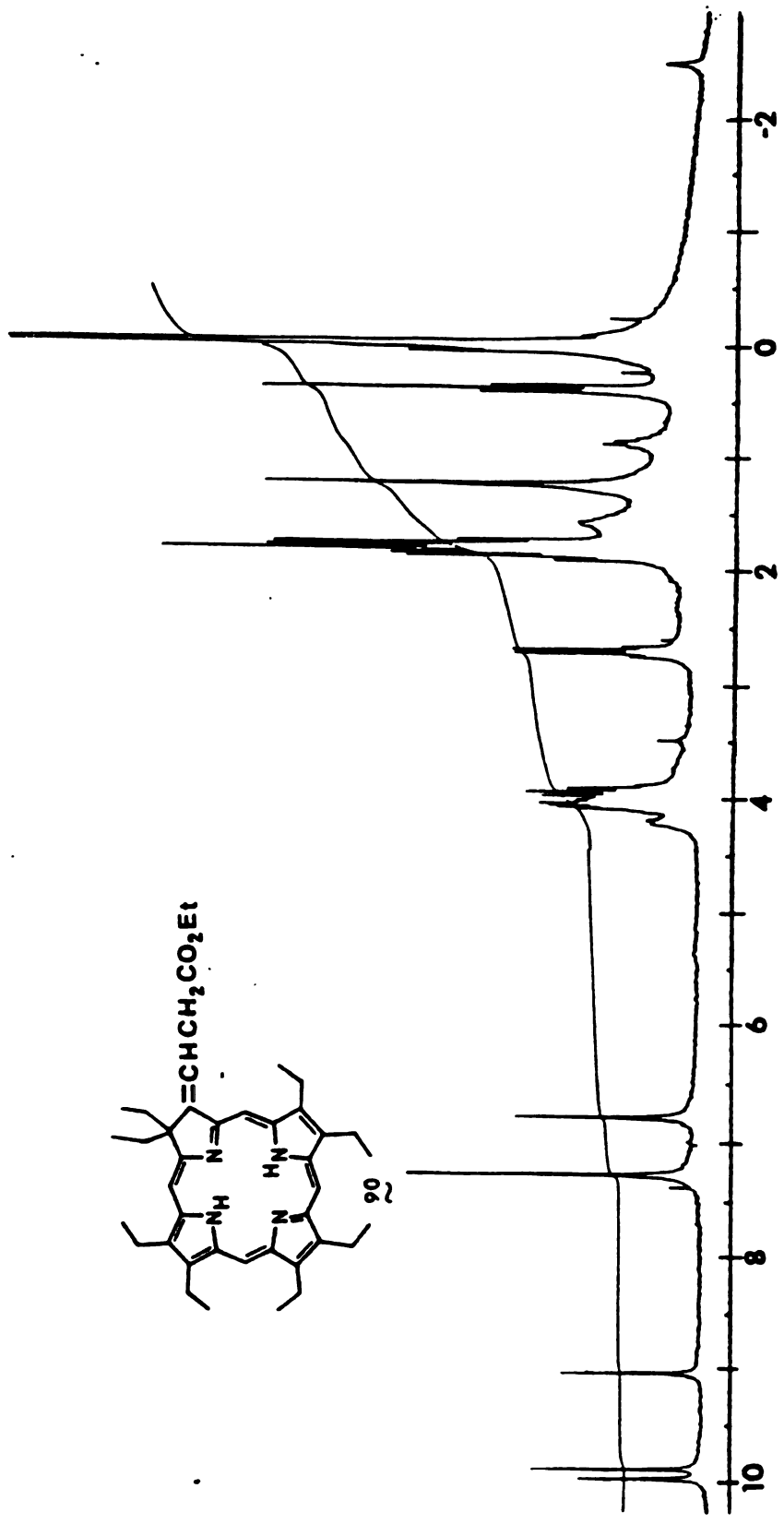

Figure A57. 250 MHz ^{1}H NMR spectrum of wittig generated chlorin 90.

Figure A58. 250 MHz ^1H NMR spectra of alkylated chlorins; (a) R = CH_2CO_2Et (88); (b) R = CH_2CH_2OH (91).

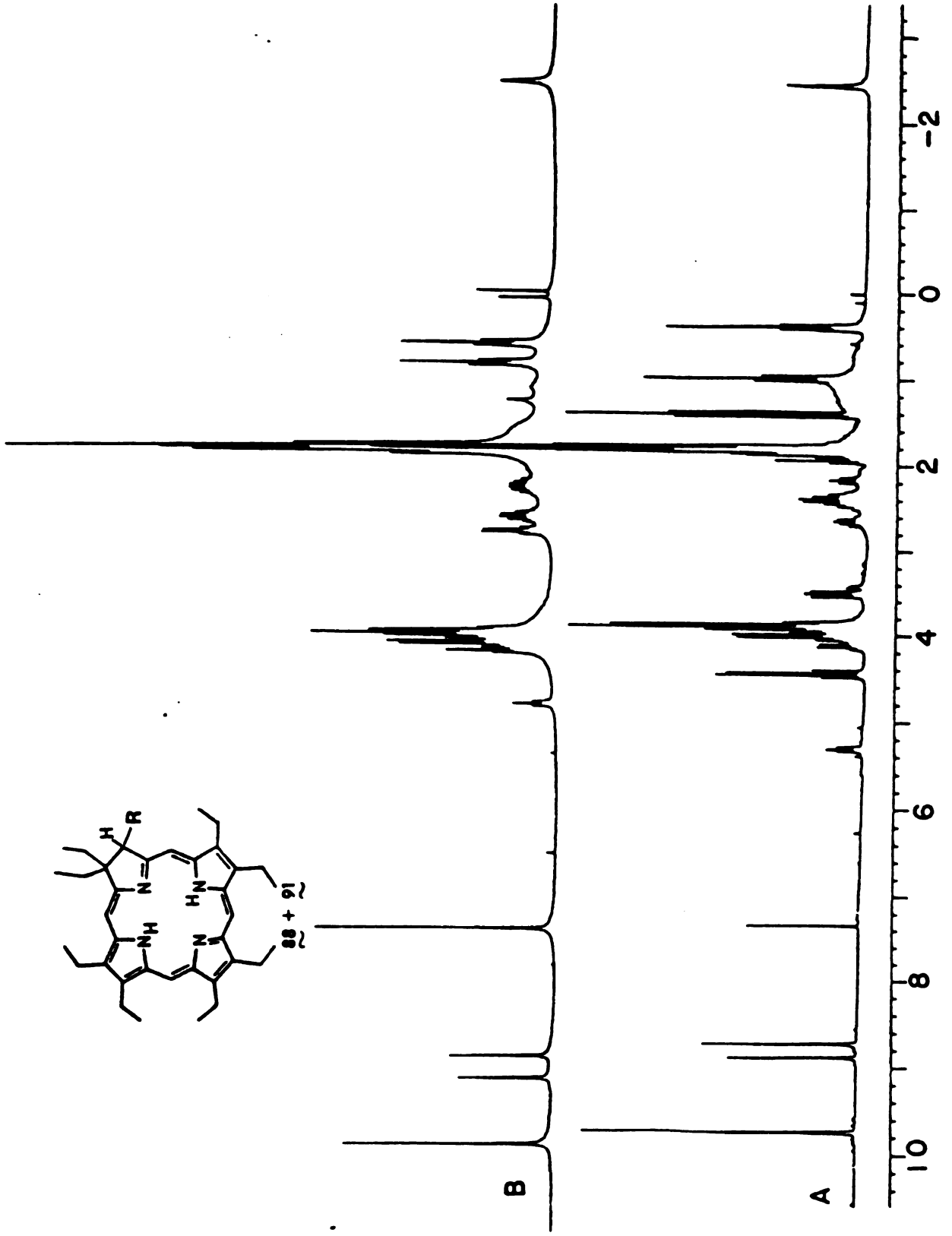
B
A
10
8
6
4
2
0
-2
R
H
N
NH
88 + 91

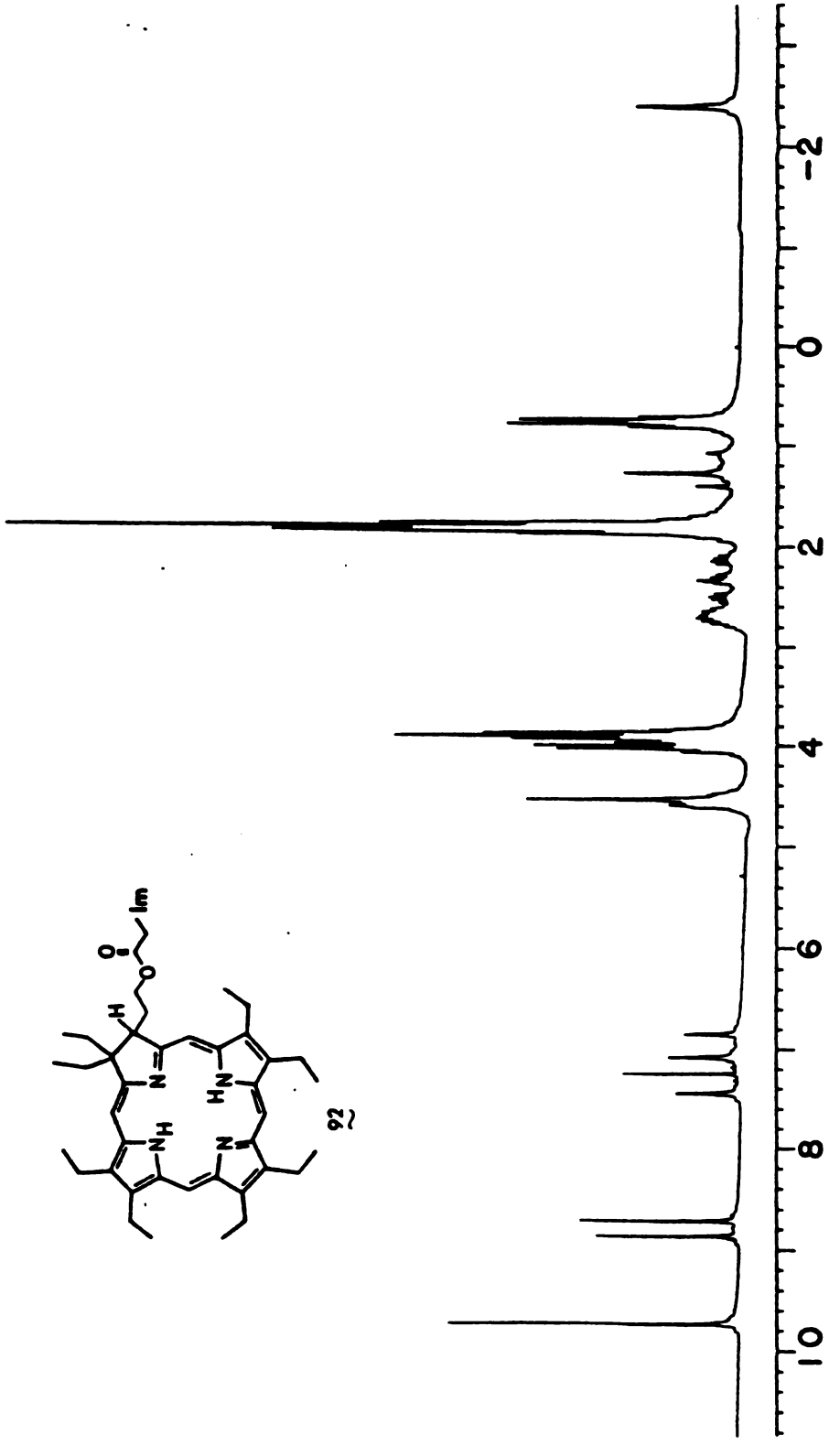

Figure A59. 250 MHz ^1H NMR spectrum of ester linked imidazole chlorin 92.

Figure A60. 250 MHz ^{1}H NMR spectra of (a) (R, R') = O, 2,3 diketone 68; (b) R = OH, R' = Me, isobacteriochlorin 95.

Figure A60. 250 MHz ^{1}H NMR spectra of (a) (R, R') = O, 2,3 diketone 68; (b) R = OH, R' = Me, tautomeric equilibrium 95.

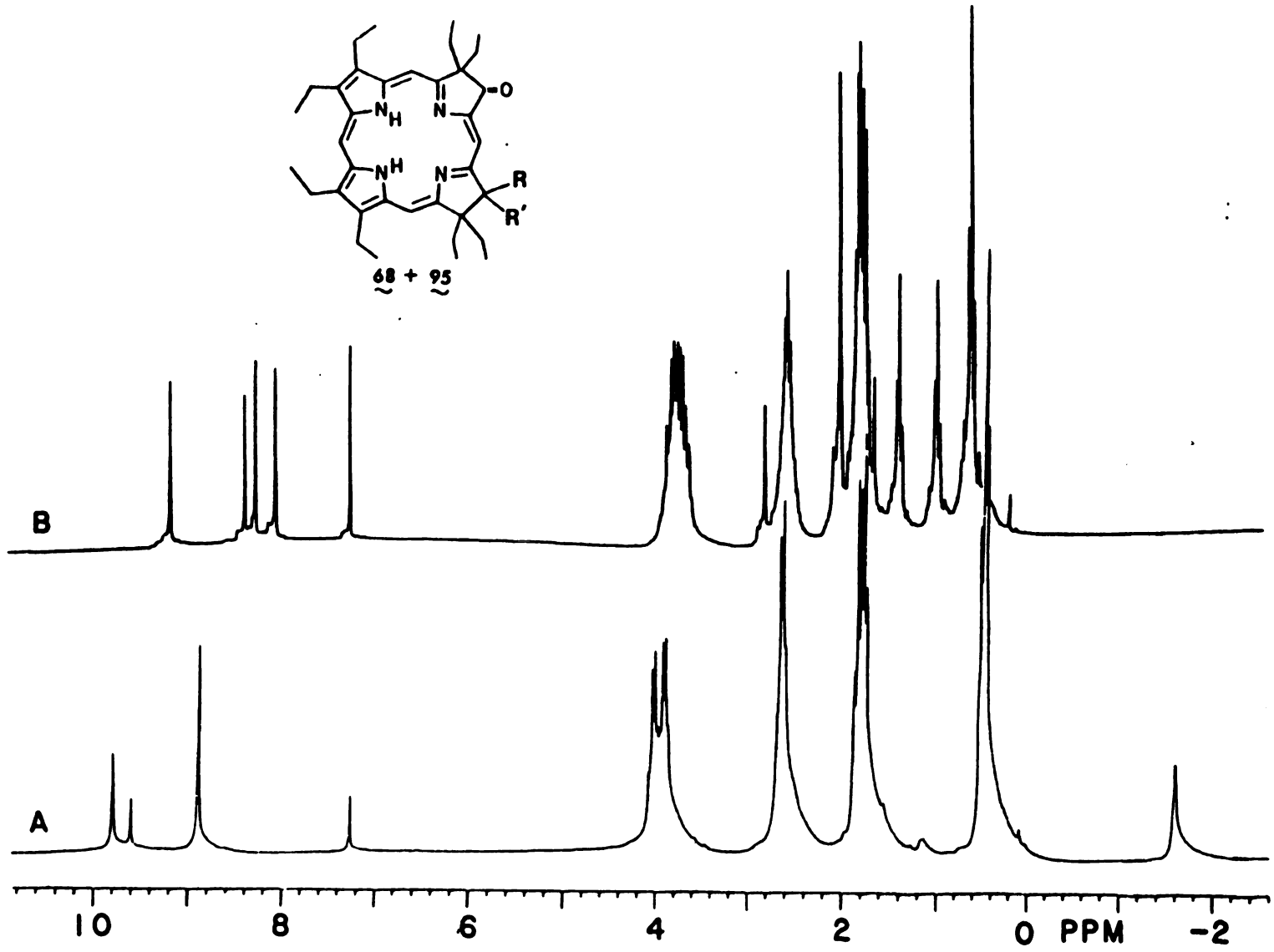

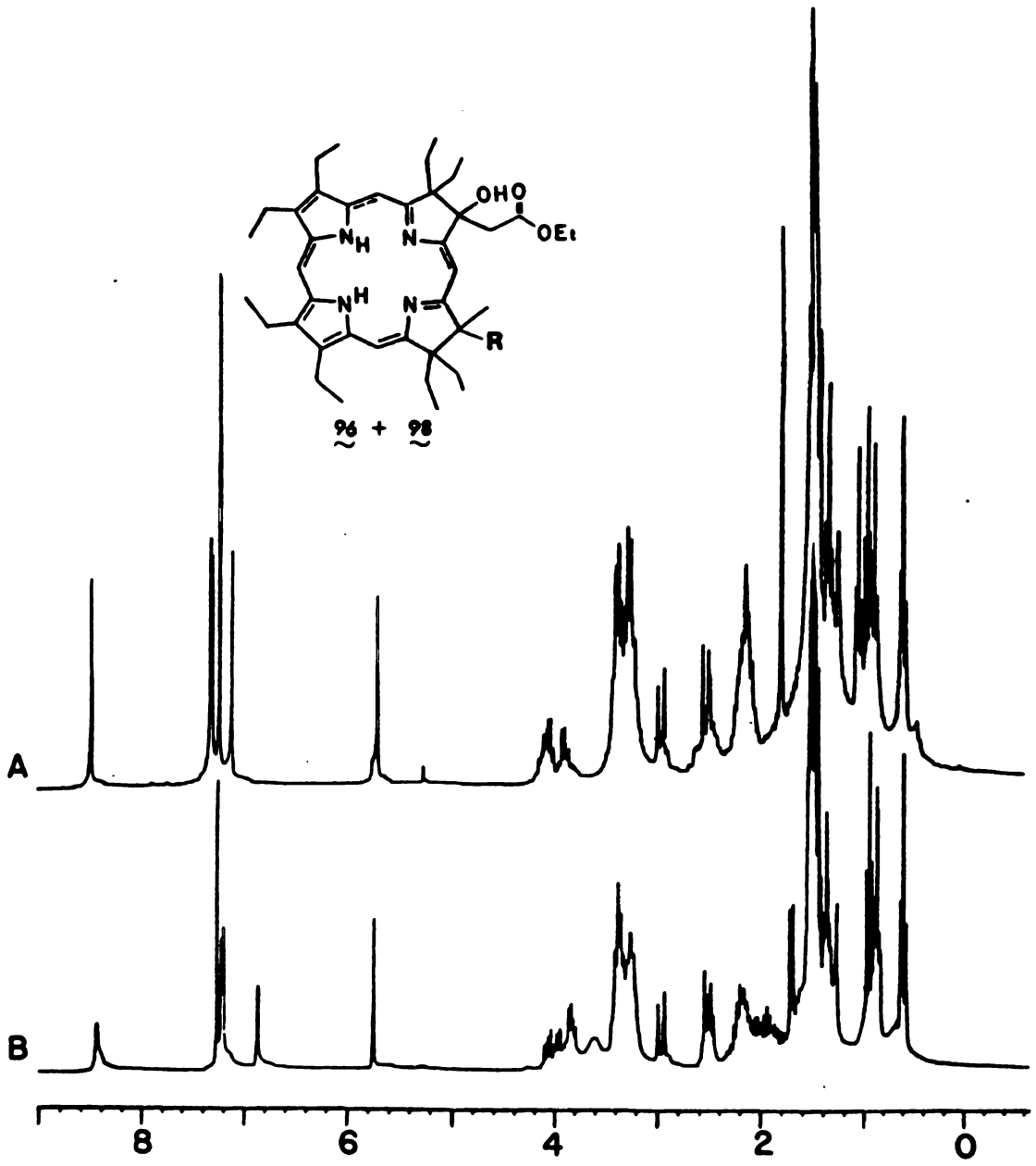

Figure A61. 250 MHz ^{1}H NMR spectra of alkylated isobacteriochlorins; (A) R = OH (96); (B) R = H (98).

Figure A62. 250 MHz ^1H NMR spectra of alkylated isobacteriochlorins; (A) R = H (100); (B) R = $COCH_2CH_2Im$ (101).

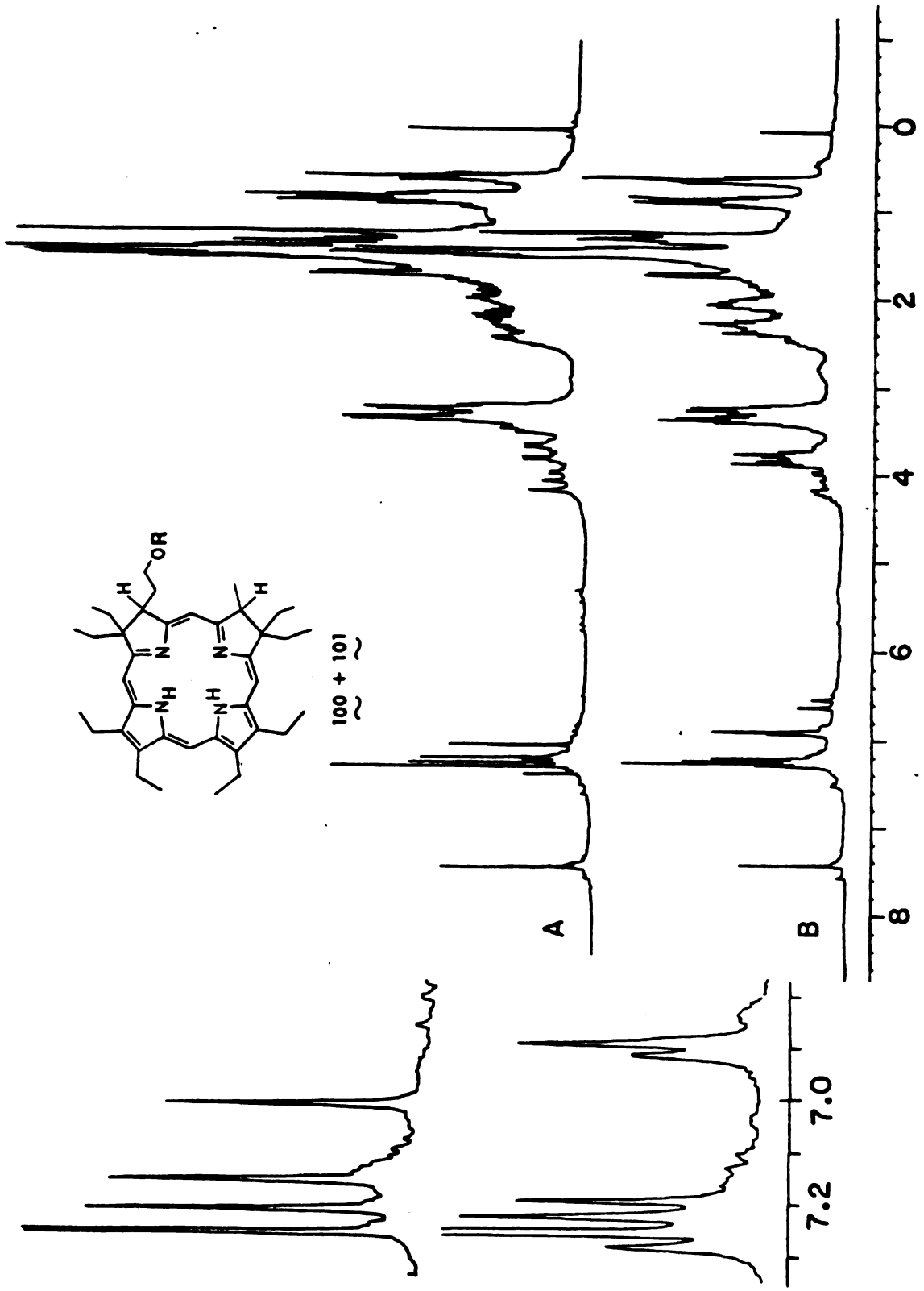
OR
H
H
N
N
H
H
N
N
100 + 101
A
B
0
2
4
6
8
7.0
7.2

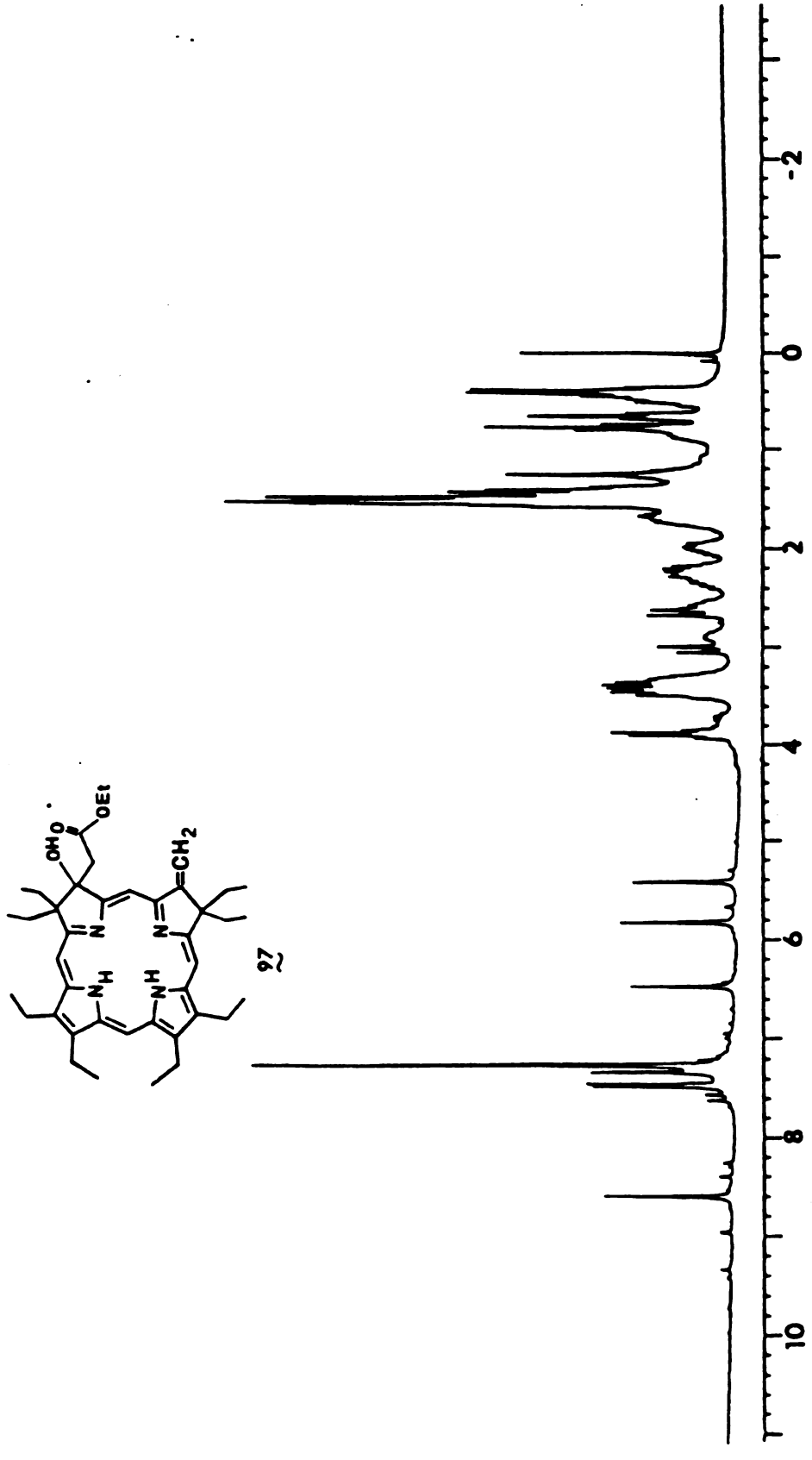

Figure A63. 250 MHz ^1H NMR spectrum of alkylated isobacteriochlorin 97.

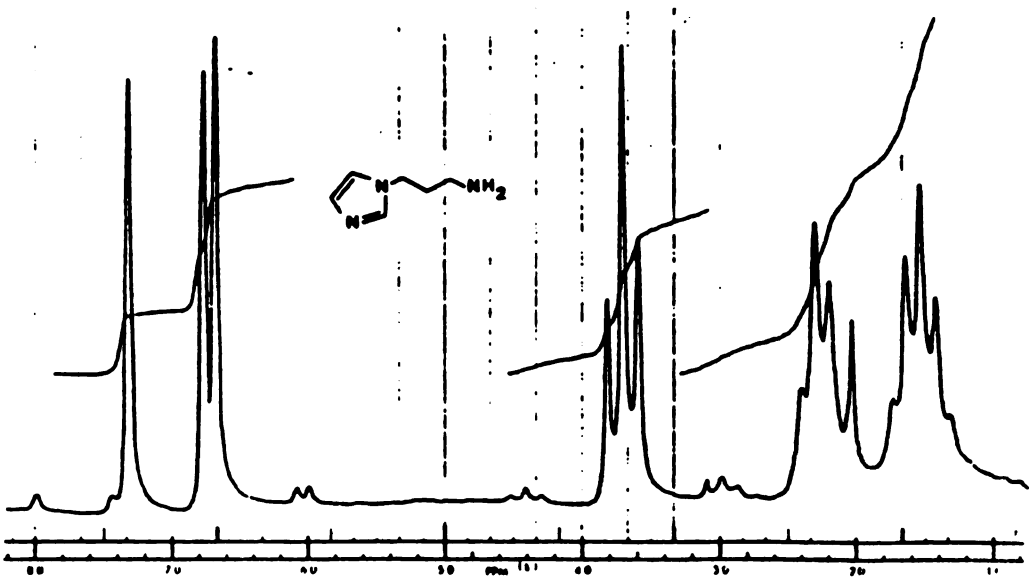

Figure A64. 60 MHz ^{1}H NMR spectrum of 3-(N-imidazolyl) propylamine, neat.

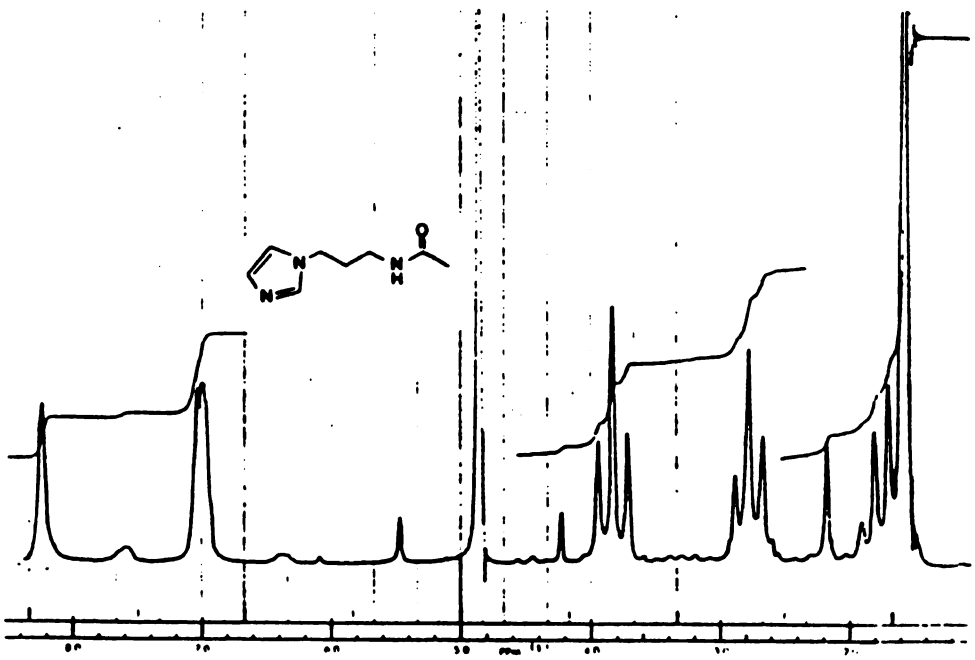

Figure A65. 60 MHz ^{1}H NMR spectrum of N-acetyl 3-(N-imidazolyl)propylamine, D_2O.

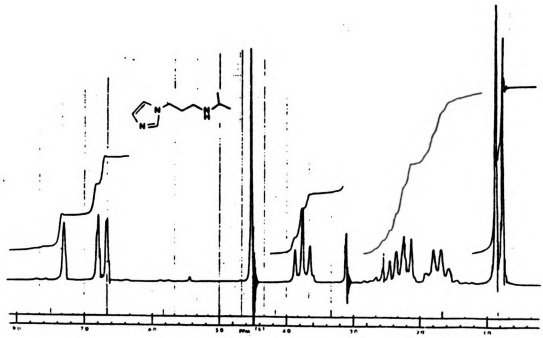

Figure A66. 60 MHz ^1H NMR spectrum of N-isopropyl 3-(N-imidazolyl)propylamine, D_2O.

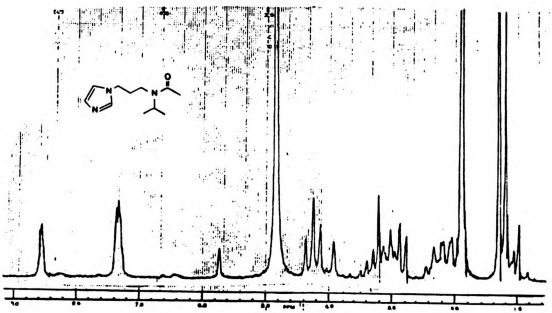

Figure A67. 60 MHz ^1H NMR spectrum of N-acetyl N-isopropyl 3-(N-imidazolyl)propyl amine.

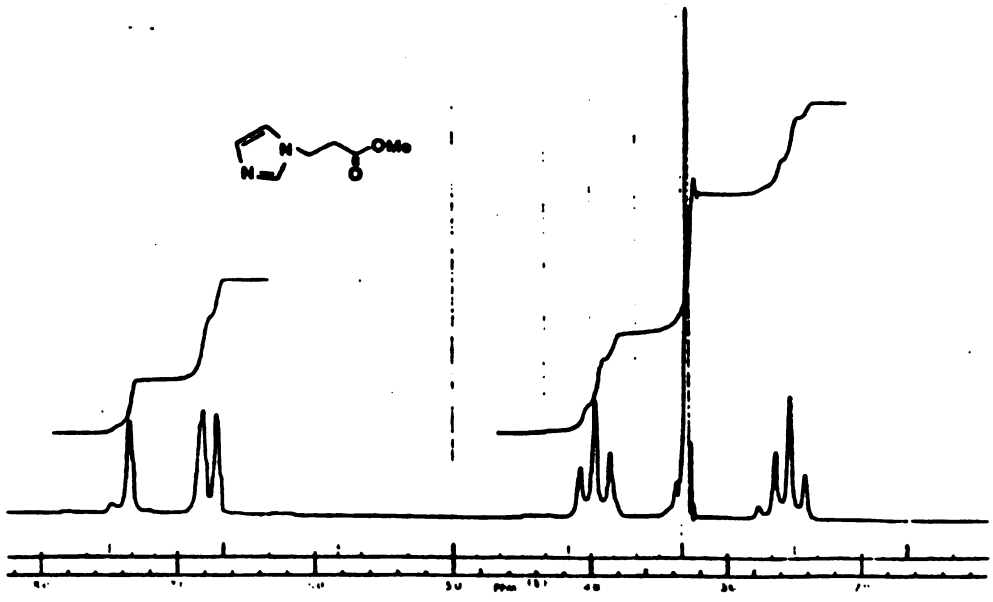

Figure A68. 60 MHz ^{1}H NMR spectrum of methyl 3-(N-imidazolyl)proprionate, neat.

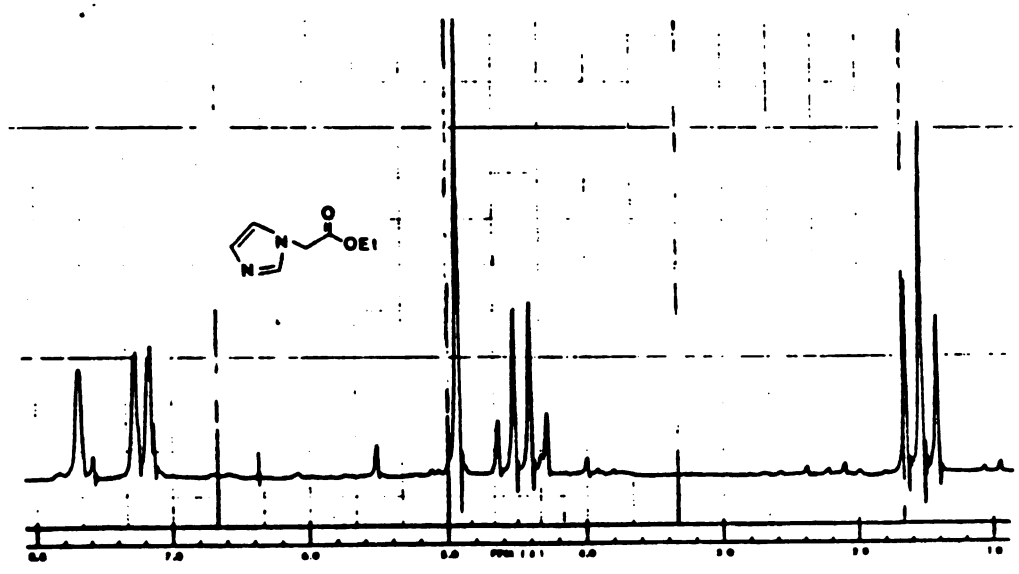

Figure A69. 60 MHz ^{1}H NMR spectrum of ethyl 2-(N-imidazolyl)acetate, $CDCl_3$.

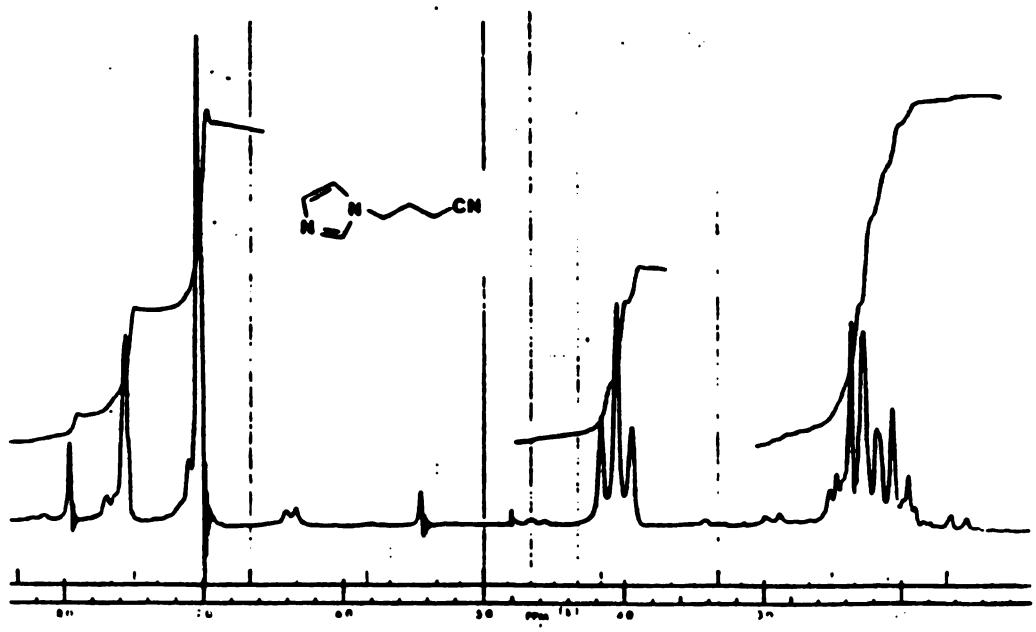

Figure A70. 60 MHz ^1H NMR spectrum of 4-(N-imidazolyl) butyronitrile, neat.

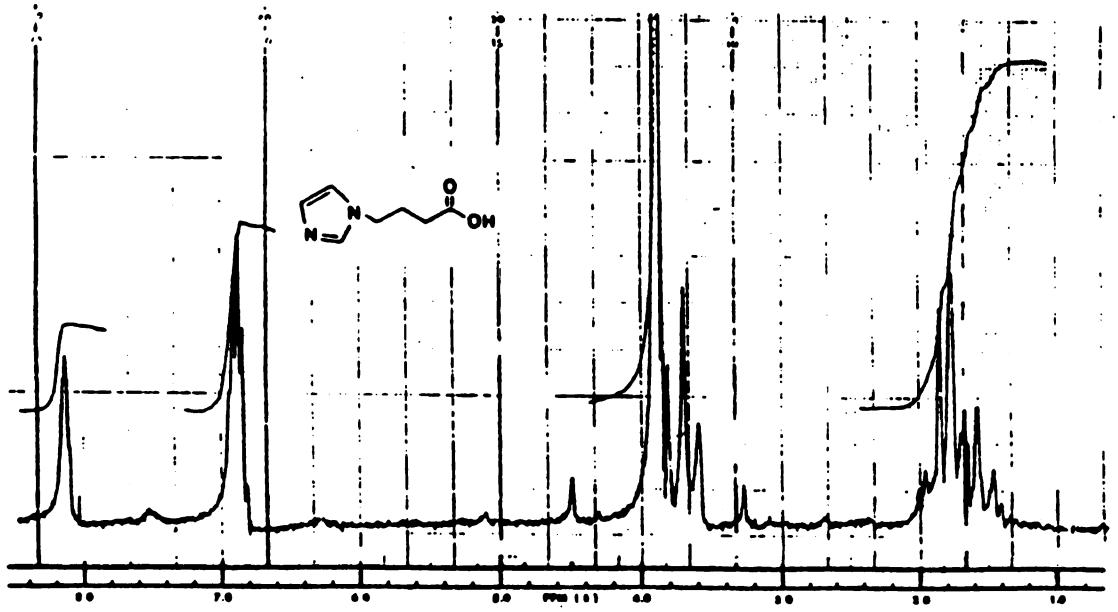

Figure A71. 60 MHz ^1H NMR spectrum of 4-(N-imidazolyl) butyric acid, D_2O.

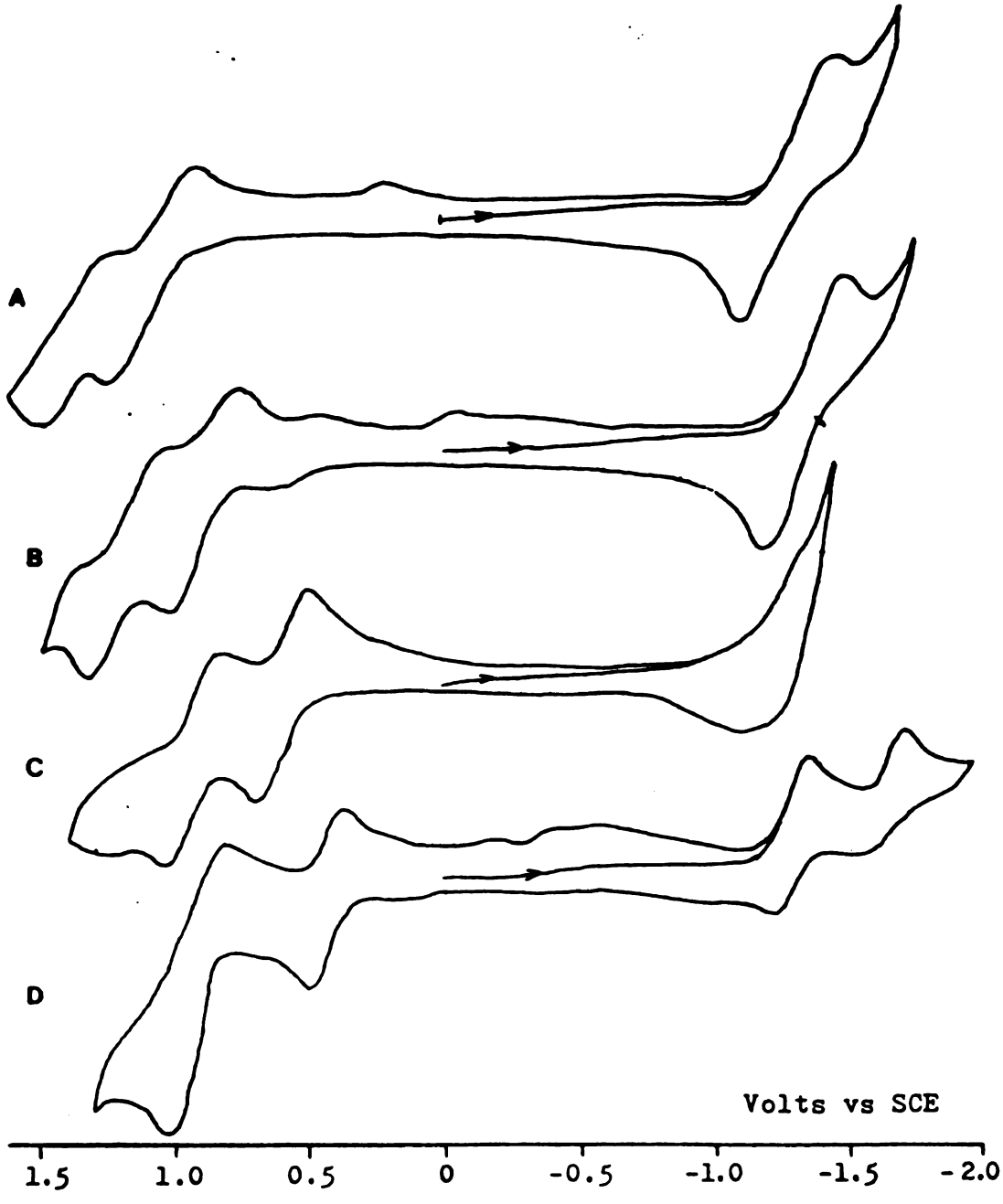

Figure A72. Cyclic voltammograms of (A) tetraphenylporphyrin; (B) tetraphenylchlorin; (C) Zinc-TPC; (D) tetraphenylbacteriochlorin. Spectra measured in CH_2Cl_2 with $(Bu)_4NClO_4$ as supporting electrolyte.

List of References

REFERENCES

1. a. Collman, J.P.; Gagne, R.R.; Halbert, T.R.; Marchon, J.C.; Reed, C.A., J. Am. Chem. Soc. 1973, 95, 7868.

   b. Collman, J.P.; Gagne, R.R.; Reed, C.A.; Halbert, T.R.; Lang, R.; Robinson, W.T., J. Am. Chem. Soc. 1975, 97, 427.

2. a. Baldwin, J.E.; Almog, J.; Dyer, R.L.; Peters, M., J. Am. Chem. Soc. 1975, 97, 226.

   b. Almog, J.; Baldwin, J.E.; Huff, J., J. Am. Chem. Soc. 1975, 97, 427.

   c. Hashimoto, T.; Dyer, R.L.; Crossley, M.J.; Baldwin, J.E.; Basolo, F., J. Am. Chem. Soc. 1982, 104, 2101.

3. a. Baldwin, J.E.; Klose, T.; Peters, M., J. Chem. Soc., Chem Comm. 1976, 881.

   b. Battersby, A.R.; Buckley, D.G.; Hartley, S.G.; Turnbull, M.D., J. Chem. Soc., Chem. Comm. 1976, 879.

   c. Momenteau, M.; Look, B.; Mispelter, J.; Bisagni, E., Nouv. J. Chim., 1979, 3, 77.

   d. Momenteau, M.; Mispelter, J.; Look, B.; Bisagni, E., J. Chem. Soc., Perkin Trans 2 1983, 189.

   e. Momenteau, M.; Lavalette, D.J., J. Chem. Soc., Chem. Comm. 1982, 341.

   f. Ward, B.; Wang, C.B.; Chang, C.K., J. Am. Chem. Soc. 1981, 103, 5236.

   g. Battersby, A.R., Bartholomew, S.A.J.; Nitta, T., J. Chem. Soc., Chem Comm. 1983, 1291.

4. a. Chang, C.K.; Traylor, T.G., J. Am. Chem. Soc. 1973, 95, 5810.

   b. Chang, C.K.; Traylor, T.G., Proc. Natl. Acad. Sci. U.S.A. 1973, 70, 2647.

5. Gunter, M.J., Mander, L.N., J. Org. Chem. 1981, 46, 4792.

6. Gunter, M.J.; Mander, L.N.; Murray, K.S.; Clark, P.E., J.Am. Chem. Soc. 1981, 103, 6784.

7. Collman, J.P.; Brauman, J.I.; Doxsee, K.M.; Halbert, T.R.; Bunnenberg, E.; Linder, R.E.; LaMar, G.N.; DelGaudio, J.; Lang, G.; Spartalian, K., J. Am. Chem. Soc. 1980, 102, 4182.

8. a. Ward, B. Ph.D. Dissertation, Michigan State University, East Lansing, Michigan, 1983.

b. Ward, B.; Young,R.; Hunt, K.; Chang, C.K., manuscript in preparation.

9. Freitag, R.A.; Mercer-Smith, J.A.; Whitten, D.G., J. Am. Chem. Soc. 1981, 103, 1226.

10. LaMar, G.N.; Walker, F.A., in "The Porphyrins", Dolphin, D., ed.; Academic Press: New York, 1979; Vol. IV, pp 61-175, and references therein.

11. Walker, F.A.; LaMar, G.N., Ann. N.Y. Acad. Sci. 1973, 206, 328.

12. LaMar, G.N.; Walker, F.A., J. Am. Chem. Soc. 1973, 95, 1782.

13. White, W.I., in "The Porphyrins", Dolphin, D., ed. Academic Press: New York, 1979; Vol. V, p 318.

14. Cheng, R.-J.: Latos-Grazynski, L.; Balch, A.L., Inorg. Chem. 1982, 21, 2412.

15. Cense, J.M.; Le Quan, R.-M., Tetrahedron Lett. 1979, 3725.

16. Groves, J.T.; Haushalter, R.C.; Nakamura, N.; Nemo, T.E.; Evans, B.J., J. Am. Chem. Soc. 1981, 103, 2884.

17. Suslick, K.S.; Fox, M.M., J. Am. Chem. Soc. 1983, 105, 3705.

18. Harel, Y.; Felton, R.H., J. Chem. Soc., Chem. Comm. 1984, 206.

19. Gunter, J.J.; Mander, L.N.; Murray, K.S., J. Chem. Soc., Chem Comm. 1981, 799.

20. LaMar, G.N.; Eaton, G.R.; Holm, R.H.; Walker, F.A., J. Am. Chem. Soc. 1973, 95, 63.

21. Botulinski, A.; Buchler, J.W.; Lay, K.L.; Ensling, J.; Twilfer, J.; Billecke, J.; Leuken, H.; Tonn, B. in "Adv. in Chem. Series", No. 201, Kadish, K.M., ed.; A.C.S. publication, Chapter 12.

22. a. Diekmann, H.; C.K. Chang, C.K.; Traylor, T.G., J. Am. Chem. Soc. 1971, 93, 4068.

b. Traylor, T.G.; Campbell, D.; Tsuchiya, S., J. Am. Chem. Soc. 1979, 101, 4748.

c. Traylor, T.G.; Campbell, D.; Tsuchiya, S.; Mitchell, M.; Stynes, D.V., J. Am. Chem. Soc. 1980, 102, 5939.

d. Traylor, T.G.; Mitchell, M.J.; Tsuchiya, S.; Campbell, D.; Stynes, S.V.; Coga, N., J. Am. Chem. Soc. 1981, 103, 5234.

23. Warne, P.K.; Hager, L.P., Biochemistry 1970, 9, 1606.

24. Geibel, J.; Cannon, J.; Campbell, D.; Traylor, T.G., J. Am. Chem. Soc. 1978, 100, 3575.

25. a. Lavalette, D.; Momenteau, M., J. Chem. Soc., Perkins Trans. 2 1982, 385.

b. Mispelter, J.; Momenteau, M., J.; Lavalette, D.; Lhoste, J.-M., J. Am. Chem. Soc. 1983, 105, 5165.

c. Momenteau, M.; Loock, B.; Lavalette, D.; Tetreau, C.; Mispelter, J., J. Chem. Soc., Chem. Comm. 1983, 962.

26. Traylor, T.G.; Berzinis, A.P., J. Am. Chem. Soc. 1980, 102, 2844.

27. Goff, H., J. Am. Chem. Soc. 1980, 102, 3252.

28. a. Walker, F.A., J. Am. Chem. Soc. 1980, 102, 2844.

b. Walker, F.A.; Buehler, J.; West, J.T.; Hinds, J.L., J. Am. Chem. Soc. 1983, 105, 3052.

29. Ward, B., unpublished results.

30. a. Collman, J.P.; Brauman, J.I.; Collins, T.J.; Iverson, B.L.; Lang, G.; Pettman, R.B.; Sessler, J.L.; Walters, M.A., J. Am. Chem. Soc. 1983, 105, 3038.

b. Collman, J.P.; Brauman, J.I.; Iverson, B.L., Sessler, J.L.; Morris, R.M.; Gibson, Q.H., J. Am. Chem. Soc. 1983, 105, 3052.

31. Vogel, M.I., "A Textbook of Practical Organic Chem." 4th ed., Longman: New York, 1978: p 531.

32. a. Tweedle, M.F.; Wilson, L.J.; Garcia-Iniguez, L.; Babcock, G.T.; Palmer, G., J. Biol. Chem. 1978, 253, 8072.

b. Moss, T.H.; Shapiro, E.; King, T.E.; Beinert, H.; Hartzell, C., J. Biol. Chem. 1978, 253, 8072.

33. a. Babcock, T.T.; Vickery, L.E.; Palmer, G., J. Biol. Chem. 1976, 251, 7907.

b. Palmer, G.; Babcock, G.T.; Vickery, L.E., Proc. Natl. Acad. Sci. U.S.A. 1976, 73, 2206.

c. Babcock, G.T.; Vickery, L.E., Palmer, G., J. Biol. Chem. 1978, 253, 2400.

34. Buckingham, D.A.; Gunter, M.J.; Mander, L.N., J. Am. Chem. Soc. 1978, 100, 2899.

35. Gunter, M.J.; Mander, L.N.; McLaughlin, G.M.; Murrsy, K.S.; Berry, K.J.; Clark, P.E.; Buckingham, D.A., J. Am. Chem. Soc. 1980, 102, 1470.

36. Chang, C.K.; Koo, M.S.; Ward, B., J. Chem. Soc., Chem. Comm. 1982, 716.

37. Chang, C.K. in "Biochemical and Clinical Aspects of Oxygen", Caughey, W.S., ed.; Academic Press; New York, 1979; p 437.

38. Collman, J.P.; Elliot, C.M.; Halbert, T.R.; Tovrog, B.S., Proc. Natl. Acad. Sci., U.S.A. 1977, 74, 18.

39. Ogoshi, H.; Sugimoto, H.; Yoshida, Z., Tetrahedron Lett. 1977, 169.

40. a. Chang, C.K.; Koo, M.-S.; Wang, C.-B., J. Heterocycl. Chem. 1977, 14, 943.

b. Chang, C.K., J. Heterocycl. Chem. 1977, 14, 1285.

41. a. Collman, J.P.; Denisevich, P.; Konai, Y.; Marrocco, M.; Koval, C.; Anson, F.C., J. Am. Chem. Soc. 1980, 102, 6027.

b. Collman, J.P.; Anson, F.C.; Barnes, C.E.; Bencosme, C.S.; Geiger, T.; Evitt, E.R.; Kreh, R.P.; Meier, K.; Pettman, R.B., J. Am. Chem. Soc. 1983, 105, 2694.

c. Collman, J.P.; Bencosme, C.S.; Durand, Jr., R.R.; Kreh, R.P.; Anson, F.C., J. Am. Chem. Soc. 1983, 105, 2699.

d. Collman, J.P.; Bencosme, C.S.; Barnes, C.E.; Miller, B.D., J. Am. Chem. Soc. 1983, 105, 2704.

42. Ooi, G.K.S.; Magee, R.J., J. Inorg. Nucl. Chem. 1970, 32, 3315.

43. Barnick, J.W.F.K.; Van Der Baan, J.L.; Bickelhaupt, F., Synthesis 1979, 787.

44. Goff, H., in "Physical Biorganic Chem. Series", Lever, A.B.P.; Gray, H., eds. Part 1, Chapter 4, p 237.

45. a. Katz, J.J., in "Inorganic Biochemistry", Vol. 2, Eichorn, G.L., ed., Elsevier Publishing Co., Amsterdam 1973, Chapter 29.

b. Clayton, R.K.; Sistrom, W.R. "The Photosynthetic Bacteria", Plenum Press, New York, 1978.

46. a. Siegel, L.M.; Murphy, M.J.; Kamin, H., J. Biol. Chem. 1973, 248, 251.

b) Murphy, M.J.; Siegel, L.M.; Kamin, H.; Rosenthal, D., J. Biol. Chem. 1973, 248, 2801.

c) Murphy, M.J.; Siegel, L.M., Tove, S.R.; Kamin, H., Proc. Natl. Acad. Sci. U.S.A. 1974, 71, 612.

d) Vega, J.M.; Garrett, R.H.; Siegel, L.M., J. Biol. Chem. 1973, 248, 251.

47. Hucklesby, D.P.; James, D.M.; Banewell, J.; Hewitt, E.J., Phytochemistry 1976, 15, 599.

48. Battersby, A.R.; McDonald, E., Bioorganic Chem. 1978, 7, 161.

49. Deeg, R.; Krienler, H.P.; Bergmann, K.H.; Muller, G., Z. Physiol. Chem. 1977, 358, 339.

50. Scott, A.I.; Irwin, A.J.; Siegel, L.M.; Shoolery, J.N., J. Am. Chem. Soc. 1978, 100, 7987.

51. Scheer, H., in "The Porphyrins", Dolphin, D., ed., Academic Press: New York, 1979; Vol. II, Chapter 1, pp 1-44, and references therein.

52. Scheer, H.; Inhoffen, H.H., in "The Porphyrins", Dolphin, D., ed., Academic Press: New York, 1979, Vol II, p 49.

53. Barret, J., Biochem. J. 1956, 64, 626.

54. a. Yamanaka, T.; Ota, A.; Okunuki, K., Biochim. Biophys. Acta 1960, 44, 397.

b. Yamanaka, T.; Kihimoto, S.; Okunuki, K., J. Biochem. 1963, 53, 416.

55. Kuronen, T.; Ellfolk, N., Biochim. Biophys. Acta 1972, 275, 308.

56. Newton, N., Biochim. Biophys. Acta 1969, 185, 316.

57. Iwasaki, H.; Matsubara, T., J. Biochem, 1971, 69, 847.

58. Inhoffen, H.H.; Nolte, W., Liebigs Ann. Chem. 1969, 725, 167.

59. Chang, C.K., Biochemistry 1980, 19, 1971.

60. a. Roomi, M.W.; MacDonald, S.F., Can. J. Chem. 1970, 48, 139.

b. Paine, J.B. in "The Porphyrins", Dolphin, D., ed.: Academic Press: New York, 1979: Vol. I, p 124.

61. Whitlock, H.W.; Hanauer, R.; Oester, M.Y.; Bower, B.K., J. Am. Chem. Soc. 1969, 91, 7485.

62. Inhoffen, H.H.; Muller, N., Tetrahedron Lett. 1969, 3209.

63. Scheer, H.; Svec, W.A.; Cope, B.T.; Studier, M.H.; Scott, R.G.; Katz, J.J., J. Am. Chem. Soc. 1974, 96, 3714.

64. a. Richardson, P.F.; Chang, C.K.; Hanson, L.K.; Spaulding, L.D.; Fajer, J., J. Phys. Chem. 1979, 83, 3420.

b. Chang, C.K.; Fajer, J., J. Am. Chem. Soc. 1980, 102, 848.

c. Chang, C.K.; Hanson, K.K.; Richardson, P.F.; Young, R.; Fajer, J., Proc. Natl. Acad. Sci., U.S.A. 1981, 78, 2652.

d. Chang, C.K., in "The Biological Chemistry of Iron", Dunford, H.B.; et al., eds. D. Reidel Publishing Co. 1982, p 313.

65. Stolzenberg, A.M.; Spreer, L.O.; Holm, R.H., J. Am. Chem. Soc. 1981, 103, 4763.

66. Fujita, I., Brookhaven Natl. Lab., preliminary results.

67. a. Stolzenberg, A.M.; Strauss, S.H.; Holm, R.H., J. Am. Chem. Soc. 1981, 103, 4763.

b. Strauss, S.H.; Holm, R.H., Inorg. Chem., 1982, 21, 863.

68. Strauss, S.H.; Silver, M.E.; Ibers, J.A., J. Am. Chem. Soc. 1983, 105, 62.